DOCTOR OF PHILOSOPHY

A metabolomics-based approach to study abiotic stress in Lolium perenne

Foito, Alexandre

Award date:
2010

Awarding institution:
University of Dundee

DOCTOR OF PHILOSOPHY

A metabolomics-based approach to study abiotic stress in Lolium perenne

Alexandre Foito

2010

University of Dundee

A metabolomics-based approach to study abiotic stress in *Lolium perenne*

Alexandre M M Foito

A Thesis Submitted for the Degree of

Doctor of Philosophy

University of Dundee

June 2010

Table of Contents

List of tables

List of figures

Acknowledgements

Firstly, I would like to take this opportunity to thank Teagasc and SCRI, in particular to Susanne Barth, Derek Stewart and Stephen Byrne, for giving me the opportunity to study for a PhD.

I gratefully acknowledge the past and present members of the laboratories in which I have worked for their help and assistance throughout my project, in particular Derek Stewart for his continued guidance and advice, Susanne Barth for her continued support and advice, Stephen Byrne for all the help in experimental set-up transcript analysis and fruitful discussions, and Claire Halpin for some advice. I would also like to express gratitude to Tom Shepherd for his expertise in GC-MS analysis, Christine Hackett for an excellent statistical analysis support, Pete Hedley and Jenny Morris for performing the microarray analysis. Additionally, I would like to thank Rob Hancock for helping me to optimise the HPAEC protocol, Nicola Stewart for helping me to set up the FT-IR analysis, Johannes Rauscher for his excellent practical advice over GC-MS sample preparation, Susan Verrall for helping me to wrestle with GenStat, Colin Alexander for statistical advice, Gary Dobson for his expertise in biochemical analysis and Julie Sungurtas for advice on data processing. Thanks must go to Kathleen McMillan for helping me to develop my writing skills and proof-reading a substantial part of my thesis.

On a personal note I would like to thank my family: mom and dad for their continued support over the years. I want to thank Kirstin for always being there for me. Finally, but not least, I want to thank all my friends back home and the friends I've gained throughout this journey that was my PhD.

Declaration

I hereby declare that the following thesis is based on the results of a joint research project and that the investigations, unless otherwise clearly stated, were conducted by myself. This thesis has not, in whole or in part, been previously presented for higher degree or qualification. Work other than my own is clearly indicated in the beginning of each chapter and in the text by reference to the relevant researchers or their publications.

Alexandre M M Foito

We declare that Alexandre Foito has fulfilled the conditions of the relevant Ordinance and Regulations of the University of Dundee and is qualified to submit the accompanying thesis in application for the degree of Doctor of Philosophy.

Dr Susanne Barth Dr Derek Stewart Dr Claire Halpin

Disclaimer

This thesis was based on a wider project which involved the collaboration between researchers. Due to the relevance of the results obtained by other researchers involved in this project they have been used to complement data acquired by the author. Furthermore, this project involved the collaboration between two different research institutes based on different countries. As a result of this, plant growth was performed in Teagasc, Ireland whereas metabolomic work was carried out in SCRI, Scotland. It is therefore extremely relevant to acknowledge the experimental contribution of those researchers for this project.

A major content of chapter 3 formed the basis of Foito *et al*. (2009). That chapter presents the results of a collaboration between two researchers, Dr. Stephen L. Byrne and the author. Dr. Stephen L. Byrne was responsible for performing transcript analysis whilst I was responsible for the metabolite profiling. However, the transcript analysis was particularly relevant to understand the global response of plants and allowed a degree of integration between two complementary approaches. It may further support or generate new hypotheses on the response of perennial ryegrass to drought conditions.

Chapter 4 presents the results of a collaboration between researchers, Dr. Stephen L. Byrne, Dr. Pete Hedley and the author. Dr. Pete Hedley was responsible for the microarray analysis while Dr. Stephen L. Byrne was responsible for performing physiological experiments and quantitative real-time RT-PCR. My responsibility was to undertake the metabolite profiling. However, the transcriptomic analysis was particularly relevant to understand the global response of plants and allowed a degree of integration between two complementary approaches. It may further support or generate new hypotheses on the response of perennial ryegrass to P-limitation.

Chapter 5 also presents the results of a collaboration between researchers, Dr. Stephen L. Byrne and the author. Dr. Stephen L. Byrne was responsible for performing physiological experiments while my responsibility was to undertake the metabolite profiling. Furthermore, statistical analysis was performed with the aid of Dr. Christine Hackett.

Abstract

In the United Kingdom and Ireland, a major percentage of fertilized agricultural area is devoted to grasslands, which helps to support the associated milk and beef production industries. In temperate grasslands, perennial ryegrass (*L. perenne*) is the major forage grass and this species is particularly suitable as a forage grass due to its high yield and digestibility, when compared with other species. However, perennial ryegrass is not well adapted to abiotic stress conditions which are likely to occur in its natural environment. Some of the abiotic stress factors which have significant impacts on plant growth and development include water and nutrient availability. Therefore, this project set out to unravel some of the mechanisms involved in the adaptation of perennial ryegrass to limited water, phosphorous and nitrogen. In order to understand the metabolic mechanisms acting in response to these stresses, metabolite profiling was performed using GC-MS. Furthermore, for the water- and phosphorous-limitation studies this approach was complemented with transcript analysis.

In order to study water-limitation a hydroponics system supplemented with polyethyleneglycol (PEG) was used to induce water-limitation for a period of one-week. A clear difference in the metabolic profiles of the leaves of plants grown under water stress was observed. Differences were principally due to a reduction in fatty acid levels in the more water stress-susceptible genotype Cashel and an increase in sugars and compatible solutes in the drought-tolerant PI 462336 genotype. Sugars exhibiting a significant increase included, raffinose, trehalose, glucose, fructose and maltose. Raffinose was identified as the metabolite exhibiting the largest accumulation under water-stress in the more tolerant genotype and may represent a target for engineering superior drought tolerance or form the basis of marker-assisted breeding in perennial ryegrass. The metabolomics approach was combined with a transcriptomics approach in

the water stress tolerant genotype PI 462336 which identified genes in perennial ryegrass that were regulated by this stress.

The characterization of the response to phosphorus-limitation was performed in a hydroponics system containing two solutions with different levels of phosphorus. Samples were collected from the roots and leaves of two genotypes 24 hours after being exposed to stress. Internal phosphate concentrations were reduced and significant alterations were detected in the metabolome and transcriptome of two perennial ryegrass genotypes. Results indicated a replacement of phospholipids with sulfolipids in response to P deficiency and that this occurs at the very early stages of P deficiency in perennial ryegrass. Additionally, the results suggested the role of glycolytic bypasses and the re-allocation of carbohydrates in response to P deficiency

The characterization of the metabolic response of *L. perenne* leaves to different levels of nitrogen supply was performed for seven different genotypes with variability in the regrowth response rate to nitrogen supply in a hydroponics system. This facilitated the identification of common mechanisms of response between genotypes to nitrogen. The metabolic response observed included modifications of the lipid metabolism, as well as alterations of secondary aromatic metabolite precursors in plants exposed to nitrogen-deficit. In contrast, plants grown in a nitrogen saturated media appeared to modify to some extent the metabolism of ascorbate. Additionally, it was found that amino acid levels increased with increasing concentrations of nitrogen supplied. This study suggested that the involvement of secondary metabolism, together with lipid and ascorbate metabolism, is of crucial importance in the early-adaptation of perennial ryegrass plants to different levels of nitrogen supply.

List of abbreviations

6G-FT- fructan:fructan 6G-fructosyltransferase
ABA- abscisic acid
ADP – adenosine diphosphate
AMDIS- Automated mass spectral deconvolution and identification system
ANOVA- Analysis of variance
APCI- atmospheric pressure chemical ionisation
ArMet- architecture for metabolomics
ATP – adenosine triphosphate
ATR – attenuated total reflectance
cDNA- complementary deoxyribonucleic acid
CE-MS – Cappilary electrophoresis mass spectrometry
DFA- discriminant function analysis
DGDG – digalactosyldiacylglycerol
DI-MS- direct injection mass spectrometry
DNA- deoxyribonucleic acid
DP- degree of polymerization
EI- electron impact
ESI- electrospray ionisation
FA- fatty acid
FAD- flavin adenine dinucleotide
FT-ICR-MS- Fourier-transform ion cyclotron resonance mass spectrometry
FT-IR- Fourier-transform infrared
GC-MS- Gas chromatography mass spectrometry
GOGAT- NADPH-dependent glutamine:2-oxoglutarate amidotransferase
GRIN – Genomic resources Information network
GSH- glutathione
HATS- High-affinity transport system
HPAEC – High pH anion exchange chromatography
HPLC- High peformance liquid chromatography
LATS-Low-affinity transport system
LC-MS – Liquid chromatography mass spectrometry
MGDG – monogalactosyldiacylglycerol
MIAME- minimum information about a microarray experient

MIAMET- minimum information about a metabolomics experiment
mRNA- messenger ribonucleic acid
MS- mass spectrometry
MSI- Metabolomics standard initiative
MSTFA – N-methyl-N-(trimethylsilyl)-trifluoroacetamide
NAD+ - Nicotinamide adenine dinucleotide
NADH- Nicotinamide adenine dinucleotide
NADP+- Nicotinamide adenine dinucleotide phosphate
NADPH - Nicotinamide adenine dinucleotide phosphate
NCBI – National Center for biotechnology information
NIST- National Institute of Standards and Technology
NMR- Nuclear magnetic resonance
NUE – nitrogen use efficiency
PAR – Photosynthetically active radiation
PCA- principal component analysis
PCR- polymerase chain reaction
PEDRo- Proteomics experimental database repository
PEG – Polyethylene glycol
PEP- phosphoenolpyruvate
PEPCase- phosphoenolpyruvate carboxylase
PFK – phospfructokinase
PFP- pyrophosphate:fructose 6-phosphate 1phosphotransferase
Ppm – parts per million
PTV – programmable temperature vaporising
QTL – quantitative trait loci
RNA- ribonucleic acid
ROS- reactive oxygen species
RT-PCR- reverse transcriptase polymerase chain reaction
RWC – Relative water content
SIC – selected ion chromatogram
SMRS- standard metabolic reporting structure
SSH- Supression subtractive hybridization
TF- transcription factor
TOF- time of flight
UDP- uridine diphosphate
USDA- United States Department of Agriculture

UTP- uridine triphosphate

UV – Ultraviolet

VLCFA – very-long-chain fatty acids

Chapter 1

Introduction

1.1 Metabolomics

Developments in the field of genomics, which relates to the study of the genomes of organisms, have allowed the sequencing of a large number of genes whose function is yet undetermined. Therefore, systematic and comprehensive approaches aimed at elucidating the functions of genes have began to attract some significantly more attention (Trethewey *et al.*, 1999; Fiehn, 2002; Saito *et al.*, 2004; Bino *et al*., 2004). Studies of the transcriptome and proteome, which correspond to the collection of the transcripts and proteins, respectively, present in an organism, have been used in functional genetics approaches which attempt to identify the functions of genes. However, these approaches have their own limitations, and do not provide complete information on how changes in the levels of mRNA or the proteins influence biochemical pathways (Trethewey 1999). A change in the levels of mRNA cannot be used to predict reliably the change in the levels of proteins, and similarly, the levels of proteins in the cell do not necessarily correlate with their putative activity (Trethewey 1999). Thus the emergence of metabolomics as a methodology may aid functional genomics studies by providing additional information about gene functions, particularly with respect with their involvement in the metabolism.

1.1.1 A recent history

Metabolomics is one of the most recent fields in functional genomics. The term was coined recently by Oliver *et al*.(1998) and refers to the study of the metabolome, which is the qualitative and quantitative collection of all the metabolites present in a cell (Oliver *et al.*,

1998). Since then, there has been a growing interest in all life sciences and in particular plant sciences (Fiehn *et al*., 2002; Shulaev *et al*., 2008; Guy 2008). This can be illustrated by the increase of the number of publications per year in the field (Figure 1.1).

The application of metabolomics to many plant biological studies is diverse in focus, ranging from biotic and abiotic stress response studies including, for example, disease resistance (Dixon, 2001), drought tolerance and temperature tolerance (Rhizky *et al*., 2004), evaluations of effects of food processing in the nutritional value of tomatoes (Capanoglu *et al*., 2008), to the taxonomic discrimination between species (Frederich *et al*., 2004). By its very nature, the use of metabolomics in functional genomics may have some advantages over the study of the complementary proteome and transcriptome. Quantitative changes in individual enzymes often result in small effects on metabolic fluxes, however, they can be responsible for significant changes on the absolute levels of numerous metabolites (Goodacre *et al*., 2004).

Additionally, the metabolome is a 'downstream' result of gene expression and protein activity. Therefore, the changes in the metabolome are expected to be amplified, reflecting more accurately the metabolic status of the cell (Goodacre *et al*., 2004; Bino *et al*., 2004). Unlike proteins and RNA sequences which show inter-specific variation, the nature of a particular metabolite remains the same regardless of the organism in which it is found. This characteristic allows the detection of common metabolic pathways between different species and has underwritten the explosion in metabolomic efforts such as the ever-expanding databases.

Some of the databases used in metabolomics can be categorised as reference spectral databases, compound- and species-specific metabolite profile databases and metabolic pathway databases (Go, 2010). The reference spectral databases, such as the NIST (national institute of standards and technology) mass spectral libraries or the Golm metabolome database (GMD) (Kopka *et al.*, 2005), include a mass spectral archive of standard compounds and may also include information about retention times and experimental methods used to generate the respective spectra.

A notable example of a species-specific metabolite profile database include the human metabolome database (www.hmdb.ca), which contains a curated collection of human metabolites and human metabolism data (Wishart *et al*., 2007). Similarly, the Lipid MAPS structure database constitutes a prime example of a compound-specific database, which includes information about the chemical structure and formula of lipids (Go, 2010).

Among the metabolic pathway databases it is possible to include the Kyoto Encyclopedia of Genes and Genomes (KEGG) (http://www.genome.jp/kegg/), which provides information about metabolic and regulatory pathways, protein-protein interactions, genes of completely and partially sequenced genomes, glycans, small molecules and reactions (Go, 2010). Furthermore, MetaCyc (http://metacyc.org) and AraCyc (http//Arabidopsis.org/tools/aracyc) are metabolic pathway databases derived from experimental data and provide a general database for metabolism in a variety of organisms and a species-specific database for *Arabidopsis,* respectively, that contain curated metabolism data (Zhang *et al*., 2005).

1.1.2 Standardization efforts in metabolomics and metabolic databases

Although reference databases of chemical information and ontology already existed to support the nascent metabolomic studies ten years ago (for example, NIST mass spectral libraries, www.nist.gov), there was a lack of databases which would describe the metabolite complement in their experimental context (Jenkins *et al.*, 2004). However, at present notable examples of an open access database for plant metabolomic-related information exist such as the GMD (Kopka *et al.*, 2005). The significant amount of information generated by functional genomics technologies can be an important source of information, as long as data is shared and made available in convenient and supportive ways for statistical analysis. In order to do this, well designed data standards are required. These have already been developed for transcriptomic (MIAME) (Brazma *et al.*, 2001) and proteomics studies (PEDRo) (Taylor *et al.*, 2003). These data reporting standards include information such as checklists, outlining of the minimal information content that should be provided, common syntax, defining the transmission formats that facilitate the exchange of information, and common semantics which add an interpretative layer to the data (Fiehn *et al.*, 2007).

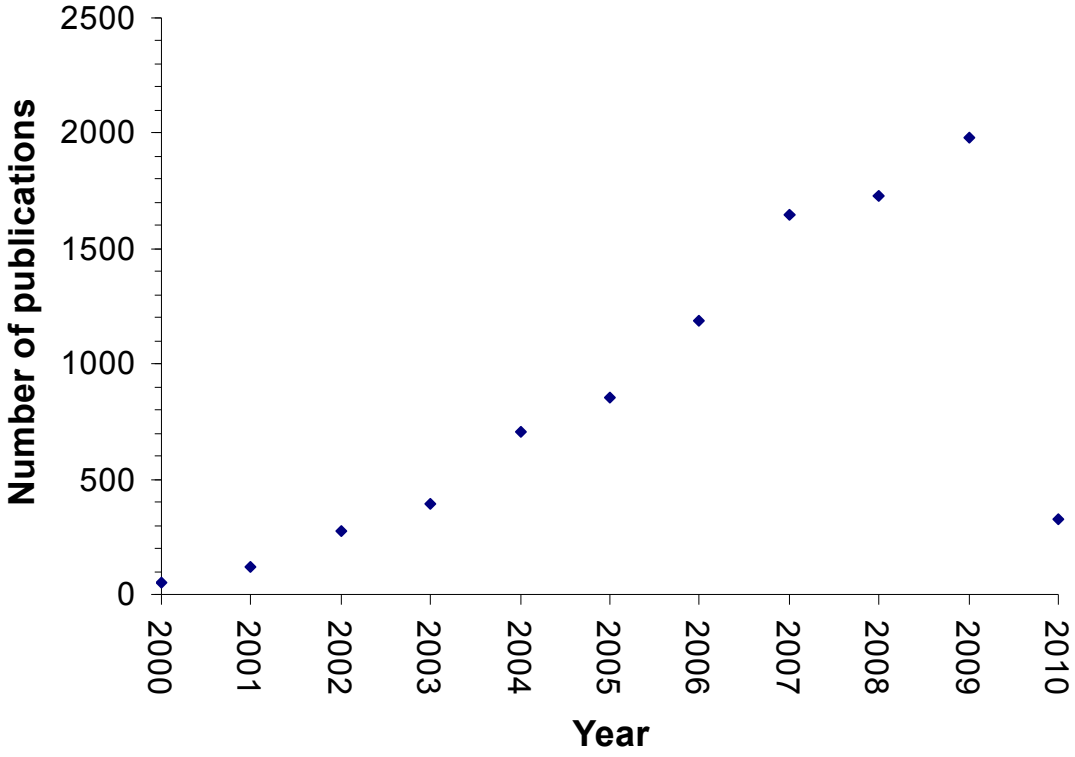

Figure 1.1 – Number of plant related peer-refereed journal articles by year of publication as retrieved from Scholar.Google using the Boolean search string [plant AND metabolomics] on 8th of March of 2010

The efforts taken to standardize data reporting in metabolomics date back to 2001, when a consortium using proton-Nuclear Magnetic Resonance (^{1}H-NMR) metabolomics (metabonomic) to assess toxicity started generating databases spectra of body fluids from animal models (Lindon *et al.*, 2005). The collaborative work, over several institutions, demanded exchange of information in common formats which eventually led to the formation of the SMRS (Standard Metabolic Reporting Structure) initiative in 2003 (Lindon *et al*., 2005). Simultaneously, a plant-focused consortium was working on a data model to provide a basis for data exchange and storage called Architecture for

Metabolomics (ArMet). These two efforts provided to be complementary, since ArMet focused on the conceptual framework of metabolomic data organization and its supporting information, whereas the SRMS initiative developed detailed recommendations of the parameters and data to be reported (Fiehn *et al.*, 2007).

In 2005, participants from both institutions joined efforts along with further interested scientists and formed the Metabolomics Standards Initiative (MSI) (Fiehn *et al.*, 2007). Subsequently, a recent small-scale study has been used to illustrate how metadata can be reported while fulfilling the MSI reporting standards (Fiehn *et al*., 2008).

1.2 Different approaches in metabolic studies

In order to study the metabolome, or part of it, two fundamentally different approaches exist: (i) targeted analysis and (ii) untargeted analysis.

Targeted analysis is the most developed approach in metabolic studies and aims to detect and quantify a limited number of metabolites. This is a quantitative approach in which it is necessary to know the structure of the target metabolites and to have developed analytical methods in order to determine their concentration in the samples (Shulaev, 2006). For example, targeted analysis approaches have been used to study terpenoids (Opitz *et al.*, 2008), amino acids (Thornton *et al*., 2007) and water soluble carbohydrates (Pavis *et al.*, 2001).

The main limitation of targeted analysis, however, is that it does not provide any information about the untargeted, potential pathway-related, metabolites which can be

relevant for a particular response (Shulaev, 2006). The introduction of bias by using protocols optimized for extracting particular groups of compounds while excluding others goes against the 'omics' concept of ´metabolomics´ which attempts to quantify and identify the entire metabolite complement. Nevertheless, the quantitative information provided by this approach is invaluable and enriches the knowledge obtained from the more global, but at best semi-quantitative, untargeted approaches.

Within the untargeted approaches, distinction should be made between two types of approach: metabolite profiling and metabolite fingerprinting (Nielsen and Oliver, 2005). Metabolite fingerprinting does not attempt to identify or quantify the metabolites present in a sample. Instead, it focuses on the pattern recognition of the total metabolite profile. Multivariate pattern recognition tools, such as principal component analysis (PCA) or discriminant function analysis (DFA), are used to identify features of the profile and differentiate two different samples (Nielsen and Oliver, 2005).

The usefulness of metabolic fingerprinting has usually been associated with biomarker discovery and disease diagnosis **(**Yang *et al*., 2004; Choi *et al*., 2004). Data acquisition is commonly obtained with NMR (Choi *et al*., 2004), Fourier transform infrared spectroscopy (FT-IR) (Gidman *et al*., 2003) or Fourier transform ion cyclotron resonance mass spectrometry (FT-ICR-MS) (Oikawa *et al*., 2006).

Despite the global, unbiased nature of this approach, the metabolites are not necessarily identified or absolutely quantified. Therefore, conclusions about metabolic pathways involved are limited. Nevertheless, metabolic fingerprinting has been used successfully to discriminate different plant ecotypes (Ward *et al.*, 2003), elucidate metabolic responses of

plants following physical wounding (Boccard *et al.*, 2007) and in the discrimination of human serum samples between healthy and diseased individuals (Yang *et al.*, 2004). An extension of metabolite fingerprinting is metabolite footprinting where the target of analysis is the media in which the organism is grown. This approach allows monitoring of metabolites taken up and secreted by the organism. Using the same principles as metabolite fingerprinting, it is possible to distinguish two different metabolic states of an organism by using pattern recognition tools (Kell *et al.*, 2005).

Unlike metabolite fingerprinting, metabolite profiling seeks to measure the concentrations of the metabolite complement in a sample. This approach makes no assumptions on the metabolites likely to be encountered. Thus, it aims to be have a global unbiased quantitative nature (Shulaev, 2006). Metabolite profiling has experienced an increase in applications within the field of functional genomics in the past 10 years. It has been postulated that metabolite profiling could aid the identification of gene functions, even in situations where a macroscopic response is not observed (Oliver *et al.*, 1998). In 2001, Raamsdonk *et al.* developed a methodology called **F**unction **AN**alysis of **C**o-response in **Y**east (FANCY) which uses metabolite profiling data to reveal the site within a metabolic network where a silenced gene is involved (Raamsdonk *et al.*, 2001).

In plants, the use of metabolomics has also been applied to aid the functional characterization of silent phenotypes. For example, Weckwerth *et al.*, (2004a) used Gas-Chromatography (GC) coupled to MS to characterize a potato line suppressed in expression of sucrose synthase 2 (SS2) while displaying a silent phenotype. The authors were able to

detect metabolic differences between SS2 suppressed lines and wild type lines, mainly with respect to the amino acid and carbohydrate metabolism (Weckwerth *et al.*, 2004a).

The response of plants to the environment is often monitored in order to understand the biochemical mechanisms involved. For instance, Kaplan *et al.* (2004) used a metabolite profiling approach coupled with induced variation in the ambient temperature, which allowed researchers to obtain an overview of the acclimation processes in the plant. This study resulted in the identification of several potential metabolic targets, such as sugar signalling processes, which were suggested to pave the way for further studies (Kaplan *et al.*, 2004). Environmental variations and genetic induced changes have been extensively studied in a similar fashion and will be discussed in more detail later in this chapter.

In order to perform metabolite profiling, there are several analytical platforms available. The most widely used are NMR, chromatography-based mass spectrometry (such as GC-MS, liquid chromatography MS [LC-MS]) and capillary-electrophoresis mass spectrometry (CE-MS). Each platform has advantages and drawbacks, which will be discussed in detail below, but a combination of these techniques generally allows complementation of data, thus, making it a very powerful approach (Nielsen and Oliver, 2005;Shulaev, 2006).

1.3 Experimental and analytical methodologies for metabolic studies

The metabolome has a dynamic nature, which by definition changes over time. In order to obtain a representative snapshot of the metabolic state of the cell, it is critical for metabolic studies to stop all the cellular processes at the time of sampling. In the same way as in transcriptomic and proteomics studies, samples should be flash-frozen in liquid nitrogen

and subsequently stored at -80ºC (Dunn and Ellis, 2005). The metabolite extraction method is the key determinant regarding metabolome coverage. Additionally, it may provide ways of inactivating enzymes, which could promote degradation or inter-conversion of metabolites (Shulaev, 2006). In targeted analysis, extraction protocols are often designed to purify particular chemical classes of metabolites such as sugars or amino-acids. However, in metabolite profiling approaches, the extraction procedure attempts to retain as much information as possible. The development of universal, robust and reproducible sampling and sample preparation methods that are not biased towards chemical classes will remain a challenge unlikely ever to be solved (Dunn and Ellis, 2005). While attempting to purify one compound, other unrelated compounds can inevitably be destroyed or excluded. Therefore, researchers should adapt their methodology according to the analytical platform being used and to the range of metabolites being studied (Shulaev, 2006).

1.3.1 Fourier-transform infra-red spectroscopy

Fourier transform infra-red spectroscopy analysis (FT-IR) is often used in metabolite fingerprinting approaches. FT-IR is a rapid, normally non-destructive technique that invariably does not require reagents and ultimately allows high-throughput analysis (Dunn and Ellis, 2005). This analytical technique is based on the irradiation of samples with electromagnetic radiation in the range of infra-red wavenumber (4000-670 cm^{-1}). Chemical bonds absorb the radiation and vibrate in a variety of ways. Depending on the compound chemical configuration, specific wavelengths are absorbed. For example, vibrations from CH_2 and CH_3 groups which are normally associated with fatty acids are absorbed in the

range of 3050-2800 cm^{-1} (Dunn and Ellis, 2005). As a consequence, peaks in the spectrum generally correspond to a compound class rather than an identified metabolite. In FT-IR all of the infrared frequencies are measured simultaneously resulting in a signal called interferogram. Because the interferogram data cannot be directly interpreted, a fourier transform is applied which will generate a frequency spectrum (conversion of time-domain into frequency-domain). However, FT-IR provides a wide range of analyte detection simultaneously (for example, carbohydrates, amino acids, lipids and polyphenolics), hence it is used in metabolite fingerprinting approaches. For example, Kim *et al*. (2009) has used an FT-IR based fingerprinting approach combined with multivariate statistical analysis to discriminate between the leaf tissues of five different strawberry cultivars. Additionally, the authors extended their approach to the fruit tissue and achieved a similar separation between cultivars (Kim *et al.*, 2009).

1.3.2 Nuclear Magnetic Resonance

Nuclear magnetic resonance spectroscopy (NMR) allows the detection of molecules containing one or more atoms with a non-zero magnetic moment, which include ^{1}H, ^{13}C, ^{14}N, ^{15}N and ^{31}P (Krishnan *et al.*, 2005). All the main metabolites include at least one NMR signal, which is characterized by their frequency (chemical shift), intensity and magnetic relaxation properties (Krishnan *et al.*, 2005) and these depend on the chemical environment that the specific nucleus occupies. The magnetic relaxation from an upper (excited) to a lower state (relaxed) is accompanied by a release of energy in the radio frequency range, which is detected and converted in the visualisations referred to as NMR spectra. In most

metabolic studies the instruments used operate in the 300-600MHz range (Krishnan *et al.*, 2005). The different regions of the NMR spectrum correspond to different chemical environments. For example, the proton associated with the α-carbon in alanine has a chemical shift of 3.76 ppm (parts per million) whereas the protons associated with the β-carbon have a resonance of 1.46 ppm (Berliner and Reuben, 1992, pp. 5). NMR based on ^{1}H or ^{13}C allows the identification and quantification of a wide range of organic compounds, providing a valuable tool in metabolomics. For example, NMR-based methods have been applied to the metabolite fingerprinting of *Arabidopsis* (Ward *et al.*, 2003), metabolite profiling in *Papaver somniferum* (Hagel *et al.*, 2008) and metabolic flux analysis in *Linum usitatissimum* (Troufflard *et al.*, 2007). NMR can be a non-destructive method, requiring minimal sample preparation methodologies, thus allowing the analysis of metabolite changes *in vivo* (Ratcliffe, 1997).

The NMR spectra obtained often contains several peaks derived from a single compound, which provides valuable structural information. However, the presence of complex mixtures of metabolites in biological samples generally results in peak overlapping. Consequently, the process of metabolite identification and quantification, particularly in ^{1}H-NMR, becomes a laborious and difficult task (Shulaev, 2006). Therefore, NMR data is commonly combined with multivariate analysis tools in metabolic fingerprinting approaches (Defernez and Colquhoun, 2003).

However, when compared to mass spectrometry based approaches, NMR spectroscopic approaches have a major drawback. The lower sensitivity of NMR restricts the quantification to the most abundant compounds or classes of compounds (Lenz *et al.*, 2004;

Krishnan *et al.*, 2005; Shulaev, 2006). Despite the usefulness of NMR spectroscopy in targeted approaches and in metabolite fingerprinting, it has a more limited use in metabolite profiling approaches and in plants is generally confined to primary metabolism studies. Nevertheless, the ability to provide insights into the structure of metabolites and changes in the predominant metabolites makes this technique invaluable in solving one of the major bottlenecks in metabolite profiling (Kopka *et al.*, 2004).

1.3.3 Mass spectrometry

Mass spectrometry has become one, if not the main analytical platform used in metabolomic studies due to its high sensitivity and to the wide range of analyte coverage. This technique relies on the ionization of chemical compounds to generate charged molecules or molecule fragments and subsequently measure their mass-to-charge ratio (m/z), which may allow the elucidation of the chemical structure and/or thr elemental composition of molecules.

Direct Injection MS (DI-MS) has been used as a high-throughput approach for a analyzing a wide range of samples (Kaderbhai *et al.*, 2003; Stewart 2007; McDougall *et al.*, 2008). Relatively crude sample extracts are injected and experience electrospray ionization, which results in a single mass spectrum representing the sample metabolite composition in total, or at least the ionisable components. This allows for a very high-throughput sample analysis. However, when several compounds with low ionization efficiencies are being analyzed, their signal can be misrepresented or under-represented in the mass spectrum due to a phenomenon known as co-suppression (Dunn and Ellis, 2005). Furthermore, the

identification of metabolites is often hindered by the overlapping of mass peaks. The different mass peaks may result from several metabolites and/or their mass fragments.

Fourier-transform ion cyclotron resonance coupled to a powerful MS (FT-ICR-MS) may overcome this limitation by providing high resolving power and high mass accuracy (Dunn and Ellis, 2005). Due to the high number of mass peaks obtained, this technique has been mostly used in metabolic profiling approaches, including the clarification of herbicide inhibiting pathways in *Arabidopsis thaliana* (Oikawa *et al.*, 2006), and the discrimination of development stages in strawberry fruit (Aharoni *et al.*, 2002). More recently, this technique was used to monitor the presence of endophyte-infection associated metabolites in perennial ryegrass cut leaf fluids and guttation fluids (Koulman *et al.*, 2007). This study revealed for the first time the mobilization of fungal alkaloids into the host plant in grass-endophyte associations (Koulman *et al.*, 2007).

Conversely, this technique cannot distinguish between isomers and enantiomers, due to their identical molecular masses (Kopka *et al*., 2004), although some insight into isomer presence can be gained from the relative proportion of the known mass fragments . In order to avoid this problem mass spectrometers are often coupled with separation techniques such as gas chromatography (GC-MS) and liquid chromatography (LC-MS) or even with electrophoretic separation (capillary electrophoresis mass spectrometry, CE-MS) (Shulaev, 2006).

1.3.3.1 Mass spectrometry coupled to gas-chromatography

The extensive use of GC-MS, particularly in plant metabolite profiling approaches, ranges from profiling leaf extracts of four genetically different lines of *Arabidopsis thaliana* (Fiehn *et al.*, 2000), mapping quantitative fruit metabolic loci in *Solanum lycopersicum* (Schauer *et al*., 2006), studying boron toxicity effects of the metabolism of *Hordeum vulgare* (Roessner *et al*., 2006), to comparisons of leaf extracts from *Lolium perenne* differentially exposed to nitrogen supply, carbohydrate supply and fungal endophyte infection (Rasmussen *et al.*, 2008). Unless the study is only focused on volatile compounds, the samples generally require extraction and derivatization steps to ensure that the metabolites become volatile over the GC operating range, usually 100-320ºC. This requirement for volatility comes at a cost, restricting the number of metabolites in the extract amenable to analysis. In other words, larger metabolites often generate derivatives with molecular mass outside the detector range (between m/z 650-1000), thereby limiting or negating volatility and passage through the GC column (Halket *et al.*, 2005).

GC can separate compounds with mass spectral similarities (for example, enantiomers and isomers), while the mass spectrum provides fragmentation patterns specific for particular compounds and chemical classes. Therefore, it allows the differentiation of co-eluting chemically diverse compounds (Kopka *et al.*, 2004). This method is capable of detecting simultaneously several hundred different chemical compounds, including organic acids, sugars, sugar alcohols, most amino acids, fatty acids and aromatic amines (Shulaev, 2006). As stated above, volatile low molecular weight metabolites can be readily analysed in GC-MS, however non-volatile metabolites require derivatization to provide volatility and

thermal stability allowing prior to MS analysis (Dunn and Ellis, 2005). The most common method of derivatization employs silylating agents (Kopka *et al.*, 2004) in a two-stage reaction. First, where necessary, carbonyl functional groups are oximated (C=O → C=N-OH) followed by replacement of exchangeable protons with trimethylsilyl (TMS) groups (Dunn and Ellis, 2005).

Upon chromatographic separation through the GC, metabolites are usually ionized by electron impact (EI) which is a reproducible approach that does not suffer ion suppression effects (Kopka *et al.*, 2004). Detection is usually performed with either single, triple or quadrupole detectors, ion trap detectors or time of flight detectors (TOF) (Kopka *et al.*, 2004).

The identification of the eluting peaks involves comparing the retention indexes (or retention times) and the mass spectrum with pure compound standards previously analysed under the same experimental conditions (Dunn and Ellis, 2005). However, the GC-MS output derived from complex biological samples often reveals a high number of unknown metabolites with no comparative standards available (Kopka *et al.*, 2004). In general, the mass spectrum can be compared with readily available MS databases containing hundreds of thousands of compounds (for example, the NIST mass spectral library). Most of these databases, however, are not specific for natural occurring metabolites and contain a significant number of synthetic products, since they were predominantly prepared to service the pharmaceutical industry (Shulaev, 2006). Therefore, the development of mass spectral databases specific for natural occurring compounds could eventually help to solve one of the major bottlenecks in metabolite profiling.

1.3.3.2 Mass spectrometry coupled to liquid-chromatography

LC-MS takes advantage of the high-separating power of liquid chromatography, which allows the study of high molecular weight metabolites that cannot be analyzed by GC-MS (Kopka *et al.*, 2004). Since the chromatography does not require the volatilization of metabolites, sample preparation for LC-MS is in general less complex and allows a wider range of analyte polarity and mass (Halket *et al.*, 2005). Following chromatographic separation, metabolites are introduced into the mass spectrometer and experience a soft ionization method such as electrospray ionization (ESI) or atmospheric pressure chemical ionization (APCI). ESI instrumentation operates in positive and negative modes, detecting metabolites which are ionized by protonation (ESI+) or deprotonation (ESI-). Metabolites usually ionise much more efficiently in one mode compared to the other, so by monitoring both modes it is possible to obtain a wider coverage of the metabolome (Dunn and Ellis, 2005). However, the identification of unknown metabolites is hindered due to the lack of transferable mass spectral libraries (Shulaev, 2006). Structural information can be obtained by tandem MS (MS/MS), which induces collision-induced dissociation. The resulting fragmentation pattern can then be compared with fragmentation databases of known compounds (Kopka et al., 2004). In contrast with GC-MS databases, these are much less populated. Nevertheless, the structural information provided by the fragmentation pattern may aid the characterization and identification of unknown metabolites (Shulaev, 2006).

LC-MS has been used in targeted approaches, mainly secondary metabolites, such as monitoring isoprenoid biosynthesis in peppermint oil gland secretory cells (Lange *et al.*,

2001), profiling of seed dormancy and germination related hormones in lettuce (Chiwocha *et al.*, 2003), assessing glycoalkaloid profiles in transgenic field-grown potatoes (Zywicki *et al*., 2005), chemical discrimination of two different species from the genus *Opuntia* (Kim and Park, 2009) to list just four examples. The range of metabolites detected by LC-MS, both with respect to structure and molecular mass, provide a very valuable feature for metabolite profiling and could be especially powerful when used to complement GC-MS data (Kopka *et al.*, 2004).

1.3.3.3 Mass spectrometry coupled to capillary-electrophoresis

Capillary-electrophoresis (CE) MS provides some advantages over the other established separating techniques such as GC-MS and LC-MS. This method allows the separation of uncharged compounds, cations and anions in a single analytical run without requiring sample derivatization. Additionally, the sample preparation is quick and common to all types of metabolites which, allied to minimal sample amount requirements (1-20 nL) makes this a very promising technique for high-throughput untargeted approaches (Saito *et al*., 2004; Monton and Soga, 2007; Timerbaev, 2009). However, the reproducibility of retentions times (and hence retention indexes) obtained, in addition to the lack of available commercial libraries limits the current use of this technique (Shulaev, 2006).

At present there is no single procedure able to quantify and identify the entire range of the metabolite complement. Each analytical method has their advantages and disadvantages (Table 1.1) and bias is introduced during extraction procedures, sample preparation and ultimately by the analytical method chosen. Therefore, screening the entire metabolome is a

Table 1.1 – Summary of the advantages and disadvantages of each analytical platform used in metabolomics (Shulaev, 2006).

Analytical method	Advantages	Disadvantages
GC/MS	- Sensitive - Robust - Large linear range - Large commercial and public libraries	- Slow - Often requires derivatisation - Many analytes thermally-unstable or too large for analysis
LC/MS	- No derivatisation required - Many modes of separation available - Large sample capacity	- Slow - Limited commercial libraries
CE/MS	- High separation power - Small sample requirements - Rapid analysis - Can analyze neutrals, anions and cations in a single run - No derivatization	- Limited commercial libraries - Poor retention time reproducibility
NMR	- Rapid analysis - High resolution - No derivatization required - Non- destructive	- Low sensitivity - Convoluted spectra - More than one peak per component - Libraries of limited use due to complex matrix
FT-IR	- Rapid analysis - Complete fingerprint of sample chemical composition - No derivatization needed	- Extremely convoluted spectra - More than one peak per component - Metabolite identification impossible - Requires sample drying

difficult task. The complementation of some of the techniques described above suggests that their combination is the most powerful and utilitarian approach towards the analysis of the entire metabolome.

1.4 Plant stress and metabolomics

In order to understand the function of genes, functional genomic approaches often introduce changes into the environment or in the genetic profile (for example gene deletions or over-expression of genes), and monitor the consequent response of the transcriptome, proteome or metabolome (Ideker *et al.*, 2001; Raamsdonk *et al.*, 2001; Thornton *et al.*, 2007). These approaches seek to understand the mechanisms involved in the response and identify the functions of the expressed genes. Metabolomics as a tool for functional genomic studies is a particular comprehensive approach for studying any potential metabolic pathways involved. In plant sciences, it is used to study transgenic plants (Zywicki *et al.*, 2005), establish the basis of difference between plant varieties (Dobson *et al.*, 2010) and for functional approaches regarding response of plants to environmental stresses (Johnson *et al.*, 2003; Kaplan *et al.*, 2004; Last *et al.*, 2007).

Environmental stresses are the result of conditions which hamper the optimal growth and development of organisms (Shulaev *et al.*, 2008). These can be classified according to their origin as either biotic or abiotic stresses. Biotic stresses are the result of biological interactions with competing organisms, predators, pathogens or parasites while abiotic stresses (non-biological) are caused by non-optimal levels of the physical components in

the environment (Kaplan *et al.*, 2004). Stresses from different origins can often result in similar consequences for the cell. For instance, oxidative damage may result from a wide range of stresses such as drought, pathogen attacks and high concentrations of heavy metals in the environment (Mittler, 2002). Since plants are sessile organisms and have only limited mechanisms for stress avoidance, their survival depends on acquired tolerance mechanisms (Schutzendubel and Polle, 2002). These mechanisms are responsible for overall improved stress tolerance, which may allow the plants to survive and recover from unfavorable conditions. Many metabolites, such as compatible solutes like trehalose, proline and fructans which may accumulate in the cell to relatively high levels without resulting in toxic effects (Chen and Murata, 2002), have been reported to increase cell tolerance to a multitude of stresses (Vinocur and Altman, 2005). Therefore, components of the metabolome may have a crucial role in the acquired tolerance mechanisms, and these can be monitored simultaneously by metabolomics approaches.

1.4.1 Biotic stresses

Bbiotic stress resistance is often associated with secondary metabolite production (Kutchan, 2001). Most of these metabolites are derived from isoprenoid, phenylpropanoid, alkaloid or fatty acid pathways and represent a significant energy commitment by the plant (Dixon, 2001). Nevertheless, these classes of secondary metabolites are generally regarded as important effectors of the response to biotic stress (Dixon, 2001; Shah, 2005).

1.4.1.1 Response to pathogens

The presence of plant secondary metabolites with anti-microbial activities is well documented and it is generally assumed that they are synthesized to confer resistance against microbe attacks (Wallace, 2004). Different classes of compounds have been associated with response to pathogens, such as indole and indole-sulfur compounds (Glazebrook and Ausubel, 1994), gluconisolates (Li *et al*., 2000; Tierens *et al*., 2001; Wittstock *et al*., 2003) and phenylpropanoid-polyamine conjugates (Kaur *et al*., 2010). Related plant families usually rely on structurally similar metabolites for defence, such as accumulation of isoflavonoids in Leguminosae and sesquiterpenes in Solanaceae (Dixon, 2001). However, some groups of metabolites such as terpene derivatives have been reported to accumulate in a wider range of species (Dixon, 2001). The ability of plants to respond to infection and synthesize anti-pathogen metabolites can be illustrated by a few targeted metabolic profiling studies, which have successfully provided discrimination between infected and healthy plants. For example, the infection of *Cataranthus roseus* (Madagascar periwinkle) with ten types of phytoplasmas was followed by NMR analysis of the corresponding leaf material (Choi *et al*., 2004). Multivariate analysis revealed a segregation of the phytoplasma-infected tissue from the uninfected material. The authors observed an increase in NMR signals associated with metabolites from phenylpropanoid or terpenoid indole alkaloid biosynthetic pathways, and these drove the differences in the PCA between control and infected plants (Choi *et al*., 2004).

1.4.1.2 Response to mechanical wounding

Mechanical wounding, which can be caused by herbivore attacks (for example biting arthropods and grazing animals), may provide potential infection sites for pathogens (Reymond *et al*., 2000). Therefore, plants have developed appropriate metabolic responses to provide a barrier against opportunistic microorganisms (Reymond *et al.*, 2000). Upon mechanical wounding *Cataranthus roseus* seedlings were reported to accumulate monoterpenoid alkaloids, which have also been reported to accumulate in response to phytoplasma infection (Vasquez-Flota *et al.*, 2004).

A study was carried out in *Gossypium hirsutum* (cotton) plants to study the response to mechanical damage, herbivory attacks by *Spodoptera littoralis* and jasmonic acid treatments (Opitz *et al.*, 2008). Terpenoid levels were increased successively from control to mechanical damage, herbivory and jasmonic acid treatments. Since the relative levels of the terpenoid products were not substantially different among the treatments, the authors suggested that the induction of terpenoid biosynthesis in cotton is a non-specific wound response mediated by jasmonic acid (Opitz *et al.*, 2008).

Besides terpenoid products, glucosinolates and their hydrolysis products have also been widely studied for their role in plant defense against generalist insect herbivore species and may function as feeding deterrents, being toxic to unadapted species (Li *et al.*, 2000).

An alternative strategy that plants may use includes the production of volatile compounds which attract predators of insect herbivores (Mercke *et al.*, 2004). A combined transcriptomic and metabolomic approach was used to study the production of volatile

compounds in cucumber plants as response to spider mite infection. These results revealed an increase in volatile compounds such as (E,E)-α-farnesene (sesquiterpene) which is known to attract carnivorous arthropods (Mercke *et al.*, 2004).

Furthermore, mechanical damage in food crops during harvest and subsequent handling may be detrimental for product quality (Strehmel *et al*., 2010). A metabolite profiling approach was used to study the time-course effect of mechanical damage in potato tubers on the primary metabolism (Strehmel *et al*., 2010). The authors observed characteristic changes in central metabolism and parts of the amino acid metabolism but not in the levels of phenylalanine and tyrosine (Strehmel *et al*., 2010).

1.4.2 Abiotic stress

In their natural environment, plants may have to endure unfavorable conditions such as flood/drought, high temperature and nutrient shortage. These conditions are caused by physical properties of the environment and are classified as abiotic stresses. Abiotic stresses may restrain growth and development at the tissue or whole plant level, and may ultimately lead to plant death (Chen and Murata, 2002). One of the mechanisms which plants employ to cope with abiotic stress is the accumulation of compatible solutes. These are small neutral molecules which can accumulate at high concentrations without resulting in a toxic effect (Valliyodan and Nguyen, 2006). The range of compatible solutes varies across plant species and can include sugars, polyalcohols and amino acids (Chen and Murata, 2002). Hence, the metabolism plays an important role in abiotic stress response and monitoring it, through the use of metabolomic approaches, may result in the discovery of important

mechanisms of acquired stress tolerance, which can be exploited to generate crops with greater endurance properties in a changing climate.

1.4.2.1 Water and salt stress

Water limitation is currently one of the major factors affecting plant productivity in the world (Chaves *et al.*, 2009). In plants, water limitation may arise through simple drought or by increasing salinity of the medium, consequentially increasing the osmotic potential with a decreased water uptake (Sanchez *et al.*, 2008). Metabolomic approaches have been previously used to study the response of higher plants to salt-induced stress.

An early study used metabolic fingerprinting approaches to study the salt stress response in tomato (Johnson *et al*., 2003). Whole fruit flesh extracts of two tomato varieties, Edkawy and Simge F1, exhibiting differential salinity tolerance, were fingerprinted by using FT-IR spectroscopy. Principal component analysis was unable to distinguish the control from salt-treated samples in any of the varieties. However, with subsequent discriminant function analysis (DFA) it was possible to discriminate salt-treated samples from the controls in both cultivars. Data mining of the DFA loading plots allowed the identification of regions in the FT-IR spectrum associated with salinity tolerance. These regions corresponded to saturated and unsaturated nitrile compounds, cyanide-containing compounds and other nitrogen containing compounds (Johnson *et al.*, 2003).

A combined transcriptomic and metabolomic approach was used to monitor the response to short term salt stress in both *Thellungiella halophyla* and *A. thaliana* (Gong *et al.*, 2005).

The metabolic profiles of the control samples differed greatly between both species. Before exposure of the plants to high salinity, fructose, glucose, sucrose and proline along with malic, succinic and citric acid were present in higher levels in *T. halophyla* compared to *A. thaliana*. This suggests that there was perhaps a constitutive adaptation mechanism in the halophile species since these metabolites have been previously associated with response to salinity. Upon stress exposure, glutamic acid, *myo*-inositol, raffinose and galactinol levels were relatively increased to a greater extent in *T. halophyla* than in *A. thaliana*, while phosphoric, aspartic, and fumaric acids were decreased in the halophile suggesting the involvement of these metabolites in the stress response (Gong *et al.*, 2005).

In *Lolium perenne* cv Bravo, a LC-based targeted metabolic approach combined with gene expression analysis was used to determine changes in the levels of water soluble carbohydrates in response to drought (Amiard *et al.*, 2003). The levels of long-chain fructans increased as a result of drought exposure. However, in this study the levels of raffinose, loliose (a galactosyl trissacharide structurally similar to raffinose), myo-inositol and galactinol were unaffected by drought exposure (Amiard *et al.*, 2003).

1.4.2.2 Temperature stress

The ability of plants to tolerate temperature stresses largely relies on acquired tolerance mechanisms (Guy *et al.*, 2007). Plants, which are exposed to non-lethal temperature stresses, may acquire enhanced tolerance to otherwise lethal stress conditions by a process termed acclimation (Kaplan *et al.*, 2004). It is well accepted that temperature acclimation

results from complex processes involving a number of physiological and biochemical responses (Kaplan *et al.*, 2004). The role of metabolites in such responses has been highlighted in several metabolomic studies.

A GC-MS based metabolite profiling approach was used to study the temporal dynamics associated with thermo-tolerance and chilling tolerance mechanisms in *A. thaliana* (Kaplan *et al.*, 2004). Cold-shock revealed extensively more changes in the metabolite profile than heat-shock. However, comparison of heat and cold-shock patterns revealed, for the first time, some similarities of the heat-and cold-shock responses. These patterns included increases in the levels of amino acids derived from pyruvate and oxaloacetate, polyamine precursors and compatible solutes (Kaplan *et al.*, 2004). A subsequent study attempted to combine metabolomic with transcriptomics data in order to understand the mechanisms involved in cold-acclimation in Arabidopsis (Kaplan *et al.*, 2007). Changes in the transcript abundance for many biochemical processes such as amino acid and soluble carbohydrate biosynthesis were observed. Correlations of the transcripts were found for some of the metabolic processes but not all of them. The authors concluded that the regulatory processes which are independent of transcript abundance, such as feedback regulation could play a crucial role in the metabolic adjustments involved in cold acclimation (Kaplan *et al.*, 2007).

1.4.2.3 Nutrient deficiency

Mineral nutrients that are required in large quantities by plants, often referred to as macronutrients, are essential for growth and productivity (Shin *et al.*, 2005). Nitrogen (N)

and Phosphorus (P) in particular are the most limiting mineral nutrients in crop production (Hammond and White, 2008) Therefore, metabolomic approaches have already been applied to the investigation of the metabolic response of a variety of plants to the different nutrient supply levels of N and P.

The response of common bean (*Phaseolus vulgaris*) roots under phosphorous deficient growth conditions was compared to phosphorus sufficient growth conditions with a combination of transcriptomic and metabolomic approaches (Hernandez *et al.*, 2007). Metabolite profiling was carried out using GC-TOF-MS, and the metabolite profiles revealed an overall increase in the levels of amino acids, polyols and sugars when plants were exposed to lower phosphorous concentrations. Additionally, several candidate genes have been identified that may contribute to the adaptation to phosphorous deficiency (Hernandez *et al.*, 2007).

In *Hordeum vulgare* L. (barley), a GC-MS based metabolite profiling was conducted with the aim of characterizing the metabolic response of plants exposed to phosphate-limiting growth conditions (Huang *et al.*, 2008). Under severe deficiency, the authors observed an increase in the levels of di- and trisaccharides, particularly in shoots while the levels of phosphorylated intermediates and organic acids were reduced. It was concluded that P-limited plants attempted to maintain essential cellular functions by salvaging inorganic phosphate (P_i) from a variety of P-containing metabolites and by modifying their carbohydrate metabolism in order to reduce P consumption. As a consequence, the levels of organic acids decreased due to a decrease in carbohydrate supply to the TCA cycle particularly in the roots (Huang *et al.*, 2008).

The consequence of different nitrate regimes in the metabolome of *Solanum lycopersicum* was evaluated by metabolite profiling (Urbanczyk-Wochniak and Fernie, 2005). Wild type tomatoes were grown under nitrogen controlled conditions supplied with media saturated, optimal or deficient in nitrate content. The metabolite profiles acquired by GC-MS appeared to be extensively influenced by the nitrate concentration. Under low nitrate concentrations a decrease in the levels of many organic and amino acids was observed while there was an increase in the levels of some carbohydrates and phosphoesters (Urbanczyk-Wochniak and Fernie, 2005).

Metabolite profiling of perennial ryegrass lines differing in their water soluble carbohydrate content was used to investigate their response to differential nitrogen supply (high concentration and control) (Rasmussen *et al.*, 2008). Leaf blades were analyzed by GC-MS and the metabolite profiles of samples supplied with high nitrogen content revealed an overall increase in the amino acid levels. The high nitrogen supply also caused a reduction in the levels of carbohydrates mainly due to their conversion, through glycolysis and citric acid cycles, into organic acids such as malic, succinic and citric acid. High levels of nitrogen were also reported to cause reduction in fibre content and increased lipid content (Rasmussen *et al.*, 2008).

1.4.2.4 Heavy metal stress

Toxic pollutants, such as heavy metals, are often accumulated in soils mainly as a result of exposure to human activities (Schutzendubel and Polle, 2002) and may have a significant

impact in the optimal development of plants. The influence of heavy metal pollutants in the metabolome has been studied in order to understand the mechanisms involved in response to toxicity/tolerance and/or study the potential use for soil remediation.

Plant cell extracts of *Silene cucubalus* (bladder campion) cell cultures were exposed to high cadmium (Cd) levels and analyzed by metabolic fingerprinting approaches (Bailey *et al*., 2003). The biochemical consequences of elevated Cd treated plants were analyzed by combined ^{1}H-NMR spectroscopy and PCA, and revealed relative increases in malic acid and acetate levels as well as decreases in the levels of glutamine and branched amino acids (Bailey *et al*., 2003).

Another example includes a combined approach using proteomics, ^{1}H-NMR metabolomics and biophysical analysis which was used to investigate the influence of potassium in the response of *A. thaliana* cells to caesium (Cs) exposure (Lay *et al*., 2006). This study revealed that under Cs stress, sugar metabolism and glycolytic pathways are affected depending on the potassium medium levels (Lay *et al*., 2006).

1.4.2.5 Combination of stresses

Usually, plant stress responses are studied using a reductionist approach, by applying a single stress condition. However, in the natural environment this seldom happens and plants are exposed to a combination of different stresses to varying degrees (Shulaev, 2008) with, for example, drought and temperature stresses often occuring simultaneously.

In *A. thaliana*, a multifactorial experiment was conducted to study the combination of drought and heat stress (Rizhsky *et al.*, 2004). The metabolite profiling approach revealed an accumulation of sucrose and other sugars such as maltose and gulose in plants exposed to stress conditions (Rizhsky *et al.*, 2004). However, the authors noted that proline, which was found to be accumulated under drought conditions, was not significantly increased in plants grown under a combination of stresses (Rizhsky *et al.*, 2004). Thus, it was concluded that a combination of drought and temperature stress imposes a different type of internal stress (as opposed to a single stress condition) which requires sucrose instead of proline as osmoprotectant (Rizhsky *et al.*, 2004).

However, the metabolic responses of plants to a wide range of stresses are often common. As described previously, alkaloids can be accumulated as result of pathogen attack (Choi *et al.*, 2004) and mechanical wounding (Vasquez-Flota *et al.*, 2004). Similarly, compatible solutes are often accumulated in response to water limitation (Amiard *et al.*, 2003), salinity (Gong *et al.*, 2005) and temperature stress (Kaplan *et al.*, 2004).

Nevertheless, responses to different types of stresses can often result in opposing differences in the levels of particular metabolites, as cited above (Rizhsky *et al.*, 2004). Therefore, the metabolic response to a range of combinations of stresses cannot be easily predicted from individual stress experiments. To understand the response of plants to a range of stress combinations further more complex studies are required (Shulaev, 2008).

1.5 Perennial ryegrass: an overview

A great majority of the plant metabolomic studies have been limited to model and crop species. Despite the importance of forage grasses, metabolite profiling has remained under-explored in comparison with barley and rice. However, in the United Kingdom and Ireland, a major percentage (~54% and ~89%, respectively) of fertilized agricultural area is devoted to grasslands (Anon, 2002, pp. 32,45) which helps to support the associated milk and beef production industries (Humphreys *et al.*, 2005). In temperate grasslands perennial ryegrass (*L. perenne*), an out-crossing species, is the major forage grass (Humphreys, 2005) and this species is particularly suitable as a forage grass due to its high yield and digestibility, when compared with other species (Wilkins and Humphreys, 2003). However, perennial ryegrass is not well adapted to abiotic stress conditions which are likely to increasingly occur in their natural environment (Good *et al.*, 2006; McElwain and Sweeney, 2007), such as severe winters and hot summers (Wilkins and Humphreys, 2003). This may result in a yield, quality and ultimately productivity loss, therefore, an improvement in tolerance of perennial ryegrass to abiotic stress, is likely to result in considerable economical and benefits.

However, a lack of publicly accessible micro-arrays for perennial ryegrass resulted in few global gene expression studies in this species (Foito *et al.*, 2009; Foito *et al*., 2010 under review). Consequently, most of the knowledge on the molecular events taking place during abiotic stress has been deducted from studies in model plants. Although the knowledge from comparison with model species provides valuable insight into the mechanisms of stress tolerance, the conclusions obtained are not always transferable to the species of

interest (Gong *et al*., 2005). Thus, there is a need to study further the mechanisms of tolerance to abiotic stress in perennial ryegrass.

1.5.1 Future challenges

Climate change predictions emphasize the need to further address to this subject. For example, predictions for the north and west regions of Europe suggest a slow increase in basal temperature with an increase in weather extremes, consequently exacerbating a water stress with swing from too much to too little (Good *et al.*, 2006; McElwain and Sweeney, 2007). This is likely to increase the frequency of soil water logging and drought, both with negative consequences for plant development (Dickin and Wright, 2008). Currently, water limitation is one of the major factors affecting global plant productivity (Chaves *et al.*, 2009). Therefore, one of the aims of this project was the characterization of the metabolic response of perennial ryegrass to water uptake limitation. In order to achieve this aim, a GC-MS-based metabolite profiling approach was used and complemented with data obtained from a transcript profiling approach.

Nutrient limitation, in addition to water limitation, is also a major factors affecting the productivity of plants worldwide. Nitrogen and phosphorus, in particular, are the most limiting mineral nutrients in crop production (Hammond and White, 2008). For example, P deficiency limits crop productivity on 30-40% of the arable land in the world (Wissuwa *et al.*, 2005). In order to prevent productivity limitations, fertilizers are added to soils. However, the overuse of fertilizers has negative impacts in the ecosystem (Wassen *et al*., 2005). Surplus nutrients are liable to be lost to aqueous and atmospheric environments.

Consequently, this may lead to the eutrophication of fresh waters and a decrease of biodiversity in the ecosystem (Wassen *et al.*, 2005). In order to tackle agricultural-derived pollution and to promote biodiversity, international agreements have been created, such as the EU Nitrate directive 91/6/76/EEC (Andrews *et al.*, 2007).

In addition to environmental benefits, there are also economic benefits in applying strategies which attempt to rely on reduced fertilizer usage. Andrews *et al*. (2007) has illustrated the economical benefits of using a strategy which allows similar yields for perennial ryegrass whilst relying on a reduced nitrogen fertilizer input. Furthermore, phosphorus fertilizers are dependent on mineral phosphorus supply which is limited (Vance *et al.*, 2003). A continuous increase in demand will deplete global supplies, which may result in escalating prices, threatening the sustainability of agriculture (Vance *et al.*, 2003).

Accordingly, forecasts for fertilizer consumption in the EU are predicting changes in fertilizer usage (Figure 1.2) (Anon, 2009). While the use of N and P fertilizers is expected to increase in wheat, coarse grains and oil seeds. Grasslands, however, are expected to experience a decrease of both nitrogen and phosphorus fertilization.

Fertilized grasslands account for a majority of the total nitrogen fertilizer used in UK and Ireland (~46% and ~90% respectively) (Anon, 2002, pp. 32,45). Similarly, a major proportion of the phosphorus fertilizer is allocated to grasslands in UK and Ireland (~31% and ~76% respectively) (Anon, 2002, pp. 32,45).

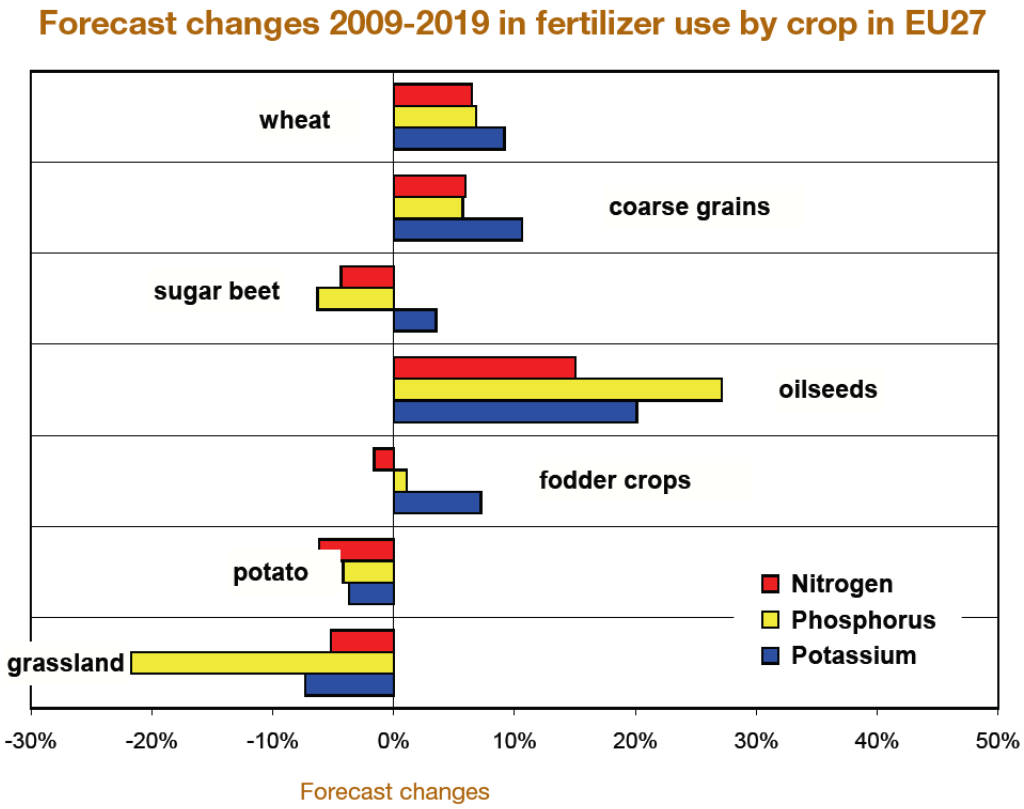

Figure 1.2 –The 10-year forecast for changes in fertilizer usage by crop in the European Union (Anon EMFA, 2009).

This highlights how a reduction in fertilizer usage in grasslands would contribute towards the overall reduction in fertilizer consumption in UK and Ireland. However, in order to reduce fertilizer inputs, without impacting greatly on grassland productivity, it is important to improve nutrient usage efficiency in plants.

1.6 Aims

Although the implications of abiotic stress in the metabolome have been studied in numerous species, there is a lack of such studies in perennial ryegrass. The aim of this work was to characterize the metabolite response of perennial ryegrass to a variety of abiotic stresses, particularly water and nutrient stress.

Drought studies have been performed in perennial ryegrass, however they have mainly focused on specific classes of metabolites such as fructans. Instead, this project aimed to initially perform a global metabolite analysis on water-stressed plants and complement this data with transcriptomic analysis results. It was expected that these results would elucidate some of the global biochemical mechanisms involved in water-stress tolerance in perennial ryegrass.

Differential nutrient supply studies have focused mainly in the medium/long-term response (3 days or more) of plants to stress, leaving the study of short-term nutrient stress responses largely under-explored. An additional aim of this project was to characterize the short-term global metabolite response to different levels of either P or N supply. Sampling of stressed and control material was performed 24 hours after the treatment was applied. This is expected to allow the elucidation of some biochemical mechanisms which will allow plants to temporarily optimize their nutrient usage in the short term.

Chapter 2

General Materials and Methods

Materials and Methods

This section of materials and methods describes only the methodology which is generally used throughout the different experiments. Methodologies which were only applied to a specific experiment are described in the appropriate section as well as minor adjustments to the methodology described below.

2.1 Genotype vegetative propagation

L. perenne is an out-crossing species, so each accession (a group of genotypes collected from multiple points in a region and collected into a single seed lot) will contain multiple alleles at a given locus. For each accession selected seeds have been planted and allowed to develop. A single seedling per accession was selected and propagated vegetatively in order to obtain sufficient number of clones. Therefore, the results presented in this thesis refer to a single genotype of each accession rather than a characterization of an entire accession. Therefore, results obtained may not be necessarily applied to the entire set of genotyopes present in the accession.

2.2 Sampling Material for 'omic' Analysis

The sampling of tissue for metabolite analysis was performed similarly throughout the different experiments. Either leaves or roots were separated from the whole plant and flash frozen in liquid nitrogen and kept at -80 ^{0}C until further processing.

2.3 Sample extraction for metabolite profiling

Standards and reagents were purchased from Sigma-Aldrich Co. Ltd. (Poole, UK). Solvents were of Distol grade and were supplied by Fischer Scientific UK (Loughborough, UK). Frozen tissues of roots and leaves were freeze dried and homogenized using tungsten beads in a Retsch mill. Frozen tissue powder (accurately weighted and recorded) was extracted with 100% methanol (3 ml) and polar (100 µl aqueous ribitol, 2 mg ml $^{-1}$) and non-polar (100 µl methanolic methyl nonadecanoate, 0.2 mg ml^{-1}) internal standards for the metabolites were added. The mixture was shaken vigorously on a vortex shaker at 30 ^{o}C for 30 min. Water (0.75 ml) and chloroform (6 ml) were added sequentially, and after each addition the mixture was shaken at 30 ^{o}C for 30 min. Water (1.5 ml) was added and the mixture was manually shaken and then separated by centrifugation for 10 minutes generating a biphasic system. The upper (polar) and lower (non-polar) fractions were isolated by pipette and were either subjected immediately to further processing, derivatisation and analysis, or alternatively stored at -20 ^{o}C, awaiting further processing. Polar fractions could be stored directly whereas non-polar fractions were first evaporated to dryness under nitrogen and then re-dissolved in isohexane containing 50 ppm 2,6-di-*t*-butyl-4-methyl-phenol (BHT).

2.4 Derivatization of the polar extract

An aliquot (250 µl) of the polar fraction was evaporated to dryness using a centrifugal evaporator. Oximation was performed adding methoxylamine hydrochloride (20 mg ml^{-1}) in anhydrous pyridine (80µl) at 50 ^{o}C for 4h. Silylation was then carried out at 37 ^{o}C for 30 min with 80 µl of N-methyl-N-(trimethylsilyl)-trifluoroacetamide (MSTFA). A sub-sample (40µl) was added to an autosampler vial containing a retention standard mixture (undecane, tridecane, hexadecane, eicosane, tetracosane, triacontane, tetratriacontane and octatriacontane, each at a concentration of 0.2 mg ml^{-1} in isohexane) previously evaporated. The sample was diluted with pyridine (1:1) and analyzed by GC-TOF-MS.

2.5 Derivatization of the non-polar extract

The totality of the non-polar fraction was evaporated to dryness using a centrifugal evaporator and trans-esterified at 50 ^{o}C overnight with 1% (v/v) methanolic sulphuric acid (2ml). Sodium chloride (5 ml, 5% (w/v)) and chloroform (3 ml) were added and the mixture was manually shaken and left to separate into two layers. The upper-phase was discarded and the lower-chloroform layer was shaken with 2% (w/v) potassium bicarbonate (3 ml). The extract was left to separate into two layers, and the lower chloroform layer was collected and dried through an anhydrous sodium sulphate column and then evaporated to dryness. The concentrate was solubilised in chloroform (40 µl). Pyridine (10µl) was added

and silylation was then carried out at 37 ^{o}C for 30 min with MSTFA (80µl). A sub-sample was prepared as described for the polar fraction.

2.6 Metabolite analysis using GC-MS based systems

During this project three different GC-MS instruments were used: analysis of samples from the drought experiment were performed using a GC-TOF-MS system; samples from the phosphorus experiment were analysed with a Thermo Finnigan DSQ system; and samples collected from the nitrogen experiment were analysed using the Thermo Finningan DSQII system.

2.6.1 Metabolite analysis using the GC–TOF–MS system

The polar and non-polar samples were analysed similarly using a Thermo Finnigan Tempus GC–(TOF)–MS system. Samples (1 µl) were injected into a programmable temperature vaporizing (PTV) injector with a split of 80 : 1. The PTV conditions were injection temperature 132 °C for 1 min, transfer rate 14.5 °C s^{-1}, transfer temperature 320 °C for 1 min, clean rate 14.5 °C s^{-1} and clean temperature 400 °C for 2 min. Chromatography was carried out on a DB5-MS^{TM} column (15 m × 0.25 mm × 0.25 µm; J&W, Folsom, CA, USA) using helium at 1.5 mL/min in constant flow mode. The GC temperatures were 100 °C for 2.1 min, 25 °C/min to 320 °C, then isothermal for 3.5 min. The GC–MS interface temperature was 250 °C. Mass spectra were acquired under electron impact (EI) ionization conditions at 70 eV over the mass range 35–900 a.m.u at four spectra/s with a source temperature 200 °C and a solvent delay of 1.3 min. Acquisition rates were set to

give approximately ten data points across a chromatographic peak. Data were acquired using the Xcalibur^{TM} (Thermo Scientific, Waltham, MA, USA) software package V. 1.4.

2.6.2 Metabolite analysis using the GC-DSQ-MS system

The polar and non-polar samples were analysed similarly using a Thermo Finnigan DSQ-MS system. Samples (1 µl) were injected into a programmable temperature vaporising (PTV) injector with a split of 40:1. The PTV and chromatography conditions used are similar as described above. Mass Spectra were acquired under electron impact (EI) ionisation conditions at 70 eV and 100 mA of emission current over the mass range 35-900 a.m.u at 6 scans s^{-1} with a source temperature 200^{o}C and a solvent delay of 1.3min, Acquisition rates were set to give approximately ten data points across a chromatographic peak. Data were acquired using the Xcalibur^{TM} software package V. 1.4. Acquired total ion chromatograms and mass spectra were analysed using XcaliburTM software package v2.0.7 (ThermoFinnigan, Manchester, UK).

2.6.3 Metabolite analysis using the GC-DSQII-MS system

The polar and non-polar samples were analysed similarly using a Thermo Finnigan DSQ-MS system. Samples (1 µl) were injected into a programmable temperature vaporising (PTV) injector with a split of 40:1. The PTV and chromatography conditions used are similar as described above. Mass Spectra were acquired under electron impact (EI)

ionisation conditions at 70 eV and 100 mA of emission current over the mass range 35-900 a.m.u at 6 scans s^{-1} with a source temperature 200^{o}C and a solvent delay of 1.3min, Acquisition rates were set to give approximately ten data points across a chromatographic peak. Data were acquired using the Xcalibur^{TM} software package V. 1.4. Acquired total ion chromatograms and mass spectra were analysed using XcaliburTM software package v2.0.7 (ThermoFinnigan, Manchester, UK).

2.7 Data processing and analysis

A number of representative chromatograms for both leaf and root tissues were used to create a processing method for the polar and non-polar extracts of perennial ryegrass (Figure 2.1 and 2.2). During the initial stages of method development all peaks were annotated with respect to retention time and major quantifying ion mass. Furthermore, a minimum of 5 mass spectrum scans was used for the annotation of a chromatographic peak. The mass spectrum for each peak was compared with the NIST mass spectral database and the results obtained analysed with respect with their relevance: due to the large number of compounds present in the database, the results obtained from a library search often contain synthetic compounds or non-sylilated metabolites which are inconsistent with the methodology applied, therefore, caution is required when assigning identities based on library searches alone. The peaks which did not reveal any similarity to relevant compounds were annotated as unidentified peaks. Mass spectra which had good positive matches with relevant metabolites in the library were temporarily assigned putative identities. For example L-5-oxoproline was assigned identity based on the NIST mass

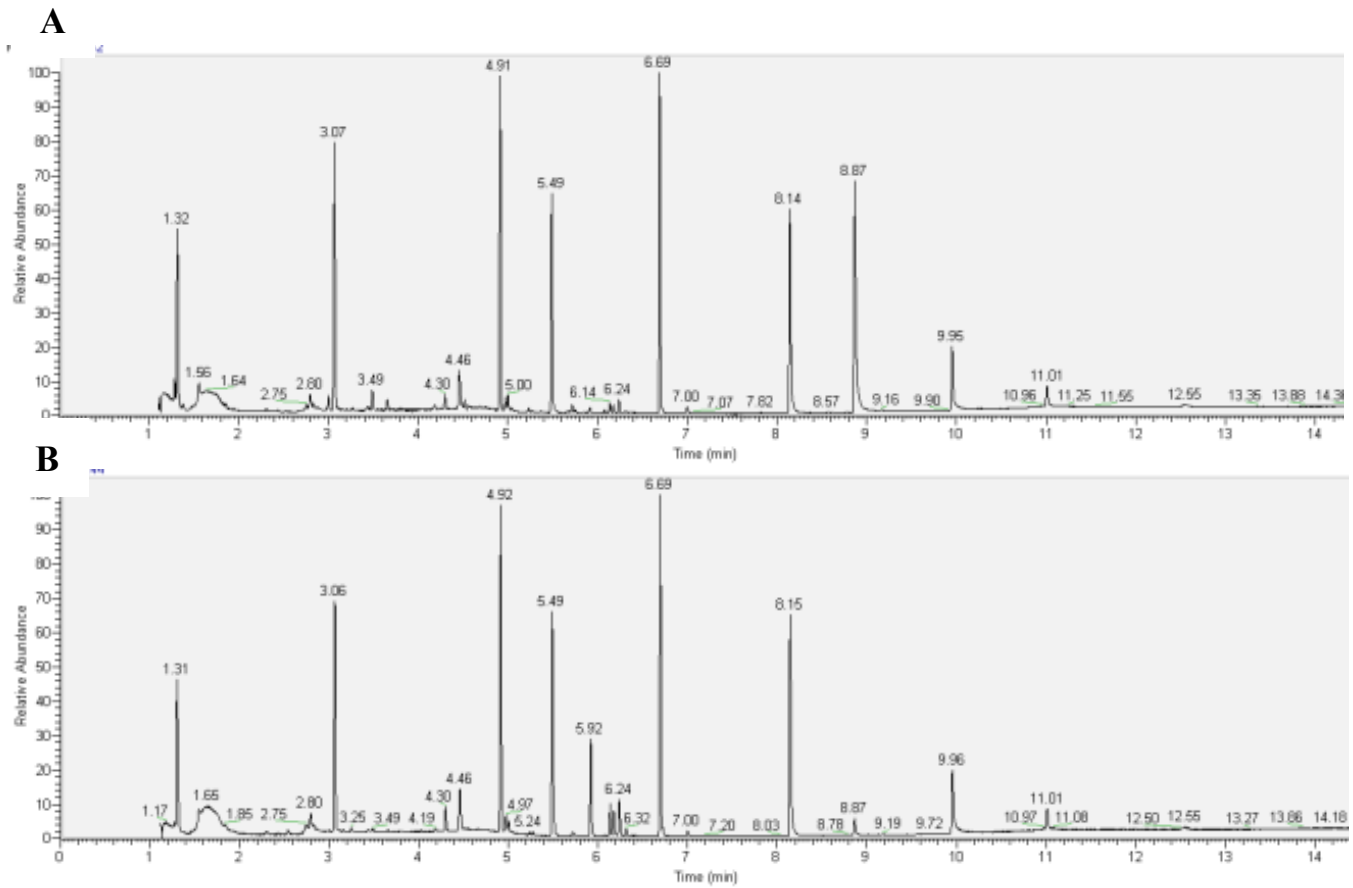

Figure 2.1 – GC-TOF-MS chromatograms from polar extracts of perennial ryegrass leaf and root samples. A- polar extract from leaf tissue of perennial ryegrass. B- Polar extract of root tissue from perennial ryegrass.

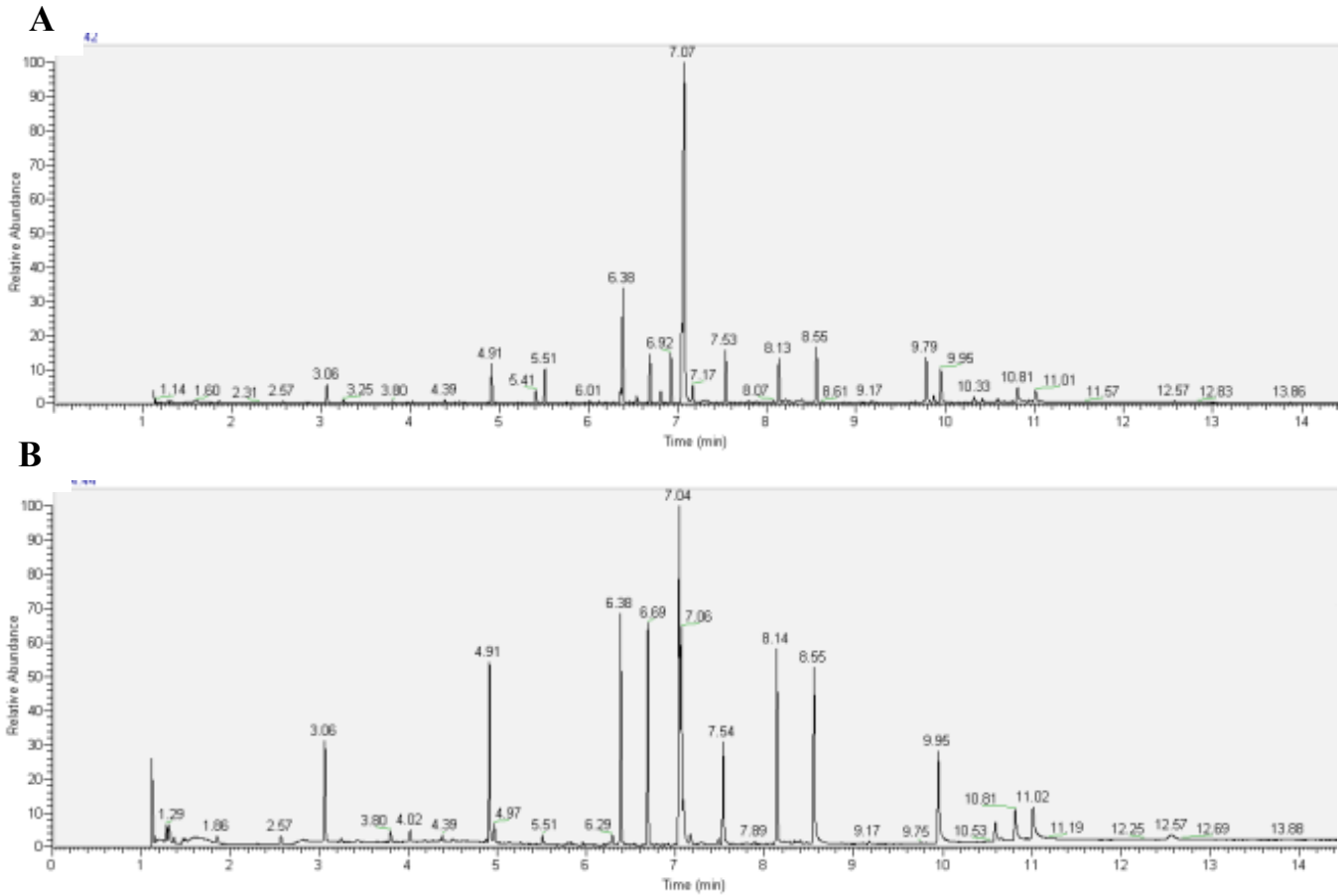

Figure 2.2 – GC-TOF-MS chromatograms from non-polar extracts of perennial ryegrass leaf and root samples. A – non-polar extract of leaf tissue of perennial ryegrass B- non-polar extract of root tissue of perennial ryegrass.

spectral library search (Figure 2.3). Subsequently, these metabolites were compared with the SCRI standard database which consists of a collection of spectra and ion mass list from standards and their respective retention times and retention indexes. The calculations of retention indexes for metabolites are based on the comparison of retention times of metabolites with the retention time of the retention standards which are added to the vials (undecane, tridecane, hexadecane, eicosane, tetracosane, triacontane, tetratriacontane and octatriacontane, view table 2.1).

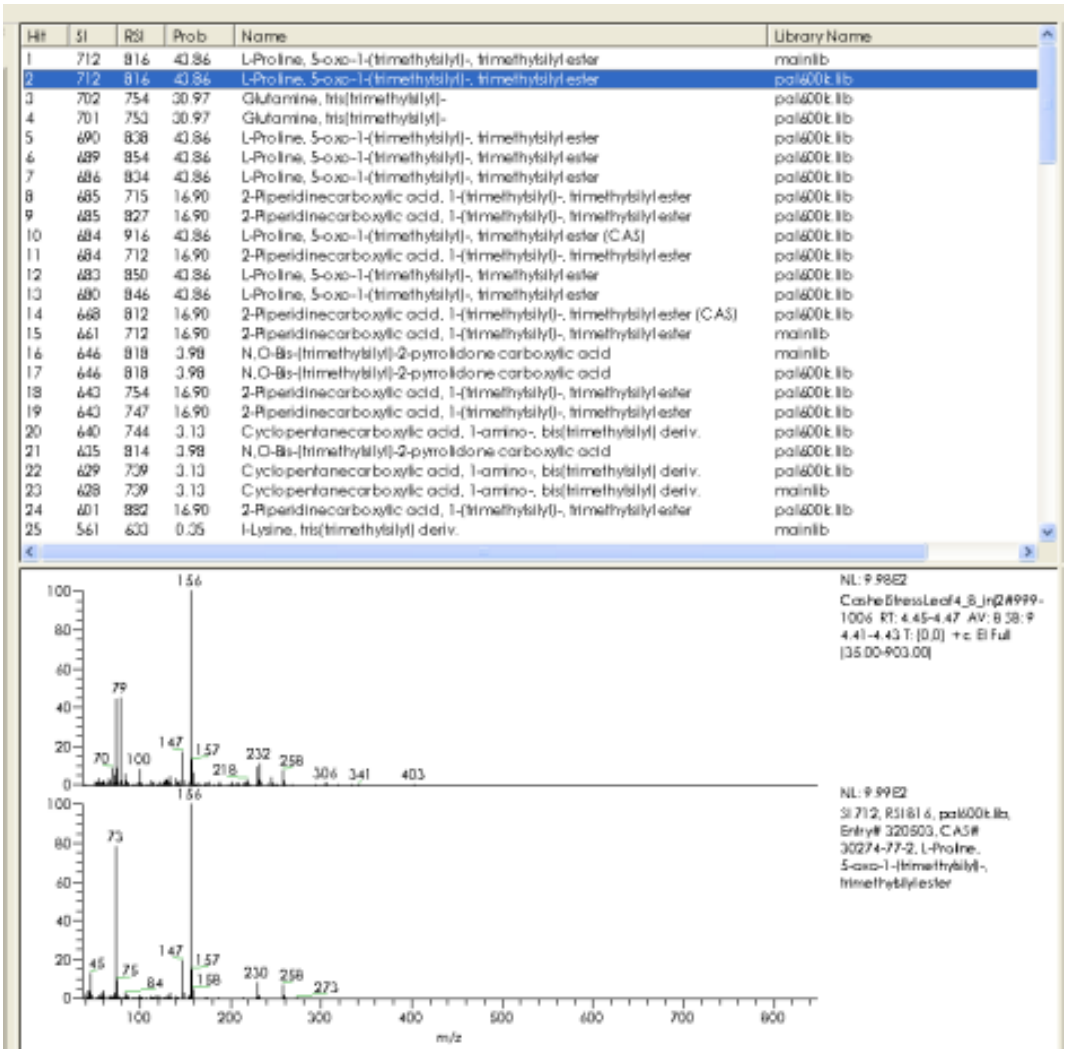

Figure 2.3 – Results from the mass spectral search on the NIST library and respective match of the sample mass spectrum with L-Proline 5-oxo-1(trimethylsylyl, trimethylsylyl ester).

The retention standards have an associated retention index (table 2.1) and by associating the retention index with the retention times in a chromatography it is possible to calculate the retention index of a metabolite based on their retention times.

A prerequisite for the positive identification of a metabolite during this process was a close proximity of the retention index of the putative identified metabolites with the ones present in the SCRI database (see example in figure 2.4 and 2.5). Furthermore, the sample mass spectrum needs a significant similarity to the mass spectrum present in the database. Additionally, identity assignment is confirmed with the GC-MS expert analyst.

Table 2.1 – Table representing the retention index of each retention standard used for GC-MS analysis.

Retention standard	Retention index
Undecane	1100
Tridecane	1300
Hexadecane	1600
Eicosane	2000
Tetracosane	2400
Triacontane	3000
Tetratriacontane	3400
Octatriacontane	3800

However, in some cases the top relevant matches from the NIST library search did not match any of the metabolites present in the SCRI standard database. In these cases, the spectrum was closely evaluated by the GC-MS analyst and was either assigned a putative identity where the spectra revealed a good match or its identity was disregarded and it was

annotated as an unidentified peak. The result of this process is the creation of a list ordered by retention time which includes the metabolite identity (where it has been assigned) or a name, and the main distinguishing mass in the spectra (Appendix I).

The selection of the main mass has mainly to fulfill two criteria: have significant signal level intensity and have a unique mass in the specific chromatographic region. The first criteria will allow the integrated data to be more accurate while the second criteria will ensure the correct identity of the chromatographic peak.

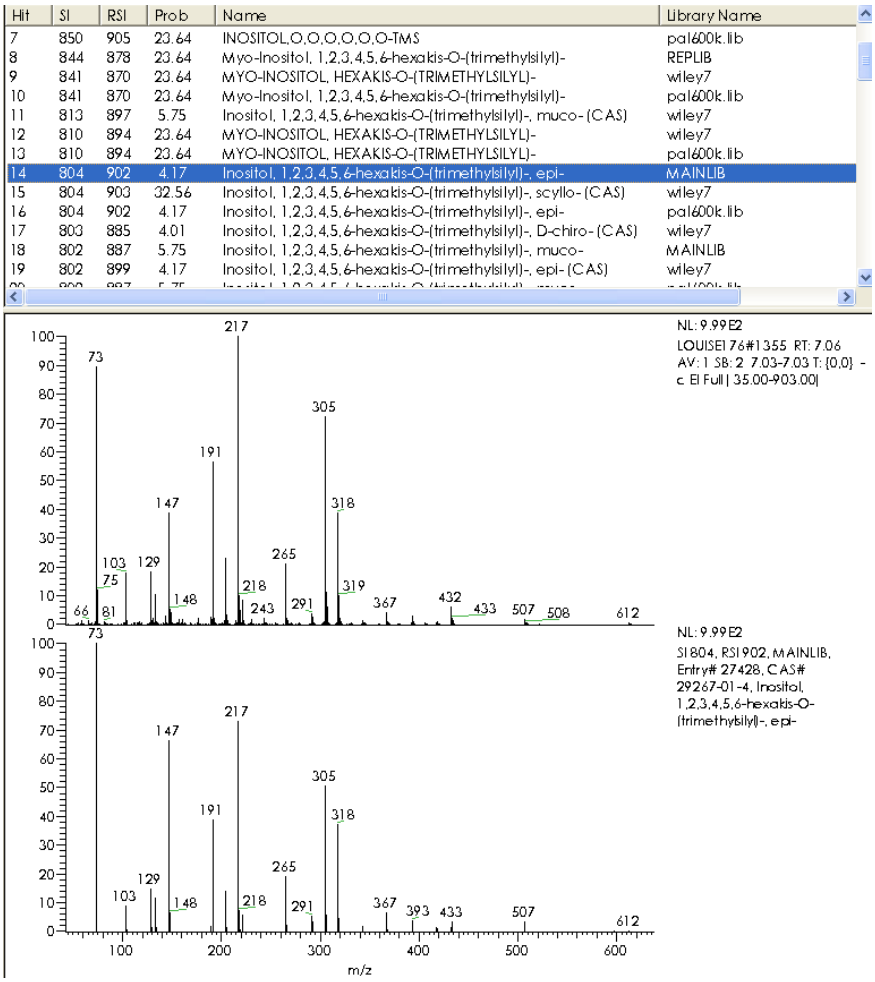

Figure 2.4 –Mass spectral search results for a chromatographic peak corresponding to inositol standard with the retention index of 2086.

For example in figure 2.6 it is possible to observe two different selected ion chromatograms from the same sample using two different selected mass ions. The chromatographic differences between the two SIC are significant and it was observed that m/z 205 provided a single chromatographic peak in that region as opposed with m/z 147.27.

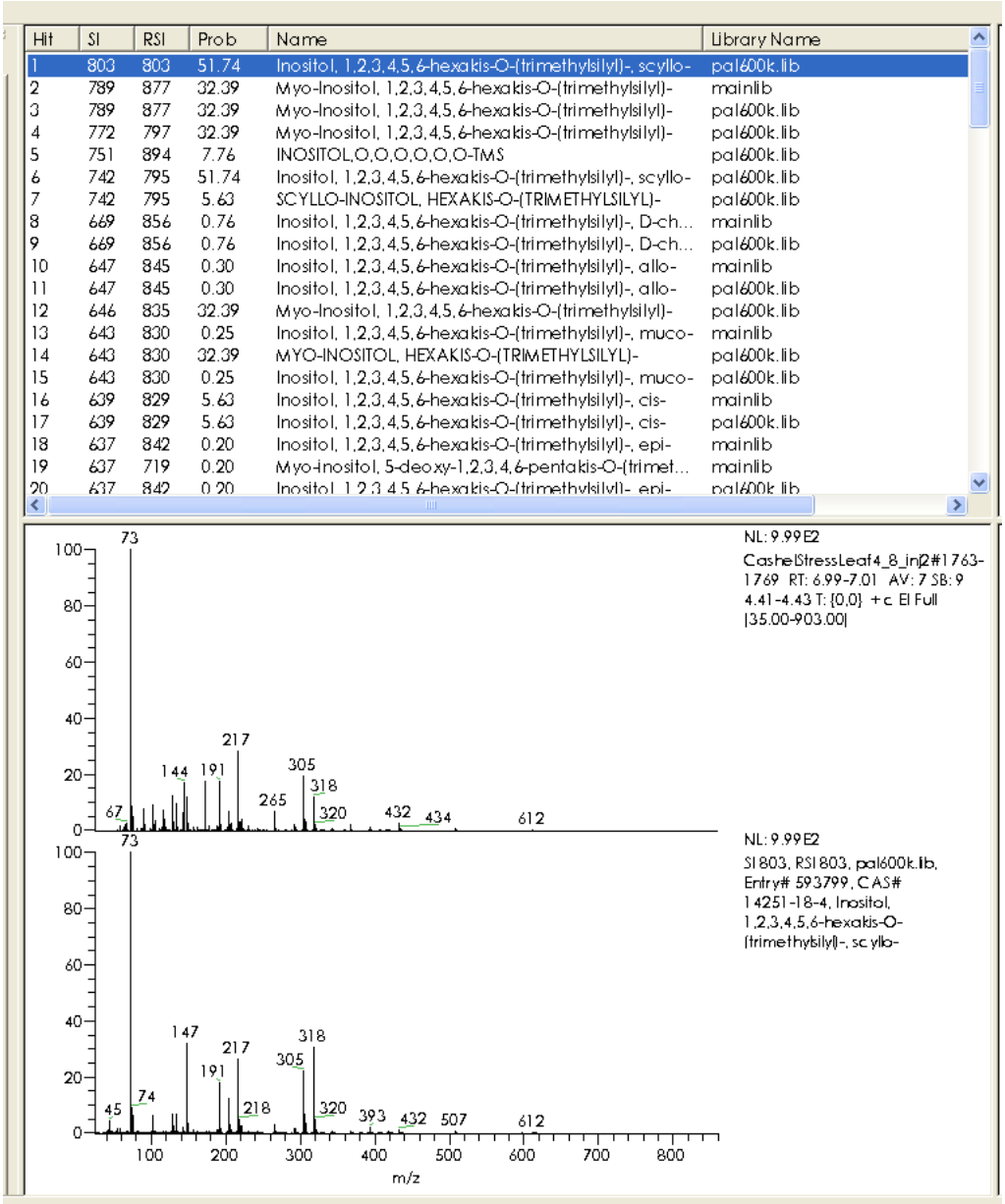

Figure 2.5 –Mass spectral search results for a chromatographic peak present in leaf samples with the retention index of 2085.

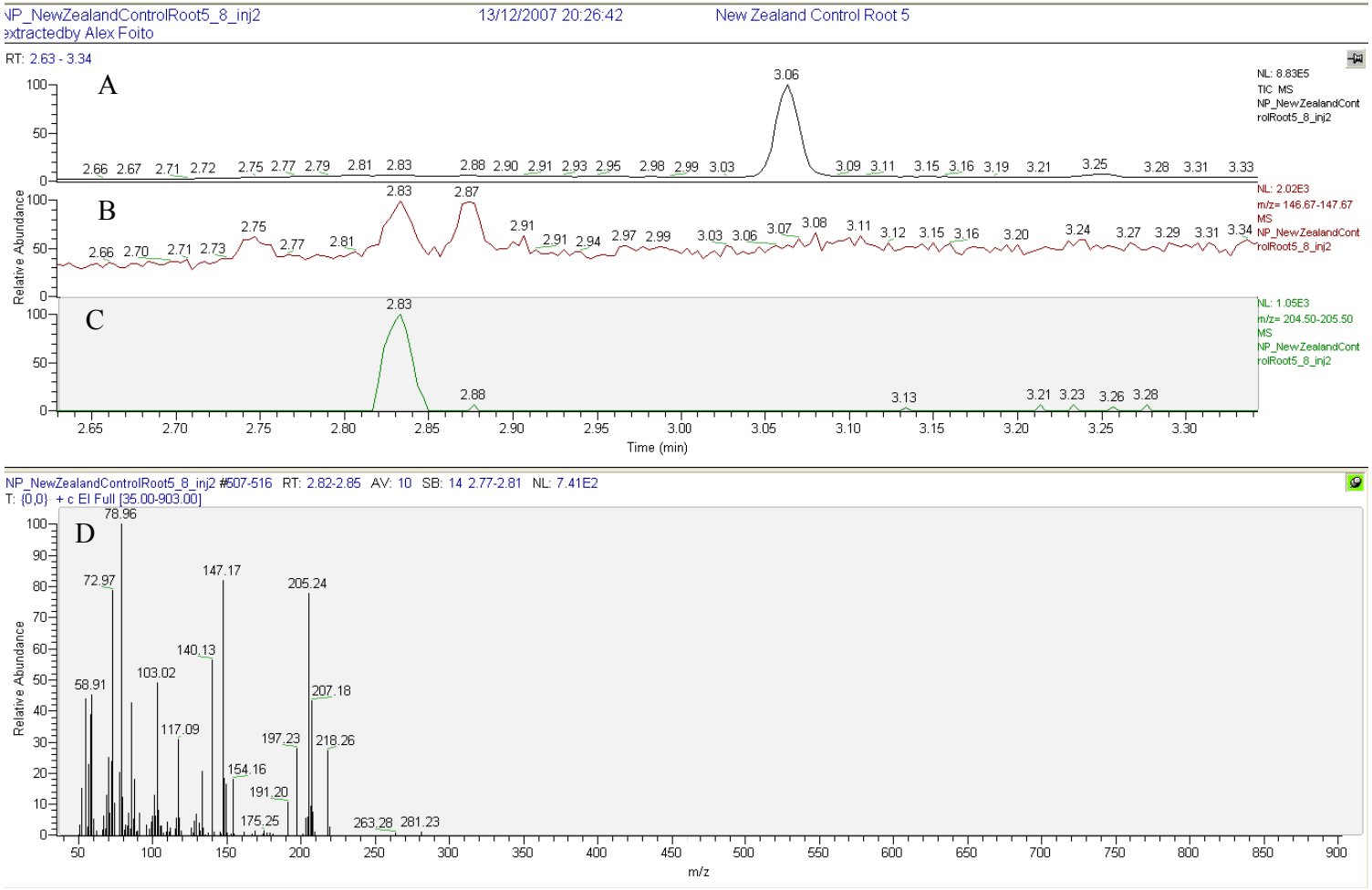

Figure 2.6– Total and selected ion chromatograms of leaf polar extracts illustrating at retention time of 2.83 minutes a peak identified as glycerol and its respective mass spectrum. A – total ion chromatogram B- selected ion chromatogram for m/z 147.17 C- selected ion chromatogram for m/z 205. D- average mass spectrum for retention time 2.82-2.85 minutes indentified through library search as glycerol

In summary, the creation of a processing method is an iterative process which can be illustrated in figure 2.7, that requires the presence of a standard database for corroboration of compound identity, as well as expertise in GC-MS analysis in order to determine false positive matches returned in the library searches.

The processing method was created in Xcalibur ™ v. 1.4 using the retention times and masses listed in appendix I using the Genesis algorithm (included with the program) for peak integration. The values set as default for the Genesis peak integration were set as 1 smoothing point, 0.5 signal/noise threshold with enabled valley detection and expected peak width of 1.50 seconds. However, in some cases these values have been adjusted for optimised detection and consistent integration. The expected retention time for each peak was adjusted using the retention times of the retention standards. The integrated values for each target compound were normalised against the integrated area of the respective internal standard, ribitol and nonadecanoic acid for polar and non-polar extracts respectively.

The initial processing method was created using the GC-TOF-MS data and the subsequent processing methods were adapted from the initial method. The subsequent versions (see appendix I) included a lower number of mass peaks which can be attributed to a reduced sensitivity of the instrument (phosphorus experiment) or reduced amount of samples (nitrogen experiment). Furthermore, an additional selection process was performed with the goal of removing low level unidentified peaks from the processing method. Data was integrated using the developed processing methods which automatically integrate the mass peaks present in the selected ion chromatograms, however this process has been thoroughly monitored for every peak and samples, and where necessary, manual adjustments were performed to correct abnormalities in the selected integrated data (an example of such case is included in figure 2.7).

A

B

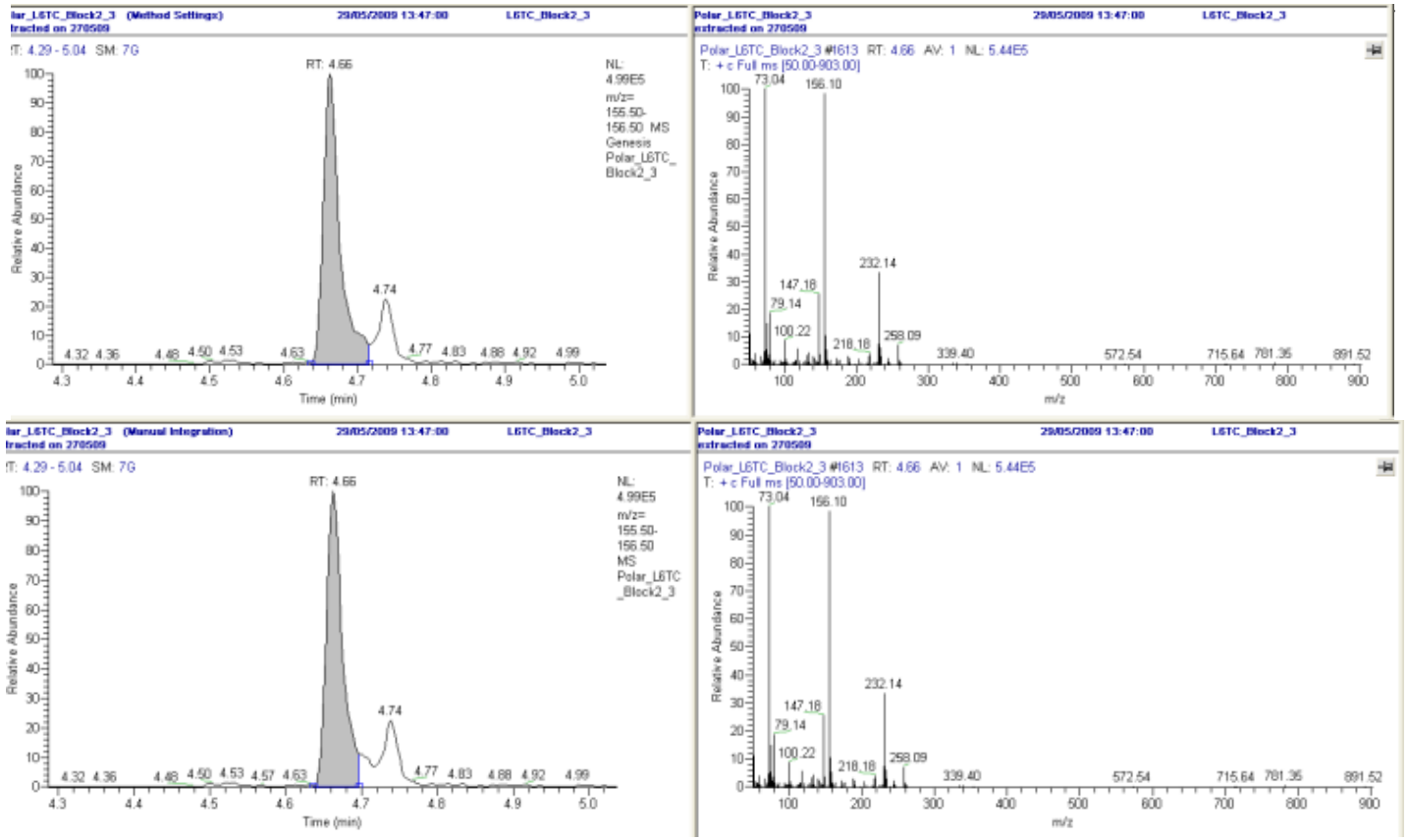

Figure 2.7 – Selected ion chromatograms for m/z 156 with the peak at retention time 4.66 minutes being putative identified as L-5-oxoproline. A – represents the selected ion chromatogram and its respective integrated area shadowed using automatic setting. B – Represents the selected ion chromatogram and its respective integrated area manually adjusted.

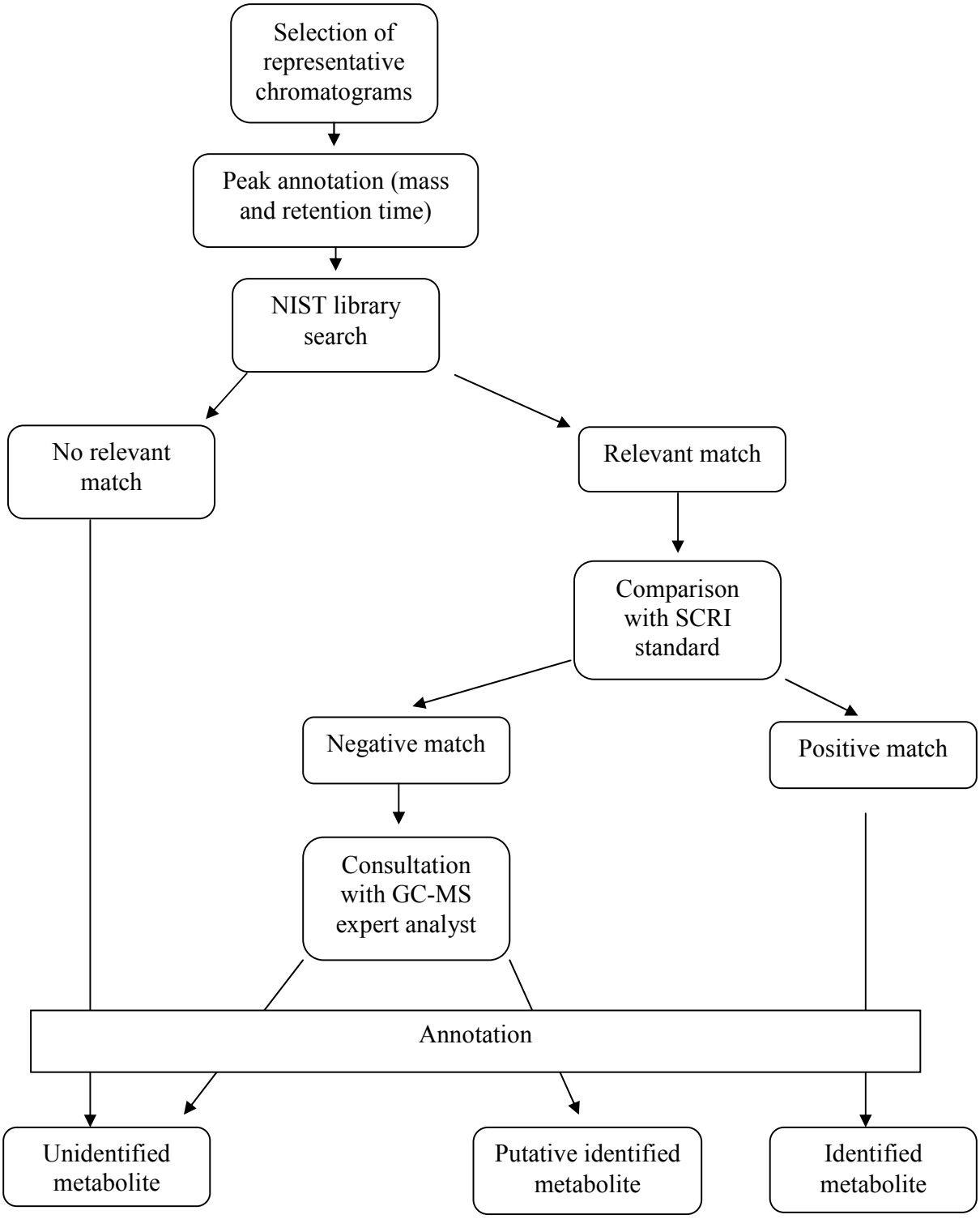

Figure 2.8 – Graphical representation of the workflow used for method development

The output obtained from the integration of each mass peak using the processing method consists of a table which includes the sample name (corresponding to one chromatography) with its associated annotated peak area ratios (Table 2.2). These data were subsequently statistically analysed using GenStat version 9.2.0.153 for multivariate analysis and analysis of variance.

Principal component analysis (PCA) was initially performed for all the samples, including the quality controls (blanks and reference potato sample) with the goal of determining any unusual effects (for example, unusual levels of the internal standard will affect all the area ratios given for a single sample) which may result in the presence of outlier samples.

Table 2.2 – Table representing the data spreadsheet output from the processing methodology for a m number of peaks present in the processing method and n samples analysed.

	Area ratios			
Sample name	**Metabolite 1**	**Metabolite 2**	**...**	**Metabolite m**
Sample 1	...	...	...	...
Sample 2	...	...	...	...
...	...	...	...	...
Sample n	...	...	...	...

These outlier samples (if present) were further investigated for the detection of possible errors and only if the levels of internal standard are unusually low/high or if the chromatography reveals any abnormalities (a misinjection, for example) are these samples excluded from further analysis. One of the requirements for samples to successfully pass the quality control is that samples from perennial ryegrass leaf and root tissues cluster

differently from the reference potato samples since they have different biological origins. Additionally, a good clustering between the reference samples will indicate a degree of consistence in the methodology used.

Once samples pass the quality control further PCA was performed to evaluate whether the differences in treatments resulted in alterations of the metabolic profiles of perennial ryegrasses. Subsequently, a one-way analysis of variance was performed in order to determine the metabolites which are significantly affected by treatment. Additionally, for these metabolites the ratios between the means of the area ratios of the metabolites from both treatments were calculated.

Chapter 3

Drought in perennial ryegrass

3.1 Summary

Metabolite profiling was undertaken in *Lolium perenne* L. (perennial ryegrass) to uncover mechanisms involved in the plant's response to water stress. When leaf and root material from two genotypes exhibiting a contrasting water stress response were analysed by GC-MS, a clear difference in the metabolic profiles of the leaf tissue under water stress was observed. Differences were principally due to a reduction in fatty acid levels in the more susceptible Cashel genotype and an increase in sugars and compatible solutes in the more tolerant PI 462336 genotype. Sugars with a significant increase included, raffinose, trehalose, glucose, fructose and maltose. Raffinose was identified as the metabolite with the largest accumulation under water-stress in the more tolerant genotype and may represent a target for engineering superior drought tolerance in perennial ryegrass. The metabolomics approach was combined with a transcriptomics approach in the water stress tolerant genotype PI 462336 which identified genes in perennial ryegrass that are regulated by this stress.

3.2 Introduction

One of the major environmental factors restricting the productivity of plants in the world is water limitation. Water-deficit conditions induce a range of physiological and biochemical responses which include stomatal closure, repression of cell growth and photosynthesis, and activation of respiration (Shinozaki and Yamaguchi-Shinozaki, 2007).

In order to maintain water balance, plant tissues may display mechanisms of drought avoidance, drought tolerance, or both (Valliyodan and Nguyen, 2006). Plants often avoid stress with morphological changes, such as the modification of root architecture and root:shoot ratios. In rice, for example, the development of an extensive and deep root system may be beneficial for upland rice (rice grown in dry soil) because it enables the access to water held deep in the soil under upland levels (Wang *et al.*, 2009a). For the same reasons, the ability of the root system to penetrate soil is considered a key characteristic contributing to increased drought adaptation (Wang *et al.*, 2009a).

Some of the constitutive traits in plants, such a root thickness, may aid plants growing under water-limiting conditions (Valliyodan and Nguyen, 2006). However, these are traits that are present even in the absence of stress (Valliyodan and Nguyen, 2006). In contrast, plants may respond by activating specific defense systems in order to survive and sustain growth, which constitutes an adaptive trait (Valliyodan and Nguyen, 2006).

The study of these adaptive responses to drought has been extensively focused at the cellular and molecular level. For example, the transcriptomic responses from the two model

plant species, *Arabidopsis* and rice, were monitored using microarray approaches and resulted in the identification of hundreds of genes regulated by drought (Shinozaki *et al*., 2003; Shinozaki and Yamaguchi-Shinozaki, 2007). These regulated genes were classified into two major groups, in which one group was classified in the regulation of signal transduction and transcriptional control, whereas the other group was attributed to directly protect cell integrity (Shinozaki *et al*., 2003; Shinozaki and Yamaguchi-Shinozaki, 2007). The first group included genes encoding various transcription factors (TF), protein kinases, protein phosphatases, phospholipid-related enzymes and additional signalling molecules such as calmodulin-binding proteins, while the second group included genes encoding key enzymes for osmolyte biosynthesis, sugar and proline transporters, water channel proteins and detoxification enzymes (Shinozaki *et al*., 2003; Shinozaki and Yamaguchi-Shinozaki, 2007).

The study above highlights the range of effector mechanisms responsible for increased tolerance to drought, as well as the role of signal transduction and transcriptional control in regulating those mechanisms.

Abscisic acid (ABA) is a major phytohormone which is thought to be responsible for regulating stomatal closure and inducing the expression of drought stress-related genes (Seki *et al.*, 2007). The main transcription factor involved in the specific response to stress mediated by ABA is an ABA-responsive element (ABRE) binding protein (AREB)/ABRE-binding factor (ABF) (Shinozaki and Yamaguchi-Shinozaki, 2007; Nakashima *et al.*, 2009). However, the characterization of genes that are induced under drought conditions but not by exogenous ABA application suggests the existence of ABA-independent

signaling pathways which are also involved in mediating cellular responses to dehydration (Nakashima *et al.*, 2009). Moreover, the dehydration responsive element binding protein 2 (DREB2) is a TF that mediates ABA-independent responses to drought in *Arabidopsis* (Liu *et al.*, 1998; Shinozaki and Yamaguchi-Shinozaki, 2007).

The mechanisms of cell protection are regulated by some of the transcript factors described above. These include the accumulation of metabolites (such as, antioxidants, radical-oxygen-species (ROS) scavengers and osmoprotectants), water channel proteins, detoxification enzymes and chaperone-like proteins (Valliyodan and Nguyen, 2006; Seki *et al*, 2007; Shinozaki and Yamaguchi-Shinozaki, 2007).

Aquaporins are water channel proteins which are among some of the relevant molecules regulated by water limitation (Shinozaki and Yamaguchi-Shinozaki, 2007). These proteins play an important role in radial water transport in both roots and leaves. Furthermore, it has been suggested that transport of water mediated by aquaporins accounts for 20-85% of the overall water transport depending on the species (Parent *et al*., 2009). In order to understand further the physiology of aquaporins in rice, particularly RWC3, a transgenic approach was used (Lian *et al*., 2004). The authors introduced a stress-inducible promoter SWPA2 to regulate the RWC3 expression under stress conditions. The resulting transgenic line displayed better water status under water limitation suggesting a role of RWC3 in adjusting water movement across plasma membrane (Lian *et al*., 2004). However, there are a number of studies which reveal contradictory findings and report a negative impact on survival of transgenic lines overexpressing aquaporins under water-limitation (Aharon *et al*., 2003; Jang *et al*., 2007).

Adverse environmental conditions, such as drought, may lead to an imbalance between antioxidant defenses and the amount of reactive oxygen species (ROS), resulting in oxidative damage (Munne-Bosch and Penuelas, 2003). The accumulation of ROS may result in damage to subcellular components, such as the chloroplast which may consequently impact on the photosynthetic machinery of the cell (Munne-Bosch and Penuelas, 2003; Chaves *et al.*, 2009). In order to protect the cells from oxidative damage, plants have enzymatic mechanisms that remove ROS, namely, superoxide dismutase (Mittler, 2002). Additionally, the accumulation of metabolites with antioxidant activity, for example, ascorbic acid, may aid in protecting cell membranes against oxidative damage (Mittler, 2002). As an illustration of the importance of ascorbic acid in the tolerance to abiotic stress, it was found that an *Arabidopsis* mutant *soz1*, which has suppressed ascorbic acid levels, displayed increased sensitivity to abiotic stress conditions such as ultraviolet B irradiation (Conklin *et al.*, 1996).

Plants often respond to stress by accumulating compatible solutes. Osmoprotectants, are compatible solutes thought to protect the cell by decreasing the osmotic potential in cells, increasing water influx into the cell, thus maintaining cell turgor. Additionally, these molecules may interact with cell membranes and proteins producing a stabilizing effect (Valliyodan and Nguyen, 2006). Osmoprotectants encompass a variety of compound classes, including sugars, sugar alcohols, amino acids and polyamines (Valliyodan and Nguyen, 2006).

The accumulation of a variety of saccharides, such as raffinose, trehalose and fructans, and polyols, such as mannitol, has been correlated with drought tolerance (Valliyodan and

Nguyen, 2006; Seki *et al*., 2007). Mannitol has been proposed to enhance tolerance to water limitation primarily through osmotic adjustment (Abebe *et al.*, 2003; Valliyodan and Nguyen, 2006). However, a transgenic study in wheat revealed that, although plants with higher levels of mannitol were able to tolerate water-stress, the changes in mannitol levels did not translate into significant changes in the total osmotic adjustment (Abebe *et al.*, 2003). Instead, it was suggested that the beneficial effect of mannitol resulted from additional protective mechanisms, such as the scavenging of hydroxyl radicals or the stabilization of macromolecular structures (Abebe *et al.*, 2003).

Trehalose is a non-reducing disaccharide of glucose which acts as reserve carbohydrate and stress protectant, stabilizing proteins and protecting them from denaturation (Elbein *et al*., 2003). This solute is accumulated under abiotic stress, ranging from dehydration to temperature stress in a wide variety of organisms, such as bacteria, fungi and plants (Elbein *et al*., 2003). The role of trehalose in protecting plants against damage resulting from water limitation has been illustrated by transgenic studies aiming to increase the levels of trehalose in the cell. For example, Garg *et al*. (2002) generated transgenic rice lines which accumulated up to 3-10 fold more trehalose when compared with the non-transgenic lines. Additionally, these transgenic lines displayed sustained growth and less photo-oxidative damage when grown under abiotic stresses, such as drought, compared with the non-transgenic lines. The authors also observed that trehalose levels correlated with an overall increase in photosynthetic activity and soluble carbohydrate levels, which suggested an important role of this solute in modulating the sugar sensing and carbohydrate metabolism (Garg *et al*., 2002).

Raffinose family oligo-saccharides, such as raffinose and stachyose, have been suggested to act as anti-stress agents in both vegetative and generative tissues (Wu *et al.*, 2009). Moreover, a study of transgenic *Arabidopsis* lines overexpressing OsUGE-1 (which encodes for a UDP-glucose 4 epimerase which interconverts UDP-D-glucose and UDP-D-galactose) revealed that these had considerable higher levels of raffinose and tolerance to drought, salt and freezing stress. Thus, the authors suggested that the tolerance to abiotic stress could be mediated by elevated raffinose levels (Liu *et al*., 2007).

Another group of compounds which are associated with higher tolerance to some abiotic stresses are fructans, which consist of a family of oligo- and poly-fructoses (Seki *et al*., 2007). For example, Pilon-Smits *et al*. (1995) compared the performance of fructan-accumulating transgenic tobacco with wild-type plants under water limiting conditions. The authors observed that the growth rate, fresh weight and dry weight yields were considerably higher in the transgenic lines. Additionally, it was observed that, under control conditions, there was no significant difference in the growth and development between wild-type plants and transgenic plants (Pilon-Smits *et al*., 1995).

In addition to sugars and polyols, the accumulation of amino acids may contribute for enhanced tolerance to drought in plants. Proline, in particular, plays a highly protective role in plants exposed to stress. This amino acid is thought to have a multifunctional role in cell protection, functioning as a mediator of osmotic adjustment, detoxification of ROS, stabilization of subcellular structures, energy sink and as a stress-signal (Seki *et al*., 2007). For example, a study in rice has revealed that plants exposed to water stress respond by

accumulating proline in the leaf tissues and that this response seems to be ABA-independent (Hsu *et al*., 2003).

Polyamines, such as putrescine, spermidine and spermine, are involved in responses to abiotic stress in a wide variety of organisms (Seki *et al*., 2007). A recent transgenic study in *Arabidopsis thaliana* was able to generate plants constitutively expressing a homologous arginine decarboxylase-2 gene (Alcazar *et al.*, 2010). These transgenic lines were found to contain high levels of putrescine with no changes in spermidine and spermine levels even when plants were grown under drought conditions. Additionally, the authors found that the degree of drought tolerance in the plants correlated with putrescine content (Alcazar *et al.*, 2010).

The biochemical adaptations of plants to water limitation are diverse, as outlined above. In order to understand the corresponding metabolic response of perennial ryegrass, a metabolite profiling approach will be used. Since a majority of the responses cited include primary metabolites, it is expected that a GC-MS-based metabolite profiling approach may be able to provide insight into the metabolite response of perennial ryegrass to water limitation.

Many different experimental systems have been used to simulate water limitation in plants such as benchtop drying (Zhou *et al*., 2007; Seki *et al*., 2002), field drought (Semel *et al*., 2007), controlled soil-based experiments (Rizhsky *et al*., 2004) and polyethylene glycol (PEG)-induced drought. The utility of PEG to control the osmotic pressure of plant nutrient solutions was first described by Lagerwerff *et al*., (1961). Since then, it has been widely

used to provide osmotic stress in order to simulate drought (Pilon-Smits *et al*., 1995; Zheng *et al*., 2006). A high concentration of PEG in the media results in a decrease of water potential, interrupting the normal flow of water from the media to the roots. As a result, this high concentration mimics soil drying by causing a loss of water from the plant cell wall and cytoplasm (Verslues and Bray, 2004). PEG can be useful in experimental systems because it allows control of the level of water stress imposed and allows easy access to root material for sampling. Furthermore, a gene expression study in maize indicated similar responses between PEG-induced water stress and a progressive drought imposed by withholding water (Zheng *et al*., 2006).

Therefore, the aim of this chapter is to characterize the molecular and metabolic response of perennial ryegrass under a PEG-induced water stress. A metabolic profiling of leaf and root tissue was undertaken on two genotypes differing in their tolerance to a PEG-induced drought stress. These data were complemented with results obtained from a suppression subtractive hybridization (SSH) approach, which was used to identify transcripts up-regulated under drought stress in both leaf and root tissue of a genotype displaying tolerance. It is expected that this will allow the identification of genes and metabolites regulated during water stress, some of which may be potential targets for improving drought tolerance in perennial ryegrass.

3.3 Material and Methods

3.3.1 Physiological assessment of PEG-induced water stress

A total of 16 *Lolium perenne* genotypes were used to verify the suitability of PEG-induced stress to generate a relevant physiological effect. Clones of each genotype were obtained by vegetative propagation of existing plants grown in glasshouse conditions. Each genotype was replicated six times and grown for 1 week in an aerated hydroponics system supplemented with either 4.4g l^{-1} MS medium (Duchefa), which acted as a control condition, or a MS medium supplemented with 15% w/v PEG 6000. After 1 week of growth in hydroponics systems the root and above ground fresh biomass was weighed and the relative water content (RWC) was measured as described by Jones and Turner (1978). Leaf segments of approximately 1 cm were weighed (fresh wt). After recording the weight, the segments were floated in distilled H_2O for 4 hours at 25 ^oC. Afterwards the leaf segments were blotted dry and weighted (turgid wt) before being incubated overnight in an oven. The oven-dry segments were weighed (dry weight) and RWC was calculated using the following equation:

$$RWC = \frac{\text{fresh wt - dry wt}}{\text{turgid wt - dry wt}} \cdot 100$$

3.3.2 Plant Material and Drought Stress

The *Lolium perenne* ecotype PI 462336 was selected from the Genomic Resources Information Network (GRIN) operated by the USDA (http://www.ars-grin.gov/npgs/). This

accession was selected after a search for accessions being described as drought tolerant. Seeds were planted together with seeds from the cultivar Cashel. After germination a single seedling per accession was allowed to propagate vegetatively to obtain sufficient numbers of clones from both accessions for drought stress testing. Clones of Cashel and PI 462336 were allowed to establish in an aerated hydroponics system supplemented with 4.4g l^{-1} MS medium (Duchefa) in two replicates. After two weeks of growth the solutions in both systems were replaced. In the first system a MS medium supplemented with 20% w/v PEG 6000 was applied to induce osmotic drought stress and the second system contained MS salts only and acted as a control. Relative Water Content (RWC) was measured at mid-day after 24 hrs and 1 week according to the method described in the above section. Dry weights (DW) for above and below ground biomass were determined after two weeks of induced drought.

3.3.3 Sampling Material for Omic Analysis

The experiment was setup as described above and material for transcript and metabolite analysis was harvested after 1 week under both stress and control conditions as described in the material and methods chapter.

3.3.4 Metabolite profiling

Both sample extraction and derivatization procedures for metabolite analysis were performed exactly as described in Chapter 2. Additionally, the metabolite profiles we

acquired using a GC-TOF-MS and the resulting data was analysed as described in materials and methods

3.3.5 Suppression Subtractive Hybridization (performed by SLB)

Suppression Subtractive Hybridization (SSH) was performed to identify transcripts up-regulated in the documented drought tolerant accession PI 462336 after one week of a 20% PEG induced drought stress. Total RNA was isolated from leaf and root material with Tri Reagent (Ambion). A DNA digestion was performed using a DNA-*free* kit (Ambion) according to the manufacturer's protocol. cDNA was generated from total RNA using the Smart cDNA synthesis kit (BD Biosciences). SSH was performed according to the protocol of Desai *et al*. (2000) using stress and control material as tester and driver, respectively. Subtracted libraries for root and leaf tissue were generated independently. The two libraries were cloned using the pGEM T-easy cloning system (Promega) and transformed into *E. coli* TOP10 using electroporation.

3.3.6 Differential Screening of SSH libraries and Verification (Performed by SLB)

In total 384 colonies were randomly selected from each library and their inserts were amplified by PCR. cDNA dot blots were prepared in duplicate and hybridized to cDNA generated with SuperScript III (Invitrogen) from 500ng stressed and control RNA. cDNA labeling and detection was done using an AlkPhos direct labeling and ECF detection system (Amersham Biosciences). Clones showing differential expression had their inserts

sequenced and were assigned putative functions by searching against the NCBI database using tblastx (http://blast.ncbi.nlm.nih.gov/blast.cgi). Quantitative RT-PCR was used to confirm differential expression. cDNA was synthesized using Superscript III and real time assays were performed with Power SYBR green PCR master mix (Applied Biosystems) according to the manufactures recommendations. Normalization was carried out using a LpGAPDH primer set (Petersen *et al*., 2004). Normalised relative quantities were calculated using QBase (Hellemans *et al*., 2007). Reaction specificity was demonstrated by performing dissociation analysis.

3.3.7 Real-time RT-PCR profiling of Lfd03 (performed by SLB)

The expression profile of fructan:fructan 6G-fructosyltransferase (6G-FFT) was characterized in both Cashel and PI 462336 genotypes during stress and control treatments using real-time RT PCR as described above. For this purpose the drought stress experiment was repeated as described previously. Leaf and root material was harvested from stressed and control plants at time 0, + 4 hours, + 24 hours and + 1 week PEG induced drought stress. Two independent biological replicates were collected at each time point and for real-time analysis three technical replicates were performed for each PCR reaction.

3.3.8 Leaf blade fructan extraction and analysis

A targeted metabolite fingerprinting approach was used in order to analyse fructan profile response to water stress in both Cashel and PI 462336 genotypes. For this purpose the drought experiment was repeated and material was collected as described above and leaf

samples were collected from stressed and control plants at time 0, +24 hours and +1 week. Plant leaves were then flash frozen in liquid nitrogen immediately after harvesting, freeze dried and then homogenized using tungsten beads in a retsch mill. Frozen tissue powder (approximately 10 mg accurately weighted and recorded) was extracted twice with 20% methanol (v/v) in portions of 660 µL at 100 ºC for 15 min each time. In order to adsorb phenolic compounds, insoluble polyvinylpyrrolidone (PVP, Sigma-Aldrich) was added in the extraction steps. The pooled extracts were further extracted with water-saturated *n*-butanol and the final water phase was analysed by HPLC.

Carbohydrate content analysis was performed on an anionic exchange column PA-1 (Dionex Sunnyvale, CA, USA) using a Dionex HPLC system ICS-3000 equipped with an amperometric detector as described by Sprenger *et al*. (1997). Samples were eluted initially with 100 mM NaOH for 2 mins at a flow rate of 1 ml min^{-1}. Monosaccharides were then eluted in a gradient of NaOH from 100 mM to 300 mM from 2 to 7 min at a flow rate of 1 ml min^{-1}. Disaccharides and carbohydrates with a degree of polymerization (DP) >2 were then separated by a gradient of 0–500 mM sodium acetate in 300 mM NaOH from 7 to 32 min, at the same flow rate. Product identification was done using retention times that were determined by pure and defined standards. Maltose polymers with different DP, such as maltotriose, maltotetraose, maltopentose, maltohexose and maltoheptose, were used in combination with chicory fructooligosaccharide standards to determine the approximate DP of the metabolites in leaf tissue (Appendix B).

3.4 Results

3.4.1 Physiological assessment of PEG-induced water stress

The extent of physiological adaptations of 16 *L. perenne* genotypes to water-limitation, achieved in a medium containing 15% of PEG, was assessed by monitoring the relative water content in leaves and the ratio of [root]:[above-ground] fresh biomass. The general response of plants grown in a medium containing 15% of PEG was an increase in the [root]:[above-ground] fresh biomass ratio which may result from either an increase of root growth, a decrease in shoot growth or both (Figure 3.1a). However, this increase in root ratio is only significant ($p<0.05$) for L019-31, L023-10 and L023-22 genotypes. Furthermore, although the RWC of leaf tissue experiences an overall decrease in all genotypes (Figure 3.1b), that difference was only statistically significant in 4 genotypes (J43, J51, S13 and T42/45/6/8/9B219/12). In summary, the majority of genotypes seem to experience an increase in [root]:[shoot] ratio and a reduction of the RWC upon exposure to stress.

3.4.2 Differential physiological response of genotypes to a PEG-induced drought stress

The accession PI 462336 was obtained from the germplasm resource information network (GRIN) collection since it was annotated in the GRIN database as drought tolerant. Initial experimentation focused on verifying superior drought tolerance. Accession Cashel was

selected as a representative example of an Irish perennial ryegrass variety which was not documented to have particular sensitivity or tolerance to drought.

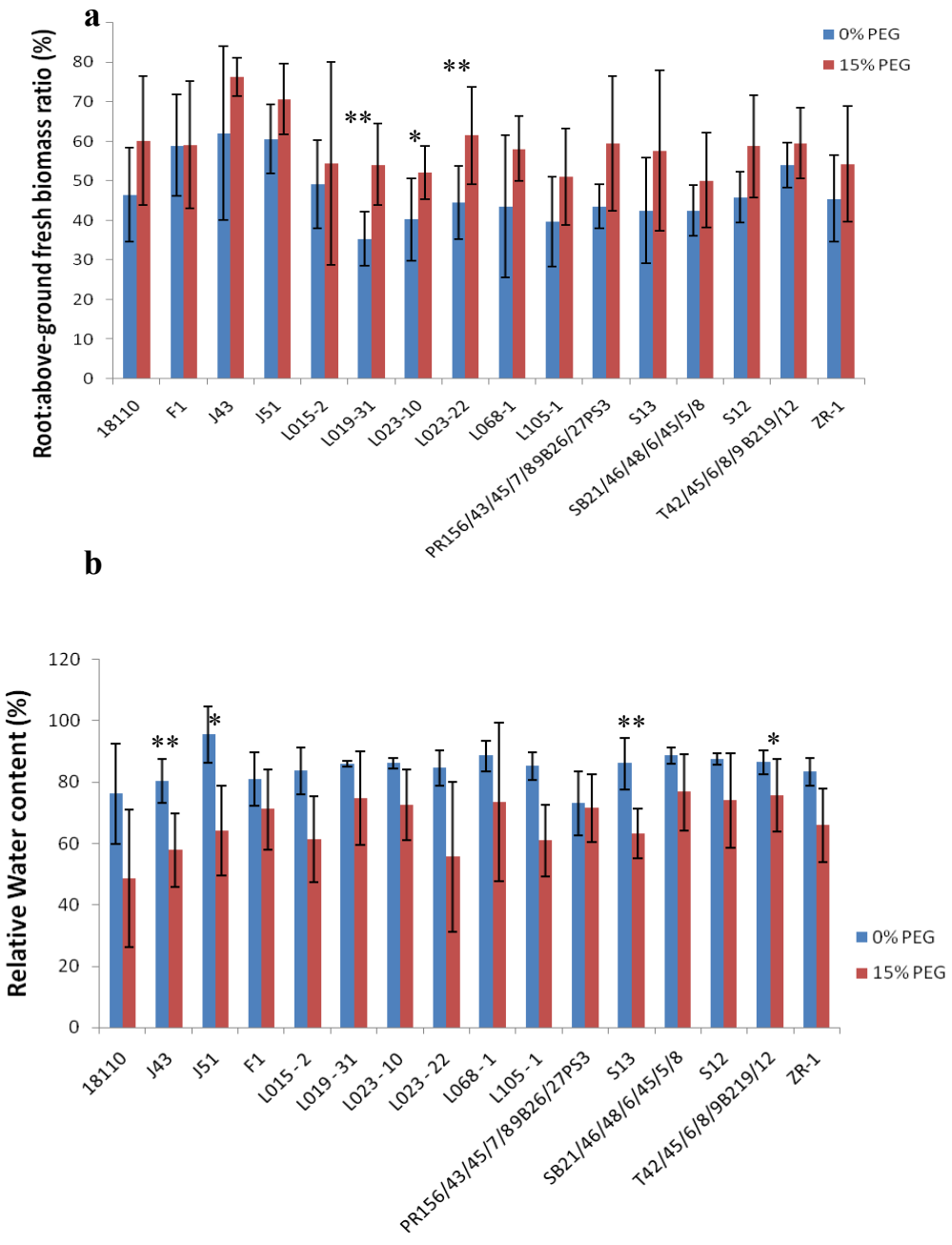

Figure 3.1 – Physiological reactions of 16 different *L. perenne* genotypes screened after a period of 1-week of exposure to either medium with either 0% or 15% PEG (a) ratio of the root:above ground fresh biomass.. (b) overall RWC levels of the 16 genotypes. (* *P<0.05*. ** *P<0.01* N=6)

Individual genotypes from the accession PI 462336 and the cultivar Cashel were subjected to a 20% PEG-induced drought stress in periods of one week in order to compare their performance. In order to further enhance stress conditions, the PEG concentration was adjusted to 20% from 15% as used in the screening experiment. After a one week period of water limitation, PI 462336 genotypes displayed higher relative water content (RWC) compared to Cashel (Figure 3.2a). The RWC of Cashel genotypes decreased to 46% after 24 hrs of exposure to stress, and those levels remained relatively stable after a period of one week, despite the small increase of the RWC levels to 52%. In contrast, PI 462336 did not experience significant changes in the RWC as a result of exposure to water-limiting conditions. Both genotypes appeared to have similar root growth rates under control conditions (Figure 3.2b). However, upon 1 week of water limitation, PI 462336 increased its root growth relative to both the controls and Cashel under stress (Figure 3.2b and 3.2c). After a 2 week period of exposure to water-stress the visual differences between genotypes was remarkable (Figure 3.3). These results demonstrate that, when the selected genotypes grown under PEG-mediated water-limiting conditions, they respond differently at the physiological level.

3.4.3 Identification of transcripts up-regulated in PI 462336 root and leaf tissue under PEG-induced water stress.

Suppression Subtractive Hybridization (SSH) was used to generate two subtracted libraries for leaf and root tissue enriched for genes up-regulated in the more drought tolerant PI 462336 accession after one week of a PEG-induced drought stress. In total, 384 clones were randomly selected from each library and analyzed by differential screening using a cDNA

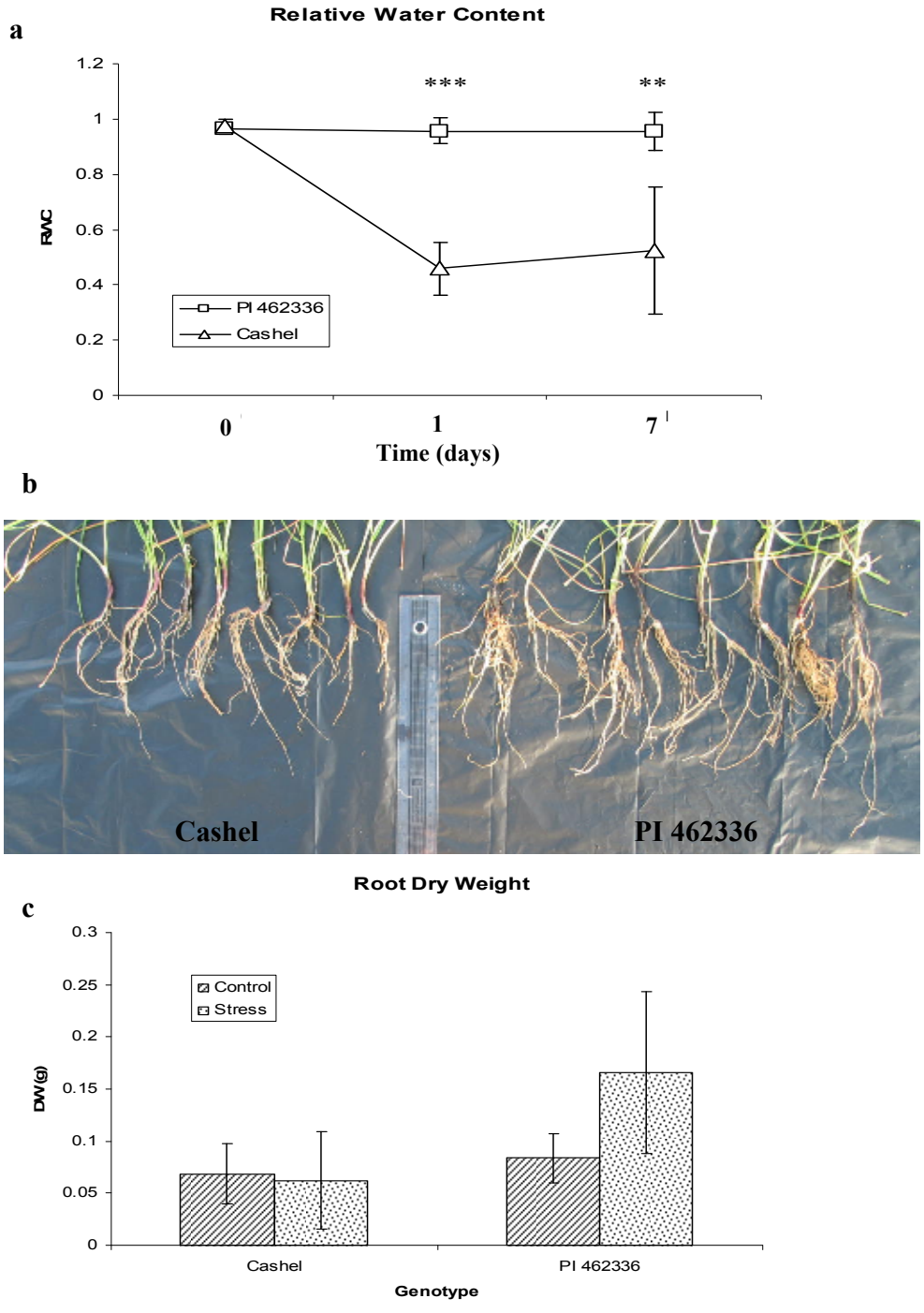

Figure 3.2 - Physiological plant reactions to the PEG-induced drought stress experiment (a) Relative water content (RWC) levels of Cashel and PI 462336 under PEG induced drought stress during 1 week of drought stress (b) Root biomass of PI 462336 in comparison to Cashel under PEG induced drought stress after 2 weeks. (c) Root dry weight of Cashel and PI 462336 genotypes under control conditions and PEG induced drought stress after 2 weeks (** difference significant at *P<0.01* N=8) (** *P<0.01*. *** *P<0.001* N=6).

dot blot approach. They were probed with stressed and control PI 462336 material to identify transcripts up-regulated under drought stress.

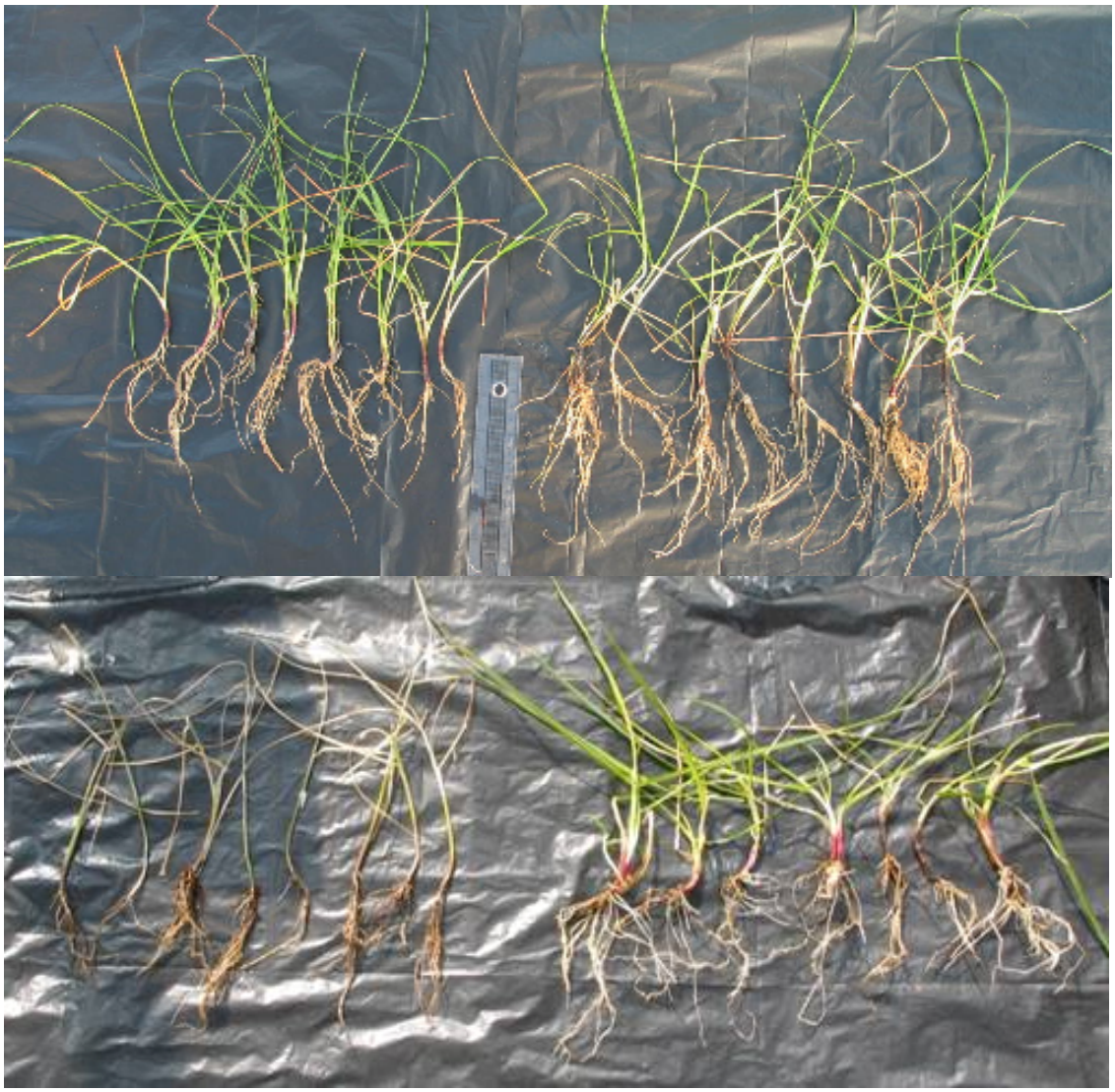

Figure 3.3 - Visual comparison between Cashel (left) and PI 462336 (right) genotypes after being exposed to PEG-induced water stress for a period of 1 week (top) and 2 weeks (bottom).

From this, 96 clones showing the strongest up-regulation were selected from each library and sequenced. Comparison of sequences from the leaf-subtracted library to known sequences in the NCBI database identified 38 non-redundant sequences with significant homology (Table 3.1). Three transcripts (Lfe06, Lfd01 and Lfa07) were present multiple times in the library.

The root-subtracted library revealed only 15 non-redundant sequences with significant homology to known plant sequences (Table 3.2). The majority of the sequences identified in the root library matched to ribosomal genes from fungi (data not shown). Although no major differences were observed, this may indicate fungal growth around roots being more prevalent in the PEG than the control solution, resulting in enrichment of their genes in the subtracted library. The transcripts Lfg01 and Rtb09, with homology to a dehydration responsive element binding (DREB) transcription factor and an aquaporin, respectively, were identified in the leaf- and root-subtracted libraries, respectively.

Real-time RT-PCR was employed to verify differential expression of a number of transcripts from both libraries (Tables 3.1 and 3.2). The genes with the highest up-regulation under water-stress included a vacuolar processing enzyme, DUF6 domain containing protein, thioredoxin F isoform, putative esterase D, glycosyl transferase family 8 protein, peroxisomal ascorbate peroxidase, MADS-box protein 3, sulphate transporter protein, ThiC, exonuclease family protein and a ubiquitin conjugating enzyme. In the root,choline phosphate cytidyl transferase exhibited a significant increase in expression.

Table 3.1- Putative functions assigned to SSH transcripts from the leaf library after TBLASTX analysis on NCBI: SSH ID (The numbers in brackets show the number of times that particular transcript appeared in the library), accession number assigned to SSH ID in public database, homology to gene in database, species to which gene is homologous, E.values of database hits, percent identity and expression of transcript under PEG induced drought stress relative to control.

SSH ID (Hits)*	Acc No.	Putative Function	Species	E.value	aa/aa id (%)	Relative expression (rest P value)*
LFa01	GE298826	NAD-dependent epimerase/dehydratase family protein	*O. sativa*	3e-39	70/80 (87%)	0.109 (0.179)
LFa02	GE298827	Ubiquitin domain containing protein	*O. sativa*	3e-13	34/40 (85%)	
LFa04	GE298828	NADH dehydrogenase subunit 9	*L. angustifolius*	3e-38	64/65 (98%)	
LFa05	GE298829	Glycosyl transferase, family 8 protein	*O. sativa*	3e-114	172/188 (91%)	1.959 (0.000)
LFa06	GE298830	putative thiamine biosythesis protein ThiC	*P. secunda*	2e-57	55/61 (90%)	1.905 (0.003)
LFa07 (10)	GE298831	photosystem II associated 10kD protein	*H. vulgare*	1e-40	64/90 (71%)	
LFa09	GE298832	DUF6 domain containing protein	*O. sativa*	7e-27	61/69 (88%)	63.157 (0.000)
LFa10	GE298833	tRNA-binding arm domain containing protein	*O. sativa*	5e-30	60/79 (75%)	
LFa12	GE298834	peroxisomal ascorbate peroxidase	*T. aestivum*	1e-71	127/134 (94%)	1.336 (0.045)
LFb04	GE298835	CYTOCHROME C-2	*A. thaliana*	1e-07	24/25 (96%)	
LFb05	GE298836	adenosine 5'-phosphosulfate reductase6	*Z. mays*	6e-14	24/36 (66%)	1.181 (0.402)
LFb09	GE298837	MADS-box protein 3	*H. vulgare*	7e-08	18/26 (69%)	2.062 (0.008)
LFb11	GE298838	one helix protein	*D. antarctica*	2e-76	123/146 (84%)	
LFc02	GE298839	vacuolar protein sorting 55 containing protein	*O. sativa*	4e-46	74/86 (86%)	0.902 (0.658)
LFc03	GE298840	60S ribosomal protein L19	*O. sativa*	1e-18	29/39 (74%)	
LFc06	GE298841	Vacuolar processing enzyme, alpha-isozyme precursor	*O. sativa*	2e-70	111/135 (82%)	3.683 (0.000)
LFd01 (3)	GE298842	ribulose-1,5-bisphosphate carboxylase/ oxygenase large subunit	*L. perenne*	2e-72	110/110 (100%)	
LFd03	GE298843	fructan:fructan 6G-fructosyltransferase	*L. perenne*	3e-122	139/140 (99%)	0.871 (0.805)
LFd07	GE298844	thioredoxin F isoform	*O. sativa*	4e-19	25/43 (58%)	1.155 (0.016)
LFd09	GE298845	Arf1_5/ArfA-family small GTPase	*P. patens*	1e-64	103/109 (94%)	1.050 (0.804)
LFd10	GE298846	sucrose synthase type 1	*T. aestivum*	4e-11	17/29 (58%)	
LFe01	GE298847	Putative Esterase D	*O. sativa*	9e-33	59/69 (85%)	94.431 (0.000)
LFe05	GE298848	Vacuolar protein sorting 29	*O. sativa*	4e-106	156/162 (96%)	1.251 (0.111)
LFe07	GE298849	1-acylcerol-3-phosphate acyltransferase-like protein	*O. sativa*	4e-66	107/117 (91%)	
LFe08	GE298850	unknown function DUF298 family protein	*O. sativa*	4e-28	53/58 (91%)	
LFe11	GE298851	Ubiquitin-conjugating enzyme E2	*O. sativa*	2e-83	126/131 (96%)	1.410 (0.045)
LFf01	GE298852	Sulphate transporter protein	*O. sativa*	4e-115	180/196 (91%)	2.073 (0.000)
LFf03	GE298853	Translation initiation factor SUI1 family protein	*O. sativa*	1e-27	53/61 (86%)	
LFf05	GE298854	asparaginyl endopeptidase	*O. sativa*	2e-70	111/135 (82%)	
LFf06 (2)	GE298855	23S ribosomal RNA gene	*F. arundinacea*	2e-38	67/67 (100%)	
LFf07	GE298856	cysteine protease	*L. multiflorum*	3e-30	52/54 (96%)	
LFg01	GE298857	DREB transcription factor 5A	*T. aestivum*	2e-36	52/80 (65%)	1.194 (0.551)
LFg03	GE298858	Mitochondrial basic amino acid carrier	*O. sativa*	2e-47	90/107 (84%)	1.262 (0.347)
LFg05	GE298859	Unknown	*H. vulgare*	5e-19	18/29 (62%)	
LFg07	GE298860	Unknown	*H. vulgare*	1e-04	13/21 (61%)	
LFh03	GE298861	atp-2 mRNA for ATP synthase beta subunit	*T. aestivum*	2e-30	31/36 (86%)	1.0364 (0.487)
LFh05	GE298862	Unknown	*H. vulgare*	4e-07	24/34 (70%)	
LFh11	GE298863	exonuclease family protein	*A. thaliana*	1e-40	67/100 (67%)	1.570 (0.079)

*Mean factor by which the transcript is up-regulated in stress tissue compared with control. Value in parenthesis is the P values generated using REST 08 and are associated with the alternative hypothesis that the difference between the control and stress group is due to chance. Results are based on three biological replicates, each performed in triplicate.

3.4.4 Comparison of the metabolic profiles of Cashel and PI 462336 leaf and root tissues under control and water stress

Results for quality control assessments and assurance of metabolite analysis are shown and described in Appendix A. The relative metabolite levels of root and leaf tissues of Cashel and PI 462336 grown over 1 week of induced water-limitation or control conditions were compared. Principal component analysis (PCA) (Figure 3.4) was performed using data for all measured metabolites and revealed a separation between root and leaf tissues by the first component, which represented about 23.9% of the variation between samples. The fourth component differentiated the tissues submitted to drought from the control explaining 6.9% of the variation. PCA plots for the second and third principal components are represented in Appendix A (Figure A.4).

Table 3.2: Putative functions assigned to SSH transcripts from the root library after BLASTX analysis on NCBI: SSH ID (The numbers in brackets show the number of times that particular transcript appeared in the library), accession number assigned to SSH ID in public database, homology to gene in database, species to which gene is homologuous, E.values of database hits, percent identity and expression of transcript under PEG induced drought stress relative to control, as determined by real time RT-PCR analysis.

SSH ID (Hits)	Acc No.	Homology	Species	E. value	aa/aa id (%)	Relative expression (rest P value)*
RTa05	GE298811	wali7	*T. aestivum*	9e-26	21/21 (100%)	
RTa07	GE298812	putative transcription factor gene	*Z. mays*	1e-24	43/49 (87%)	
RTa08 **(2)**	GE298813	ATP/ADP translocator	*O. sativa*	1e-14	20/40 (50%)	
RTb04	GE298814	Unknown	*H. vulgare*	9e-04	19/26 (73%)	
RTb09	GE298815	HvPIP1;4 mRNA for aquaporin	*T. aestivum*	1e-68	112/118 (94%)	0.973 (0.919)
RTc04	GE298816	Choline phosphate cytidylyltransferase	*O. sativa*	5e-30	54/55 (98%)	44.068 (0.000)
RTc06	GE298817	18S ribosomal RNA	*S. cereale*	9e-99	151/155 (97%)	
RTc08	GE298818	benzothiadiazole-induced homeodomain protein 1	*O. sativa*	6e-10	21/26 (80%)	
RTe06	GE298819	vacuolar proton-ATPase subunit A	*T. aestivum*	2e-74	105/107 (98%)	0.966 (0.865)
RTe08	GE298820	polyubiquitin	*N. tabacum*	5e-40	73/77 (94%)	
RTg04	GE298821	cytochrome P450	*A. strigosa*	5e-13	24/28 (85%)	
RTg07	GE298822	glycine-rich RNA-binding protein	*L. perenne*	4e-31	58/64 (90%)	
RTg10	GE298823	type 1 membrane protein, putative	*A. thaliana*	8e-09	29/46 (63%)	
RTh06	GE298824	Unknown	*H. vulgare*	2e-12	36/64 (56%)	
RTh10	GE298825	S25 ribosomal protein family protein	*O. sativa*	2e-22	48/53 (90%)	

*Mean factor by which the transcript is up-regulated in stress tissue compared with control. Value in parenthesis is the P values generated using REST 08 and are associated with the alternative hypothesis that the difference between the control and stress group is due to chance. Results are based on three biological replicates, each performed in triplicate.

Samples of Cashel leaf tissue responded to water-limitation by segregating from the control leaf samples as well as from PI 462336 leaf tissue samples. The leaf control samples from both varieties formed overlapping clusters revealing no significant segregation. PI 462336 leaf tissue samples of stressed plants formed a separate cluster from the respective control in the opposite direction of the Cashel water limited samples. In the root tissue, the control samples of both Cashel and PI 462336 appeared to cluster together in the same region. Upon water-limitation, a separation of the respective clusters was observed.

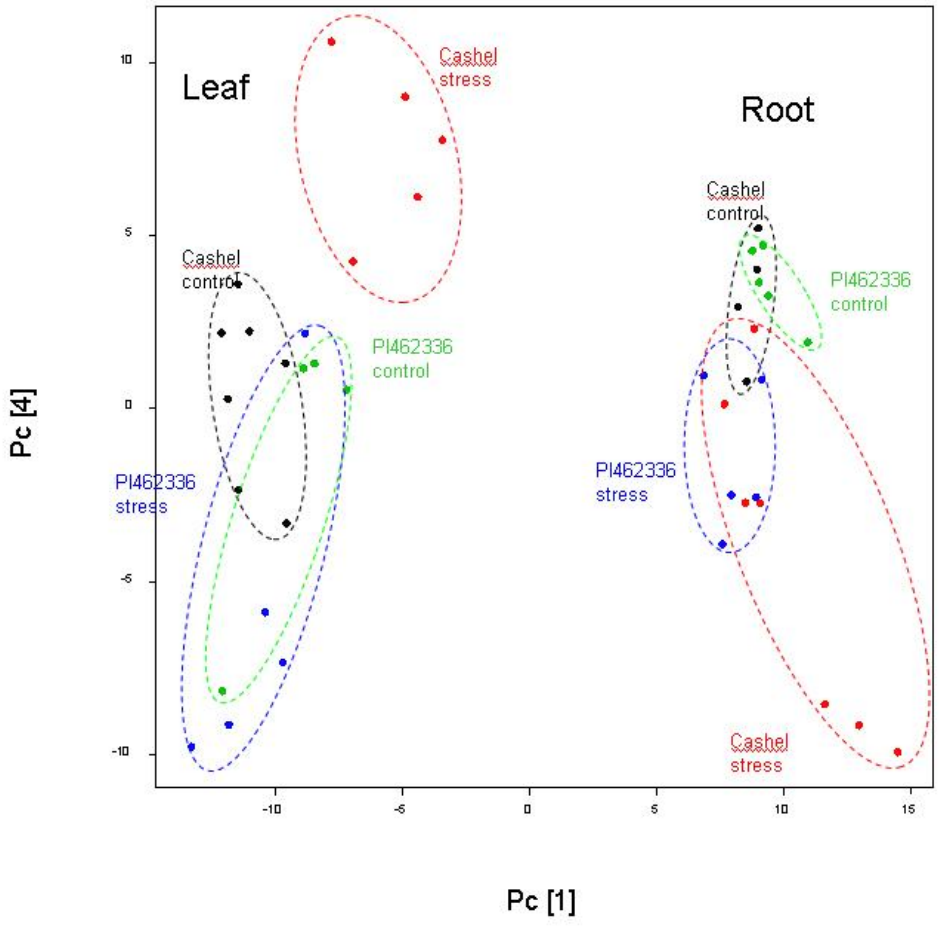

Figure 3.4- Principal component analysis (PCA) plot of all metabolite compounds found, following GC-TOF-MS analysis of the root and leaf tissues of Cashel and PI 462336. Components 1 and 4 explained up to 23.9% and 6.9% of the variation, respectively.

Both varieties experienced similar changes in their metabolic profiles following water-limitation and consequently segregating away from the control treatment.

3.4.5 The metabolic response of Cashel leaf and root tissue to water-limitation

The metabolite profiles of Cashel leaf and root tissue were compared for treatment effects by ANOVA. Metabolites showing significant differences ($P<0.05$) were identified, and fold changes were calculated for both tissues (Table 3.3). Following exposure to drought conditions a large number of metabolite levels decreased in the leaf tissue, including amino acids (10), fatty acids (12), fatty alcohols (4) and phytosterols (4). However, a small number of metabolites such as malic acid (2.0-fold), gluconic acid, (2.2-fold) docosane (8.0-fold), octadocane (12.2-fold) and eicosanoic acid (4.0-fold) increased upon drought. Similarly, the exposure of root tissue to water limitation resulted in a pronounced decrease of metabolite levels. Amino acids (6), fatty acids (8) and urea (61-fold decrease) were among the affected metabolites. An increase in metabolite levels was only experienced for sucrose (5.7-fold), γ-aminobutyric acid (2.2-fold) and n-ethydiethanoamine (1.9-fold).

3.4.6 The metabolic response of PI 462336 leaf and root tissue to water-limitation

The metabolite profiles of PI 432336 of both leaf and root tissue were analysed by ANOVA, as described above. Metabolites showing significant differences ($P<0.05$) were

Table 3.3 – Comparison between the levels of metabolites from Cashel plants under control conditions (0% PEG) and water-limiting conditions (20% PEG). Results are limited to putatively identified significant metabolites (P<0.05).

Metabolite	0% PEG average	Standard error of the mean	20% PEG average	Standard error of the mean	Log_{10}(Stress avg/ control avg)	p-value (uncorrected)
Leaf						
Eicosanoic acid	0.0001	0.0000	0.0004	0.0001	0.6021	0.043
Gluconic acid	0.0056	0.0016	0.0126	0.0040	0.3522	0.043
Malic acid	0.1675	0.0295	0.3285	0.0683	0.2925	0.032
Alanine	1.3817	0.2310	1.1916	0.6430	-0.0643	0.048
Hexadecanoic acid	1.5022	0.0437	1.1589	0.1080	-0.1127	0.007
Hexadecenoic acid	0.1084	0.0079	0.0643	0.0094	-0.2268	0.004
Hexacosanol	3.5604	0.3030	1.8909	0.5980	-0.2748	0.020
β-Sitosterol	0.1440	0.0086	0.0677	0.0117	-0.3278	0.000
2,3-Dihydroxypropanoic acid	0.0727	0.0100	0.0333	0.0050	-0.3391	0.011
Putrescine	0.0504	0.0070	0.0228	0.0058	-0.3445	0.048
Serine	0.4388	0.0616	0.1964	0.0756	-0.3491	0.008
Proline	1.7626	0.3290	0.7661	0.3660	-0.3619	0.011
Valine	0.1827	0.0196	0.0767	0.0227	-0.3769	0.012
Phosphate	1.3652	0.3400	0.5494	0.2200	-0.3953	0.005
4- or 3-hydroxy-cinnamic acid	0.0098	0.0021	0.0036	0.0008	-0.4349	0.028
(n-9)Octadecenoic acid	0.0602	0.0061	0.0214	0.0078	-0.4492	0.002
Hexadecenoic acid ethyl ester	0.0017	0.0004	0.0006	0.0002	-0.4523	0.036
Threonine	0.1268	0.0151	0.0405	0.0182	-0.4957	0.015
(n-9)Tetracosenoic acid	0.0017	0.0004	0.0005	0.0002	-0.5315	0.023
Phytol C	0.0201	0.0031	0.0057	0.0015	-0.5473	0.003
(n-6)Octadecadienoic acid	0.4883	0.0489	0.1336	0.0304	-0.5629	0.000
Aspartic acid	0.3832	0.0674	0.1031	0.0268	-0.5702	0.001
Glutamic acid	0.4611	0.1430	0.1211	0.0079	-0.5807	0.000
Phytyl methyl ether	0.1861	0.0153	0.0469	0.0061	-0.5986	0.000
Phytol B	0.0282	0.0018	0.0068	0.0011	-0.6177	0.000
Campesterol	0.0589	0.0034	0.0137	0.0027	-0.6334	0.000
Stigmasterol	0.0096	0.0011	0.0022	0.0007	-0.6398	0.000
Ergost-7-en-3-ol	0.0122	0.0021	0.0024	0.0009	-0.7061	0.002
5-Oxoproline	3.4160	0.3930	0.5887	0.1960	-0.7636	0.000
anteiso-Hexadecanoic acid methyl ester	0.0063	0.0013	0.0011	0.0004	-0.7579	0.005
Phytyl methyl ether 2nd peak	0.7502	0.0270	0.1165	0.0192	-0.8089	0.000
Ornithine	0.0545	0.0164	0.0085	0.0056	-0.8070	0.022
Tricosane	0.0558	0.0054	0.0086	0.0018	-0.8121	0.000
(n-3)Octadecatrienoic acid	2.2589	0.1550	0.3258	0.0527	-0.8409	0.000
3- or 4-hydroxy-cinnamic acid	0.0041	0.0009	0.0005	0.0002	-0.9138	0.007
Nonadecanoic acid	0.0246	0.0029	0.0020	0.0005	-1.0899	0.000
Phytol	0.0709	0.0083	0.0052	0.0026	-1.1346	0.000
Glutamine	0.0443	0.0130	0.0029	0.0013	-1.1840	0.050
Root						
Sucrose	0.2136	0.0493	1.2152	0.2820	0.7550	0.010
γ-Aminobutyric acid	0.0545	0.0093	0.1181	0.0230	0.3359	0.048
n-Ethydiethanoamine	0.2409	0.0568	0.4667	0.3620	0.2872	0.017
Serine	0.0650	0.0119	0.0561	0.0287	-0.0640	0.015
Phosphate	0.5327	0.0573	0.2952	0.2030	-0.2564	0.000
Glutamic acid	0.1180	0.0212	0.0622	0.0115	-0.2781	0.041
Aspartic acid	0.1647	0.0120	0.0866	0.0594	-0.2792	0.000
2-Hydroxydocosanoic acid	0.0155	0.0014	0.0065	0.0013	-0.3774	0.002
Eicosanoic acid	0.0390	0.0044	0.0162	0.0025	-0.3815	0.001
Glycerol	0.0623	0.0157	0.0249	0.0070	-0.3983	0.006
Pentadecanoic acid	0.0211	0.0008	0.0079	0.0025	-0.4267	0.005
Phytyl methyl ether 2nd peak	0.0189	0.0007	0.0071	0.0011	-0.4252	0.000
Hexadecanoic acid	1.3919	0.1670	0.5209	0.0987	-0.4269	0.001
Ergost-7-en-3-ol	0.0089	0.0010	0.0033	0.0009	-0.4309	0.004
Phytyl methyl ether	0.0050	0.0003	0.0018	0.0004	-0.4437	0.000
Threonine	0.0182	0.0055	0.0058	0.0019	-0.4966	0.037
(n-3)Octadecatrienoic acid	0.3517	0.0491	0.1060	0.0257	-0.5209	0.001
Asparagine	0.0536	0.0055	0.0161	0.0065	-0.5229	0.007
Putrescine	0.0522	0.0134	0.0145	0.0065	-0.5563	0.005
(n-6)Octadecadienoic acid	1.2505	0.1680	0.3244	0.0870	-0.5860	0.000
Tricontanol	0.0030	0.0006	0.0006	0.0003	-0.6990	0.002

5-Oxoproline	2.6083	0.5120	0.5427	0.4270	-0.6818	0.000

Table 3.3 (continued)

Allantoin	0.0056	0.0005	0.0010	0.0007	-0.7482	0.003
Tricosane	0.0024	0.0003	0.0004	0.0002	-0.7782	0.000
Ribose	0.0090	0.0021	0.0016	0.0005	-0.7501	0.002
Caffeic acid	0.0027	0.0011	0.0003	0.0002	-0.9542	0.025
Sorbitol	0.0052	0.0025	0.0005	0.0002	-1.0170	0.034
Tricontanoic acid	0.0037	0.0006	0.0003	0.0001	-1.0911	0.000
2,3,4-Trihydroxybutyric acid	0.0009	0.0005	0.0001	0.0000	-0.9542	0.033
Phytol	0.0041	0.0015	0.0002	0.0002	-1.3118	0.004
Urea	0.0119	0.0038	0.0002	0.0001	-1.7745	0.002

identified, and fold changes were calculated for both tissues (Table 3.4). In the leaf tissue, the metabolomic response appeared to be different from the leaves of Cashel. A decrease in the levels of amino acids (8), some fatty acids (2) and fatty alcohols (2), in addition to a noticeable decrease in the levels of allantoin, was found. However, the most prominent trend was revealed by the upregulated metabolites, which included sugars (raffinose with 15.4-fold, glucose with 8.7-fold, trehalose with 6.9-fold, fructose with 5.3-fold and maltose with 3.4-fold), inositol (2.4-fold), shikimic acid (7.1-fold) and allantoic acid (14.1-fold). In PI 462336 root samples a similar trend was observed as described with Cashel root tissue. There was a decrease in the levels of amino acids (10), fatty acids (18), phytosterols (3) and urea (78.9-fold decrease). However, the upregulated metabolites, which included fumaric acid (2.8-fold), raffinose (4.6-fold), dotriacontanoic acid (5.0-fold) and hydroxylamine (8.3-fold) were not common across genotypes.

3.4.7 Comparison of the metabolite profiles of both genotypes under control and water stress conditions

The metabolic complements of root and leaf tissue of Cashel and PI 462336, grown for one week in control media, were compared in an initial analysis. Metabolite profiles of the

Table 3.4 – Comparison between the levels of metabolites from PI 432336 plants under control conditions (0% PEG) and water-limiting conditions (20% PEG). Results are limited to putatively identified significant metabolites (P<0.05).

Metabolite	0% PEG average	Standard error of the mean	20% PEG average	Standard error of the mean	Log_{10}(Stress avg/ control avg)	p-value
Leaf						
Raffinose	0.0292	0.0118	0.4495	0.1310	1.1873	0.034
Allantoic acid	0.0001	0.0001	0.0020	0.0006	1.3010	0.019
Glucose	0.1391	0.0183	1.2093	0.1800	0.9392	0.002
Shikimic acid	0.0830	0.0177	0.5884	0.1580	0.8506	0.042
Trehalose	0.0043	0.0016	0.0295	0.0072	0.8364	0.032
Fructose	0.2754	0.0235	1.4566	0.0973	0.7234	<0.001
Maltose	0.0124	0.0038	0.0426	0.0036	0.5366	0.014
Inositol	0.1310	0.0123	0.3142	0.0342	0.3799	0.007
Octadecanol	0.1067	0.0156	0.0577	0.0094	-0.2670	0.028
Docosanol	0.0457	0.0054	0.0214	0.0059	-0.3295	0.030
Valine	0.1782	0.0396	0.0827	0.0173	-0.3334	0.044
Serine	0.2933	0.0593	0.1300	0.0271	-0.3534	0.026
Alanine	1.2087	0.2070	0.4718	0.1450	-0.4086	0.031
Glutamic acid	0.2728	0.0521	0.0875	0.0102	-0.4938	0.007
Proline	2.0180	0.1650	0.5410	0.1450	-0.5717	0.001
Ornithine	0.0148	0.0038	0.0023	0.0008	-0.8085	0.009
Aspartic acid	0.2810	0.0350	0.0385	0.0076	-0.8632	0.000
anteiso-Pentadecanoic acid	0.0006	0.0002	0.0001	0.0001	-0.7782	0.040
Asparagine	0.1226	0.0317	0.0073	0.0037	-1.2241	0.013
5-Oxoproline	5.5586	1.4740	0.0939	0.0211	-1.7723	0.004
Allantoin	0.0008	0.0003	0.0000	0.0000	n.d.	0.021
Root						
Hydroxylamine	0.0270	0.0091	0.2250	0.0590	0.9208	0.031
Dotriacontanoic acid	1.2E-05	0.0000	0.0001	0.0000	0.9208	0.024
Raffinose	0.0306	0.0055	0.1399	0.0508	0.6601	0.029
Fumaric acid	0.0045	0.0007	0.0126	0.0041	0.4472	0.011
Ornithine	0.0058	0.0010	0.0038	0.0023	-0.1836	0.016
Octadecanol	0.0787	0.0090	0.0478	0.0080	-0.2165	0.028
Threonine	0.0273	0.0049	0.0158	0.0054	-0.2375	0.021
Serine	0.0894	0.0136	0.0518	0.0186	-0.2370	0.010
iso-Pentadecanoic acid	0.0226	0.0044	0.0125	0.0017	-0.2572	0.026
Tyrosine	0.0052	0.0007	0.0028	0.0008	-0.2688	0.009
Octadecenoic acid	0.2669	0.0402	0.1353	0.0061	-0.2951	0.009
Octadecanoic acid	0.1232	0.0130	0.0611	0.0053	-0.3046	0.001
Alanine	1.0166	0.2040	0.5015	0.1670	-0.3069	0.043
Pentadecanoic acid	0.0191	0.0014	0.0089	0.0012	-0.3316	0.000
Heptadecanoic acid	0.0131	0.0015	0.0058	0.0012	-0.3538	0.003
Hexadecanoic acid	0.0330	0.0059	0.0145	0.0038	-0.3571	0.025
2-Hydroxyeicosanoic acid	0.0314	0.0024	0.0135	0.0026	-0.3666	0.001
Hexadecenoic acid	1.2530	0.0880	0.5358	0.0582	-0.3689	0.000
Tetradecanoic acid	0.0958	0.0191	0.0403	0.0054	-0.3761	0.019
Stigmasterol	0.0381	0.0071	0.0154	0.0029	-0.3934	0.014
Glutamic acid	0.1427	0.0189	0.0575	0.0193	-0.3948	0.001
Pentacosanoic acid	0.0183	0.0021	0.0073	0.0013	-0.3991	0.001
Tricosanoic acid	0.0264	0.0026	0.0102	0.0017	-0.4130	0.000
Campesterol	0.2332	0.0240	0.0878	0.0098	-0.4242	0.000
Tetracosanoic acid	0.0706	0.0081	0.0266	0.0047	-0.4239	0.001
β-Sitosterol	0.2181	0.0244	0.0807	0.0089	-0.4318	0.000
(n-9)Tetracosenoic acid	0.0124	0.0014	0.0045	0.0010	-0.4402	0.001
2-Hydroxytetracosanoic acid	0.0699	0.0090	0.0241	0.0052	-0.4625	0.001
Phytyl methyl ether 2nd peak	0.0237	0.0057	0.0080	0.0006	-0.4717	0.022
2-Hydroxydocosanoic acid	0.0214	0.0026	0.0072	0.0017	-0.4731	0.001
Phytyl methyl ether 1st peak	0.0074	0.0019	0.0024	0.0003	-0.4890	0.028
(n-6)Octadecadienoic acid	0.9109	0.0664	0.2922	0.0440	-0.4938	0.000
(n-3)Octadecatrienoic acid	0.3410	0.0541	0.1022	0.0154	-0.5233	0.002
Ribose	0.0139	0.0008	0.0036	0.0015	-0.5867	0.000
Allantoin	0.0054	0.0006	0.0014	0.0009	-0.5863	0.001
Homoserine	0.0037	0.0006	0.0009	0.0005	-0.6140	0.000
Aspartic acid	0.1300	0.0181	0.0313	0.0128	-0.6184	0.000
Asparagine	0.1450	0.0210	0.0261	0.0257	-0.7464	<0.001
Putrescine	0.0669	0.0041	0.0102	0.0041	-0.8168	0.000

Table 3.4 (continued)

Glutamine	0.0284	0.0055	0.0037	0.0024	-0.8851	0.001
Phosphate	0.9316	0.1660	0.1062	0.0369	-0.9431	0.002
Diamino-1,3-propane	0.0136	0.0029	0.0009	0.0004	-1.1793	0.005
Tricosane	0.0032	0.0010	0.0001	0.0001	-1.5051	0.013
5-Oxoproline	8.5887	1.8910	0.1884	0.0898	-1.6588	0.002
Urea	0.0107	0.0034	0.0001	0.0001	-2.0294	0.010

leaves (Table 3.5) revealed that substituted cinnamic acid (2.7-fold), octadecenoic acid (1.8 fold) and octadecanol (1.4-fold) were significantly higher in PI 462336, whilst conversely phytil methyl ether (1.4-fold), maltose (2.2-fold), threonine (2.3-fold) and raffinose (3.2-fold) were significantly higher in Cashel. In root tissue (Table 5) the levels of amino acids such as alanine (4.2-fold), 5-oxoproline (3.3-fold), glutamine (2.8-fold) and asparagine (2.7-fold) together with the sugars fructose (2.0-fold) and glucose (1.9-fold), were higher in PI 462336. Cashel appeared to have higher levels of fatty alcohols such as docosanol (1.9-fold), hexacosanol (2.0-fold), tetracosanol (4.2-fold) and nonadecanol (18.1-fold). Overall, the differences under control conditions were not as pronounced as those under stress.

Table 3.5 – Comparison between the levels of metabolites from PI 432336 and Cashel plants under control conditions (0% PEG). Results are limited to putatively identified significant metabolites (P<0.05).

Metabolite	**Cashel**	**PI 462336**	**Log_{10}(PI 462336/ Cashel avg)**	**p-value**
Leaf				
4- or 3-hydroxycinnamic acid	0.0098	0.0268	0.4369	0.045
(n-7)Octadecenoic acid	0.0061	0.0107	0.2441	0.034
Octadecanol	0.0756	0.1067	0.1496	0.030
Phytyl methyl ether 2nd peak	0.7502	0.5415	-0.1416	0.001
Maltose	0.0283	0.0124	-0.3591	0.043
Threonine	0.1268	0.0541	-0.3699	0.034
Raffinose	0.0942	0.0292	-0.5087	0.020
Root				
Alanine	0.2428	1.0166	0.6219	0.009
5-Oxoproline	2.6083	8.5887	0.5176	0.025
Glutamine	0.0103	0.0284	0.4405	0.023
Asparagine	0.0536	0.1455	0.4336	0.004
γ-Aminobutyric acid	0.0545	0.1365	0.3987	0.019
Fructose	0.4920	0.9632	0.2918	0.014
Glucose	0.2523	0.4845	0.2834	0.009
Glyoxime	0.0663	0.1103	0.2211	0.042
Methoxy hydroxyl cinnamic acid	0.0475	0.0361	-0.1192	0.006
Docosanol	0.0109	0.0058	-0.2740	0.016
Hexacosanol	0.0285	0.0144	-0.2965	0.041
Heptadocane	0.0015	0.0006	-0.3979	0.029
Tetracosanol	0.0062	0.0015	-0.6163	0.004
Dotriacontanoic acid	0.0001	1.2E-05	-0.9208	0.031
Nonadecanol	0.0017	0.0001	-1.2304	0.005

Large differences under stress were expected due to the apparent differences in tolerance of the genotypes to a PEG induced water stress.In leaf tissue many metabolites responded differently to water-stress and the most notable trend was an overall higher level of metabolites present in PI 462336 (Table 3.6). Following the PEG treatment only glutamic acid (1.4-fold), allantoic acid (2.3-fold), sorbitol (2.5-fold) and the alkanes octadocane (9.8-fold) and docosane (84.6-fold) appeared to be significantly higher in Cashel. In PI 462336 quinic acid (18.5-fold) and shikimic acid (15.9-fold) showed significant higher levels compared with Cashel. However, changes were also observed in the levels of phytosterols (campesterol, stigmasterol and β-sitosterol with 4.1, 3.2 and 2.5-fold increase, respectively), raffinose (7.0-fold), inositol (3.3-fold) and fructose (2.4-fold) among many other metabolites. In root tissue, overall metabolite levels were also higher in PI 462336. The metabolites which accumulated to a higher level in PI 462336 (Table 3.6) were sorbitol (10.1-fold), cinnamic acid (5.1-fold), lysine (4.5-fold), tricontanol (3.5-fold) and the fatty acids eicosanoic acid (2.2-fold), anteiso-pentadecanoic acid (1.8-fold) and tetradecanoic acid (3.7-fold).

3.4.8 Real-time RT-PCR profiling of Lfd03

The expression profile of 6G-FFT was characterized in both Cashel and PI 462336 genotypes during stress and control treatments using real-time RT PCR. There was no significant trend in expression of 6G-FFT in response to water limitation in either genotype. However, dramatic differences in the expression of 6G-FFT were found between both genotypes. These differences were in the range of 1000-fold at all the different time-points sampled (Figure 3.5).

Table 3.6 – Comparison between the levels of metabolites from PI 432336 and Cashel plants under water-limiting conditions (20% PEG). Results are limited to putatively identified significant metabolites (P<0.05).

Metabolite	Cashel	PI 462336	Log_{10}(PI 462336/ Cashel avg)	p-value
Leaf				
Quinic acid	0.0230	0.4268	1.2685	0.033
Shikimic acid	0.0369	0.5884	1.2026	0.017
Nonadecanoic acid	0.0020	0.0163	0.9112	0.005
Phytol	0.0052	0.0421	0.9083	0.000
(n-3)Octadecatrienoic acid	0.3258	2.4271	0.8721	0.000
Raffinose	0.0644	0.4495	0.8438	0.030
Phytyl methyl ether 2nd peak	0.1165	0.7672	0.8186	0.000
Phytyl methyl ether 1st peak	0.0469	0.2714	0.7624	0.001
3 or 4-hydroxy-cinnamic acid	0.0005	0.0029	0.7634	0.007
(n-6)Octadecadienoic acid	0.1336	0.6593	0.6933	0.000
Phytol B	0.0068	0.0333	0.6899	0.000
Tricosane	0.0086	0.0415	0.6835	0.000
Campesterol	0.0137	0.0563	0.6138	0.000
4- or 3-hydroxy-cinnamic acid	0.0036	0.0135	0.5740	0.009
Inositol	0.0964	0.3142	0.5131	0.002
Stigmasterol	0.0022	0.0069	0.4964	0.008
(n-9)Tetracosenoic acid	0.0005	0.0015	0.4771	0.031
anteiso-Hexadecanoic	0.0011	0.0033	0.4771	0.001
Phytol C	0.0057	0.0164	0.4590	0.019
Ergost-7-en-3-ol	0.0024	0.0068	0.4523	0.023
(n-9)Octadecenoic acid	0.0214	0.0596	0.4448	0.018
β-Sitosterol	0.0677	0.1674	0.3932	0.002
Fructose	0.6000	1.4600	0.3862	0.026
2,3-Dihydroxypropanoic acid	0.0333	0.0737	0.3450	0.033
Hexadecanoic acid	1.1589	2.0178	0.2408	0.015
γ-Aminobutyric acid	0.3067	0.4409	0.1576	0.029
L-glutamic acid	0.1211	0.0875	-0.1411	0.012
Allantoic acid	0.0045	0.0020	-0.3522	0.014
Sorbitol	0.0021	0.0008	-0.4191	0.009
Root				
Phytol B	0.0000	0.0006	n.d.	0.042
Sorbitol	0.0005	0.0051	1.0086	0.018
4- or 3-hydroxy-cinnamic acid	0.0118	0.0596	0.7034	0.047
L-Lysine	0.0009	0.0042	0.6690	0.010
Tetradecanoic acid	0.0110	0.0403	0.5639	0.000
Tricontanol	0.0006	0.0022	0.5643	0.033
Eicosanoic acid	0.0162	0.0351	0.3358	0.001
antesiso-Pentadecanoic acid	0.0200	0.0359	0.2541	0.025

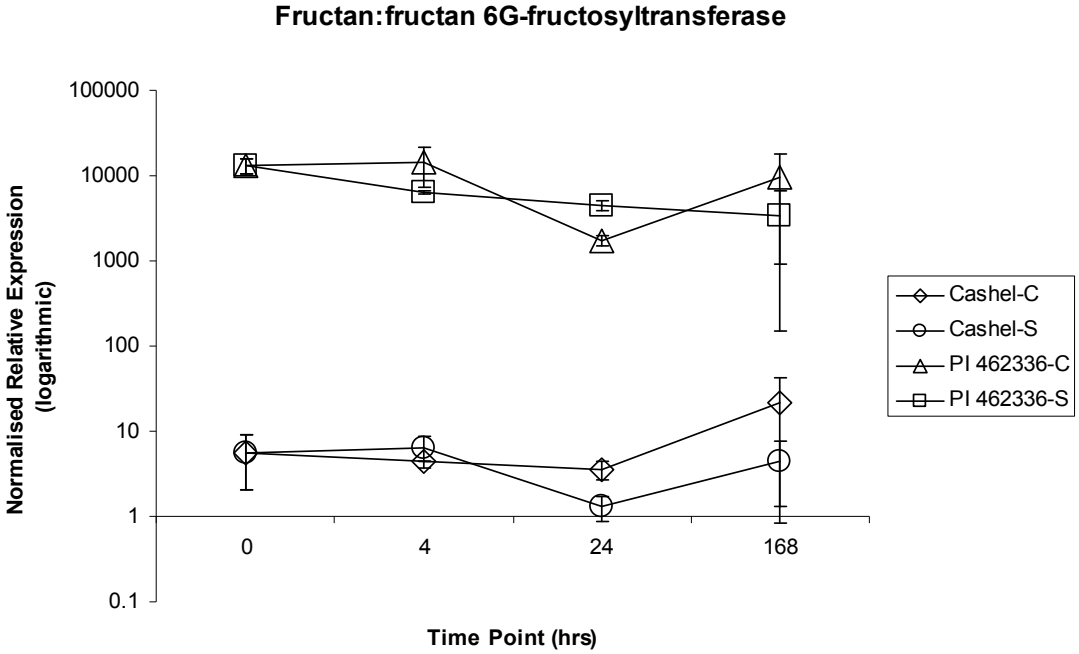

Figure 3.5 - Relative expression of fructan:fructan 6G-fructosyltransferase during 1 week of PEG induced water stress (S) and control conditions (C) in Cashel and PI 462336 leaf material. Biological replicates were each tested in triplicate and normalized to the LpGAPDH housekeeping gene and relative quantities calculated using qBase (Hellemans *et al*., 2007). The graph shows the average of the two biological replicates with their standard deviation.

3.4.9 Analysis of fructan content

In order to compare fructan levels with the expression levels of fructan:fructan 6G-fructosyl transferase in both genotypes under different conditions, fructans were extracted with a method adapted from Sprenger *et al.,* (1997). The approximate DP of the metabolites in leaf tissue was estimated using maltose polymers with varying degrees of polymerization (DP) in combination with chicory fructo-oligosaccharide standards (Appendix B). Peaks from the latter regions of the chromatogram (retention time >14.1min) (Appendix B, Figure B.2) corresponding to a DP>2 were integrated generating 53 individual peaks. Principal component analysis was performed and revealed differential clustering of the different

genotypes in the third component (Figure 3.6). Neither different environmental conditions nor different times of sampling appeared to have a significant effect over the fructan profile (Appendix B). The metabolites responsible for differential clustering between the 2 genotypes were mainly high DP fructans (approximate DP≥20).

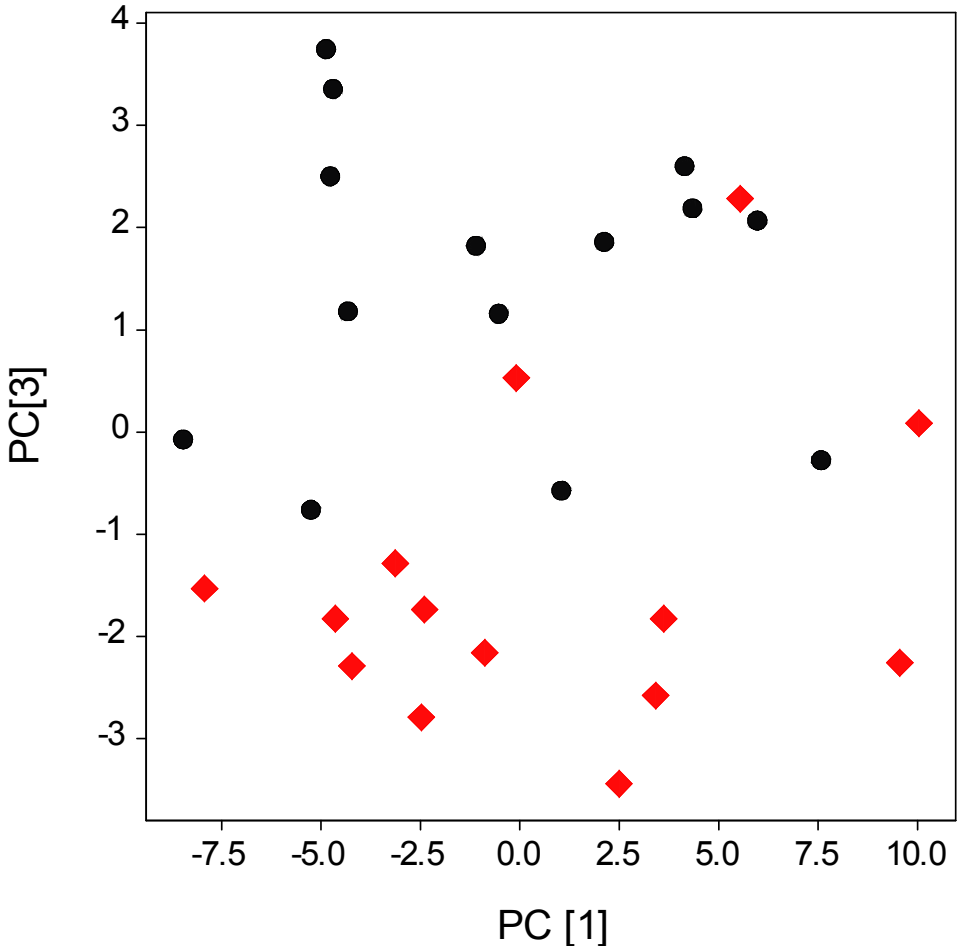

Figure 3.6 - Principal component analysis (PCA) plot of all metabolites with DP ≥2 found, following HPAEC-PAD analysis of leaf blades of Cashel and PI 462336. Components 1 and 3 explained up to 45% and 7.5% of the variability, respectively. ● represent PI 462336 and ♦ represent Cashel

3.5 Discussion

The aim of this chapter was to characterize the response of a PEG-induced water stress in perennial ryegrass. In order to achieve this aim, a metabolite profiling approach was undertaken in combination with transcript analysis. Initial screenings were carried out with a variety of 16 genotypes. These experiments allowed the physiological distinction between control and plants grown in 15% PEG medium. However, the statistical significance levels are relevant for only a small number of genotypes, 4 and 3 for RWC measurements and root:above-ground fresh biomass ratio, respectively. Therefore, it was decided to increase the levels of PEG to 20% in the media in order to obtain higher level of stress. Initial characterization of the RWC of genotypes Cashel and PI 462336 suggested that these have significant different degrees of tolerance to water-limitation. Furthermore, it was observed that, in genotype PI 462336, which displayed higher tolerance to water-deficit, there was an increase in dry biomass. Metabolite analysis and transcript profiling have uncovered putative components of the mechanisms which may be responsible for an enhanced tolerance to a PEG-induced water stress.

3.5.1 Metabolite profiling

Metabolic profiling initially showed a greater difference between tissues than between distinct genotypes, as reflected in the associated PCA plot (Figure 3.3). These findings are in agreement with another metabolic profiling study characterizing these two different tissues in barley (Roessner *et al*., 2006). In addition, the greatest metabolic differences

detected were between the leaf samples of the two genotypes under stress. The leaf samples of PI 462336 under stress clustered closely to the control samples, whereas contrastingly, Cashel stressed leaf samples clustered apart from the associated control samples. This is the result of a significant decrease in a high number of metabolites in Cashel leaf tissue after one week of stress (Table 3.3). The decrease of metabolites was accompanied by a reduction in water content of the leaves. Some of the metabolites which were exclusively reduced in Cashel included a significant number of fatty acids. A previous study, where total leaf lipid content was monitored in *Arabidopsis* plants grown for 14 days under water-limiting conditions, revealed that total lipid content decreased progressively as the RWC of leaves decreased (Gigon *et al*., 2004). Additionally, the authors correlated the decrease of lipid content with an increase in both the lipolytic activity in leaf extracts and the expression of genes involved in lipid degradation (Gigon *et al*., 2004).

The decreases in lipid content had previously been correlated with increase in lipolytic activities (Matos *et al*., 2001) as well as with the inhibition of lipid biosynthesis (Monteiro de Paula *et al*., 1993). Due to the lack of transcript profiling in Cashel, it is not possible to verify whether genes involved in lipid degradation are being regulated under water limitation. However, the metabolite levels reveal an overall decreasing trend in both tissues accompanying the onset of stress. This suggests that water-limitation is constraining source activity in the plant, possibly by affecting the photosynthetic machinery in the cell (Chaves *et al.*, 2009). This may result in a decrease of metabolite intermediates and consequently lead toward a decrease in the levels of fatty acid biosynthetic precursors resulting in inhibition of fatty acid biosynthesis. Additionally, the levels of phosphate (P_i) appeared to experience a down-regulation in both tissues under stress conditions. Monteiro de Paula *et*

al. (1993) have also reported that P_i could be limited in plants grown under water-limiting conditions due to a reduction of absorption by the roots. Therefore, it is possible that this P limitation contributes to the limitation of phospholipid biosynthesis (Gigon *et al*., 2004).

Another significant proportion of metabolites which experience a down-regulation trend under water-stress are N-containing metabolites (Table 3.3 and 3.4). These decreasing trends are comparable in both genotypes and seem to suggest an interaction of water-limitation with N metabolism (Figure 3.7 and 3.8).

3.5.2 Accumulation of osmolytes

The accumulation of non-toxic metabolites is one of the generally accepted mechanisms that cells use to cope with dehydration. This results in an increase of cell osmolarity, subsequently leading to an influx of water and/or reduced efflux of water (Hare *et al.*, 1998). Many of the osmolytes accumulated by plants in response to environmental stress conditions include polyhydroxylic compounds (saccharides, polyhydric alcohols) and zwitterionic alkylamines (amino acids and quaternary ammonium compounds).

There was a significant increase in the accumulation of known compatible solutes in PI 462336. (Figure 3.7) In this current study, a significant increase in the levels of trehalose in the drought tolerant genotype PI 462336 was observed while Cashel did not experience such changes. This increase indicates a beneficial role for trehalose in perennial ryegrass leaves during times of water stress.

There was also an increased accumulation of glucose, fructose, maltose and inositol under water stress which was specific to the leaves of the more tolerant genotype PI 462336 (Figure 3.7). Rizhsky *et al*., (2004) investigated polar compounds under drought and heat stress. In their study, glucose and fructose were accumulated under drought stress alone and in combination with heat stress, whereas inositol and maltose were only accumulated under a combined drought and heat stress. The results presented indicate that these metabolites appear to be involved in enhancing tolerance to PEG-mediated water-limitation in perennial ryegrass.

One compound with a widely regarded role in water stress tolerance is proline (Bartels and Sunkar, 2005). However, a decrease in proline levels under water stress was observed in the leaf tissue of both genotypes. Proline has been reported to accumulate in *Sesevium portulacastrum* plants under stress conditions similar to the stress experiments described in this study (Slama *et al.*, 2007). Rizhsky *et al*., (2004) observed a large accumulation of proline under drought stress compared to the control, but no increased accumulation under a heat and drought combination. Instead, the authors reported a very large accumulation of sucrose which, they hypothesized, was required as a replacement osmoprotectant for proline under a combined heat and drought stress. Furthermore, it was suggested that the proline accumulation would result in increases in the levels of intermediates of proline biosynthesis which could be toxic for plant cells under these stress conditions. Previous work in perennial ryegrass has revealed that proline accumulates mainly in the basal region of leaves during the initial stages of drought stress, while at later stages, during severe drought, it accumulates in the leaf blades (Thomas, 1991). It was suggested that accumulation in leaf laminae occurs prior to or as a result of injury. Therefore, it is possible

that accumulation of proline occurred in the basal region of the leaves, but not on the sampled material collected which comprised leaf blades. Alternatively, the role of proline as a compatible solute might have been compensated for by the accumulation of a different osmolyte.

Of particular interest was a dramatic increase in raffinose levels in both the leaves and roots of PI 462336 under water stress. This increased accumulation was only observed in the more tolerant genotype PI 462336 and not in the more susceptible Cashel genotype. Raffinose has previously been correlated with increased dehydration tolerance in vegetative tissue of *Arabidopsis* (Taji *et al.*, 2002). However, a targeted metabolomic study undertaken in perennial ryegrass suggested that raffinose did not play a role in desiccation tolerance because it did not accumulate under drought stress (Amiard *et al*., 2003). This observation is in disagreement with the results presented in the current chapter where raffinose was the metabolite with the largest increase under water stress (15.4-fold) in leaf tissue and had the third largest increase in root tissue (4.6-fold). These contradictory results may be explained by the differences in the experimental system used to apply water-limitation. Whilst Amiard *et al*. (2003) withheld water-supply (and nutrient) in plants grown in perlite-filled pots, in this study PEG was used at a 20% concentration to generate water-limiting conditions. It is therefore possible that raffinose may accumulate under PEG-mediated water-limiting conditions but not according to the method used by Amiard *et al*. (2003). Alternatively, differences in raffinose response to water limitation may result from genotypic differences. Amiard *et al*. (2003) used cv. Bravo in their analysis while in the present study 2 different genotypes were used with contrasting levels of water stress tolerance. However, while cv. Bravo may or may not display tolerance to water limitation,

genotype PI 462336 definitely displayed enhanced tolerance to water stress when compared to Cashel. Therefore, it is probable that raffinose plays an important role in improving tolerance to water-limitation in perennial ryegrass.

3.5.3 Reactive oxygen species

In addition to its role as an osmoprotectant, a role for raffinose in ROS scavenging has also been recently proposed (Nishizawa *et al*., 2008). ROS can accumulate due to abiotic stress, ultimately resulting in oxidative stress and cellular damage (Mittler, 2002). Plants can combat this threat through enzymes that remove ROS and/or through the production of antioxidants that react with ROS. Nishizawa *et al*. (2008) generated transgenic *Arabidopsis* plants with high intracellular levels of raffinose and galactinol. These high levels were correlated with increased tolerance to a methylviologen treatment (used to generate ROS), salt and chilling stress. Furthermore, an *in vitro* approach demonstrated that both raffinose and galactinol protected salicylate from hydroxyl radicals (Nishizawa *et al*., 2008).

Additional strategies of ROS protection were identified by differential expression analysis in PI 462336. A gene with homology to peroxisomal ascorbate peroxidase was identified as being up-regulated following PEG-induced water stress (LFa12; Table 3.1). Ascorbate peroxidase has an important role in detoxifying hydrogen peroxide that has been formed by the reduction of superoxide by superoxide dismutase (Apel and Hirt, 2004). For example, transgenic studies in tobacco and *Arabidopsis* over-expressing ascorbate peroxidase showed increased protection against oxidative stress (tobacco) and heat tolerance (*Arabidopsis*) (Wang *et al*., 1999; Shi *et al*., 2001).

Glutathione (GSH) also has a key role as an antioxidant and redox buffer in plants (Noctor and Foyer, 1998). In the γ-glutamyl cycle, 5-oxoproline can be converted by oxoprolinase to L-glutamate which in turn can be used in GSH synthesis. In both PI 462336 and Cashel, a decline in both 5-oxoproline and glutamate was observed under water stress in leaf and root material (Tables 3.3 and 3.4). The decrease of 5-oxoproline levels was more pronounced in the PI 462336 genotype: indeed it was one of the metabolites with the largest decrease. Both genotypes experienced relatively high levels of 5-oxoproline under control conditions. The significant decline of 5-oxoproline may in part be result of an increased synthesis of GSH as a defence against the consequences of water stress. Interestingly, a thioredoxin F isoform (Lfd07; Table 3.1) was identified as significantly up-regulated under water stress. Michelet *et al*. (2005) proposed a cross-talk between the thioredoxin and GSH systems. The authors demonstrated that, in *Arabidopsis* and *Chlamydomonas reinhardtii*, only f-type chloroplastic thioredoxins underwent glutathionylation. Thioredoxin f is involved in the activation of Calvin-cycle enzymes (Schurmann and Jacquot, 2000) and it was proposed that glutathionylation of thioredoxin f was a mechanism which reduced its activity during increased ROS production, thereby reducing the activity of thioredoxin targets in the Calvin-cycle (Michelet *et al*., 2005). The increased expression of thioredoxin f observed may be result of a mechanism for compensating for the glutathionylation-mediated reduction in thioredoxin f activity.

3.5.4 Transcriptional response

The differential gene expression study was aimed at finding genes up-regulated under water stress in PI 462336. Transcripts with homology to genes with a known involvement in drought stress were identified in both the leaf and root library. A Dehydration Responsive Element Binding (DREB) transcription factor was up-regulated in leaf tissue under water stress (LFg01; Table 3.1). DREB transcription factors are involved in the induction of abiotic stress-related genes independent of abscisic acid. They contain specific sequences that recognize and bind to the Dehydration Responsive Element (DRE) motif of stress responsive genes. The particular transcript identified as being up-regulated under water-limitation had a significant similarity to a DREB transcription factor 5A from *Triticum aestivum*, for which very little is known. It appears from the current study that LFg01, sharing homology to DREB 5A (65%), is regulated by water stress and may be a target for improving drought tolerance in the forage grasses. Superior drought tolerance has already been engineered into *Arabidopsis* by over-expression of DREB transcription factors (Liu *et al*., 1998; Kasuga *et al*., 1999; Haake *et al*., 2002; Sakuma *et al*., 2006).

In the root tissue choline phosphate cytidylyltransferase (RTc04, Table 3.2) appeared to be upregulated.. This enzyme is involved in the synthesis of choline which is a precursor for glycine betaine formation. Glycine betaine is a compatible solute and the engineering of plants to accumulate glycine betaine has been achieved in many plants resulting in superior tolerance to many abiotic stresses including drought (for review see Chen and Murata, 2008). However, no significant effects in the concentrations of glycine in response to water stress were observed in the metabolite profiles. Nevertheless, it was observed that the

choline phosphate cytidylyltransferase was significantly up-regulated in our study by a mean factor of 41.39 in response to a water stress that may signify a switch to an increased accumulation of glycine betaine.

3.5.5 Fructan response to water-stress

A gene for fructan:fructan 6G-fructosyltransferase (6G-FFT) was identified as being regulated by water stress in the PI 462336 subtracted library (Table 3.1). In a repeated experiment, the expression of this gene through PEG induced water stress in Cashel and PI 462336was monitored at different time points. A significant difference in expression of the gene between the two genotypes was found, although a clear differential regulation between control and water stress conditions was not observed for the gene expression profiles of the leaf blades after one week (Figure 3.4). A study by Amiard *et al.*, (2003) reported fructan accumulation in *L. perenne* leaf sheaths under drought conditions and a role in inducing drought tolerance in vegetative tissues was proposed. However, the large differences observed in 6G-FFT expression in the leaf blades did not translate into major differences in fructan profiles (Appendix B). Nevertheless, a multivariate analysis revealed segregation between genotypes (Figure 3.5), although no significant clusters were formed for time of sampling or treatment effects. It was found that the DP of fructans driving the segregation corresponded to DP>20.

A study by Lasseur *et al*., (2006) also observed situations where 6G-FFT expression did not correlate with fructan accumulation and the authors suggested post-transcriptional regulation of expression. However, the low level of fructan content found in leaf blades is

in partial agreement with the study by Amiard *et al.*, (2003) where it was reported that fructan accumulated in the leaf sheath but not in the leaf blades under drought conditions. A study by Pavis *et al.* (2001) used the same *L. perenne* variety as Amiard *et al.* (2003) and focused on analysis of fructans in different parts of the leaf tissue under different fructan-inducting conditions. The authors also concluded that fructans were significantly accumulated in leaf sheaths and elonganting leaf bases but not in leaf blades. Guerrand *et al*. (1996) made a similar approach with fructan-inducing conditions and suggested that fructans accumulated in leaf blades only when the storage capacity of leaf sheaths and then expanding leaves has been decreased. These reports suggest that fructans accumulated in leaf sheaths, however, no samples from those tissues were collected here for fructan analysis. A possible future approach would include analysis of leaf sheaths, leaf bases and leaf blades in these two genotypes in order to access the fructan partition in the tissues of these genotypes. This would aid in determining whether fructan levels correlate with increased drought tolerance. By contrast, a recent study by Turner *et al*. (2008) reported a negative relationship between fructan accumulation and drought resistance and suggested that fructan content by itself cannot be responsible for increased drought tolerance. Instead, the authors suggested that complex patterns of carbon partitioning and metabolism may be responsible for increased tolerance (Turner *et al*., 2008). Nevertheless, the results described in this chapter, particularly the accumulation of fructans may result from a consequence of water-limitation in the primary metabolism rather than a specific response to water-stress.

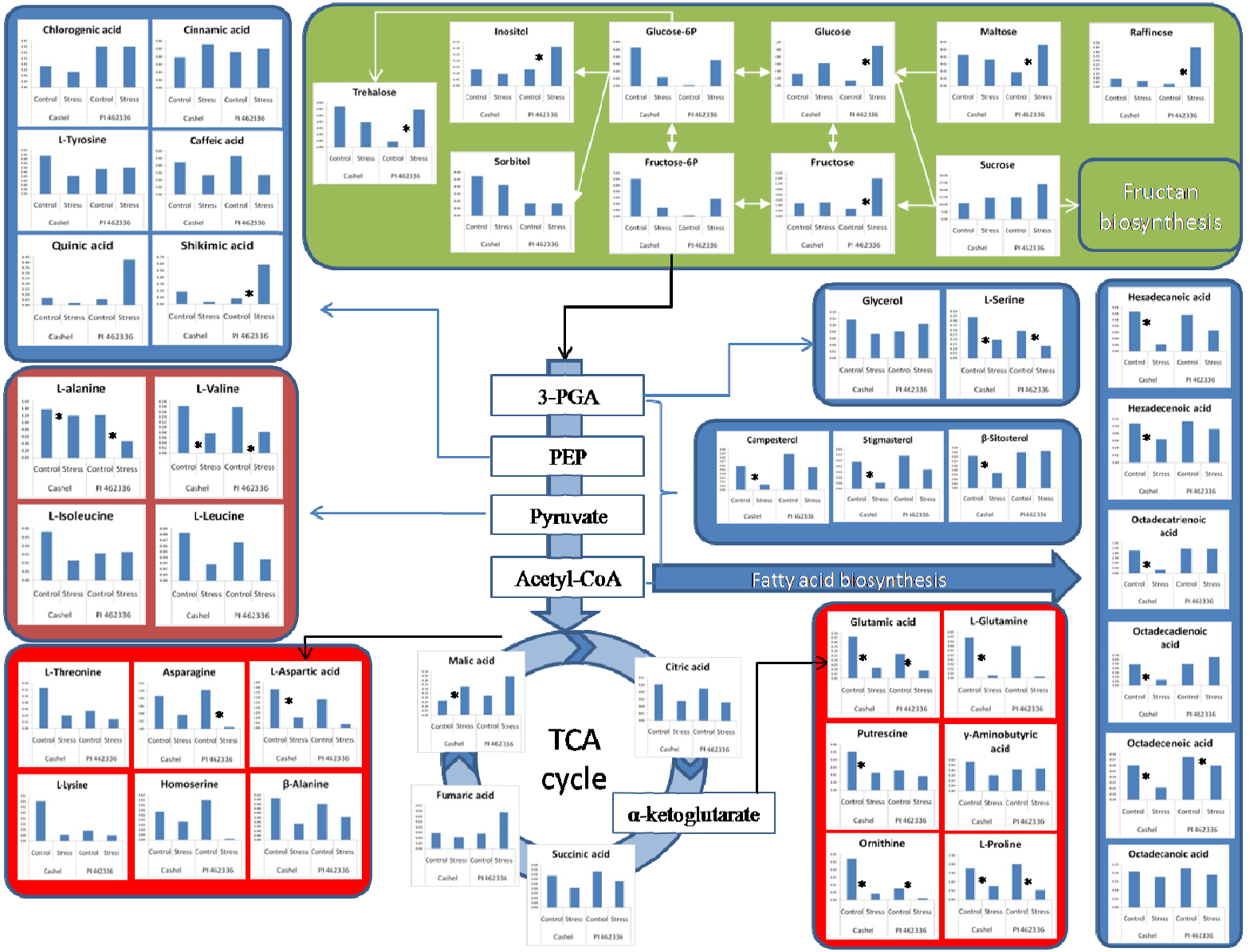

Figure 3.7 - Diagram representing the means metabolite levels in the leaf tissue of PI462336 and Cashel plants grown under control and water-stress conditions . Significant differences (p-value < 0.05) between the means of control and water-stressed plants are represented with *. Red boxes represent pathways which display an overall negative regulation in response to stress, whereas green boxes represent pathways which display a positive regulation in response to stress.

The levels of fructans and raffinose may possibly increase due to the overall increase in the levels of sugar precursors (Figure 3.7), and perhaps they may act as carbon storage compounds. One of the major physiological responses of plants to water-limitation includes stomata closure, which aids in preventing water-loss due to transpiration. This will result in a reduced gas-exchange which will directly affect the CO_2 levels in the leaf tissue consequently reducing carbon assimilation. Perhaps an increased pool of carbon storage compounds would allow the plant to sustain reduced carbon assimilation associated with water-limitation for longer periods of time. Furthermore, the overall decrease in aminoacid levels may indicate a remobilization of carbon flux from aminoacid biosynthesis favouring the accumulation of sugars.

Overall, the majority of genes identified in the root libraries shared significant homology to fungal transcripts and may indicate more prevalent growth of micro-organisms around the roots in the PEG treatments. Despite this, there were no observable differences with regard to fungal growth between roots in PEG and control treatments. However, the possibility that an increased fungal growth in the PEG stress may have resulted in a combined fungal and osmotic stress should not be disregarded. Nevertheless, a number of transcripts with homology to genes with a known involvement in drought stress response, such as DREB transcription factor (LFg01; Table 3.1), were identified in both the leaf and root libraries. This suggests the existence of a specific response to water limitation.

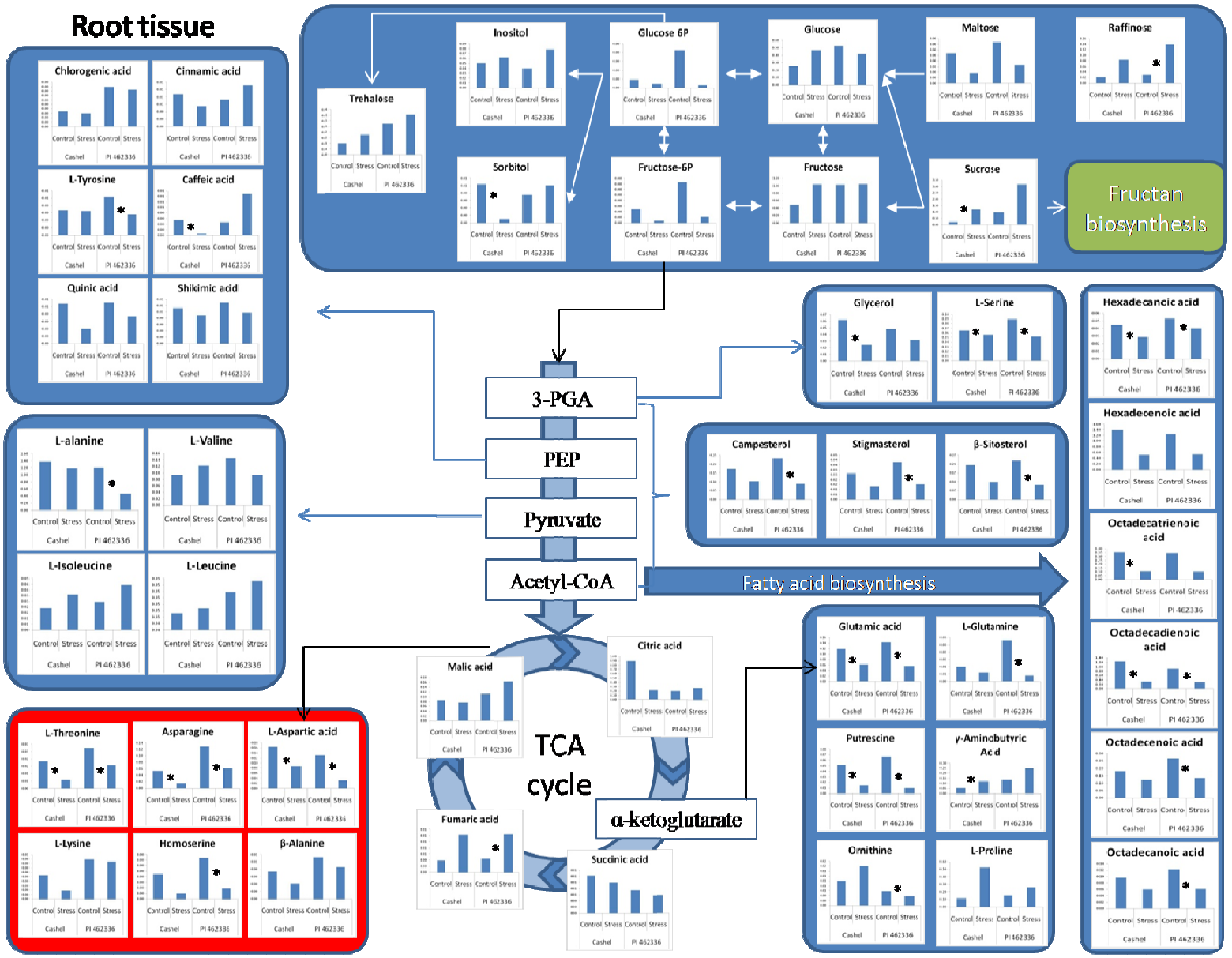

Figure 3.8 - Diagram representing the means metabolite levels in the root tissue of PI462336 and Cashel plants grown under control and water-stress conditions . Significant differences (p-value < 0.05) between the means of control and water-stressed plants are represented with *. Red boxes represent pathways which display an overall negative regulation in response to stress.

3.6 Conclusions

Metabolite profiling has provided an overview of changes in the metabolism of perennial ryegrass under a PEG induced drought stress, in particular, the identification of potential sugars that may play a key function in assisting ryegrass to tolerate water stress (Figure 3.7 and 3.8). The increase in raffinose levels in the leaves and roots of PI 462336 under water stress seems to suggest a relevant role in adaptation of perennial ryegrass to water limitation. It has been proposed that raffinose is a multifunctional metabolite, functioning in both osmoregulation and scavenging of reactive oxygen species. In addition to raffinose, other well-documented responses to drought, such as trehalose accumulation and mechanisms of response to ROS, appeared to be regulated under water-deficit conditions. In contrast, other proposed widespread mechanisms of drought response, such as proline accumulation, were not observed. Additionally, the results of the present study suggest that the different genotypes have different fructan levels and that these may be correlated with differences in drought tolerance.

Chapter 4

P-limitation in perennial ryegrass

4.1 Summary

Improving phosphorus (P) nutrient efficiency in *Lolium perenne* L. (perennial ryegrass) is likely to result in considerable economic and ecological benefits. To date, there has been limited research into the global transcriptomic and metabolomic responses of perennial ryegrass to P deficiency and in particular to early response mechanisms to P-deficit. This study aimed to identify molecular mechanisms activated in response to the initial stages of P deficiency. A barley microarray was successfully used to study gene expression in perennial ryegrass and gene expression work was complemented with gas chromatography-mass spectrometry (GC-MS) metabolic profiling to obtain an overview of the 'omic' response to early stages of P deficiency. After 24 hrs P deficiency, internal phosphate concentrations were reduced and significant alterations were detected in the metabolome and transcriptome of two perennial ryegrass genotypes. Results indicate a replacement of phospholipids with sulfolipids in response to P deficiency and that this occurs at the very early stages of P deficiency in perennial ryegrass. Additionally, the results suggested the role of glycolytic bypasses and the re-allocation of carbohydrates in response to P deficiency.

4.2 Introduction

Phosphorous (P) is a macronutrient which is required in great abundance for the normal functioning of plant activities (Raghothama, 1999). Nevertheless, it is estimated that up to 30-40% of world's arable land is exposed to P limitation (Wissuwa *et al*., 2005). The deficit of P generally results in yield losses, resulting from decrease in growth and photosynthetic activity. However, plants are sessile organisms and their survival depends on mechanisms of adaptation to stress. The morphological and physiological mechanisms that plants use to adapt to low P supply include increases in root:shoot ratio as well as modification of photosynthetic activity (Wissuwa *et al*., 2005).

Low levels of P_i have been suggested to affect the photosynthetic machinery of the plants. For example, in wheat it has been demonstrated that P-deficit results in decreased photosynthetic activity under high light intensity (Rodriguez *et al.*, 1998). The reduction of cytosolic P_i results in a decrease in the activity of ATP-synthases in the thylakoid membrane and ribulose 1,5-biphosphate carboxylase (RuBisCO) resulting in a reduction of carbon assimilation through the Calvin-cycle (Hammond and White, 2008).

The P present in soil displays low mobility, therefore the presence of a root system able to explore a greater soil volume is recognized as an important adaptation to limited-P supply. Increases in lateral root growth have been observed for both bean (Lynch and Brown, 2001) and *Arabidopsis* (Ticconi *et al*., 2004). However, Wissuwa *et al*. (2005) reported that in rice P deficiency stimulated root elongation instead. These are differences which illustrate that root architecture experiences modifications in response to low P availability. These often indicate an increase in root:shoot ratio which is another trend typical of P limitation (Vance *et al*., 2003; Hammond and White, 2008).

Additionally, there are biochemical adaptations of plants to low-P_i which include a variety of responses. These include mechanisms for increasing P uptake, the induction of phosphate scavenging and recycling enzymes, induction of alternative glycolytic and respiratory pathways as well as the induction of tonoplast H^+-pumping pyrophosphatase (Plaxton, 2004).

Under phosphorous starvation, one of the strategies adopted by plants is the enhancement of P_i uptake. The increase in such uptake is believed to be modulated by the activity of transporter proteins under P-limitation (Plaxton, 2004). It has been proposed that low- and high-affinity P transporters exist, which are responsible for translocation of P towards the roots (Raghothama, 1999). These allow the uptake of inorganic P in the form of PO_4^{3-}, HPO_3^{2-} and $H_2PO_4^-$ (Raghothama, 1999).

However, a majority of the P present in soils occur in organic form and it is estimated to account for 50% to 80% of the total phosphate in soils (Wang *et al*., 2009b). Furthermore it has been estimated that phosphate monoesters constitute a majority (estimated at 90%) of the organic phosphorous in soils while a minor percentage (~5%) is accounted for as sugar phosphates or diester phosphates (Richardson *et al*., 2009). Since the roots of plants are only able to take up inorganic P, plants require mechanisms which enable the release of P present in phosphorus monoesters and hence increase P availability.

Acid phosphatases (APases) are hydrolytic enzymes that catalyze the breakdown of P monoesters. This catalytic activity results in the release of Pi from organic compounds and may play an important role in P nutrition (Wang *et al*., 2009b). APase activity has

been found both at the intracellular (vacuole) and extracellular (secreted) level and its induction has been widely associated with limited P availability (Plaxton, 2004). Intracellular APases are thought to be involved in remobilizing P_i from older leaves and vacuoles whereas extracellular APases are thought to be involved in mobilization of extracellular P_i from organic compounds in soil (Wang *et al*., 2009b). As an illustration of the importance of APases in the P metabolism in the plant an *Arabidopsis* mutant *pup3* (phosphatase under-producer) which produces a reduced level of APases compared with wild-type genotypes was found to accumulate 17% less P in shoot when supplied with organic P as main phosphorous source (Tomscha *et al.*, 2004). In soybean (*Glycine max*) a transgenic approach was used with the aim of constitutively overexpressing a purple acid phosphatase from *Arabidopsis* (Wang *et al*., 2009b). When plants were grown in sand with phytate, a monoester P compound, as the sole P source, the authors observed substantial increases in plant biomass and P content when compared with wild-type plants (Wang *et al*., 2009b). These results were accompanied by an increase in phytase activity both in leaves and root exudates. Additionally, the authors found that the transgenic lines had enhanced yield, compared with wild-type plants, when grown in field conditions in acid soils (Wang *et al*., 2009b).

Although P monoesters constitute the majority of organic P present in soils, diester phosphates are also present most notably represented by nucleic acids. These are present in decaying organic matter and represent an additional source of extracellular P which can be explored by plants experiencing P-deficit (Plaxton, 2004). The secretion of nucleases and nucleotide phosphodiesterases appears to be P_i-starvation induced and may allow plants to liberate P contained in those molecules resulting in the increase of available phosphate in the soil.

As described previously, only a minority of soil P is present in its mineral form (P_i). The majority of the P_i is in precipitated form or adsorbed to soil constituents such as organic matter and clays (Richardson *et al*., 2009). Precipitated forms of P in alkaline soils are usually associated with calcium ions (Ca^{2+}) whereas in acidic soils these are often associated with iron (Fe^{2+}) or aluminium (Al^{3+}) ions (Richardson *et al*., 2009) However, plants have the ability to modify their rhizosphere under P starvation in order to release unavailable inorganic P. The exudation of organic acids, such as citric acid, malic acid or oxalic acid, has been extensively reported as one of the universal responses to P deficit in plants (Raghothama, 1999; Uhde-Stone *et al*., 2003; Richardson *et al*., 2009). It is thought that an increase in the levels of organic acids in the rhizosphere will chelate ions such as Ca^{2+}, Fe^{2+} or Al^{3+}, thus allowing the inorganic phosphate to be released for plant uptake (Vance *et al*.,2003). For example, Zhang *et al*. (1997) compared the exudation of organic acids from roots of *Raphanus sativus* L. (radish) and *Brassica* napus L. (rape) when grown under P-deficit or P-sufficient conditions. It was reported that the levels of organic acids increased in both plant species with the onset of P starvation. Furthermore, the authors observed that the two species exudated different organic acids. Since rape was commonly grown in calcareous soils while radish was found in acid soils, the authors suggested that plants had adapted specifically to the type of soil found in their natural environment (Zhang *et al*., 1997).

The deficit of P often results in substantial alteration in the membrane lipid composition. A majority of the membranes in plants are composed of phospholipids, such as phosphatidylcholine (PC) phosphatidylethanolamine (PE), phosphatidylinositol (PI), phosphatidyl-serine (PS), phosphatidylglycerol (PG) and phosphatidic acid (PA). Additionally, membrane lipid composition may include sulfolipids and galactolipids,

such as monogalactosyldiacylglycerol (MGDG) and digalactosyldiacylglycerol (DGDG) (Li *et al*., 2006). However, it has been suggested that under P-limiting conditions plants may replace membrane phospholipids with non-phosphorous lipids. For example, a study in *Arabidopsis* demonstrated that under P-starvation conditions the membrane lipid composition is affected in both the leaf and root tissue (Li *et al*., 2006). In addition to a wild-type genotype, the authors used phospholipase D knock-out mutants and reported an overall decrease in the levels of phospholipids while the levels of galactolipids increased. In the leaf tissue the amount of phospholipid decrease was balanced by the increase in galactolipid levels, while in the root tissue the phospholipid was greater. However, the phospholipase D mutants experienced a lesser extent of phospholipid decrease and a slight increase in the levels of DGDG in the roots. Thus, the authors suggested that the hydrolysis of PC contributed to the increase in Pi levels for the cell metabolism and provides diacylglycerol moieties for galactolipid biosynthesis (Li *et al*., 2006). Furthermore, an *Arabidopsis* mutant, *sqd2*, disrupted in a gene involved in sulfoquinovosyl diacylglycerol (SQDG) synthesis, displayed a complete lack of sulfolipid content and a reduced growth under P deficient conditions (Yu *et al*., 2002). As result of this, the authors hypothesised that sulfolipids may substitute for anionic phospholipids under P deficient conditions in order to scavenge P_i from phospholipids (Yu *et al*., 2002).

The decline of available P to the plant has severe repercussions with respect to cytoplasmatic P_i and associated decreases in ATP and related nucleoside concentrations. The phosphate deficit may result in a reduction of glycolytic flux through enzymes dependent on P_i or ATP. Therefore, in order to sustain glycolysis, plants require additional mechanisms some of which are in the form of glycolytic bypasses. There are at least 6 glycolytic bypass mechanisms in plants which include steps catalysed by

phosphate-starvation inducible enzymes such as sucrose-synthase (SuSy) UDP-glucose pyrophosphorylase, pyrophosphate:fructose 6-phosphate 1-phosphotransferase (PP_i-PFK), non-phosphorylating NADP-glyceraldehyde 3-phosphate dehydrogenase, phosphoenolpyruvate carboxylase (PEPCase) and phosphoenolpyruvate phosphatase (PEPP)(Plaxton, 2004).

The conversion of fructose 6-phosphate to fructose 1,6-bisphosphate has a strategic role in the regulation of glycolysis. This reaction can be catalyzed by an ATP-dependent phosphofructokinase (PFK) which is found both in the cytoplasm and chloroplasts, and catalyses the forward reaction. Additionally, PP_i-PFK catalyses the above reaction reversibly by using pyrophosphate as the phosphoryl donor hence being often referred to as PP_i-dependent phosphofructotransferase (PFP) (Nadas *et al.*, 2008). Duff *et al.* (1989) observed an increase of PFP activity up to 5-fold in *B. nigra* plants experiencing P-starvation, thus suggesting the involvement of PFP in the response to P starvation through the mediation of a glycolytic bypass. Furthermore, it was shown that the α-subunit of PFP has a regulatory role over the β-subunit and that its forward activity is stimulated by P_i deprivation (Theodorou *et al.*, 1992). This bypass would allow glycolysis to proceed despite decreases in adenylate phosphates (Duff *et al.*, 1989; Plaxton, 2004) under P-starvation. Additionally PP_i levels appear to be insensitive to P-limitation (Plaxton, 2004) so by converting PP_i to P_i the plant would generate and access further internal P which would aid in mitigating P_i decline.

Additionally in the study cited above, the authors reported an additional increase in the activity of non-phosphorylating NADP-glyceraldehyde 3-phosphate dehydrogenase, phosphoenolpyruvate carboxylase (PEPCase) and a phosphoenolpyruvate phosphatase (Duff *et al.*, 1989).

The non-phosphorylating NADP-glyceraldehyde 3-phosphate dehydrogenase catalyses the conversion of glyceraldehyde 3-phosphate to 3-phosphoglycerate with the concomitant reduction of NADP to NADPH. This bypass avoids the synthesis of a phosphorylated intermediate (1,3-bisphosphoglycerate) and its subsequent dephosphorylation which yields one ATP. The alternative bypass does not require phosphate, therefore allowing the intracellular P_i to be available for other metabolic processes.

PEP-phosphatase is thought to be involved in the dephosphorylation of phosphoenolpyruvate (PEP) to pyruvate in the vacuole (Duff *et al.*, 1989). Unlike pyruvate kinase which catalyses the analogous reaction in the cytosol the acceptor of the phosphoryl group is not ADP, but it is instead converted into P_i. The resulting P_i and pyruvate can subsequently be mobilized to the cytosol.

The PEPCase enzyme mediates the carboxylation of PEP to oxaloacetate in the cytosol. During this reaction HCO_3^- is consumed and PEP is dephosphorylated generating free P_i. Oxaloacetate is subsequently reduced by NADH to form NAD^+ and malate, with the latter available for transportation to the mitochondria and interactions in the TCA cycle. This bypasses the metabolic step catalysed by pyruvate kinase which mediates the dephosphorylation of PEP to pyruvate, using ADP as the phosphoryl acceptor resulting in the synthesis of ATP.

The accumulation of anthocyanins, which have antioxidant capacity (Kalt *et al.*, 1999), is often considered a symptom of P deficiency in a variety of plant species (Halsted and Lynch, 1996). However, their accumulation is not specific to P-deprivation. Instead,

anthocyanin levels have been found to increase in response to a large number of abiotic stresses, including drought, exposure to UV radiation and limitation of N supply (Trull *et al*., 1997). Furthermore, anthocyanin accumulation may not necessarily be involved in response to P-limitation in some plant species (Halsted and Lynch, 1996). In other cases, it has been reported that anthocyanin levels increase only upon long-term P-deficiency (Misson *et al*., 2005).

PP_i is a by-product of a host of anabolic reactions, including the terminal steps of macromolecule synthesis (Plaxton, 2004). The accumulated levels of PP_i may be employed by plants to improve the energetic efficiency of several cytosolic processes (Plaxton, 2004). However, plant cells, unlike animal cells, lack PP_iase which generates relatively high levels of cytosolic PP_i. Environmental conditions, such as Pi deprivation, may cause a decline in the levels of ATP (but not PP_i), therefore, plants have adapted important mechanisms which utilize PP_i, instead of ATP. The induction of PP_i-PFP under phosphorous starvation, as cited above, represents a prime example of such mechanisms. These mechanisms are thought to act by circumventing ATP-limited conditions, thereby conserving limited ATP pools and liberating P_i from PP_i molecules (Plaxton, 2004). The existence of additional metabolic processes which recycle Pi from PP_i, such as the conversion of sucrose to hexose-phosphate and the induction of tonoplast proton-pumping pyophosphatase, may further contribute to plant cell homeostasis under P-limitation (Plaxton, 2004).

The aim of this chapter is to characterize the early molecular and metabolic response of two perennial ryegrass genotypes under P-limitation. An initial screen was carried out in order to select genotypes with contrasting capacity of removing P from nutrient solution. The selected genotypes were then grown in a hydroponics solution containing

two different levels of P supply. Both leaf and root samples were analysed using metabolite profiling and a microarray-based approaches. Since the response of plants to P deficit includes extensive effects at the primary metabolism levels it is expected that the metabolite profiling approach will allow the characterization of the metabolic response of perennial ryegrass even in the early-stage of response to P-limitation. Additionally, results from transcriptome analysis will provide a wide-scope analysis of the response to P-limitation and are expected to complement the metabolomic approach. These results may, therefore, contribute to an increase in the knowledge of the response of *Lolium perenne* to P-deficit which should consequently result in the identification of potential targets to improve phosphate usage efficiency.

4.3 Material and Methods

4.3.1 Selection of genotypes (performed by SLB)

A screen was carried out on five genotypes from each of 34 ecotypes and 2 cultivars with the aim of identifying material with a high capacity to remove P from solution. Selection of ecotypes and cultivars was determined by availability of seed. Seeds were germinated on filter paper and transferred to perlite. After five days, seedlings were weighed, transferred to 50ml test tubes containing 40ml nutrient solution ($CaCl_2.2H_2O$,0.75 mM: $MgSO_4.7H_2O$, 0.38 mM; MS Micro Salts (Duchefa), 0.146 g l^{-1}; NH_4NO_3, 5 mM; $Ca(NO_3)_2.4H_2O$,2.33 mM; KH_2PO_4 0.31 mM) and placed in a growth room maintained at 23°C with a 16hr daylight regime (PAR = 360 µmol.m^{-2}.s^{-1}). After three days, a volume of 200 µl was taken from each solution and the phosphorus content determined using the molybdenum blue assay (He and Honeycutt, 2005). In order to perform the molybdenum blue assay, a reagent solution was prepared with 875µl of

Splittgerber's reagent, 250µl of 300mM Ascorbic acid solution and 125 µl of 2mM potassium antimonyl tartrate solution (all reagents purchased from Sigma-Aldrich). A volume of 20µl of reagent solution was added to the 200µl of sample while dilutions of initial nutrient solution were used to generate a standard curve (R^2=0.99). The reaction was incubated in darkness overnight, and absorbance was measured at 880nm. Results were analysed in GenStat V10 (VSNi, Hemel Hempstead, UK) using a one way ANOVA (without blocking). The fresh weights of seedlings at the start of the experiment were used as covariates in the analysis. Two genotypes (IRL-OP-02538_P and Cashel_P) were selected from this screen and propagated to provide adequate clonal replicates for the experiments described below.

4.3.2 Experimental conditions (performed by SLB)

Seedlings of IRL-OP-02538_P and Cashel_P were cleaned of soil and transferred to perlite medium held inside plug trays (84 inserts) floated on the plant nutrient solution (see above). Solutions were placed in two 25 litre tanks and aerated with an aquarium pump. Experiments were performed in a controlled glass house with a mean daily temperature of 22^{o}C and supplemented with lighting (PAR = 650 µeinsteinl.m^{-2}.s^{-1}) for 16hrs. The plants were allowed to acclimatise for one week to the hydroponics growth conditions before applying treatments. At the start of the treatment the solutions in both tanks were replaced with either solution A, identical to above, or solution B, identical to above except that the KH_2PO_4 content was reduced to 0.016 mM. After 24 hours (midday) root and leaf tissues were separated and flash frozen in liquid nitrogen. Separate experiments were performed to obtain samples for array hybridisations and

metabolite profiling and independent biological replicates (four in total) were sampled for each.

4.3.3 Microarray processing: genomic DNA hybridisations (performed by PH)

Genomic DNA (gDNA) was isolated according to the method of Doyle and Doyle (1987) with minor modifications. DNA quality was assessed on an EtBr stained agarose gel and quantified by measuring absorbance at 260 nm. Throughout this study, a custom microarray SCRI_Hv35_44k_v1 (Agilent design 020599) representing approx. 42,000 barley unigene sequences from the public HarvEST database (assembly 35; http://www.harvest-web.org/) was used (ArrayExpress accession A-MEXP-1728). This microarray, along with a smaller barley array design (Chen *et al*., 2010), have been successfully utilised for gene expression analysis in our laboratory. Array procedures followed MIAME guidelines. The design of the microarray experiment and the data derived from it are detailed in the public database ArrayExpress (http://www.ebi.ac.uk/microarray-as/ae/; accession E-TABM-950). For gDNA hybridisations, fluorescent labelling and purification was carried out according to the protocol detailed in Ducreux *et al*., 2008. Microarray hybridisation and washing followed the manufacturer's protocols for gene expression arrays (Agilent Two-Color Microarray-Based Gene Expression Analysis, version 5.5). For each array, 20 µl combined purified labelled samples was mixed with 5 µl 10x Blocking Agent, heat denatured at 98^{o}C for 3 min and cooled to room temperature. GE Hybridisation Buffer HI-RPM (25 µl) was added and mixed prior to hybridization (65^{o}C for 17 h at 10 rpm). Slides were dismantled in Agilent Wash Buffer 1 and washed sequentially in Wash Buffer 1 for 1 min and Agilent Wash Buffer 2 for 1 min. Hybridised arrays were

scanned at 5 μm resolution using an Agilent G2505B scanner at 532 nm (Cy3) and 633 nm (Cy5) wavelengths.

4.3.4 Microarray processing: cDNA hybridisations (performed by PH)

Total RNA was isolated independently from replicate leaf and root tissues using the RNeasy Plant Mini Kit (Qiagen, Hilden, Germany) with on-column DNase I digestion according to the manufacturer's protocol. Samples were run on Bioanalyzer RNA 6000 Nano Chips (Agilent Technologies, CA, USA) to assess quality and integrity.

The design of the microarray experiment and the data derived from it are detailed in the public database ArrayExpress (http://www.ebi.ac.uk/microarray-as/ae/; accession E-TABM-943). The experimental design was balanced with respect to fluorescent dyes, two replicates each of Cy3 and Cy5, to minimise dye bias. RNA samples were labelled as cDNA and purified using the Quick Amp Labelling Kit (Agilent Technologies, CA, USA) as recommended using 1 μg total RNA per sample. Hybridisation, washing and scanning were performed as above.

4.3.5 Microarray processing: data extraction and analysis (performed by PH)

For data extraction, microarray images were imported into Agilent Feature Extraction (FE v.10.5.1.1) software and aligned with the array grid template (020599_D_F_20080612). Intensity data for each spot were extracted using a defined FE protocol (GE2-v5_95_Feb07) and data from each array normalised using the

LOWESS (LOcally WEighted polynomial regreSSion) algorithm (Yang *et al*., 2002). Normalised datasets for each array were subsequently loaded into GeneSpring software (v.7.3.1; Agilent Technologies, CA, USA) for analysis.

For the RNA-based microarray study, specific samples were subjected to dye-swap according to the experimental design and data with consistently low probe intensity level, flagged as absent in all replicate samples, was discarded. Comparisons were made between the two P treatments for each tissue and genotype independently using volcano plots, with thresholds of >2-fold change and a Student's T-test P value <0.05 applied, to identify significantly regulated genes. Unique and overlapping genes between the lists were selected using Venn diagrams.

4.3.6 Quantitative RT-PCR (performed by SLB)

Total RNA was isolated as described above and 200ng was converted to cDNA using SuperScript III and Oligo(dt)$_{20}$ primer (Invitrogen, CA, USA) as recommended by the manufacturer. cDNA was diluted to a final volume of 200µl with ddH_2O and real time assays were performed with SYBR Green I Master (Roche) on the LightCycler 480 according to the manufacturer's recommendations. Analysis was carried out on three biological replicates (each in technical triplicates). Reaction efficiency values were calculated by running each primer set on serial dilutions of a cDNA mixture comprising leaf and root material. The specificity of the reaction was demonstrated by performing melt curve analysis after completion of amplification. Normalization was performed using the housekeeping gene LpGAPDH (Petersen *et al*., 2004). Primers were designed from the barley sequences used for microarray probe design and details are shown in

Appendix C. Statistical analysis was performed in REST 2008 software package (Pfaffl *et al*. 2002).

4.3.7 Sample preparation and metabolite profiling

The experiment was set-up as described above and material for metabolite analysis was harvested after 24 hours under both P-limited and control conditions as described in the material and methods chapter. Both sample extraction and derivatization procedures for metabolite analysis were performed as described in materials and methods. However, the weight of frozen tissue powder used was adjusted to approximately 50 mg (accurately weighted and recorded), and the volume of the aliquots derivatized for the polar and non-polar fractions were adjusted to 750 µl and 4 ml, respectively. Additionally, the metabolite profiles we acquired using a Thermo DSQ GC-MS and the resulting data was analysed as described in materials and methods.

4.3.8 Metabolite fingerprinting by FT-IR

The FT-IR spectra of freeze-dried ground samples from both leaf and root samples were measured using a Bruker IFS66 ATR XPM spectrometer (Bruker Optik, Ettlingen, Germany) and an attenuated total reflectance (ATR) cell (Specac, UK) under ambient conditions. The spectra were collected in the wavelength over the region of 700-4000 cm^{-1} with a spectral resolution of 4 cm^{-1}. Wheat flour powder was used as external reference and was introduced in the sequence of samples every tenth sample. Background spectra were acquired initially and were performed throughout the

experiment for correction purposes. Ground material was pressed onto the crystal surface (2mm×2mm) of the ATR cell to ensure good contact with the ATR crystal. The original FT-IR spectra were corrected for atmospheric variation and normalized using OPUS 5.5 software (Bruker Optik, Ettlingen, Germany). Multivariate analysis of the FT-IR data was performed using the chemometric software package SIMCA-P+ v11.0.0.0 (Umetrics, Umeå, Sweden).

4.4 Results

4.4.1 Genotype Selection

The purpose of the pre-screen was to identify genotypes with contrasting rates of P_i removal from solution. The results showed that ecotype had an effect on P removal ($F(35, 142) = 3.07, P < 0.001$). The ecotype with the highest removal of P_i from solution was IRL-OP-02538 (Table 4.1). The genotype with the highest P_i removal, IRL-OP-02538 was propagated together with a genotype from the cultivar Cashel. The latter genotype displays a capacity of removing P_i from solution which does not contrast with the majority of genotypes analyzed. Furthermore, this genotype corresponds to a commercially available variety, and hence may illustrate better the response to P-deficit of perennial ryegrass varieties present in agricultural lands. Interestingly, among the ecotypes screened there was no ecotype with a notable lower rate of P_i removal from solution.

Table 4.1 - mean values for P_i removal from solution for 34 ecotypes and 2 cultivars. The two genotypes selected from this screen and propagated for the experiments described in this chapter are noted with an asterisk. The results are for P_i removal relative to amount of P in starting solution (0.31mM of KH_2PO_4), which was used for serial dilutions in constructing the standard curve. The standard error of difference is 6.606.

Ecotype/Cultivar	P removal relative to concentration at start of experiment (μM)
IRL-OP-02018	53.01
IRL-OP-02048	50.01
IRL-OP-02058	56.67
IRL-OP-02059	29.67
IRL-OP-02078	40.13
IRL-OP-02093	33.08
IRL-OP-02131	34.48
IRL-OP-02169	45.05
IRL-OP-02192	35.59
IRL-OP-02241	35.34
IRL-OP-02258	52.88
IRL-OP-02337	46.7
IRL-OP-02419	36.51
IRL-OP-02442	35.68
IRL-OP-02512	49.49
IRL-OP-02538 *	63.56
PI 225825	42.05
PI 231606	47.12
PI 231619	31.9
PI 231620	38.59
PI 234779	38.68
PI 237186	42.63
PI 239730	33.98
PI 249751	31.46
PI 251557	29.57
PI 267059	31.36
PI 317452	38.54
PI 321397	40.21
PI 418701	38.62
PI 577268	45.5
PI 598512	34.28
PI 610958	43.15
PI 619024	49.15
W616127	33.75
Shandon	36.14
Cashel *	41.51

4.4.2 Array hybridization across species

Initial experimentation used genomic DNA to determine the overall level of hybridisation of perennial ryegrass genome to probes on the barley microarray. This took advantage of the extreme sensitivity of the Agilent microarray platform. Approximately 40% of probes (16,000 genes) hybridised with measurable signal to perennial ryegrass genomic DNA. This level of hybridisation reflects the levels of

sequence diversity between the two species, however the 60mer probes utilised in the Agilent microarray allow for a certain degree of mismatches, as reported previously for analysis of diverse potato genotypes (Ducreux *et al*., 2008). After hybridisation with cDNA derived from leaf and root RNA, a total of ~6,800 and ~6,300 probes, respectively, produced an acceptable signal amongst replicates.

The validity of the array results was verified by the real time RT-PCR of seven selected genes (Table 4.2) identified as significantly regulated using the barley arrays. The results were in general agreement with the array results with the exception of U35_44k_v1_8347, Phospholipase C, that was not identified as being significantly up-regulated (Table 4.2). Indeed, the strong agreement confirms the efficacy of the barley arrays for analysing gene expression in perennial ryegrass.

Table 4.2 - Validation of array data by real time RT-PCR of seven genes identified as significantly regulated from leaf and root hybridisations. The fold change for both array and RT-PCR data are shown with associated significance values in brackets. Array data was analysed in GeneSpring and RT-PCR data in REST.

Description	Rice Match	Putative Function	**Array**		**RT-PCR**	
			Cashel_P	IRL-OP-02538_P	Cashel_P	IRL-OP-02538_P
Leaf						
U35_44k_v1_12109	LOC_Os02g33710.1	histidine decarboxylase	**5.85 (0.001)**	**5.80 (0.000)**	**8.22 (0.000)**	**7.38 (0.000)**
U35_44k_v1_37470	LOC_Os12g37600.1	glycerol-3-phosphate acyltransferase 1	0.94 (0.951)	**5.82 (0.005)**	0.93 (0.904)	**2.72 (0.029)**
U35_44k_v1_8347	LOC_Os03g30130.2	phospholipase C	**2.79 (0.007)**	**4.32 (0.006)**	1.35 (0.374)	1.61 (0.178)
U35_44k_v1_7335	LOC_Os01g54620.1	CESA4 - cellulose synthase	1.41 (0.702)	**6.99 (0.038)**	1.22 (0.626)	**4.03 (0.013)**
Root						
U35_44k_v1_22715	LOC_Os01g67126.1	60S ribosomal protein L5-2	3.25 (0.585)	**3.63 (0.032)**	0.64 (0.714)	**8.24 (0.000)**
U35_44k_v1_49610	LOC_Os08g43870.1	hypothetical protein	0.96 (0.939)	**2.63 (0.024)**	0.85 (0.543)	**2.82 (0.003)**
U35_44k_v1_43490	LOC_Os08g39300.1	serine-glyoxylate aminotransferase	1.16 (0.718)	**0.28 (0.021)**	0.72 (0.487)	**0.32 (0.000)**

4.4.3 Transcriptomic changes in leaf tissue under P deficiency

Using the barley arrays it was observed that that the expression profiles of two perennial ryegrass genotypes changed in response to 24 hours of P deficiency. The genes significantly regulated (≥ 2 fold and $P<0.05$) in each genotype are shown in Appendix D. The greatest number of significantly regulated genes (222) was discovered in the leaf tissue of Cashel_P under P deficiency, with 95% of these genes being up-regulated. In contrast, a much smaller number of genes (35) were significantly regulated in the leaf tissue of IRL-OP-02538_P (Figure 4.1a).

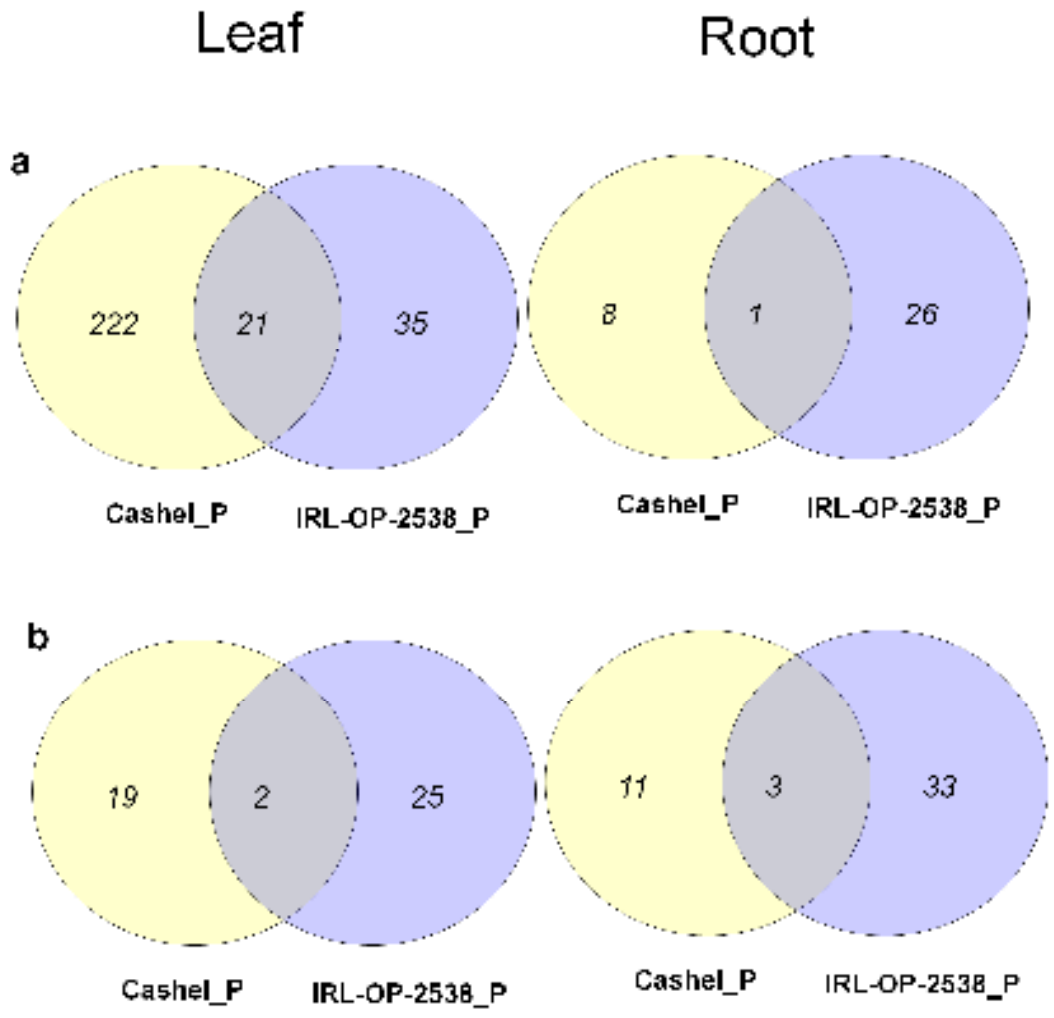

Figure 4.1- a) Number of genes from barley array hybridisations with ≥ 2-fold change in expression ($p<0.05$) under limited phosphorus for each genotype. b) Number of metabolites with significant fold change ($p<0.05$) under limited phosphorus for each genotype. Leaf tissue on left and root tissue on right.

Only 21 genes were significantly regulated in a similar fashion in both genotypes, some of which have an unknown function (Table 4.3). No genes were down regulated commonly in both genotypes. The gene with the greatest induction in both genotypes was a glycerol 3-phosphate permease.

In all cases there were a number (3) of genes encoding phosphatases up-regulated under P deficiency in leaf tissue (Appendix D). In addition, one gene encoding a phosphate transporter was also up-regulated but to a lesser extent. One group of genes was notably regulated, particularly in the Cashel_P genotype and these were those involved in cell wall synthesis with five cellulose synthase genes up-regulated under P deficiency (CESA4, CESA9, CESA1, CESA2 and CESA8). Other genes involved in cell wall modification were also identified with the gene encoding ENDO-1, 4-beta-xylanase, which catalyses the hydrolysis of the major plant hemicellulose, xylan, reporting the greatest increase in expression in Cashel_P under P deficiency.

4.4.4 Metabolite changes in leaf tissue under P deficiency

Metabolite profiling was carried out on both genotypes when grown under normal P supply and restricted P supply. Results for quality control of metabolite analysis are shown and described in Appendix E. The metabolite profiles comprised the levels of 206 metabolites (140 identified metabolites) which included 116 polar metabolites and 90 non-polar metabolites. Principal component analysis revealed distinguishing differences between the profiles of leaves from different genotypes (Figure 4.2) and, to a lesser extent, between treatments. An analysis of variance (ANOVA) identified a number of significantly different ($p<0.05$) metabolites in the different tissues and genotypes (Figure 4.1b).

Table 4.3 - Genes significantly (P<*0.05*) induced ≥ 2 fold after 24 hrs P deficiency in the leaf and root tissue of both Cashel_P and IRL-OP-02538_P genotypes.

Array ID	Best hit Rice PP5		IRL-OP-02538_P		Cashel_P	
		E value	Fold Change	P value	Fold Change	P value
Leaf						
U35_44k_v1_27526	glycerol 3-phosphate permease	1e-45	7.6	0.00	17.1	0.00
U35_44k_v1_31414	glycerol 3-phosphate permease	7e-70	7.0	0.00	12.3	0.00
U35_44k_v1_12109	histidine decarboxylase	1e-121	5.9	0.00	5.8	0.00
U35_44k_v1_7536	purple acid phosphatase precursor	1e-166	5.5	0.00	5.3	0.00
U35_44k_v1_26073	nucleotide pyrophosphatase/phosphodiesterase	1e-130	4.5	0.00	5.4	0.00
U35_44k_v1_31178	No hits found		3.7	0.00	2.9	0.01
U35_44k_v1_7801	UDP-sulfoquinovose synthase chloroplast precursor	1e-68	3.4	0.01	4.2	0.00
U35_44k_v1_27915	ids4-like protein	4e-18	3.4	0.00	5.3	0.00
U35_44k_v1_48069	No hits found		3.1	0.00	2.4	0.02
U35_44k_v1_24642	expressed protein	2e-15	2.9	0.04	5.7	0.00
U35_44k_v1_8347	phospholipase C	1e-159	2.8	0.01	4.3	0.01
U35_44k_v1_30444	expressed protein	4e-43	2.8	0.00	2.0	0.00
U35_44k_v1_36750	expressed protein	4e-85	2.7	0.00	2.4	0.04
U35_44k_v1_28139	phosphate transporter 1	1e-82	2.7	0.04	10.5	0.01
U35_44k_v1_27385	acid phosphatase/vanadium-dependent haloperoxidase related	4e-05	2.5	0.01	2.4	0.00
U35_44k_v1_28600	expressed protein	4e-65	2.4	0.01	2.5	0.00
U35_44k_v1_2801	expressed protein	3e-21	2.3	0.05	2.6	0.00
U35_44k_v1_9242	diacylglycerol O-acyltransferase 1 putative expressed	1e-97	2.1	0.05	6.3	0.01
U35_44k_v1_11282	xyloglucan endotransglucosylase/hydrolase protein 30 precursor	8e-47	2.1	0.05	2.3	0.04
U35_44k_v1_1867	pyrophosphate--fructose 6-phosphate 1-phosphotransferase alpha subunit	0.0	2.1	0.01	2.6	0.01
U35_44k_v1_6244	glycerophosphoryl diester phosphodiesterase precursor	3e-93	2.1	0.03	2.4	0.00
Root						
U35_44k_v1_5590	1,4 beta-xylanase, putative, expressed	0.0	3.3	0.03	3.3	0.04

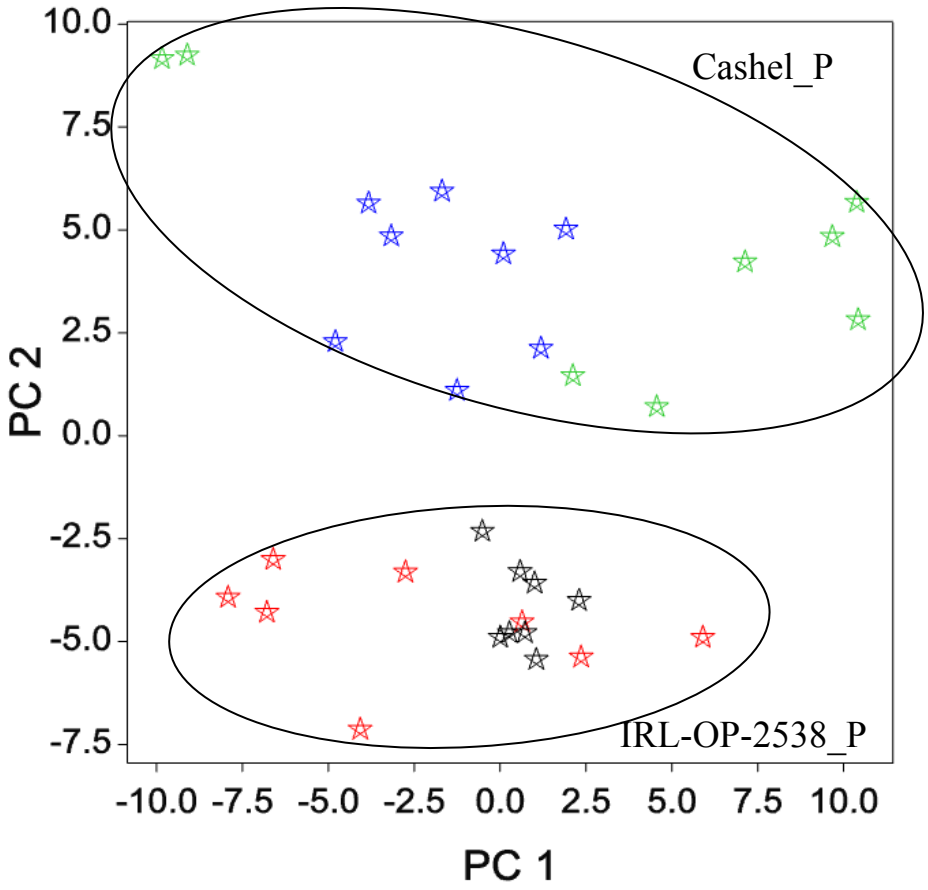

Figure 4.2 – PCA plot representing the first (PC 1) and second (PC 2) components of the metabolite profiles of leaf tissue samples. The second principal component appears to separate both genotypes. Components 1 and 2 explain 16.3 and 13.9% of the metabolite variation respectively. Cashel_P grown under P limiting conditions - ★; Cashel_P grown under P sufficient conditions - ★; IRL-OP-2538_P grown under P limiting conditions - ★; IRL-OP-2538_P grown under P sufficient conditions - ★.

In contrast to the transcriptomic data, no major difference in the number of up-regulated metabolites between genotypes was found, although the majority of metabolites were different. In the leaf tissue of IRL-OP-02538_P there were a total number of 27 regulated metabolites (including nine unidentified metabolites). One unidentified metabolite, was up-regulated under P deficiency whilst the remaining 26 metabolites (Table 4.4) were down-regulated. This is in contrast to the genotype Cashel_P where eleven metabolites were up-regulated and ten metabolites down-regulated (Table 4.5). From the total of 21 significantly regulated metabolites in Cashel_P in the leaf tissue, 4 of the metabolites remain unidentified. These differences in trends between genotypes

contributed significantly to the segregation seen in the principal component analysis (PCA) of the leaf tissue. In Cashel_P, there was a significant decrease in amino acids (asparagine, glutamine, homoserine and histidine) while the levels of putative Phytol-derived metabolites appeared up-regulated (Phytol A-C and Phytil methyl ether). Despite the overall differences in the metabolic response to P-limitation, both genotypes experienced a significant decrease in the levels of P_i.

Table 4.4 – Comparison of the mean and standard error of significantly different ($p<0.05$) metabolites in the leaves and roots of IRL-OP-2538_P genotype under sufficient and deficient phosphorous conditions.

	Average IRL-OP-2538_P under sufficient P supply	Standard error of mean	Average IRL-OP-2538_P under limited P supply	Standard error of mean	low/high	p-value	Log(ratio)
Leaf							
Unknown	1.83E-04	2.24E-05	3.10E-04	3.29E-05	1.69	0.007	0.23
Phytil methyl ether 2nd peak	4.47E-01	9.92E-03	4.01E-01	1.58E-02	0.90	0.028	-0.05
Unknown	5.17E-01	1.60E-02	4.49E-01	2.67E-02	0.87	0.045	-0.06
Unknown	1.10E-02	4.82E-04	9.22E-03	6.05E-04	0.84	0.037	-0.08
Phenylalanine	5.64E-04	2.18E-05	4.71E-04	2.53E-05	0.84	0.015	-0.08
n-Tetracosanol	1.11E-02	4.76E-04	9.01E-03	5.13E-04	0.81	0.010	-0.09
Octadecanol	5.25E-03	3.64E-04	4.02E-03	4.23E-04	0.76	0.044	-0.12
Isoleucine	3.09E-04	1.07E-05	2.13E-04	2.35E-05	0.69	0.002	-0.16
Unknown	3.71E-04	1.70E-05	2.53E-04	2.36E-05	0.68	0.001	-0.17
Unknown	5.13E-04	3.81E-05	3.48E-04	3.60E-05	0.68	0.007	-0.17
Citric acid	5.48E-03	2.69E-04	3.50E-03	7.87E-04	0.64	0.032	-0.19
Pentadecenoic acid	5.43E-03	2.98E-04	3.37E-03	4.35E-04	0.62	0.002	-0.21
□-alanine	4.94E-05	3.98E-06	3.01E-05	5.86E-06	0.61	0.016	-0.22
Leucine	4.13E-04	3.82E-05	2.49E-04	5.61E-05	0.60	0.030	-0.22
Fructose*	1.19E-02	1.27E-03	7.15E-03	6.58E-04	0.60	0.005	-0.22
Tyrosine	2.40E-04	1.99E-05	1.37E-04	3.03E-05	0.57	0.013	-0.24
Unknown	4.19E-04	7.73E-05	2.39E-04	3.10E-05	0.57	0.049	-0.24
Malic acid	1.22E-02	6.35E-04	6.73E-03	8.48E-04	0.55	<0.001	-0.26
Unknown	5.80E-05	3.70E-06	2.58E-05	5.16E-06	0.44	<0.001	-0.35
n-pentadecanoic acid	8.70E-04	1.42E-04	3.82E-04	1.42E-04	0.44	0.029	-0.36
Lysine	3.61E-05	3.07E-06	1.56E-05	6.89E-06	0.43	0.017	-0.36
Fucosterol	1.84E-03	3.34E-04	7.44E-04	2.52E-04	0.41	0.020	-0.39
Phosphate	3.06E-03	1.82E-04	1.20E-03	5.07E-04	0.39	0.004	-0.41
2-Piperidinecarboxylic acid	2.27E-05	3.78E-06	8.58E-06	3.41E-06	0.38	0.015	-0.42
Unknown	2.26E-03	5.32E-04	8.37E-04	1.65E-04	0.37	0.023	-0.43
Unknown	2.12E-03	2.20E-04	7.73E-04	1.17E-04	0.36	<0.001	-0.44
Proline	2.20E-03	7.38E-04	5.26E-04	1.41E-04	0.24	0.043	-0.62
Root							
Unknown	5.63E-04	1.35E-04	0.00E+00	0.00E+00	*	<0.001	*
Stigmastadienol	6.68E-05	6.68E-05	6.03E-04	2.16E-04	9.03	0.032	0.96
Diamino-1,3-propane	3.25E-06	2.35E-06	1.93E-05	4.70E-06	5.94	0.009	0.77
Unknown	8.96E-04	1.84E-04	3.65E-03	8.38E-04	4.08	0.006	0.61
Unknown	1.72E-03	3.92E-04	5.29E-03	9.09E-04	3.07	0.003	0.49
Unknown	4.07E-05	8.87E-06	9.54E-05	1.10E-05	2.34	0.002	0.37
D-5-avenasterol	1.63E-03	1.84E-04	3.63E-03	6.45E-04	2.23	0.010	0.35

Table 4.4 (continued)

Putrescine	7.52E-05	8.26E-06	1.62E-04	1.25E-05	2.15	<0.001	0.33
Galactose	2.89E-05	6.69E-06	5.78E-05	1.13E-05	2.00	0.046	0.30
Fructose*	1.22E-03	1.52E-04	2.35E-03	2.13E-04	1.93	<0.001	0.29
Glucose*	1.23E-03	1.51E-04	2.27E-03	1.79E-04	1.85	<0.001	0.27
Unknown	5.51E-05	7.71E-06	9.49E-05	1.04E-05	1.72	0.008	0.24
Shikimic acid	2.66E-05	2.26E-06	4.00E-05	2.30E-06	1.50	0.001	0.18
Unknown	2.07E-04	2.64E-05	3.09E-04	2.31E-05	1.49	0.011	0.17
Sucrose	7.85E-02	1.06E-02	1.16E-01	1.07E-02	1.48	0.027	0.17
n-Octadecanoic acid	7.44E-03	4.57E-04	9.96E-03	8.45E-04	1.34	0.020	0.13
Linoleic acid	2.06E-01	8.93E-03	2.62E-01	1.07E-02	1.27	0.001	0.10
α-linolenic acid	5.63E-02	2.32E-03	6.82E-02	3.65E-03	1.21	0.016	0.08
β-Sitosterol	1.55E-01	7.64E-03	1.86E-01	8.30E-03	1.20	0.017	0.08
n-Hexadecanoic acid	2.05E-01	4.83E-03	2.47E-01	1.46E-02	1.20	0.017	0.08
Valine	1.61E-03	1.05E-04	1.27E-03	8.97E-05	0.79	0.031	-0.10
Eicosanol	1.08E-02	1.10E-03	7.60E-03	6.74E-04	0.70	0.026	-0.15
Leucine	9.10E-04	7.67E-05	6.26E-04	6.74E-05	0.69	0.015	-0.16
Unknown	4.80E-04	3.89E-05	3.02E-04	6.90E-05	0.63	0.041	-0.20
Lysine	2.29E-04	2.26E-05	1.42E-04	1.42E-05	0.62	0.006	-0.21
Phosphate	1.24E-02	9.23E-04	7.33E-03	7.76E-04	0.59	<0.001	-0.23
Cinnamic acid	4.50E-02	7.17E-03	2.60E-02	4.78E-03	0.58	0.045	-0.24
4- or 3-Hydroxycinnamic acid	2.23E-02	1.64E-03	1.23E-02	1.08E-03	0.55	<0.001	-0.26
Alanine	1.83E-03	1.74E-04	9.89E-04	1.12E-04	0.54	0.001	-0.27
Unknown	5.29E-04	5.80E-05	2.75E-04	5.31E-05	0.52	0.006	-0.28
Allantoin	8.70E-04	6.48E-05	4.16E-04	6.06E-05	0.48	<0.001	-0.32
Unknown	1.25E-03	1.40E-04	5.05E-04	6.04E-05	0.40	<0.001	-0.39
Unknown	1.36E-04	1.18E-05	4.74E-05	1.70E-05	0.35	<0.001	-0.46
n-Docosanol	8.50E-04	1.61E-04	2.97E-04	6.63E-05	0.35	0.007	-0.46
Heneicosanol	9.84E-04	1.52E-04	3.15E-04	9.68E-05	0.32	0.002	-0.49
Mannitol	3.14E-04	5.80E-05	3.64E-05	1.37E-05	0.12	<0.001	-0.94

*Both Glucose and Fructose result in 2 peaks corresponding to their isomers. The levels of both isomers were combined to calculate the total value of glucose and fructose

4.4.5 Trancriptomic changes in root tissue under P deficiency

There were a much lower number of significantly regulated genes under P-deficiency in the root tissue in comparison to leaf tissue. Furthermore, the majority of the significantly regulated genes were down-regulated in both genotypes (Appendix D). In Cashel_P the down-regulated genes included those which encode a pair of ribosomal proteins, an asparagine synthetase (EC 6.3.5.4), a serine-glyoxylate aminotransferase (EC 2.6.1.45), a fructose-1, 6-bisphosphatase (EC 3.1.3.11) and a sedoheptulose-1, 7-bisphosphatase (EC 3.1.3.37). Only one gene was commonly regulated in both genotypes and this encoded a 1,4-beta-xylanase (EC 3.2.1.8), which was up-regulated.

4.4.6 Metabolite changes in root tissue under P deficiency

In the PCA of the metabolite profiles from root tissue (Figure 4.3) there was no segregation between genotypes as observed in the leaf tissue.

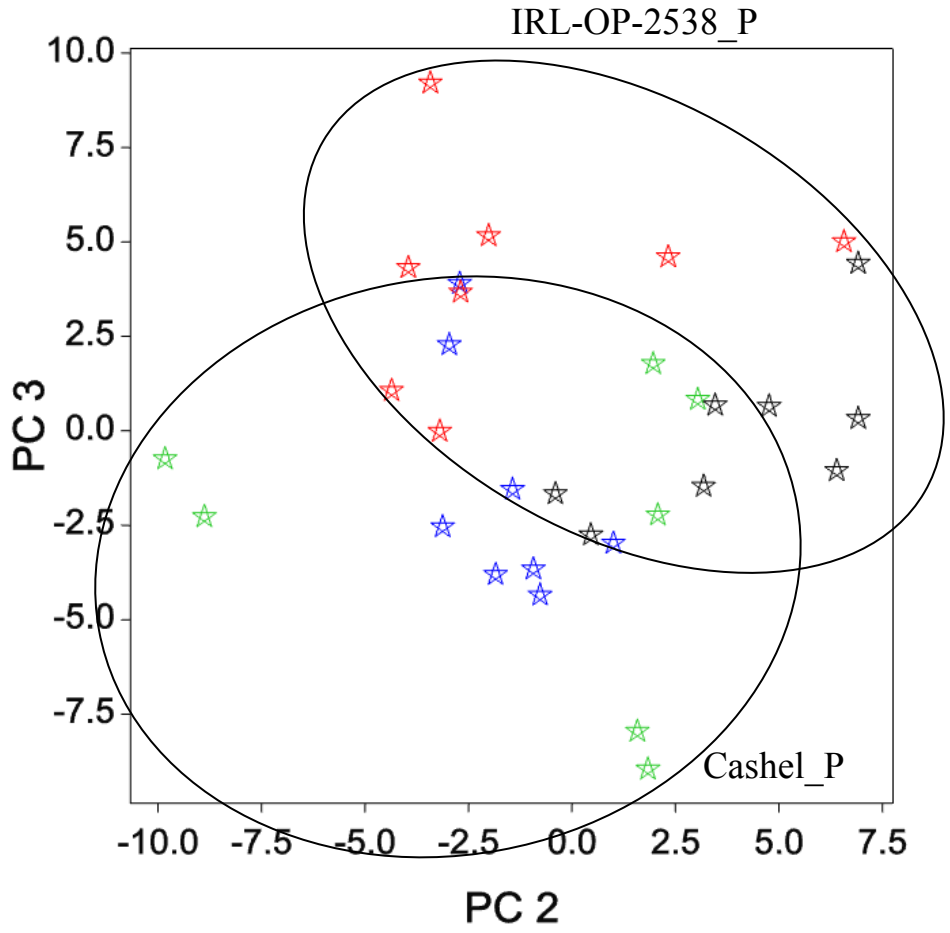

Figure 4.3 – PCA plot representing the second (PC 2) and third (PC 3) components of the metabolite profiles of root tissue samples. The second and third components explain 10.99 and 9.70% of the total variation in the metabolite profiles respectively. Cashel_P grown under P limiting conditions - ★; Cashel_P grown under P sufficient conditions -★; IRL-OP-2538_P grown under P limiting conditions -★; IRL-OP-2538_P grown under P sufficient conditions -★.

However, the ANOVA highlighted differences in the root tissue metabolites which could not be visualized using PCA. A greater difference in the number of significantly regulated metabolites was found between genotypes in the root tissue: 14 metabolites (eight unidentified) were regulated in Cashel_P plants to P limitation (Table 4.5) while in IRL-OP-02538_P that number increased to 36 (Table 4.4), which included ten

unidentified metabolites. The latter genotype experienced a general increase in sugar levels (glucose, fructose, galactose, sucrose) and fatty acids (C16:0, C18:0, C18:2 and C18:3) while some of the pyruvate-derived amino acids (alanine, leucine and valine) were decreased. Among the metabolites significantly regulated in Cashel_P, only six were putatively identified.

Table 4.5 – Comparison of significant different ($p<0.05$) metabolites in the leaves and roots of Cashel_P under sufficient and deficient phosphorus conditions.

	Average Cashel_P under sufficient P supply	Standard error of mean	Average Cashel _P under limited P supply	Standard error of mean	Low/high	p-value	Log(ratio)
Leaf							
γ-aminobutyric acid	3.41E-04	6.68E-05	6.86E-04	8.34E-05	2.01	0.006	0.30
Unknown	3.56E-05	6.31E-06	5.65E-05	5.86E-06	1.59	0.029	0.20
Galactose/glycerol conjugate	8.19E-05	1.13E-05	1.25E-04	1.55E-05	1.53	0.042	0.18
Threonic Acid	8.27E-04	6.73E-05	1.21E-03	1.47E-04	1.46	0.034	0.16
Unknown	2.60E-01	8.97E-03	3.62E-01	2.29E-02	1.4	<0.001	0.14
Phytol B	2.12E-02	8.23E-04	2.85E-02	1.64E-03	1.34	0.002	0.13
Phytol A	1.27E-02	5.89E-04	1.66E-02	6.75E-04	1.31	<0.001	0.12
Sucrose	4.01E-01	4.12E-02	5.04E-01	1.80E-02	1.26	0.038	0.10
Phytol C	6.33E-03	5.24E-04	7.88E-03	3.31E-04	1.25	0.025	0.10
n-Hexadecenoic acid	4.43E-02	2.43E-03	5.54E-02	3.10E-03	1.25	0.014	0.10
Phytil methyl ether	1.49E-01	4.32E-03	1.79E-01	7.54E-03	1.2	0.004	0.08
Homoserine	2.16E-04	4.43E-05	1.17E-04	1.05E-05	0.54	0.047	-0.27
2-Piperidinecarboxylic acid	3.95E-05	6.09E-06	2.03E-05	6.45E-06	0.51	0.048	-0.29
Unknown	7.45E-05	1.33E-05	3.18E-05	5.55E-06	0.43	0.010	-0.37
5-Oxoproline	5.29E-02	1.38E-02	2.27E-02	2.57E-03	0.43	0.049	-0.37
Histidine	7.89E-06	2.17E-06	2.04E-06	8.14E-07	0.26	0.024	-0.59
Spermidine	5.38E-06	1.74E-06	1.18E-06	8.73E-07	0.22	0.048	-0.66
Glutamine*	2.66E-03	8.22E-04	5.3E-04	1.58E-04	0.20	0.026	-0.70
Phosphate	7.64E-03	1.69E-03	1.17E-03	3.60E-04	0.15	0.002	-0.82
Asparagine*	1.11E-03	3.12E-04	1.5E-04	6.59E-05	0.14	0.009	-0.87
Unknown	3.48E-04	1.44E-04	3.10E-05	1.74E-05	0.09	0.046	-1.05
Root							
Unknown	2.40E-04	8.43E-05	5.71E-04	1.18E-04	2.38	0.045	0.38
Unknown	1.08E-04	2.75E-05	2.28E-04	3.40E-05	2.11	0.019	0.32
Unknown	3.69E-04	6.82E-05	7.56E-04	1.52E-04	2.05	0.046	0.31
Methionine	3.62E-05	7.21E-06	7.12E-05	1.15E-05	1.97	0.027	0.29
Unknown	5.11E-05	1.41E-05	9.36E-05	1.31E-05	1.83	0.046	0.26
Sucrose	5.50E-02	1.43E-02	9.70E-02	8.33E-03	1.76	0.022	0.25
Aspartic acid	5.14E-03	7.65E-04	8.28E-03	3.89E-04	1.61	0.002	0.21
Glutamic acid	6.61E-03	1.36E-03	9.84E-03	4.56E-04	1.49	0.034	0.17
n-Tetracosanoic	1.35E-02	1.94E-03	9.20E-03	6.05E-04	0.68	0.043	-0.17
Unknown	1.21E-04	1.90E-05	7.60E-05	4.18E-06	0.63	0.028	-0.20
Octadecenoic acid	4.61E-03	6.03E-04	2.53E-03	2.29E-04	0.55	0.005	-0.26
Unknown	2.09E-03	4.82E-04	1.05E-03	1.23E-04	0.50	0.044	-0.30
Unknown	6.10E-04	5.40E-05	2.69E-04	7.36E-05	0.44	0.003	-0.36
Unknown	4.32E-05	1.27E-05	1.39E-05	3.79E-06	0.32	0.035	-0.49

* Both glutamine and asparagine generate 2 TMS derivatives which were combined to generate the total levels of asparagine and glutamine. For glutamine the TMS4 derivative was multiplied by a factor of 2 before being combined with its other derivative

As a result of imposing P limitation on Cashel_P, the levels of sucrose and some amino acids (methionine, aspartic acid and glutamic acid) increased while some fatty acid levels (C24:0 and C18:1) decreased.

4.4.7 Analysis of FT-IR spectra

The comparison of samples with reference samples is described in Appendix F. The PCA derived from the FT-IR spectra of samples from both tissues revealed that samples from root tissue clustered away from leaf samples (Appendix F). Therefore, it was decided to individually analyse samples from different tissues. PCA of leaf samples (Figure 4.4) revealed that the spectrum profile of samples does not seem to be particularly affected by genotype or P supply. However, PCA of the root tissue revealed segregation resulting from treatment in both genotypes (Figure 4.5). The separation between Cashel P-sufficient and P-limited samples seems to be driven by the 4^{th} principal component while the separation between IRL-OP-02538 occurs mainly on the first principal component. Analysis of the loading plots revealed that the regions of the IR spectra that seem to have a major influence in the first principal component are 980-1100 cm^{-1} (positive), 600-700 cm^{-1}, 1500-1700 cm^{-1} and 3100-3300cm^{-1} (negative). The contribution of the regions of 1300-1450cm^{-1} (positive) and 2850-2950cm^{-1} (negative) seem to drive the major differences in the fourth principal component (see Appendix F). These regions in the range of 900-1800 cm^{-1} are generally associated with structural polymers (in grasses at least) such as hemicelluloses, celluloses, pectins and lignins. Therefore, it appears that cell components of root tissue experience some extent of modification as result of exposure to limitation of P.

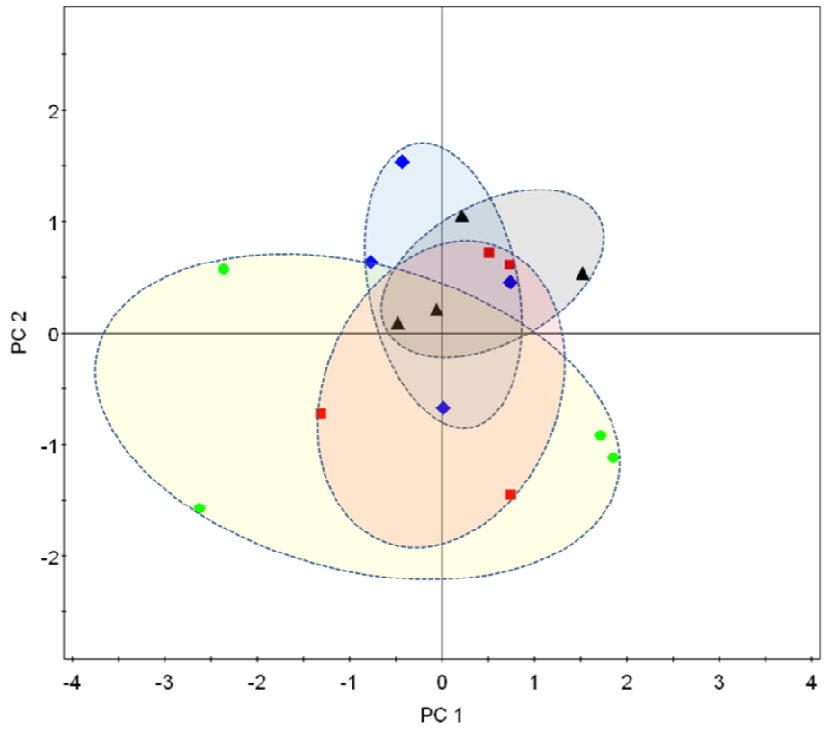

Figure 4.4 – PCA plot representing the first (PC 1) and second (PC 2) components derived from the FT-IR spectra of leaf tissue samples. The first and second components explain 54.02 and 27.60% of the total variation in the FT-IR spectra respectively. Cashel_P grown under P limiting conditions -▲; Cashel_P grown under P sufficient conditions -♦; IRL-OP-2538_P grown under P limiting conditions -●; IRL-OP-2538_P grown under P sufficient conditions -■.

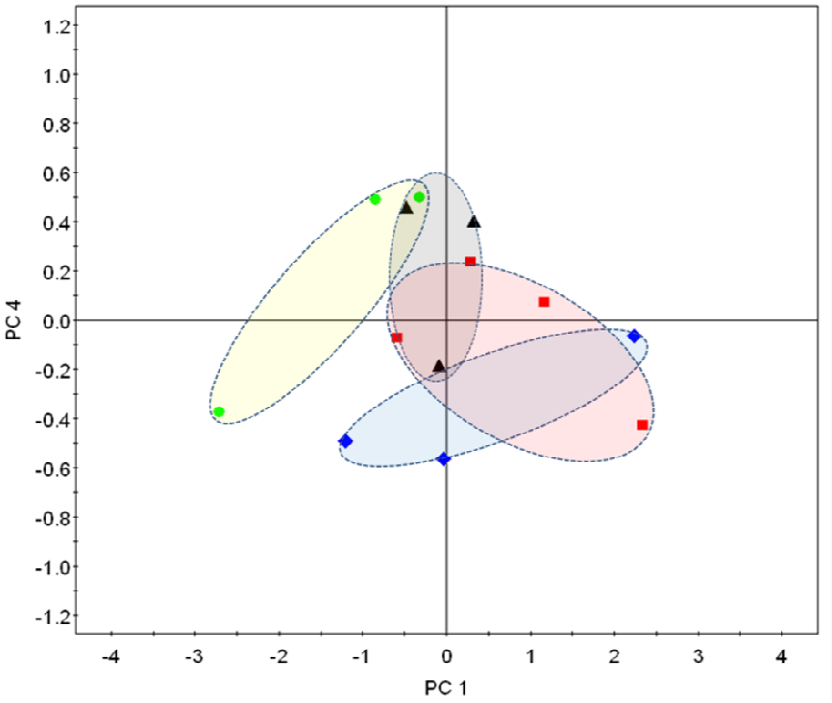

Figure 4.5 – PCA plot representing the first (PC 1) and fourth (PC 4) components derived from the FT-IR spectra of root tissue samples. The first and fourth components explain 51.96 and 4.33% of the total variation in the FT-IR spectra respectively. Cashel_P grown under P limiting conditions -▲; Cashel_P grown under P sufficient conditions -♦; IRL-OP-2538_P grown under P limiting conditions -●; IRL-OP-2538_P grown under P sufficient conditions -■.

4.5 Discussion

This chapter aimed to uncover changes in the transcriptome and metabolome of two perennial ryegrass genotypes during the initial stages of P deficiency. The analysis of the effects at the transcriptome level of exposure to P-deficit conditions has been limited to a small number of species, which include *Arabidopsis* (Wu *et al*., 2003; Hammond *et al*., 2003; Misson *et al*., 2005; Muller *et al*., 2007) and rice (Wasaki *et al*., 2006). Similarly, the global response to P-limitation at the metabolite level has been reported in a relatively low number of species, such as barley (Huang *et al*., 2008). Furthermore, the combination of both global transcript and metabolite profiling has been used to determine the response of common bean (*Phaseolus vulgaris*) to P limitation (Hernandez *et al*., 2007; Hernandez *et al*., 2009). In perennial ryegrass, however, this is the first study looking at the global transcript and metabolic responses to low P availability, thus providing an emerging insight into the early stage response mechanisms to P deficiency. Metabolic profiling demonstrated that P deficiency resulted in a Pi decrease in both genotypes (Tables 4.4 and 4.5), which confirms that the experimental conditions have successfully produced an effect on the intracellular levels of P_i and that the timeframe (24 h) was sufficient to elicit this response.

4.5.1 Signalling Mechanisms

The microarray results identified changes in the expression levels of genes involved in signal transduction that may also be involved in the leaf tissue response to P deprivation. A gene encoding phospholipase C (PLC, EC 3.1.4.3) was significantly up-regulated in the leaf tissue of both genotypes (Table 4.3). PLC catalyses the hydrolysis

of phosphatidylinositol 4,5-bisphosphate ($PI(4,5)P_2$) into diacylglycerol (DAG) and inositol triphosphate (IP_3), the latter diffusing through the cytosol releasing calcium from intracellular stores or being converted to inositol hexakisphosphate (IP_6), both of which may play roles as signalling molecules (Meijer and Munnik, 2003).

Furthermore, in IRL-OP-2538_P it was found the expression level of a putative membrane calcium-transporting ATPase 2 was up-regulated under P-deficiency, which further suggests the role of calcium-mediated response to P-limitation. This seems to be corroborated in Cashel_P, where the expression of a number of genes that are involved in calcium-mediated responses such as a putative calmodulin-binding protein and a putative calcium-dependent protein kinase isoform AK1 appear to be enhanced under P-deficiency (Appendix D).

The up-regulation of an *ids4*-like gene was observed in both genotypes (Table 4.3), which has been described in previous transcriptomic studies as being enhanced under P deficiency (Misson *et al*., 2005; Guo *et al.*, 2008). The *ids*4-like gene shares most significant homology with At2g45130 from *Arabidopsis* that contains an SPX domain, a region in PHO1 genes identified important for inorganic phosphate homeostasis (Wang *et al*, 2004). This gene, *AtSPX3*, has recently been proposed to play a role in a phosphate-signalling network (Duan *et al*., 2008). It was shown that when *AtSPX3* was repressed by RNAi it resulted in augmentation of P deficient symptoms and altered allocation of internal P leading to the conclusion that *AtSPX3* plays an important role in plant adaptation to P deficiency (Duan *et al*., 2008). The high induction of an *AtSPX3* homologue in the early stages of P deficiency in both genotypes of our study indicates it may have a similar role to play in adaptation to P deficiency in perennial ryegrass.

4.5.2 Membrane Remodelling

One mechanism of adaptation to P deficient growth conditions is the remodelling of plant lipid membranes in order to liberate Pi bound in membrane phospholipids (Plaxton, 2004). The increase reported in the expression levels of genes encoding phospholipase A1 (EC 3.1.1.32) together with increases in glycerophosphoryl diester phosphodiesterase (EC 3.1.4.46, hydrolysis of deacylated phospholipids to glyceraldehyde 3-phosphate), acid phosphatase/vanadium dependent hydrolase, and diacylglycerol O-acyltransferase 1 (EC 2.3.1.20) also seems to suggest a certain degree of phospholipid remodelling in the response to P deficiency in perennial ryegrass (Table 4.3). Photosynthetic membranes are characterized by a substantial fraction of non-phosphorus lipids, such as galactolipids or sulfolipids (for example sulfoquinovosyldiacylglycerol), which reflects the need to conserve phosphorous by plants (Benning, 2009). In this study it was observed a significant increase in expression of genes encoding UDP-sulfoquinovose synthase (EC 3.13.1.1), a key enzyme in the sulfoquinovosyldiacylglycerol (SQDG) synthesis pathway, during P deficiency in the leaf tissue of both genotypes. Misson *et al.*, (2005) have previously demonstrated in *Arabidopsis* that under Pi deficiency SQDG increased, whereas phosphatidylglycerol (PG) decreased and these results are in agreement with elevated expression of genes involved in SQDG synthesis and phospholipid degradation.

An increase was also observed in the gene expression level of a sulphate transporter in both genotypes, however, the increase was only significant in Cashel_P (Cashel_P - 5.2 fold, $P<0.001$; IRL-OP-02538_P – 2.8 fold, $P=0.054$). This has previously been observed in *Arabidopsis* and was proposed to support an increased demand for sulphur during P deficiency to meet the needs for increased sulfolipid synthesis (Misson *et al.*,

2005). Further support for lipid membrane remodelling in perennial ryegrass can be seen from the strong induction of a gene encoding glycerol 3-phosphate permease (G3PP) under P deficiency (7.5 fold and 17.1 fold, $P<0.001$ in IRL-OP-02538_P and Cashel_P, respectively). This suggests the enhanced mobilization of glycerol 3-phosphate from the cytosol into the chloroplast or endoplasmic reticulum where it could be utilised in lipid biosynthesis (Figure 4.6). The results obtained indicate that the replacement of phospholipids with sulfolipids in the membranes of photosynthetic tissue is also occurring in perennial ryegrass under P deficiency that this is a rapid response to changes in external P concentrations.

Additionally, it was found that in the roots of genotype IRL-OP-02538 there was an increase in sterol levels, such as stigmastadienol, avenasterol and β-sitosterol in response to P-starvation (Table 4.4). Sterols are primary components of the cellular membranes where they regulate fluidity and permeability (Schaller, 2003). Furthermore it has been suggested that an appropriate composition of sterols in the membranes is crucial for optimal enzymatic activity, ion and metabolite transport or channelling and also protein-protein and protein-lipid interactions (Schaller, 2003). It is plausible therefore, that the modification of sterol levels in the membranes upon P-limitation impact to some extent on these biological processes. Hypothetically, the impact on ion and metabolite transport and channelling would be particularly relevant for the root adaptation to P-deficit since some of the major responses of roots to low P include increases in phosphate uptake and organic acid excretion (Raghothama, 1999).

4.5.3 Carbon Partitioning

At the metabolome level in the leaves of IRL-OP-02538_P, P deficiency was accompanied by an overall decrease in metabolite levels whilst there were no putatively identified up-regulated metabolites. The significantly regulated metabolites included a variety of metabolite classes such as sugars, amino acids, fatty acids and organic acids. The overall decrease in metabolite levels may be symptomatic of either a decrease of source activity due to decreases in photosynthetic activity, an increase in sink activity or both. Phosphorous limitation has been reported to impact upon photosynthetic activity (Foyer and Spencer 1986, Lauer *et al*., 1989, Rodriguez *et al.*, 1998) however, increases in the root:shoot ratio are also considered typical effects of P limitation (Marschner, 1995) and may account for increased sink activity as carbohydrates are exported from the leaves to the roots. A study by Wissuwa *et al.* (2005) focused on determining whether root growth in rice is affected by either source or sink limitations when grown under P deficient conditions and they did this by comparing rice genotypes under four P levels and two light treatments. The authors reported that net photosynthesis was 70% greater in plants grown under high, compared with low, light but it was found that this did not translate into greater root growth under P limitation, leading them to suggest that assimilate supply from source leaves was not a limiting factor under P limitation.

Conversely, low P supply appears to limit root growth directly. It was proposed that the most tolerant genotype used in the experiment of Wissuwa *et al.*, (2005) preferably mobilized P to the roots, which would increase P concentrations and consequently promote growth. The levels of sugars in the roots of IRL-OP-02538_P increase in response to P limitation, which seem to suggest a decrease in sink activity, resulting from a reduction in root growth.

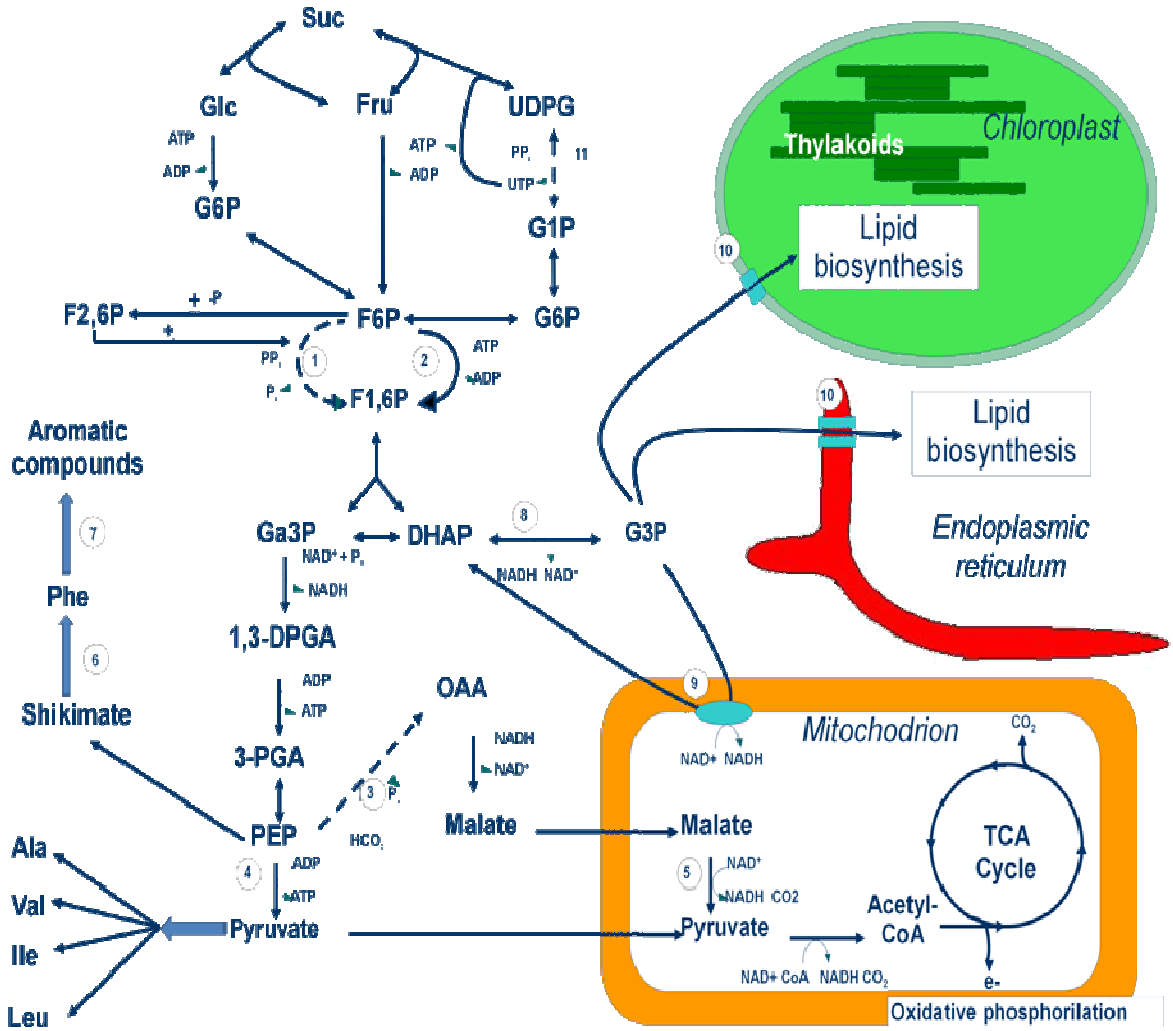

Figure 4.6 - Diagram depicting the primary metabolism in *Lolium perenne,* adapted from Hammond *et al*., 2004. Bold Arrows represent a downstream set of reactions, not single reactions. Dashed arrows highlight alternative pathways for glycolysis to conserve Pi. Microarray results indicate an increase in expression of transcripts encoding genes involved in reactions 1, 6, 7, 8 and 10. The designations are: Suc, sucrose; Glc, glucose; Fru, fructose; UDPG, UDP-glucose; G1P, glucose 1-phosphate; G6P, glucose 6-phosphate; F6P, fructose 6-phosphate; F2,6P, fructose 2,6-bisphosphate; F1,6P, fructose 1,6-bisphosphate; G3P, glycerol 3-phosphate; DHAP, dihidroxyacetone phosphate; OAA, oxalo acetic acid; Ga3P, glyceraldehyde 3-phosphate; 1,3-DPGA, 1,3- diphosphoglyceraldehyde; 3-PGA, 3-phosphoglycerate; PEP, phosphoenol pyruvate; Phe, phenylalanine; Ala, alanine; Val, valine; Ile, isoleucine; Leu, leucine. (1) pyrophosphate fructose 6-phosphate 1-phosphotransferase, EC 2.7.1.90; (2) ATP:fructose 6-phosphate 1-phosphotransferase, EC 2.7.1.11 (3) phospho*enol*pyruvate carboxykinase (ATP), EC 4.1.1.49 (4) pyruvate kinase, EC 2.7.1.40 (5) malate dehydrogenase (oxaloacetate-decarboxylating), EC 1.1.1.38 (6) involvement of anthranilate phosphoribosyltransferase, EC 2.4.2.18 (7) involvement of flavonol synthase/flavanone 3-hydroxylase (EC 1.14.11.23) (8) glycerol 3-phosphate dehydrogenase, EC 1.1.5.3 (9) glycerol-3-phosphate dehydrogenase, EC 1.1.5.3 (10) glycerol 3-phosphate permease (11) UDP-glucose pyrophosphorylase, EC 2.7.7.9

Growth inhibition in response to P limitation has been suggested to be mediated by putrescine in rice cells (Shih and Kao, 1996), and while no root:shoot ratios were measured, the significant accumulation of putrescine levels in the roots of IRL-OP-02538_P (Figure 4.8) suggests a limitation of root growth in IRL-OP-02538_P plants as an early response to P-deprivation

4.5.4 Glycolytic Bypasses

The results presented in this chapter presented evidence of glycolytic bypasses being utilised, which have previously been reported in other species as being valuable mechanisms to enable the efficient use of P during times of deficiency (Theodorou and Plaxton, 1993). A significant increase in the expression of a gene encoding an α-subunit of pyrophosphate:fructose 6-phosphate 1-phosphotransferase (PFP, EC 2.7.1.90) during P deficiency in the leaf tissue of both genotypes was observed. The phosphorylation of fructose-6-P to fructose 1-6 bisphosphate during glycolysis is efficiently catalysed by ATP:fructose 6-phosphate 1-phosphotransferase (PFK, EC 2.7.1.11), using ATP (Stryer, L., 1995). PFP can also catalyse this reaction but employing PP_i rather than ATP (Figure 4.4). It has already been demonstrated in black mustard (*Brassica nigra*) suspension cells that PFP activity is increased under P deficiency and its activity falls to below the level of PFK as solute P levels increase (Duff *et al*., 1989). Furthermore, it was shown that the α-subunit of PFP has a regulatory role over the β-subunit and that its activity is tightly regulated by intracellular Pi status (Theodorou *et al*., 1992). The results presented in this chapter demonstrate that a switch to alternative pathways during glycolysis happens at an early stage of P deficiency in perennial ryegrass.

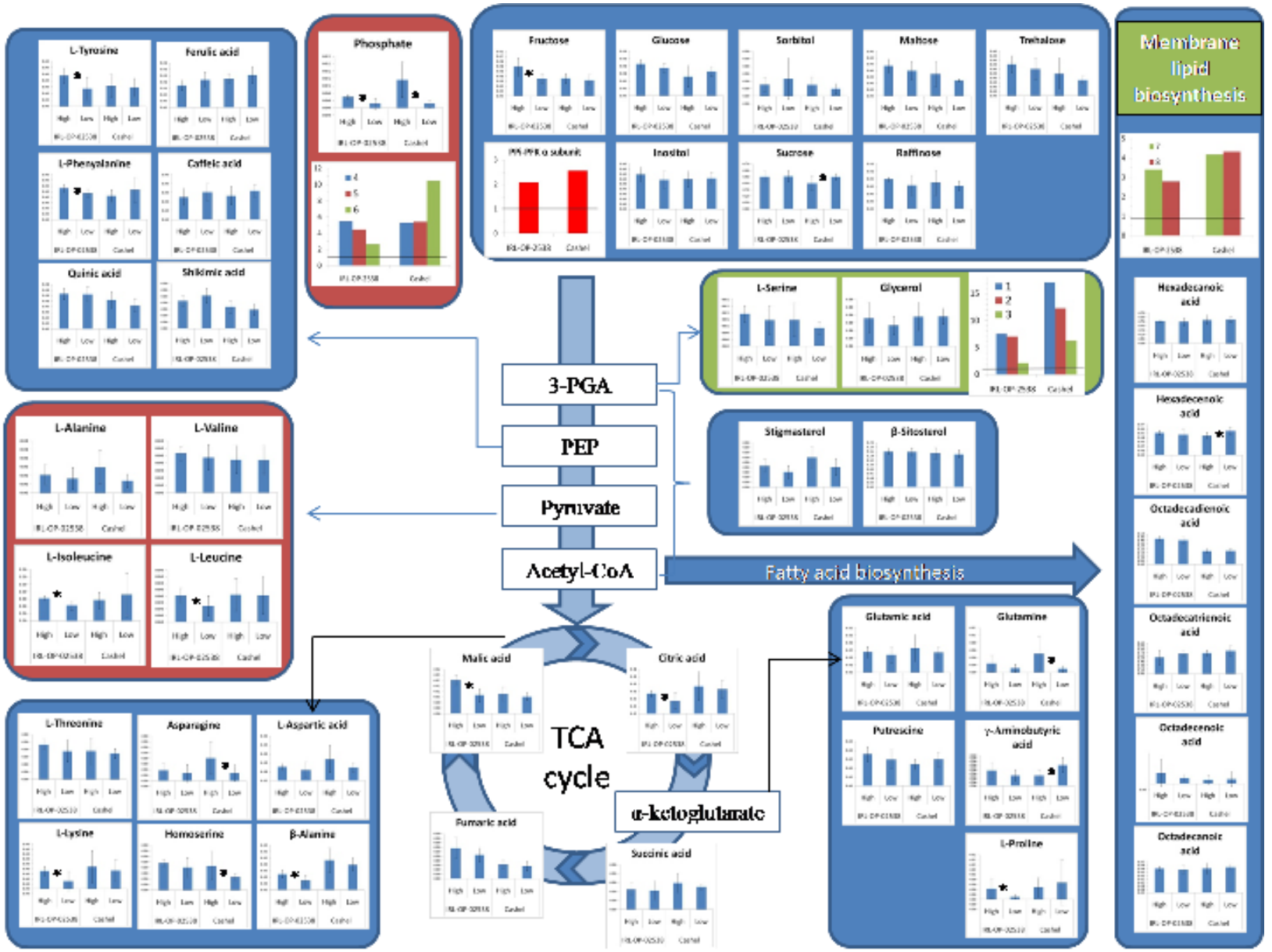

Figure 4.7 - Diagram representing the means and respective standard deviations of metabolite levels in the leaf tissue of IRL-OP-02538_P and Cashel_P plants grown under control and P-limited conditions . Significant differences (p-value < 0.05) between the means of control and water-stressed plants are represented with *. Red boxes represent pathways which display an overall negative regulation in response to stress, whereas green boxes represent pathways which display a positive regulation in response to stress. Furthermore, significant fold changes (p-value <0.05) of gene expression are represented: 1- Glycerol 3P-permease 2- Glycerol 3P-permease 3- Diacylglycerol O-acyl transferase 4- purple acid phosphatase precursor putative expressed 5- nucleotide pyrophosphatase/phosphodiesterase putative expressed 6- Phosphate transporter 1 putative expressed 7- UDP-sulfoquinovose synthsae chloroplast precursor putative expressed 8- phospholipase C putative expressed.

Another important glycolytic bypass mechanism, which is cited in the introductory section, involves the carboxylation of PEP to oxaloacetate in a reaction catalysed by PEPCase (EC 4.1.1.31) (Plaxton, 2004). This mechanism attempts to bypass the activity of pyruvate kinase, which is involved in the biosynthesis of pyruvate. However, the transcript profiling approach did not reveal any significant regulation of any PEPCase-related genes. It is possible that this resulted from the genes encoding PEPCase not being present in the number of genes which successfully hybridised with the barley microarray.

Interestingly, a study by Shinano *et al*. (2005) revealed that under P-deprived conditions rice plants experience a small increase in the expression levels of both PEPCase, and pyruvate kinase (EC 2.7.1.40). This is in contrast with the findings of Duff *et al*. (1989), who observed a significant up-regulation of PEPCase expression of at least 5-fold in *Brassica nigra* suspension cells. Shinano *et al*. (2005) suggested that, in rice plants, the pyruvate kinase bypass would modify the carbon flux from PEP to the TCA cycle, thus reducing the pyruvate levels. This would lead to a repression of alanine-related amino acid biosynthetic pathway which would not be acceptable at whole plant level.

However, the results presented in this chapter reveal that, in both leaf and root tissue of genotype IRL-OP-02538_P, the levels of some of the alanine-related aminoacids (alanine, leucine, isoleucine and valine) experience a decline in IRL-OP-02538_P plants exposed to P-limitation (Table 4.4 and figures 4.7 and 4.8). This seems to suggest that there is a decrease in the carbon flux towards this biosynthetic pathway at the whole plant level which may result from the PEPCase-mediated glycolytic bypass.

4.5.5 Aromatic secondary metabolites

A common physiological response in a wide variety of plants to long term P-limitation is the increase in anthocyanin content in leaf tissue (Hammond *et al*., 2004) and a number of studies have demonstrated the up-regulation of genes involved in anthocyanin biosynthesis during P deficiency (Hammond *et al*., 2003; Misson *et al*., 2005). It is thought that anthocyanins help protect the photosynthetic machinery during leaf senescence (Hoch *et al*., 2001). The biosynthesis of anthocyanins involves the shikimate pathway to produce phenylalanine, which eventually leads to flavonoid biosynthesis (Figure 4.4). The accumulation of anthocyanins is a general feature of long term P deficiency and the majority of the genes are specifically induced during long term deficiency (Misson *et al*., 2005). In IRL-OP-02538_P leaves after a period of 24h P deficiency, two transcripts involved in phenylalanine and flavonoid biosynthesis (anthranilate phosphoribosyltransferase, EC 2.4.2.18 and flavonol synthase/flavanone 3-hydroxylase, EC 1.14.11.9) were up-regulated. Simultaneosly there is a decrease in the levels of phenyalanine, which seems to indicate an increase in its conversion into its downstream products, which may suggest the early onset of a secondary metabolite response in this genotype.

4.5.6 Glycerol 3-phosphate shuttle

PEP is a precursor of the shikimate pathway and has an important role in the PEPC mediated glycolitic bypass. The reduction of oxaloacetate to malate in this bypass by consuming a molecule of NADH and the consequent transport of malate into mitochondria is a shuttle used to translocate NADH from the cytosol to the

mitochondria where NADH is consequently oxidized (Stryer, 1995). However, under P-deficit the leaves of genotype IRL-OP-02538_P have increased expression levels of glycerol 3-phosphate dehydrogenase. This is a central enzyme involved in an additional NADH shuttle previously identified in animals, yeast and more recently in *Arabidopsis thaliana* (Shen *et al*., 2006). This shuttle, often referred to as glycerol 3-phosphate shuttle, acts by reducing dihydroxyacetone phosphate (DHAP) to glycerol 3-phosphate in a step catalyzed by glycerol 3-phosphate dehydrogenase (EC 1.1.1.8) consuming one cytosolic NADH (Shen *et al*., 2006). Glycerol 3-phosphate subsequently diffuses through the outer mitochondria membrane and, once in contact with the inner mitochondria membrane, is oxidized in a reaction catalized by mitochondrial flavin adenine dinucleotide (FAD)-dependent glycerol 3-phosphate dehydrogenase:ubiquinone oxidoreductase (FAD-GPDH)(EC 1.1.99.5) generating DHAP and NAD^+ which then diffuses back to the cytosol. The electrons transferred to the membrane protein will then be used to reduce mitochondrial NAD+ to NADH (Shen *et al*., 2006). Therefore, the regulation of glycerol 3-phosphate dehydrogenase under low P growth conditions seems to suggest that P-limitation affects to some extent the cytosolic NADH/NAD^+ ratio. Alternatively, the increase in expression levels of glycerol 3-phosphate dehydrogenase may instead result from the extensive modification of lipid profiles in response to low P.

4.5.7 Cell Wall Metabolism

One class of genes stands out as being abundant within the list of transcripts significantly up-regulated in leaf tissue under P deficiency, particularly in the Cashel_P genotype. These are genes involved in cell wall synthesis and remodelling. Previous reports have also reported the up-regulation of genes involved in cell wall synthesis

under P-limiting conditions (Wasaki *et al*., 2003). Five genes encoding the catalytic subunit of cellulose synthase (CESA) were up-regulated between both genotypes: four in Cashel_P and one in IRL-OP-02538_P. A total of ten CESA genes are reportedly present in the *Arabidopsis* genome and the role of these in cell wall synthesis has previously been described by Scheible and Pauly (2004). The significant up-regulation of this gene family points to an increased production of cellulose during the early stages of P deficiency. However, the gene with the highest increase in expression under P deficiency in Cashel_P leaves was an ENDO-1, 4-β-xylanase (EC 3.2.1.8), a xylan hydrolase. Taken together, these results may suggest a re-modelling of cell walls, with cellulose content increasing and xylan content decreasing to allow for cell expansion. The exact role, if any, of this modification under P deficiency remains unknown. Interestingly, it has been recently demonstrated that the overexpression of a wall-bound purple acid phosphatase from tobacco (*NtPAP12*) resulted in an increased deposition of cellulose in transgenic cells (Kaida *et al*., 2009). Transcripts coding for acid phosphatases (purple acid phosphatase precursor and acid phosphatase 1) are up-regulated in both genotypes in our study. The induction of acid phosphatases is regarded as a universal symptom/response of P limitation (Duff *et al*., 1994) and their role in hydrolysing Pi from mono-esters make them important in intracellular and extracellular Pi salvage systems (Plaxton, 2004). However, the results of PCA of the FT-IR spectra of leaf samples revealed minor significant differences between varieties or treatments in the leaf tissue (Figure 4.4). This seems to suggest that the alteration in the expression levels of genes involved in the metabolism of cell wall components under P-limitation does not result in immediate significant modifications of cell wall composition. Thus, it seems that modification of cell wall components may occur at later stages of response to P-limitation. However, further experimentation would be required to monitor the response of cell wall components in the leaf tissue over a longer period of time.

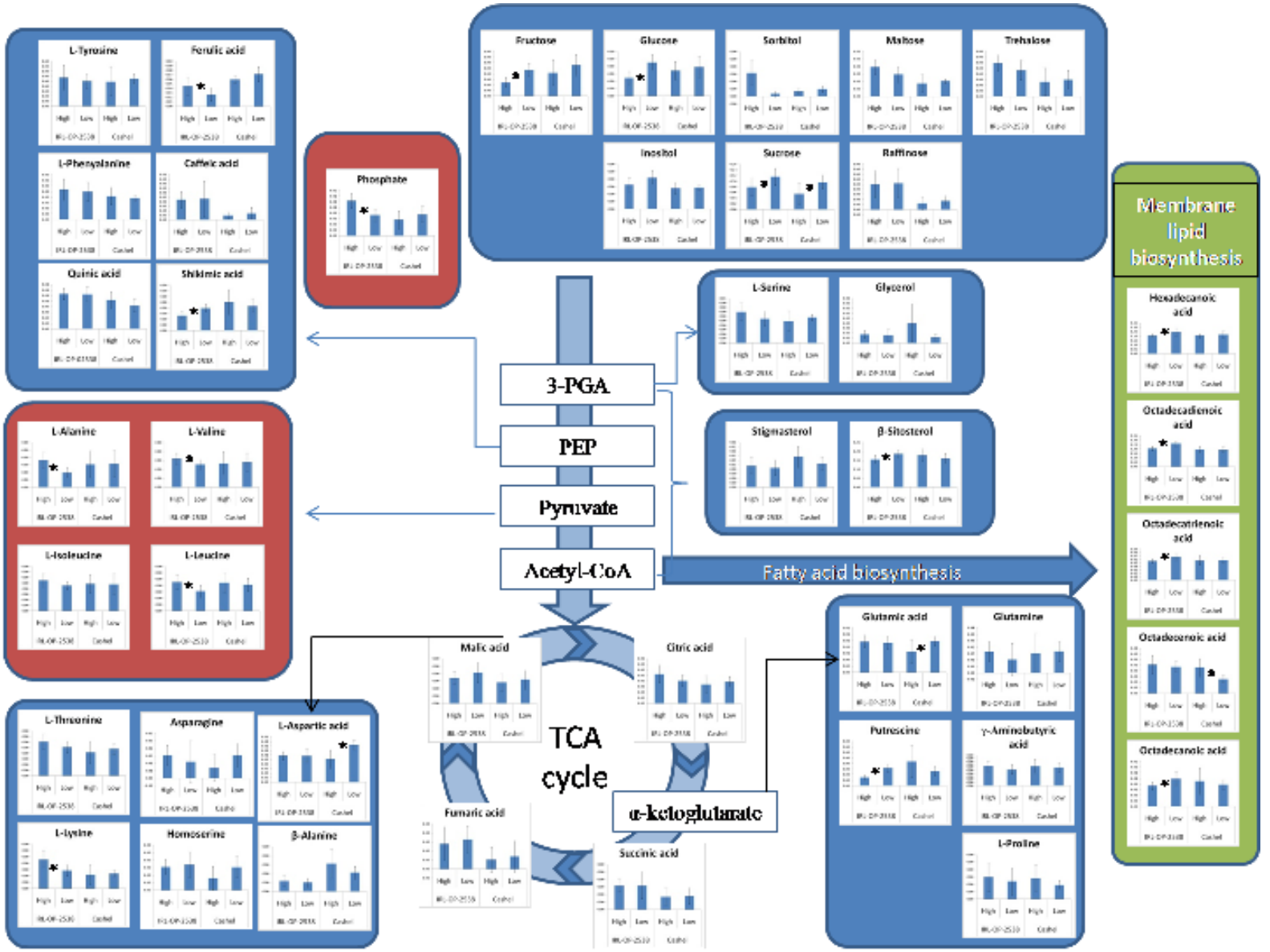

Figure 4.8 - Diagram representing the means and respective standard deviations of metabolite levels in the leaf tissue of IRL-OP-02538_P and Cashel_P plants grown under control and P-limited conditions . Significant differences (p-value < 0.05) between the means of control and water-stressed plants are represented with *. Red boxes represent pathways which display an overall negative regulation in response to stress, whereas green boxes represent pathways which display a positive regulation in response to stress.

Perhaps surprisingly, the PCA of the FT-IR data from the root tissue revealed significant differences between controls and stress tissues in both genotypes (Figure 4.5). Initially, this seems to be contradictory since there are a significantly lower number of regulated genes compared with the leaf tissue. Interestingly, the only gene which experienced a similar regulation in response to P-deficit in the roots of both genotypes was a 1,4-β-xylanase putatively expressed (Table 4.3). This gene encodes a xylan hydrolase and hence it may contribute to some extent for the regulation of the cell wall composition and/or physical structure in root tissues of perennial ryegrass.

The up-regulation of a gene encoding a xylan hydrolase also occurs in the leaf tissue of Cashel_P, however, it does not result in a significant modification of cell wall composition. Therefore, an increase in the expression of 1,4-β-xylanase is unlikely to be solely responsible for significant alteration of cell wall composition. Nevertheless, the impact of 1,4-β-xylanase in morphology and structure should also be considered.

4.6 Conclusions

Although most metabolic profiling reports aimed at studying the responses of plants to P deficiency have been performed at latter stages, it seems that a significant degree of metabolic control is evident in the early stages of response to P deficiency (figures 4.7 and 4.8). This was particularly evident in the leaves suggesting that P sensing mechanisms readily signal to the leaf tissue eliciting a metabolic response. We also observed significant changes in the transcriptome, which pointed to the utilisation of glycolytic bypasses, remodelling of lipid membranes and P scavenging mechanisms under early P deficiency. Although at an early stage these studies are providing insights

at the biochemical and genetic level that will undoubtedly facilitate hypotheses testing via transgenic methodologies and ultimately identify a way forward to improve phosphorus use efficiency in ryegrass by employing candidate genes and marker-assisted breeding approaches.

Chapter 5

N nutrition in perennial ryegrass

5.1 Summary

Nitrogen (N) is one of the major macronutrients required by plants for normal growth and development. Improving the nitrogen usage efficiency (NUE) of *Lolium perenne* L. (perennial ryegrass) will allow the reduction of the N fertilizer input. In countries where grasslands represent a significant proportion of the fertilized agricultural land, such as Ireland and the United Kingdom, this is likely to result in significant economic and ecological benefits. The characterization of the metabolic response of *L. perenne* to different levels of N supply has been limited to a small number of studies and has focused primarily on polar metabolites. In this study, the range of metabolites analysed was extended to include non-polar metabolites. Furthermore, the analysis of seven genotypes with variability in the regrowth rate response to N supply allowed the characterisation of the metabolic response of different genotypes. This will allow the identification of common mechanisms of response which are likely to be common to a large number of perennial ryegrass genotypes. The metabolic response observed included modifications of the lipid metabolism as well as alterations of secondary aromatic metabolite precursors in plants exposed to N-deficit. In contrast, plants grown in a N saturated media appeared to modify to some extent the metabolism of ascorbate. Additionally, it was found that amino acid levels increase with increasing concentrations of N supplied. This study suggests that the involvement of the secondary metabolism, together with lipid and ascorbate metabolism is of crucial importance in the early-adaptation of perennial ryegrass plants to different levels of N supply.

5.2 Introduction

Nitrogen (N) is an essential macronutrient and its availability is a major limiting factor for plant growth (Lea and Azevedo, 2006). This nutrient has a major impact in the production of forage and seed, as well as strongly influencing many of their quality traits (Lemaitre *et al*., 2008). Nitrogen can be supplied using commercial fertilizers, however, its cost often represents a significant proportion of the cost in plant production (Lemaitre *et al*., 2008). Furthermore, it has been estimated that 50-70% of the nitrogen provided to plants is lost (Hodge *et al.*, 2000) in the soil. As a consequence, this "lost nitrogen" may be leached from the soil and contaminate water bodies and, similarly to what happens with P (Chapter 4), may result in water eutrophication (Masclaux-Daubresse *et al*., 2010). Therefore, improvement in the efficiency of nitrogen usage is likely to result in large benefits, both at the ecological and economic levels.

The response of plants to N limitation generally involves mechanisms which improve the nitrogen use efficiency of plants (NUE). This has been often defined for cereal crops as the seed yield per unit of N applied (Moll *et al*., 1987). Although seed yield has great importance for cereal crops such as barley, wheat and rice, in forage grasses its agronomic value is relatively low when compared with vegetative tissue yield. Therefore, in the case of perennial ryegrass the original definition seems to be overly strict and should be adapted to include, not only seed yield, but also the yield of vegetative tissue. The NUE parameters have been associated with two components: the nitrogen uptake efficiency and the nitrogen utilisation efficiency (Lea and Azevedo, 2006). The first component has been associated with mechanisms which allow plants to interact with the environment and optimize the access to sources of nitrogen, such as nitrates and ammonium (Lea and Azevedo, 2006). The latter component has been

mainly associated with internal mechanisms which optimize the allocation of N in order to sustain a homeostatic balance within the plant.

The uptake of nitrogen by plant roots is a complex process which seems to be dependent upon different transport systems (Lea and Azevedo, 2006). There are high-affinity transport systems (HATS) and low-affinity transporter systems (LATS) which can be further classified as either constitutive or inducible (Glass *et al*., 2002).

Nitrogen may be present in soils in inorganic forms, such as nitrate, nitrite, ammonium and in organic forms, such as amino acids (Thornton *et al*., 2007).

The uptake of nitrate by plant roots is a complex process which seems to be dependent on both constitutive and inducible HATS and LATS. Genes encoding nitrate transporters have been identified in two families of genes, NRT1 and NRT2 (Lea and Azevedo, 2006). It has been reported that associated NRT1 proteins have a wide range of substrate affinities that include LATS and dual-affinity nitrate transporters (Guo *et al*., 2002). On the other hand the NRT2 family of genes seem to contribute towards HATS when nitrogen levels fall (Little *et al*., 2005). For example, a microarray study in *Arabidopsis* revealed that N-limited plants responded to the presence of nitrate by rapidly (within 30 minutes) inducing genes involved in N uptake from both NRT1 (NRT1.1) and NRT2 (NRT2.1 and NRT2.2) gene families (Scheible *et al*., 2004).

Ammonium is often present in soils, and its uptake appears to be modulated by both HATS and LATS (Glass *et al*., 2002). These transporter systems, appear to be mediated by the activity of proteins of the ammonium transporter/methylammonium permease (AMT/MEP) family, which in *Arabidopsis* include six isoforms (Yuan *et al.*, 2007). Yuan *et al*. (2007) performed a reverse genetics study in *Arabidopsis* aiming to determine the individual contribution of some of the AMT members to the overall

ammonium uptake capacity. The authors observed that the high-affinity uptake of ammonium in the root tissue derives mainly from the activity of four AMT proteins which contributed to the total of 90-95% of the ammonium uptake. Additionally, the authors observed that the activity of these proteins seems to be additive and enhanced under nitrogen deficiency (Yuan *et al.*, 2007).

Plants have also been recognized to have the potential to uptake amino acids as a source of nitrogen (Nasholm *et al*., 1998). However, the general view of N-cycling in the soils is that organic N is first mineralized and then inorganic N is up taken (Thornton *et al*., 2007). In perennial ryegrass, a study was conducted with the aim of investigating the response of plants challenged with glycine as the N source in comparison with plants supplied with an inorganic N source (Thornton *et al*., 2007). The authors concluded that plants supplied with glycine acquired less N which resulted in lower nitrate levels in the root tissue (Thornton *et al*., 2007). This seems to suggest that, although plants may acquire organic N, inorganic N is the major source of N in perennial ryegrass.

When challenged with N limitations plants often modify their root architecture in order to explore available N present in soil (Walch-Liu *et al*., 2006). Zhang and Forde's (1998) study in *Arabidopsis thaliana* provided evidence of nitrate-dependent lateral root growth, which may constitute a mechanism of exploration of nitrogen-rich patches in soils. It has been suggested that the assimilation of nitrate locally leads to an increase of influx of photosynthate which in turn stimulates the lateral root growth (Sattelmacher et al., 1993). However, an alternative hypothesis had been proposed which suggested that the nitrate ion is an important regulatory molecule in plants and that among its roles it includes the stimulation of lateral root growth (Zhang and Forde, 2000). Further studies were performed with the aim of understanding whether lateral root growth is promoted by the nitrate ion which would act itself as a signal or by its role as N source. A study

performed by Zhang and Forde (1998) revealed that mutants in nitrate reductase displayed a similar alteration of lateral root growth in response to a nitrate stimulus, which seems to suggest that the promotion of LR growth is not dependent on the assimilation of nitrate by plants. Subsequently, Zhang *et al*. (1999) performed a study in which the localized supply of N (ammonium and glutamine were provided but not nitrate), did not stimulate lateral root growth. Instead, it appears that lateral roots responded directly to the presence of nitrate ions rather than a result from N nutrition.

Furthermore, when N-starved roots of *Arabidopsis* are supplied with nitrate ions a number of genes were found to be rapidly induced (within 30mins). One of those genes is an ANR1 gene which encodes a transcription factor from the MADS-box family (Zhang and Forde, 1998). This family of transcription factors is mainly expressed in flowers and seems to be particularly relevant to control floral organ identity in plants (Theissen *et al*., 2000). However, in yeast and mammalian cells, this family of transcription factors seems to be involved in converting external signals into metabolic and developmental responses (Shore and Sharrocks, 1995, Messenguy and Dubois, 2003). Studies in which the expression of this gene was down-regulated revealed that lateral root growth was not induced by the localized supply of nitrate ions. Therefore, it was concluded that ANR1 is a component of the signal transduction pathway that stimulates lateral root growth in response to nitrate ion levels (Zhang and Forde, 1998).

Nitrogen (N_2) constitutes a major proportion of the atmosphere composition, however the biological reduction of N_2 to ammonium is a process that is only performed by prokaryotes in a process that is highly-sensitive to oxygen (Mylona *et al*., 1995). Some higher plants establish symbiotic relationships with some soil bacteria, such as the symbiotic relationship of *Rhizobia* with legumes (Mylona *et al*., 1995). In these relationships the prokaryotes fix nitrogen inside the cells of the plant, while being

separated from the cytoplasm by a membrane derived from cellular membrane (Mylona *et al*., 1995). The host plant will provide energy for the N fixation and also mechanisms of protection against oxygen (Mylona *et al*., 1995). Perennial ryegrass does not establish symbiotic relationships with N-fixating prokaryotes. However, the cultivation of perennial ryegrass with white clover (an important pasture legume), which forms symbiotic relationships with N-fixating bacteria, has been studied as an alternative strategy to reduce N fertilizer inputs (Andrews *et al.*, 2007). Some of the fixed N may be exuded by the legume to the soil or be released by senescence of legume tissue and consequently become available to the grass (Ledgard *et al*, 2001). Andrews *et al*. (2007) observed that dry matter production of a mixed pasture of perennial ryegrass and white clover cultivars was comparable to that of a perennial ryegrass pasture supplied with 200 kg N ha^{-1} annum $^{-1}$. This in essence suggests that cultivating perennial ryegrass with white clover may become a viable strategy to reduce N inputs.

The mechanisms cited above contribute greatly to increase the ability of plants to uptake N, particularly under limited N conditions. However, N utilisation efficiency also involves internal mechanisms which may respond to N-limitation and in some cases allow the plant to use N more efficiently.

Nitrate assimilation involves the activity of nitrate and nitrite reductases which reduce nitrate and nitrite, respectively (Hermans *et al*., 2006). The sequential activity of these enzymes catalyses the intracellular conversion of nitrate to ammonium. The latter can then be assimilated through the combined activity of glutamine synthase (EC 6.3.1.2) and NADPH-dependent glutamine:2oxoglutarate aminotransferase (GOGAT) (EC 1.4.1.13). In the first reaction glutamine is synthesized from ammonium and glutamate while consuming one ATP molecule. The following step, catalyzed by GOGAT, yields

two molecules of glutamate from the reaction between glutamine and 2-oxoglutarate, consuming NADPH + H^+. The net reaction can be described as:

$$NH_3 + \text{2-oxoglutarate} + ATP + NADPH + H+ \rightarrow \text{glutamate} + ADP + P_i + NADP^+$$

Therefore, the assimilation of ammonium requires the synthesis of organic acids, in particularly 2-oxoglutarate which acts as acceptor for ammonium in the GOGAT pathway (Stitt, 1999). Scheible *et al*. (1997) observed that, when intracellular nitrate levels increase, there is an increase in the expression of genes involved in organic acid biosynthesis, such as pyruvate kinase, phosphoenolpyruvate carboxylase and citrate synthase. Additionally, the authors observed that the increase in nitrate levels caused a repression in the expression of a gene encoding the regulatory subunit of ADP-glucose pyrophosphorylase, which is involved in the synthesis of starch. It was then suggested that the increase in organic acid biosynthesis results in the diversion of carbon from carbohydrate synthesis (Scheible *et al*., 1997).

Under nitrogen limitation, it has been found that leaves accumulate sugars and starch (Scheible *et al*., 2004 Hirai *et al*., 2004). Sugars may then induce the expression of nitrate transporters NRT1 and NRT2 (Lejay *et al*., 1999) as well as nitrate reductase, glutamine synthase, pyruvate kinase, phosphoenolpyruvate carboxylase and NADP-isocitrate synthase (Koch *et al*., 1996). Therefore, high levels of sucrose appear to act as a signal to stimulate the conversion of nitrate to glutamine (Stitt, 1999). Conversely, when sugar levels are low, nitrite reductase activity seems to be downregulated (Matt *et al*., 1998).

Nitrogen limitation often results in a decrease in the expression of genes involved in photosynthesis (Hermans *et al*., 2006). It has been suggested that the inhibition of photosynthetic activity is a result of sugar accumulation, which may exert feedback

regulation in some of the genes involved in photosynthesis (Hermans *et al*., 2006). This seems to be corroborated by a recent study by Araya *et al*. (2010) in *Phaseolus vulgaris*. Araya *et al*. (2010) supplied three levels of nitrogen supply, and analysed the effects of sucrose feeding on the nitrate levels, photosynthetic activity and carbohydrate content. The authors observed a negative relationship between photosynthetic rate and carbohydrate content which was not affected by the nitrogen nutrition levels. Additionally, they observed a concomitant increase in carbohydrate levels and decrease in nitrogen content which led them to conclude that nitrogen nutrition influences the photosynthetic activity by modifying the levels of carbohydrates (Araya *et al*., 2010).

Despite the importance of improving nitrogen usage efficiency (NUE) with respect to sustainable agricultural perspectives, a limited number of studies have been performed in perennial ryegrass aiming to elucidate the mechanisms underlying NUE. Nevertheless, numerous studies have been performed in the 70s and 80s which aimed to characterize some agronomic traits of perennial ryegrass pastures in response to differential nitrogen fertilization (Cowling and Locklyer, 1970; Davies, 1971; Dowdell and Webster, 1979; Gonzalez *et al*., 1989).

The metabolic adaptations to nitrogen deprivation appear to have a significant role in the adaptation of plants to N limitation. Therefore, it is perhaps surprising that the use of metabolite profiling approaches to characterize the response to this particular nutrient deprivation seems to be largely unexplored. Nevertheless, there has been some limited effort to characterize the metabolic response of perennial ryegrass to nitrogen deprivation. These efforts can be illustrated by the study of Thornton *et al*. (2007) who used a combined targeted metabolomic approach and a proteomic approach to study the response of perennial ryegrass plants challenged with glycine as N source. However, a more comprehensive metabolomic approach was used by Rasmussen *et al*. (2008), who

compared the response of two perennial ryegrass cultivars infected with endophytes grown at two different levels of N (medium and high). Although the main goal of the study was to characterise plant-endophyte relationships, it was found that one of the cultivars, which accumulates higher levels of sugars, displayed lower levels of nitrate and amino acids when compared with the other cultivar (Rasmussen *et al*., 2008). This could possibly result from the interaction of sugars with the mediation of N assimilation as cited above. Furthermore, plants infected with endophytes were found to accumulate less amino acids and nitrates while their associated water soluble carbohydrates, lipids and some organic acids were increased (Rasmussen *et al*., 2008).

The aim of this chapter was to characterize the metabolite profiles of a variety of perennial ryegrass genotypes to three different levels of nitrogen supply (high, intermediate and low). The genotypes used were found to have a wide range of regrowth rate responses to N nutrition. As result of this, it is likely that the observed results will correspond to the general mechanistic response to N supply in perennial ryegrass. Furthermore, the characterization of the response of non-polar metabolites to N supply has remained largely unexplored. The number of non-polar metabolites analysed is significantly higher when compared with the metabolite profiling study from Rasmussen *et al*., (2008). This will allow the elucidation of whether some of the non-polar metabolites respond to the supply of N in perennial ryegrass.

5.3 Material and Methods

5.3.1 Plant material (performed by SLB)

A screen was carried out on seven genotype populations (Cashel, IRL-OP-L02011, IRL-OP-02419, IRL-OP-2131, IRL-OP-2241, PI 462336 and S13) with the aim of characterizing the response of the regrowth rate in perennial ryegrass plants supplied with different levels of nitrogen. Seeds were germinated on filter paper and transferred to soil. Twelve seedlings of each genotype population were cleaned of soil and transferred to each of the three plug trays (84 inserts) containing perlite medium. These trays were floated on a plant nutrient solution A: (KH_2PO_4, 0.31 mM; $CaCl_2.2H_2O$ 0.75mM; $MgSO_4.7H_2O$, 0.375mM; NH_4NO_3, 5mM; $Ca(NO_3)_2.4H_2O$, 2.348mM; MS Micro Salts (Duchefa), 0.146 g l^{-1}) as described below.

5.3.2 Experimental growth conditions (performed by SLB)

Solutions were placed in three 25 litre tanks and aerated with an aquarium pump. Experiments were performed in a controlled glass house with a mean daily temperature of 22^{o}C and supplemented with lighting (PAR = 650 microreinsteins $m^{-2}s^{-1}$) for 16hrs. The plants were allowed to acclimatise for one week to the hydroponics growth conditions before applying treatments. At the start of the treatment the solutions in the three tanks were replaced with either solution A (intermediate N supply), identical to above, solution B, identical to above except that the NH_4NO_3 and $Ca(NO_3)_2.4H_2O$ levels were reduced to 0.133 mM and 0mM respectively; or solution C, which is identical to solution A but the levels of NH_4NO_3 and $Ca(NO_3)_2.4H_2O$ have been increased to 10mM and 4.7mM, respectively. At the start of the experiment all plants were cut down to the

same length (6 cm). At the end of each week plants were cut down to the same length and nutrient solutions were replenished. The biomass collected was dried in an oven at 80°C overnight, and the dry weight recorded. This procedure was repeated three times for a period of three weeks.

5.3.3 Sample preparation and metabolite profiling

In order to collect samples for metabolite analysis a similar experiment to the one described above was set up. A total number of six clonal replicates of each genotype were used for each treatment, and plants were initially allowed to establish in the hydroponics system described above with solution A. Plants were then exposed to different N supply treatments (Solutions A, B and C) for a period of 24h before samples from the leaf tissue were harvested (midday), extracted and derivatised as described in the material and methods chapter. However, the weight of frozen tissue powder used was adjusted to approximately 4.6 mg (accurately weighted and recorded) due to a lack of available biomass. Accordingly, the volumes used for the extraction and derivatization procedures were adjusted with the aim of improving signal/noise levels. The volumes of solvents used for the extraction protocol were reduced to half, while the volume of polar and non-polar internal standard solutions used was adjusted to 25µl and 50µl, respectively. The volumes of the aliquots derivatized for the polar and non-polar fractions were adjusted to 1.5ml and 4 ml, respectively. The metabolite profiles were acquired using a GC-DSQII-MS (see material and methods) and the resulting data was analysed as described in materials and methods.

5.3.4 Statistical analysis

A repeated measures analysis was performed for the regrowth data collected over a period of three weeks. Since the variance of the weights increased with higher means a logarithmic transform was applied before analysis. Analysis of variance (ANOVA) was subsequently performed with an adjustment (Greenhouse and Geisser, 1959) to take into account the correlation among repeated measurements.

For the metabolite data, a logarithmic transformation was also performed in order to normalise data. Subsequently, ANOVA was performed to test for effects of the different levels of N supply treatment and genotype on the levels of metabolites of all the ecotypes screened. Furthermore, the interaction of genotype and N supply was tested for effects on metabolites levels. The metabolites which reveal statistical significant ($p<0.05$) differences in response to N supply and display no significant effect ($p>0.05$) in the interaction between N supply and genotype were identified and further characterised. Individual ANOVAs were then performed to identify the N supply levels which significantly affect the levels ($p<0.05$) of metabolites in all genotypes. All statistical analysis was performed using GenStat v 12.1.0.3278 (VSN international).

5.4 Results

5.4.1 Regrowth rate under different N supply

The regrowth rates of seven genotype populations were measured weekly, for a period of three weeks (Figure 5.1). The regrowth rate levels appeared to have a high variability between the genotypes screened. A majority of the genotypes (5) have an optimum

regrowth rate at intermediate N supply levels while those levels tend to decrease under low- and high-N supply (Figure 5.2). Nevertheless, two of the genotypes appear to have a different response (Figure 5.3). Genotype IRL-OP-2131 appears to have higher regrowth rates at both intermediate- and high-N supply when compared with plants supplied with low nitrogen levels. Contrastingly, genotype IRL-OP-2241 has higher regrowth rates at low- concentrations of N supply. The variability observed in the regrowth rate responses seems to indicate that the ecotypes screened have a diverse response to N supply. Therefore, the common metabolic responses to N-supply observed in this study are more likely to be widely present in perennial ryegrass plants, in contrast with results obtained from sampling an ecotype pool with very little variability.

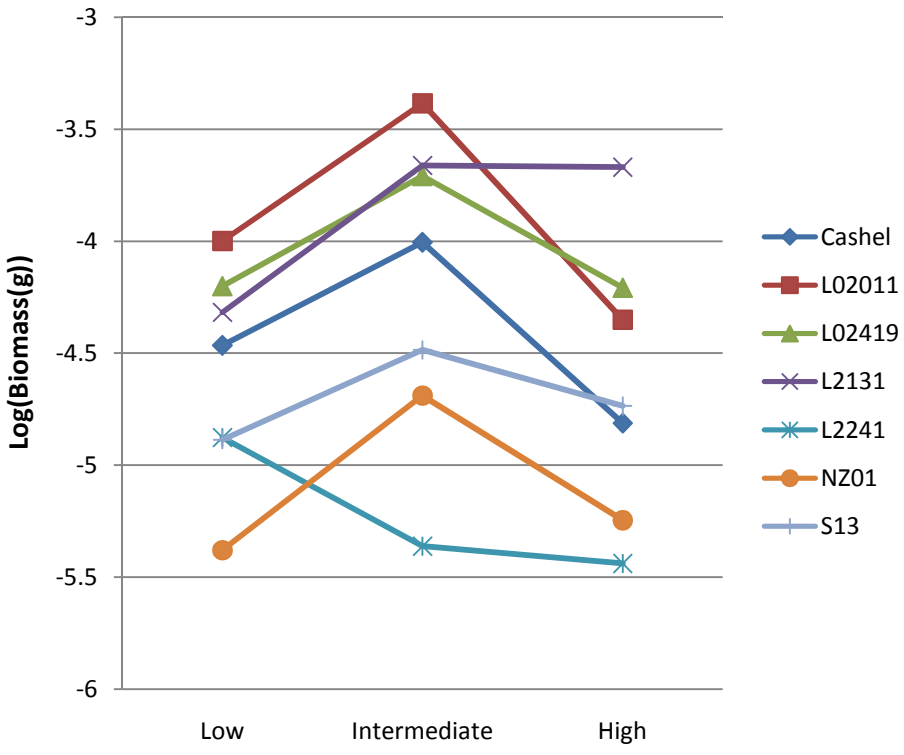

Figure 5.1- Graphical representation of the weekly regrowth rate of seven genotypes in response to N supply over a period of 3 weeks. The respective standard error bars have been omitted for simplicity of representation and are represented in figures 5.2 and 5.3.

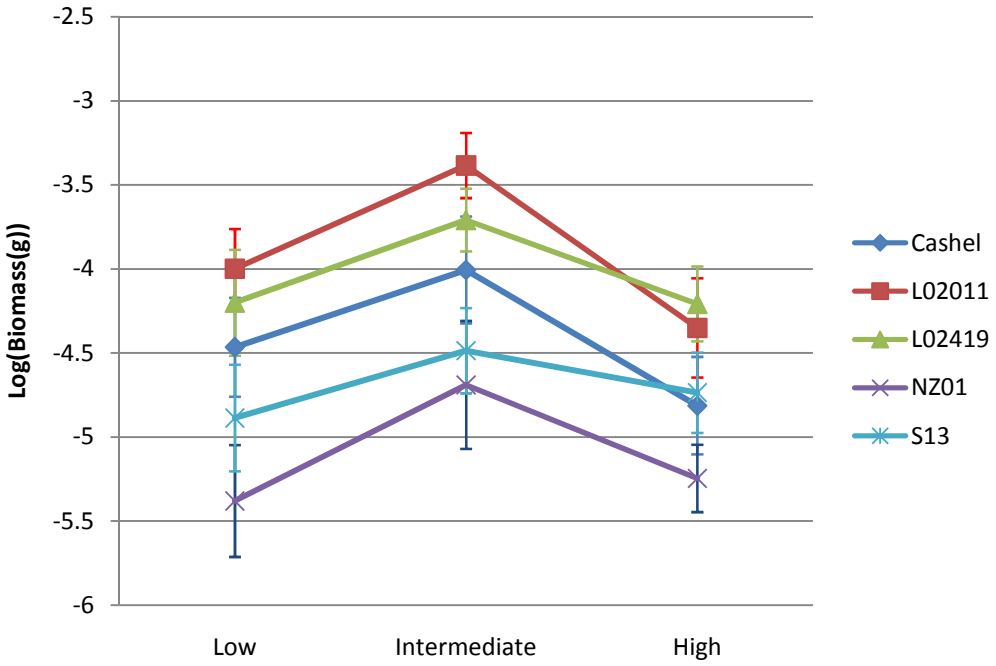

Figure 5.2 - Graphical representation of the mean and standard errors of the weekly regrowth rate of five genotypes in response to N supply over a period of 3 weeks. The genotypes represented have a maximum regrowth rate at intermediate N supply.

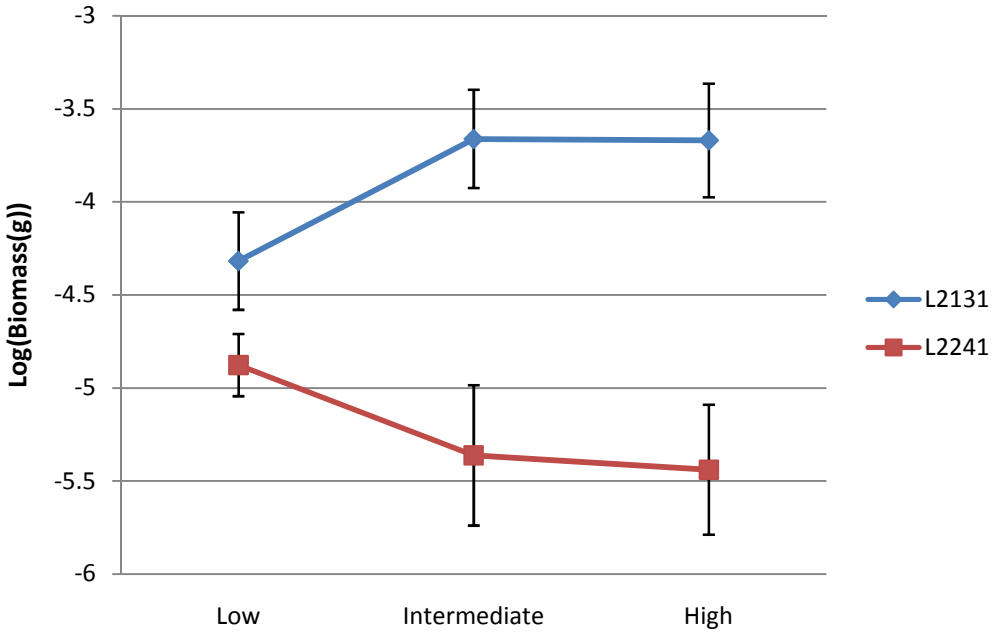

Figure 5.3 - Graphical representation of the mean and standard errors of the weekly regrowth rate of 2 genotypes in response to N supply over a period of 3 weeks. These genotypes appear to have a different type of response when compared to the majority of genotypes analysed.

5.4.2 Metabolite level response to different N levels

Metabolite profiling of the leaf tissue was performed in seven genotypes supplied with three different N supply concentrations. Results for quality control of metabolite analysis are shown and described in Appendix G. The metabolite profiles included the levels of 97 metabolites (79 categorically identified metabolites) which included 50 polar metabolites and 47 non-polar metabolites.

Analysis of variance was performed to test for effects of the different N levels and genotype on the levels of metabolites of all the screened genotypes. Furthermore, the genotype and N supply interaction was tested for effects on metabolites levels.

Table 5.1 – Table representing the means, standard errors and ANOVA test results for effects on metabolite levels caused by N supply, genotype, and interaction between N supply and genotype. The means of metabolite levels have been transformed using a logarithmic transformation.

Metabolite	**N supply**			**Standard error for N means**			**p-value**		
	Low	Medium	High	Low	Medium	High	N treatment	Genotype	N x genotype interaction
Inositol	-2.65	-2.72	-2.54	0.138	0.086	0.056	0.020	<0.001	0.095
L-Threonine	-3.94	-3.85	-3.67	0.149	0.076	0.072	<0.001	<0.001	0.579
Homoserine	-7.61	-7.08	-6.88	0.366	0.112	0.145	0.001	<0.001	0.541
Glutamic acid	-1.68	-1.53	-1.45	0.148	0.071	0.037	0.010	0.083	0.685
Oxoproline	-1.44	-1.22	-0.94	0.196	0.123	0.114	<0.001	<0.001	0.082
L-Glutamine	-3.04	-2.68	-2.42	0.324	0.155	0.244	0.007	<0.001	0.561
L-Serine	-2.20	-1.95	-1.62	0.162	0.111	0.086	<0.001	<0.001	0.465
Threonic acid	-6.02	-5.75	-4.86	0.208	0.183	0.100	<0.001	0.012	0.597
Cinnamic acid	-2.55	-2.84	-2.66	0.125	0.110	0.080	0.022	0.010	0.491
Tricosanoic acid	-4.63	-5.08	-4.95	0.176	0.128	0.079	<0.001	0.718	0.486
Tetracosanoic acid	-2.70	-2.86	-2.81	0.146	0.136	0.118	0.031	<0.001	0.613
Octacosanoic acid	-3.59	-3.85	-3.74	0.183	0.118	0.089	0.022	<0.001	0.567
2-hydroxy tetracosanoic acid	-3.66	-3.88	-3.98	0.173	0.122	0.081	0.019	0.020	0.068
Ferulic acid	-3.65	-3.87	-3.97	0.225	0.109	0.148	0.046	<0.001	0.325

The goal of this approach was to identify metabolites that were significantly affected by N supply levels, without displaying interaction with genotype. The metabolites which

appear to be regulated by solely the levels of nitrogen supplied are represented in table 5.1. In plants growing under low levels of nitrogen supply a number of amino acids (which include glutamic acid, serine and homoserine) were found to have significantly lower levels when compared with plants supplied with intermediate levels of nitrogen (Figure 5.4). In contrast, the levels of cinnamic acid, ferulic acid, and long chain saturated fatty acids (C23:0, C24:0 and C28:0) increased significantly in plants grown under N-deficit. Interestingly, the levels of 2-hydroxy tetracosanoic acid levels also increased under N limitation (Appendix H).

When the medium is saturated with N, the levels of some amino acids (serine, threonine and oxoproline) increased significantly when compared to plants supplied with intermediate N concentrations of N (Figure 5.4). The same occured with the levels of inositol and threonic acid (Appendix H).

When analysing the levels of the significant metabolites under the different levels of N supply it was observed that amino acid levels increase gradually with increasing concentrations. Interestingly, glutamine also responded to N supply levels, although the differences were only significant when comparing plants grown under low N supply with plants saturated with N, the extremes. This trend was also observed for all the previously cited amino acids (see figure 5.4).

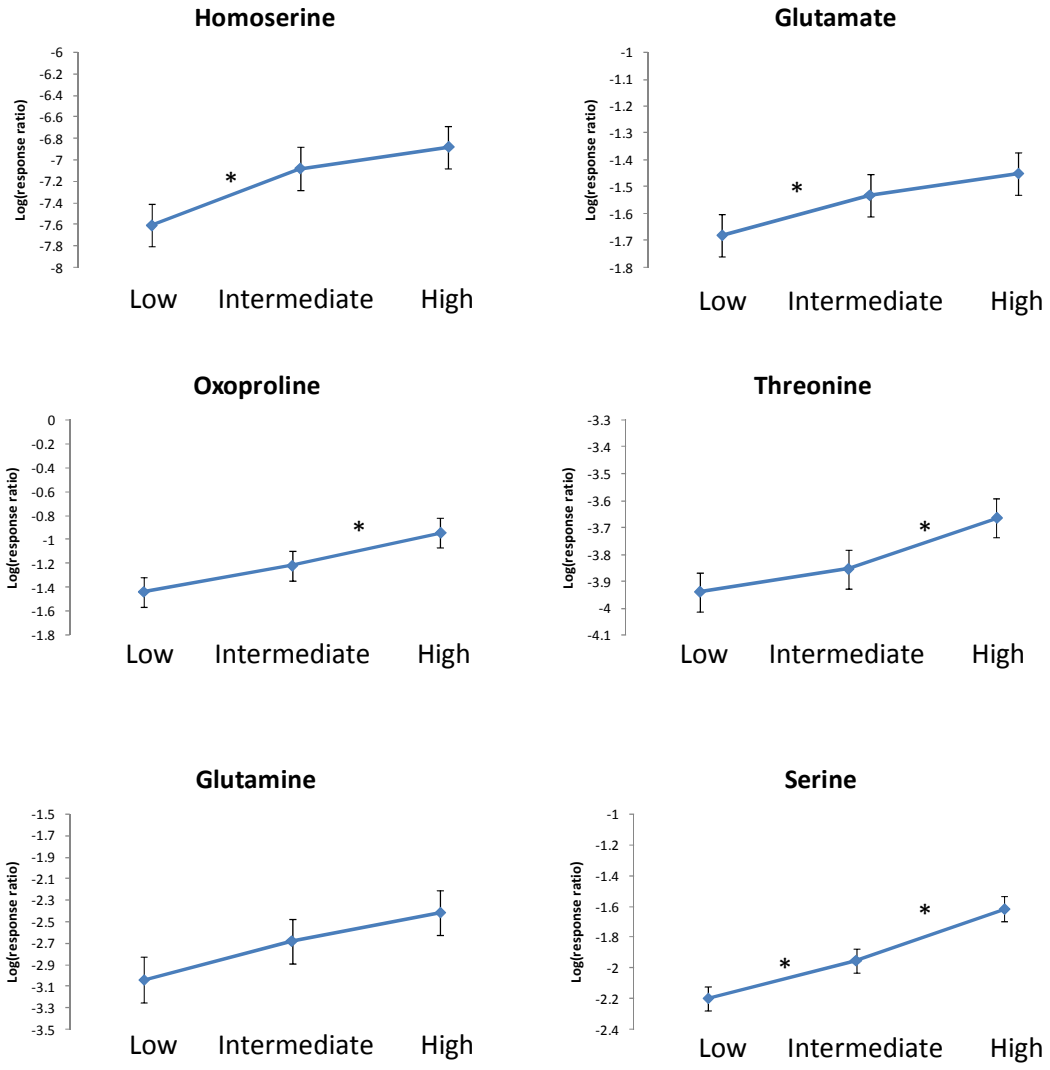

Figure 5.4- Graphical representation of the logarithm of the mean value of each amino acid found to be significantly regulated by N levels. ANOVAs between means from high and low treatments were found to be significantly different ($p<0.05$). Significant differences between high or low and intermediate treatments are annotated with *.

5.5 Discussion

5.5.1 Regrowth rate

Analysis of the regrowth rates seems to indicate that a majority of the genotypes is affected negatively by both low and high levels of N supply (Figure 5.2). This seems to indicate that intermediate levels of N correspond to the optimal range of N for the

majority of genotypes screened. However, a small number of genotypes behaved differently (Figure 5.3). Genotype IRL-OP-2241 exhibited higher levels of regrowth rates under low levels of N supply. This suggests that this genotype is particularly adapted to a system of low fertilization, and therefore an interesting genotype to study specific mechanisms of adaptation to low levels of fertilization. However, the overall regrowth rate is very low, being the lowest for all genotypes screened under intermediate and high levels of N supply (Figure 5.1). Even in conditions of low N-supply the levels of regrowth rate for genotype IRL-OP-2241 only surpass those of genotype NZ01. This suggests that the study of the specific metabolic response of genotype IRL-OP-2241 may not be applicable to plants with overall higher regrowth rates.

Contrastingly, the regrowth rate from genotype IRL-OP-2131 is not negatively affected by growing in a N-saturated medium. In fact, the regrowth rate appears to be similar under intermediate and high-levels of N supplied (Figure 5.3). This seems to suggest that the optimal range of N concentration in the medium for this ecotype occurs within the intermediate-high concentration of N used in this experiment. Another alternative is that this particular genotype displays specific mechanisms of adaptation to high-levels of N present in the medium. Therefore, it would be interesting to perform further studies with this ecotype in order to corroborate this hypothesis, and also to characterize mechanisms of adaptation to N-saturated conditions.

5.5.2 Response to low levels of nitrogen supply

5.5.2.1 Amino acids

Perennial ryegrass plants exposed to low levels of N appear to reduce the levels of some free amino acids, in particular glutamate, serine and homoserine. The assimilation of N

by plants generally involves the uptake of nitrate, which is then reduced to ammonium by the sequential activity of nitrate reductase and nitrite reductase. The nitrogen present in ammonium is then assimilated through the GS-GOGAT pathway which leads to the synthesis of glutamate from a molecule of ammonium and oxoglutarate (Stitt, 1999). The decrease in the levels of glutamate seems to suggest that under nitrogen limitation there is a decrease in overall N assimilation.

Oxoproline is a downstream product of glutamate and it is possible that the decrease observed in its levels is a consequence of a decrease in available glutamate. Glutamate also has an important role in transamination reactions which are involved in the biosynthesis of aspartate from oxaloacetate (EC 2.6.1.1) and serine from 3-phospho-hydroxy-pyruvate (EC 2.6.1.52) which is a downstream product of 3-phosphoglyceric acid (3-PGA). Therefore, it is likely the significant alterations in the glutamate levels may impact upon the levels of a wide range of amino acids. In this particular experiment the levels of aspartate seem to be unaffected by a low N supply, however, homoserine, one of its downstream products appears to be down-regulated. The levels of serine also experience a significant decrease which may also be a direct consequence of a limitation of the transamination reaction leading to the synthesis of serine.

The assimilation of nitrate into amino acids requires reductants, ATP and carbon skeletons, hence this process is tightly linked with photosynthesis and carbohydrate metabolism (Smith and Stitt, 2007).

Plants experiencing N limitation have been reported to accumulate carbohydrates and experience a decrease in the photosynthetic rate (Paul and Driscoll, 1997). For example, Araya *et al*. (2010) studied the response of *P. vulgaris* leaves to different N levels and observed that low levels of N supply resulted in significantly higher levels of carbohydrates. The authors further demonstrated that high levels of carbohydrates

contribute towards a decrease in photosynthetic rate. It was then concluded that nitrogen nutrition influences leaf photosynthesis by modifying the levels of carbohydrates (Araya *et al*., 2010) (Figure 5.6 A). However, in this study no significant alteration of carbohydrate levels was found in plants supplied with low levels of N in comparison with plants supplied with intermediate levels of N supply. According to the mechanism proposed by Araya *et al*. (2010) this seems to suggest that the photosynthetic rate of perennial ryegrass leaves is not affected at the early onset (24h) of N-deprivation (Figure 5.6 B). However, no measurements of photosynthetic rate were performed in this experiment, thus there is no data available to corroborate this hypothesis.

Evidence has been provided that the levels of 2-oxoglutarate increased up to 3-fold in *Arabidopsis* seedlings supplied with low levels of N (Scheible *et al*., 2004). However, in this study, the levels of 2-oxoglutarate and its up-stream metabolites (acyl-CoA, pyruvate and phosphoenolpyruvate) remain undetermined; therefore, it is not possible to confirm that N limitation produces an organic acid build-up. Nevertheless, the levels of carbohydrates remain unaltered while N assimilation appears to decrease (as discussed above) which may suggest the accumulation of organic acids upstream of 2-oxoglutarate.

5.5.2.2 Secondary aromatic metabolites

The increase in the levels of very-long-chain fatty acids (VLCFAs) and cinnamic acid derivatives observed in this study seems to indicate that there is a shift from organic acids towards the lipid and secondary aromatic metabolism. This shift in the metabolism may explain the unaltered carbohydrate levels observed in the leaf tissue (Figure 5.6).

Interestingly, a transcriptomic approach was used to study the short- and long-term response of *Arabidopsis* to low levels of N supply (Scheible et al., 2004), which resulted in the identification of processes involved the primary and secondary metabolism which are regulated under N deficiency. After 9 days of treatment with different levels of N the authors observed an increase in anthocyanins and a reduction in chlorophyll contents. In seedlings supplied with low nitrogen the authors also observed alterations in the secondary metabolism upon the readdition of nitrate which seems to suggest the involvement of secondary metabolites in the response of plants to N-deprivation (Scheible *et al*., 2004). More specifically, the authors observed that N-starved plants contained higher levels of ferulic acid, rutin, several unidentified peaks (flavonoids and isoprenoids), and to lesser extent cinnamic acid and caffeic acid. Additional studies have also provided evidence that under limitation of nitrogen supply the biosynthesis of anthocyanins is induced (Bongue-Bartelsman and Philips, 1995; Diaz *et al*., 2006). Furthermore, it has been found that *Arabidopsis* mutants in the NLA gene are unable to induce anthocyanin synthesis in response to nitrogen limitation, but not to phosphorus limitation (Peng *et al*., 2008). Additionally, when challenged with N deficit, plants display an early-senescence phenotype which illustrates the importance of the induction of anthocyanin biosynthesis to N limitation (Peng *et al*., 2008).

In this study, the levels of cinnamic acid and ferulic acid also increased under N limitation, which suggests that in perennial ryegrass the secondary aromatic metabolism was induced when N was limited (Figure 5.6 B). One of the possible group of molecules that could mediate response to N-limitation are anthocyanins (Peng *et al*., 2008). However, since the levels of downstream metabolites of cinnamic acid were not quantified (or seen by GC-MS), it is not possible to corroborate this hypothesis.

5.5.2.3 Very long-chain fatty acids

Lipid metabolism has also been reported to be affected by low N levels. Scheible *et al*. (2004) observed that a set of genes which included several fatty acid elongases and four fatty acid desaturases which are involved in the plastid fatty acid synthesis pathway are regulated under low nitrogen. In this study the levels of very-long-chain fatty acids (VLCFAs), which include C_{23}, C_{24} and C_{28} saturated fatty acids, appear to increase under N limitation. This is possibly a result of an increase of fatty acid elongase activity, which is in agreement with the study cited above (Scheible *et al*., 2004).

In addition to this, Scheible *et al.* (2004) observed a repression of three genes involved in the synthesis of galactolipids upon nitrogen resupply and suggested that an analogue mechanism to the one observed for adaptation to low-P supply may occur in order to increase the amounts of N available from plants by scavenging N present in phospholipids.

However, a subsequent study by Gaude *et al*. (2007) demonstrated that the total levels of galactolipids are reduced under N limitation. Nevertheless, the authors also observed that the ratio of MGDG:DGDG decreased, which the authors proposed that it would stabilise thylakoid membranes since MGDG is the only non-bilayer-forming lipid in the chloroplasts.

Additionally, the authors demonstrated that N limitation did not impact upon the levels of N-containing glycerolipids (phosphatidyl choline, phosphatidyl ethanolamine and phosphatidylserine). It was suggested that the levels of N present in glycerolipids are relatively low and therefore N would be preferably remobilized from protein bound

amino acids (Gaude *et al*., 2007). Therefore, it is unlikely that plants modify the lipid metabolism in order to scavenge N present in phospholipids.

In this study, an increase in the levels of VLCFAs under N limitation was observed. These fatty acids serve as components or precursors of structurally important molecules such as waxes, suberin and cutin, which forms the leaf cuticule (Trenkamp *et al.*, 2004). Furthermore, VLCFAs occur as storage lipids in seeds, periderm and endodermis components, glycosylphosphatidyl-inositol anchors in plasma membrane proteins and as sphingolipid components in various membranes (Trenkamp *et al.*, 2004). This appears to indicate that perennial ryegrass adapts to N limitation by modifying the leaf cuticule structural composition or by regulating the membrane lipid composition. In addition to this, it has been demonstrated in a number of studies that the impairment of VLCFA biosynthesis results in severe growth and developmental consequences (Zheng *et al*., 2005; Beaudoin *et al*., 2009). For example, the analysis of *Arabidopsis* mutant lines impaired in the expression of PAS1, a member of the immunophilin family which is known to target protein complexes and regulate their activity and assembly, provided further evidence of the role of VLCFA in the regulation of growth and development (Roudier *et al*., 2010). These mutants lines were found to have reduced levels of VLCFA and also deficiency in lateral root formation and defective cotyledon organogenesis (Roudier *et al*., 2010). The characterization of these mutants showed that PAS1 associates with the VLCFA elongase complex in the endoplasmatic reticulum, and therefore directly linked to VLCFA synthesis. The alterations in cotyledon development were suggested to be associated with auxin mobilization since it was found that mutant lines experienced alterations in auxin distribution (Roudier *et al*., 2010). This was likely caused by alteration in the cellular distribution of PIN1, an auxin efflux carrier which determines the directionality of auxin transport by means of their

polar subcellular localization (Robert and Friml, 2009). The accumulation of PIN1 in the cytosol was suggested to result from alteration in the trafficking of PIN1 caused by the lower levels of VLCFA in the mutant plants (Roudier *et al*., 2010). Interestingly, the addition of exogenous VLCFAs to mutant plants resulted in the restoration of lateral root development (Roudier *et al*., 2010). Therefore, it is possible that the increase in VLCFA levels in this study could result in alteration of auxin mobilization within the plant. One of the general responses to low N supply observed in a variety of species is an increase in lateral root growth (Zhang and Forde, 1998; Lea and Azevedo, 1999), which is promoted by auxin levels in the root (Robert and Friml, 2009). An increase in mobilization of auxin to this tissue, possibly mediated by alterations in the levels of VLCFAs, could induce the response of lateral root growth to N deficiency. Furthermore, Guo *et al.* (2002) demonstrated that auxin regulates a dual-affinity transporter gene in *Arabidopsis* suggesting that auxin not only stimulates lateral root growth, which may allow exploration of nutrient-rich patches, but also regulates to some extent the transport of nitrate within the plant. However, metabolite profiling of the root tissue was not performed in this study, thus, this hypothesis is merely speculative. This highlights the need to perform a systematic characterization of different tissues (for example, the roots and leaves) in order to gain an understanding of long-distance signalling events as well as source:sink relationships between tissues.

The levels of 2-hydroxy tetracosanoic acid (α-OH C24:0) also increase in response to low nitrogen levels. This hydroxy-fatty acid is a prevalent long-chain base of sphingolipids present in plants (Pata *et al*., 2009). This further suggests that sphingolipid composition in cell membranes may play an important role in the response to N-deficit. Sphingolipids are generally classed in four groups, glycosyl inositol phosphoceramides, glycosylceramides, ceramides and free long-chain bases (Pata *et al*.,

2009). The physiological role of sphingolipids ranges from acting as membrane anchors for proteins (Borner *et al*., 2005), which could be an important determinant in cell signalling events, to the stabilisation and regulation of membrane permeability (Pata *et al*., 2009) and response to pathogens (Liang *et al*., 2003) and also including a role in the regulation of apoptosis (Liang *et al*., 2003; Townley *et al*., 2005). However, the presence of α-hydroxylated fatty acids occurs mainly in glycosylceramides and ceramides (Pata *et al*., 2009). In fact, the occurrence of very-long chain α–hydroxylated fatty acids seems to be a particular characteristic of glycosylceramides and ceramides of plants of the *Poaceae* family (Pata *et al*., 2009). Glycosylceramides have been ascribed to have an important role in membrane stability and permeability (Pata *et al*., 2009) while ceramides have been reported to be involved in the induction of apoptosis (Liang *et al*., 2003, Townley *et al*., 2005). This seems to suggest that the observed increase in 2-OH C24:0 levels may result from the induction of an apoptotic response of the leaf tissue.

However, in the study by Townley *et al*. (2005) it was found that α–hydroxylated ceramides and ceramides with longer FA chain length were less efficient in inducing apoptosis. In addition to this, it has been reported that ceramides have lower abundance when compared with glycosyl inositol phosphoceramides and glycosylceramides. Therefore, it seems more likely that significant modifications of 2-OH C24:0 levels are linked with the levels of glycosylceramides rather than with ceramides. Nevertheless, the possibility of an induction of apoptosis in the leaves should not be ruled out. Considering this, it is likely that under N deficit plants modify the sphingolipid composition in order to stabilise cell membranes and modify their permeability in addition to a role in regulating membrane protein trafficking for the auxin carrier protein (Roudier *et al*., 2010).

Interestingly, both VLCFA, cinnamic acid and ferulic acid are both up-regulated under low N supply. Suberin is a heteropolymer comprised of polyaliphatic and polyaromatic domains, with embedded waxes (Molina *et al.*, 2009). Its monomers include fatty acids, ω-hydroxyfatty acids, α,ω-dicarboxylic acids, fatty alcohols, very-long-chain saturated fatty acids, glycerol and *p*-hydroxycinnamic acids (particularly ferulic acid) (Pollard *et al*., 2008). The deposition of suberin requires the synthesis of metabolites from both the phenylpropanoid and acyl lipid pathways (Molina *et al*., 2009), and since there is a significant increase in metabolites from both these pathways it may be possible that plants are responding to N limitation by modifying the suberin biosynthesis. Interestingly, the levels of both 2-OH tetracosanoic acid and ferulic acid display similar levels and a similar response to the three levels of N supplied (Figure 5.5). This may further suggest a relationship between these two metabolites, which could support the hypothesis of suberin metabolism being modified in response to alteration of N supply.

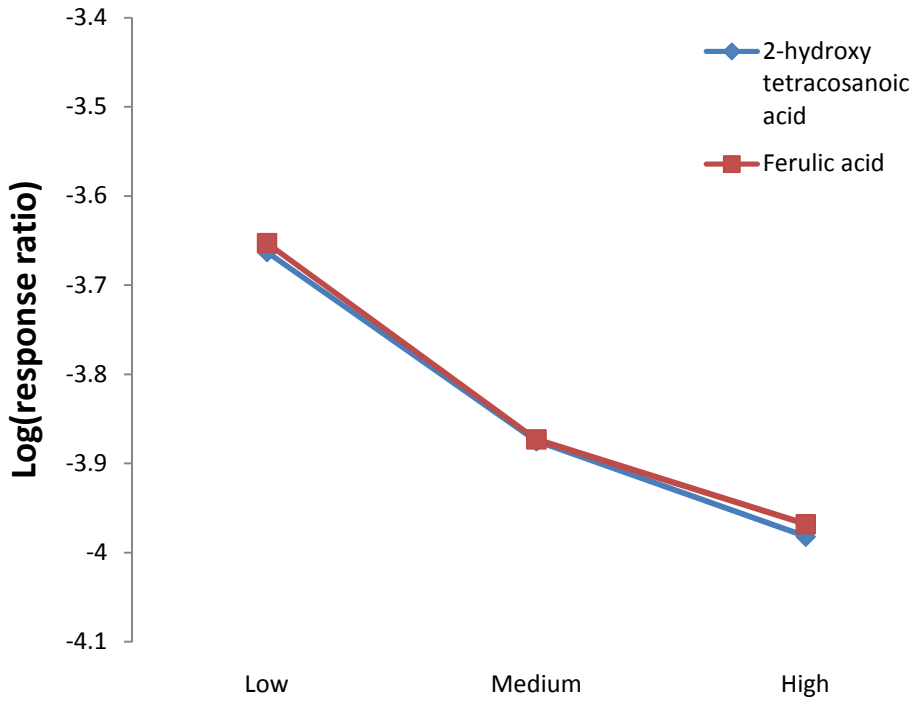

Figure 5.5- Logarithmic-transformed levels of response ratio of 2-hydroxy tetracosanoic acid and ferulic acid under different levels of N supply.

Suberin is constitutively deposited in both internal and external tissues during plant development; however, it can also be synthesized in response to wounding and stress (Pollard *et al*., 2008). One of the major roles of suberin and its associated waxes is to provide a hydrophobic barrier that can restrict the apoplastic transport which has consequences in the movement of water and solutes. Schreiber *et al*. (2005) characterized the response of suberin levels in roots of *Ricinus communis* plants challenged with NaCl and limiting N supply. The authors observed that when challenged with high levels of NaCl, plants would increase the amounts of aliphatic suberin which was suggested to prevent water loss due to osmotic effects (Schreiber *et al.*, 2005). Contrastingly, when plants were exposed to low levels of N the levels of aliphatic and aromatic suberin were reduced. The uptake of ions occurs mainly across the symplast (Enstone *et al*., 2003) so the authors speculated whether a decrease in suberin levels would result in an increase of movement of solutes which would allow an increase of available area for symplast uptake.

In this study, the results presented would suggest a hypothetical increase in suberin content. The increase in deposition of suberin would result in a decrease of apoplastic transport in the leaves and a reduction of the area available for symplastic uptake. Theoretically, this reduced area would allow the plant to exert a higher level of control upon nitrogen uptake in the leaf tissue. However, the increase in both secondary aromatic precursors and α–hydroxylated FA and VLCFAs may be a result of two independent responses to nitrogen limitation as discussed previously in this section. Therefore, a targeted approach aimed at elucidating the response of suberin metabolism in perennial ryegrass is required in order to support this speculative hypothesis.

5.5.3 Response to high levels of nitrogen supply

Plants grown under high nitrogen supply display increased levels for some amino acids, such as threonine, oxoproline and serine. This seems to suggest that one of the early-response mechanisms to increased levels of nitrogen supply is an increase in N assimilation by the plant. This is in agreement with Rasmussen *et al*. (2008) who studied the response of perennial ryegrass to a variety of conditions which included high nitrogen supply. In this study the authors observed an overall increase in a wide range of amino acids in plants supplied with higher levels of nitrogen after a period of eight weeks (Rasmussen *et al*., 2008). This seems to indicate that the first alterations in amino acid content can occur within 24h of exposure to high N concentrations and that it is likely that this trend will spread at a late-response to include a significantly higher number of amino acids.

Interestingly, the levels of the amino acids, which are significantly regulated either in response to low or to high nitrogen supply compared with intermediate, seem to be significantly different in plants grown under low- and high- nitrogen supply (Figure 5.4). A notable example is the difference in the levels of glutamine, which reveal only significant differences when comparing plants supplied with low N or high N. This suggests that the levels of amino acids increase gradually with increasing concentrations of N supplied (Figure 5.4), which is in accordance with the findings by Urbanczyk-Wochniak and Fernie (2005). Therefore, it is likely that for the range of N concentrations supplied there is a correlation between N supplied and N assimilation.

Additionally, it was found that there is an increase in the levels of threonate and inositol in plants supplied with high levels of N. Threonate is a downstream product of

ascorbate (Green and Fry, 2005), which is key metabolite regulating the presence of radical oxygen species (ROS) in cells (Apel and Hirt, 2004). The activity of ascorbate peroxidase is crucial in detoxifying hydrogen peroxide that has been formed by the reduction of superoxide by superoxide dismutase (Apel and Hirt, 2004).The role of this enzyme in response to stress conditions can be illustrated by a transgenic study in tobacco with over-expression of ascorbate peroxidase which displayed increased protection against oxidative stress (Wang *et al*., 1999). The reaction catalysed by ascorbate peroxidase results in the partial oxidation of ascorbate to monodehydroascorbate radical or the fully oxidised molecular species dehydroascorbate (DHA) (Hancock and Viola, 2005). The latter can be recycled back to ascorbate through the activity of dehydroascorbate peroxidase (EC 1.8.5.1) while oxidizing two molecules of glutathione (GSH) . However, DHA can also be channelled into two distinct enzyme-catalysed catabolic pathways in plants. One of the pathways results in the production of tartrate while the alternative pathway results in the production of oxalate and threonate, which can be subsequently oxidised to tartrate (Hancock and Viola, 2005).

Ascorbate levels have been associated mainly with its role as antioxidant, however it may also act as pro-oxidant (Podmore *et al*., 1998). Green and Fry (2005) proposed that several steps in the ascorbate catabolism may enhance the pro-oxidant activity of ascorbate by generating radical oxygen species (ROS). Thus, the authors proposed that the degradation of ascorbate, which is mainly present in the apoplast, may potentially initiate a cascade of up to five molecules of H_2O_2 from a single molecule of ascorbate (Green and Fry, 2005). The presence of apoplastic H_2O_2 and residual levels of ascorbate could generate hydroxyl radicals which could modify cell wall, enhancing cell expansion (Fry, 1998; Green and Fry, 2005). Furthermore, it is possible that the ROS production is directly involved in ROS-mediated signalling which has been previously

proposed to regulate some abiotic and biotic stress response mechanisms (Foyer and Noctor, 2005; Bailey-Serres and Mittler, 2006).

Interestingly, Wang and Lin (2003) observed that strawberry fruit experienced significantly increased ROS levels with increasing application of fertilizer and compost use. Therefore, it seems plausible that high nitrogen levels may trigger a ROS-mediated signalling response. However, Wang and Lin (2003) also observed that antioxidant components such as ascorbate (AsA), GSH, flavonol and anthocyanin experienced an increase in their levels as well as the ratios of AsA/DHA and GSH/GSSG, which they proposed to act in response to the increase in ROS. This seems to further suggest that ROS production is under fine control as reviewed by Hancock and Viola (2005).

Interestingly, the levels of inositol also increase in perennial ryegrass plants grown under high N concentrations. Recent molecular and biochemical evidence has been reported with respect to a possible biosynthetic route of ascorbate from inositol (Lorence *et al*., 2004). The proposed pathway involves the activity of *myo*-inositol oxidase (MIOX) which results in the synthesis of D-glucuronate, a precursor of one of the main biosynthetic pathways of ascorbate (Figure 5.6). Furthermore, the authors observed that the constitutive expression of MIOX4 resulted in a 2- to 3-fold increase in ascorbate levels in the leaves of *Arabidopsis* plants (Lorence *et al*., 2004).

However, this study lacks the characterization of ascorbate levels and its immediate products and precursors; therefore, it is impossible to confirm its role in regulating the response of perennial ryegrass to high levels of N. In order to confirm this hypothesis, further experiments are required aimed at characterizing both the ascorbate metabolism as well as the response of ROS.

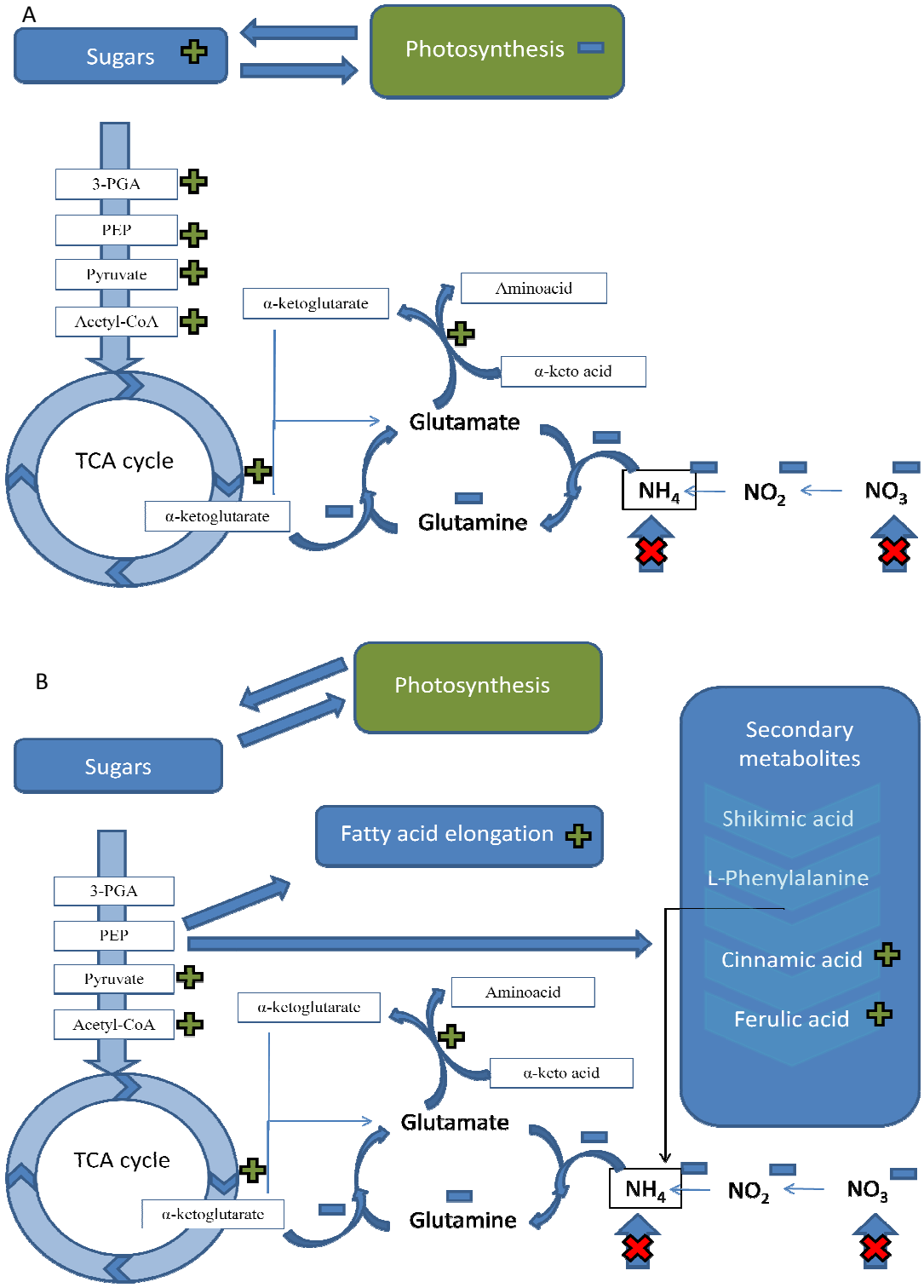

Figure 5.6 – Metabolic adaptations to N-limitation. A –It has been proposed that a decrease in N availability will result in a reduction in N-assimilation through the GS-GOGAT pathway resulting in elevated levels of organic acids. This will result in feedback inhibition of glycolysis causing the accumulation of sugars. The sugar accumulation is then thought to be responsible for decreasing the photosynthetic activity. B- This hypothesis proposed in this chapter suggests that, in order to prevent inhibition of photosynthesis by sugar accumulation, the plant diverts its metabolic flux towards the elongation of fatty acids and the production of secondary aromatic metabolites in the short term response. Furthermore, the accumulated metabolites may have functional roles to play in stress as discussed in the main text.

Myo-inositol is an important molecule that is directly involved in important metabolic and signalling processes besides the biosynthesis of ascorbate. It can become incorporated into phosphatidylinositol phosphate, *myo*-inositol phosphate and also certain sphingolipid signalling molecules which may be involved in a variety of processes, including gene expression (Alcazar-Roman *et al*., 2006), auxin receptor association (Tan *et al*., 2007), stress tolerance (Bohnert and Sheveleva, 1998) and also regulation of cell death (Liang *et al*., 2003). A study with *Arabidopsis* mutants in L-myo-inositol 1-phosphate synthase (MIPS; EC 5.5.1.4) revealed that a loss of MIPS resulted in smaller plants with curly leaves in addition to a reduction of the levels of myoinositol, ascorbic acid and phosphatidylinositol levels (Donahue *et al*., 2010). Furthermore, the authors observed elevated levels of ceramides in mutant plants, which had been previously been associated with induction of cell death (Meng *et al*., 2009). Therefore, the authors suggested that alterations in the expression of MIPS1 which had a significant effect in the levels of *myo*-inositol levels is critical for controlling the levels of ascorbic acid, phosphatidylinositol and ceramides that regulate growth, development and cell death (Donahue *et al*., 2010).

However, in this study there was no change in the levels of fatty acids in perennial ryegrass plants supplied with high levels of N. Taking into consideration that fatty acids are essential components of both ceramides and phosphatidylinositol (Pata *et al*., 2009), it appears that there is no significant alteration in both these classes of compounds in the early-response to high levels of N supply. This further suggests that alteration of the inositol levels will probably result in changes ascorbate levels, which will mediate the early-response to high N. Nevertheless, a targeted approach aiming to quantify both ceramides and phosphatidylinositol, in addition to ascorbate is essential to confirm this hypothesis.

5.6 Conclusions

A large majority of the studies aiming to study the biochemical response to different N-levels has mainly focused in the study of a relatively small number of genotypes. In this study metabolite profiling was undertaken for a total of seven different genotypes, and aimed to indentify the metabolic response to different levels of N supplied regardless of the genetic background.

The study of metabolic response to N-limitation has largely focused on studying polar molecules such as aminoacids and sugars. The general metabolic response reported for N-limitation includes a decrease in aminoacid levels and a concomitant increase in carbohydrates. In this study, it was also observed alterations in the levels of some aminoacids, which appear to correlate positively with N levels in the medium. However, there were no significant changes in the levels of sugars under N-deficit. It appears that the metabolic response of perennial ryegrass to N-depletion includes modifications of the secondary metabolism and also the lipid metabolism, with the synthesis of cinnamic acids and VLCFAs. In contrast, the response of perennial ryegrass plants to high levels of N supply appears to be linked with ascorbate metabolism, suggesting the involvement of ROS-mediated signalling.

This study highlights the importance of lipid and ascorbate metabolism for response to N-limitation and N-saturation, respectively, and suggests that further attention should be devoted to these metabolic processes by using targeted approaches.

Chapter 6

General Conclusions

General conclusions

Throughout this PhD project a number of different approaches were used to study the metabolic response of perennial ryegrass to a variety of abiotic stresses. The combination of transcript profiling and metabolite profiling proved to be powerful to elucidate several mechanisms associated with stress response. The metabolite profiling was generally achieved using GC-MS, however, it is estimated that the plant metabolome is comprised of approximately 200,000 metabolites (Fiehn, 2002), while the number of metabolites here describes only a fraction of that number (151, 140 and 97 identified metabolites for chapter 3, 4 and 5, respectively). It is clear, therefore, that the coverage of the plant metabolome in this study can only partially characterise metabolic response to stress. Nevertheless, it was observed that abiotic stresses produced effects on primary metabolism reflecting its importance for coordinating plant homeostasis. The complementation of metabolite profiling with global transcript profiling revealed, on several occasions, the involvement of secondary metabolism, which was not possible to observe using a GC-MS profiling approach. This highlights the need to further expand the coverage of the metabolites analysed, perhaps by including an LC-MS approach, to acquire an appropriate profile of the secondary metabolism. One inherent disadvantage of metabolomics is that generally all the information about cellular and sub-cellular metabolite location is generally lost during sample preparation. For example, it would be impossible to distinguish metabolites present in the cytoplasm from metabolites present in the endoplasmic reticulum. Transcript analysis often provides evidence of transport mediator regulation which may contribute to the understanding of changes in cellular metabolite, for example, the up-regulation of glycerol 3-P permease under low levels of P (Chapter 4) which was linked

to an involvement in fatty acid biosynthesis in the chloroplast/endoplasmic reticulum. Other transport mediators which are relevant for the response to abiotic stress can be observed with transcript profiling but not at the metabolome level such as the up-regulation of aquaporins in plants exposed to water-limitation (Chapter 3). The response to stress also appears to be mediated by several signalling cascades which can be identified by the up-regulation of specific genes. For example, the upregulation of an calmodulin-binding protein in plants grown under P limitation was observed (Chapter 4). Furthermore, transcript profiling may provide information about metabolic alterations in classes of metabolites which are not covered by the analytical method used. This can be illustrated in Chapter 3, where the up-regulation of a fructan:fructan 6 fructosyltransferase lead to the subsequent analysis of fructan composition in the leaves. This highlights the role of global transcript profiling in a top-to-bottom approach, where an initial global approach is used and from the subsequent transcriptomic data a further targeted approach will be used. However, transcript profiling alone also has its own limitations, such as being unable to detect post-transcriptional and post-translational modifications. One of such examples includes the glycolytic by-passing mechanism catalysed by PEPCase, which does not experience significant regulation at transcript level (Chapter 4). However, the metabolite levels indicated a decrease of amino acids derived from pyruvate which provided an indirect evidence of the bypassing mechanism (Chapter 4).

A general feature observed when integrating metabolite data with transcript profiling data in this project is that a majority of the significantly up-regulated transcripts are not directly involved in the regulation of significantly regulated metabolites. This highlights the role of biochemical regulation mechanisms which determine the steady-state levels

of metabolites and seem to have a degree of independence from transcriptional regulation.

The lack of a direct relationship between significant metabolite and transcript often makes it difficult to address whether increases in the levels of a metabolite are a result of a decrease in its downstream reaction or an increase in its biosynthesis. However, metabolites are part of a highly interconnected network, and should not be considered in isolation. Instead, metabolites should be analysed in relation to the pathways in which they are involved, and often their related metabolites provide insights into the metabolic adjustments in response to stress. For example, in chapter 4 it was observed that the levels of alanine, valine, leucine and isoleucine decreased in some plants exposed to low levels of P. All these metabolite are downstream products of pyruvate and form a "sub-network" which appears to be co-ordinately regulated. These types of "sub-networks" were also observed in chapter 5 for very-long-chain fatty acids (VLCFAs), cinnamic acids and some amino acids. However, in some cases it is not possible to define a closely related "sub-network" of metabolites. Nevertheless, it may still be possible to extract some information from the relationships between not closely related metabolites. A notable example of this is present in chapter 5 for both inositol and threonate, which seem to increase in plants grown in N-saturated media. Inositol may be involved as a precursor in biosynthesis of ascorbate and an increase in its levels may be a result of either a decrease in ascorbate biosynthesis (decrease in sink activity) or an increase in the metabolic flux towards the synthesis of ascorbate. However, since threanate (a product of ascorbate degradation) increases, it seemed plausible that there is both an increase in the synthesis and degradation of ascorbate. Inositol may also be involved in other biosynthetic routes, but this was deemed unlikely due to a lack of alteration in the levels of metabolites involved in those processes. It should be noted, however, that this

hypothesis is highly speculative compared with the hypothesis being derived from closely linked "sub-networks", as described above. This further suggests the need to expand metabolome coverage to include a significantly higher number of metabolites and therefore, define a "sub-network" for ascorbate-related metabolites. However, at the moment it seems unlikely that a single metabolite profiling approach will provide significant coverage of the metabolome, therefore in order to circumvent this limitation, the use of targeted profiling approaches aimed at characterizing specific "sub-networks" of closely related metabolites may aid in defining specific metabolite "sub-networks". This means that a targeted profiling approach should be used to validate the hypothesis suggested above for the involvement of ascorbate metabolism in response to high levels of N supply.

The different experiments performed throughout this project have distinguishing features, each with their own benefits and drawbacks. This knowledge can be used in the future to generate new experiments focusing mainly on the beneficial aspects of each experiment.

Plants exposed to stress often display alterations in their morphology and physiology (Stitt *et al*., 1999; Molnar *et al*., 2004; Kavanova *et al*., 2006). Morphological and physiological characterization of the drought response in perennial ryegrass included biomass modifications, monitoring relative water content in the leaf tissues and visual assessment. This provided valuable information for characterizing the response of each genotype to water limitation. The extent of characterization performed in the drought experiment was greater when compared with the nitrogen and phosphorous experiments. Perhaps an increased focus on monitoring the morphological and physiological responses of plants to stress (in other words, the collection of metadata) should be taken in consideration for future stress experiments.

The transcript profiling approaches used included SSH (for chapter 3) and microarrays (for chapter 4). However, time limitations meant that no transcript analysis was performed for the nitrogen experiment. This resulted in a lack of information regarding nitrate and ammonium transporters as well as in nitrate and nitrite reductases, and therefore, information regarding nitrogen assimilation was deducted from the metabolite data. Furthermore, the results presented in chapter 5 suggest indirectly an involvement of signalling pathways. Perhaps, via a complementary transcript/metabolite profiling approach additional evidence would be provided for these mechanisms. Transcript analysis by microarray appeared to have a higher coverage (in number of useful outcomes) when compared with SSH. Therefore, microarray analysis appears to have greater advantages when compared with SSH profiling. However, at present there is no publicly accessible microarray available specifically for perennial ryegrass.

For the analysis of stress in chapters 3 and 4, metabolomic data were often complemented with data generated with additional analytical techniques (HPAEC and FT-IR, respectively). These techniques were used in order to complement the GC-MS approach. In one case (chapter 3) a targeted approach was used with the aim of characterising a specific group of molecules, while the FT-IR analysis performed in chapter 4 provided a broader-range, albeit less detailed, perspective for a wide range of classes of molecules. The ability to focus on increased detail, or alternatively reduce the detail to obtain a "wider-picture" should be explored in order to gain a comprehensive understanding of the response of plants to different environmental factors.

When analysing the response of plants to abiotic stress conditions, it is of extreme importance to characterize the relevant tissues. In this project water and nutrient supply were studied as factors of environmental stress. Considering the role of root tissue in the uptake of both nutrients and water, it is important to characterise its response to the

limitation of those factors. In plants grown in soil this is a difficult task to achieve, since extraction protocols generally require relatively clean tissues. Therefore, a hydroponics system was used for all the experiments presented in this thesis, which allows access to clean roots and also allows some extent of control over media composition. However, this lack the physical restraint aspect of soil, and an alternative approach that could be used would involve an infused gel-system. Additionally, metabolomic studies of stress response often incorporate metabolite profiling of leaf tissues in addition to the root tissue (Roessner *et al*., 2006; Huang *et al*., 2008; Hernandez *et al*., 2009). The photosynthetic tissue is indeed an important source of C and energy and the photosynthetic rate is often affected by some abiotic stresses (Raghothama, 1999, Chaves *et al*., 2009).

However, analysing tissues in isolation may provide an incomplete view of the overall metabolic response to stress in plants. Chapter 5 illustrates this, since unfortunate circumstances made it impossible to perform metabolite profiling in the roots of plants grown under different levels of N supply. This limited the conclusions since it was impossible to establish relationships between metabolites in different tissues, in the manner presented in chapter 4. Therefore, the study of environmental factors related with nutrient and water supply should ideally be performed for both leaf and root tissues.

A majority of the stress-related metabolomic studies that have been performed generally focus on a small number of genotypes, normally one or two, exposed to a range of different conditions (Roessner *et al*., 2006; Gaude et al., 2007; Hernandez et al., 2007; Huang *et al.*, 2008; Hernandez *et al*., 2009). However, this may raise the question of whether the responses observed in such studies can be extrapolated to a larger pool of genotypes, or whether the differences observed are specific to those genotypes. There is

interest in characterising particularly well-adapted plants to stress conditions in order to determine some of the mechanisms which affect positively the performance of such plants. However, the availability of genotypes particularly well-adapted to stress conditions is scarce and the occurrence of genotypes described as tolerant to a particular stress (as observed in chapter 3) are the exception rather than the rule. Therefore, studying the response of a small number of genotypes which are not specifically adapted to a stress condition may result in conclusions which are specific for those genotypes. By characterizing a greater number of different genotypes it may be possible to detect a response to stress which seems to be largely independent of the genetic background as was observed in chapter 5. Altogether, this provides two ideal approaches to study stress response in plants. One approach, may include a relatively low number of genotypes screened and should aim to characterise the response of highly-adapted plants to stress in order to identify mechanisms which may be responsible for conferring enhanced tolerance to stress. The alternative (or complementary) approach, attempts to characterize a larger pool of genotypes and attempt to identify mechanisms which are common for all genotypes. Clearly a combination of both would result in a more comprehensive understanding of the response of plants to stress.

In order to gain a better understanding of the metabolic implications of water and nutrient limitation and improved nutrient usage efficiency, this project aimed to characterize the metabolic response of different perennial ryegrass varieties to different levels of water, N and P supply. Characterization of the metabolic profiles was performed with GC-MS-based metabolite profiling. Additionally, the metabolite response to a PEG-mediated water stress and different P supply was integrated with data from a transcriptomic approach.

The analysis of the metabolite profiles of perennial ryegrass plants exposed to PEG-induced water stress revealed that tolerant plants accumulated increased levels of raffinose, which may function as an osmoregulator or a ROS-scavenger. Furthermore, it was found that other osmolytes, such as trehalose, accumulated in response to stress. Additionally, the results suggested that the different genotypes had different fructan levels and that these could be correlated with differences in drought tolerance.

Metabolite profiling of perennial ryegrass plants exposed to P-deficit revealed that the response to stress involved glycolytic bypasses, induction of the secondary metabolism, induction of P-scavenging mechanisms and alterations in lipid composition.

The analysis of several genotypes supplied with three different levels of N highlighted the role of both VLCFAs and secondary metabolism in the response to N levels. Although these have been associated with structural components of the cell, the possible involvement in signal transduction mechanisms was also a possibility. The involvement of ascorbate metabolism in mediating response to high levels of N was also proposed. The major trend observed was a gradual increase in amino acid levels with increasing levels of N supply.

The pathways described above are ultimately linked via primary metabolism. This highlights its contribution to the coordination of the response to environmental factors. Primary metabolism includes metabolites which are involved in multiple pathways, and hence represent “cross-roads” in the metabolism. Such examples include PEP which may contribute as precursor of secondary metabolites through the shikimate pathway, or alternatively, be converted to pyruvate, which is subsequently oxidised in the mitochondria, or acetyl CoA which can be involved in fatty acid biosynthetic and in the tricarboxylic cycle pathways. A regulation of the metabolic flux through those branching points in metabolism appears to be of extreme importance to the adaptation to

different levels of water and nutrients in perennial ryegrass. A future perspective for stress studies should include multifactorial experiments, with for example N and water availability being altered simultaneously. In this example, it would be interesting to observe whether the metabolic adaptation to a combination of stresses would be additive or alternatively result in a different response, as observed by Rhisky *et al*. (2004).

Overall, the results obtained here yielded insights into some of the mechanisms involved in the response of perennial ryegrass to a variety of stress. However, in most cases additional experimental validation is required to support the hypotheses suggested. For example, in chapter 4 it was proposed a modification of lipid composition, thus lipid profiling should be performed.

The immediate application of the knowledge gained in this project to the applied science sector is limited. In some cases, an increase of specific mechanisms was observed, such as raffinose and trehalose in the drought experiment (chapter 3). In this case it may be possible to perform genetic engineering approaches aimed at increasing the levels of those metabolites to improve the tolerance of perennial ryegrass varieties. This has already been performed in rice by Garg *et al*. (2002) who genetically engineered plants to accumulate higher levels of trehalose. However, in the case of the response mechanisms to N levels which are likely to involve signalling mechanisms this may not be a suitable approach.

It is evident that the response of perennial ryegrass to abiotic stress still requires further characterization. There is a need to develop publicly available *Lolium perenne* microarrays in combination with further metabolomic studies to obtain a detailed overview of the metabolic response to a variety of stresses. Analysis of the response over time should be performed for those studies in order to identify the sequential

response mechanisms and perhaps gain a better understanding of the mechanisms of regulation and the function of several genes. In addition to 'omic' scale profiling, additional in-depth studies to fully characterise the molecular and metabolic regulation of several pathways involved in mediation of abiotic stress tolerance is a requirement. However, this is a daunting task requiring expertise in different areas of research and can succeed via the establishment of collaborations between different groups, perhaps via a perennial ryegrass international consortium.

Reference list

Abebe T, Guenzi AC, Martin B, Cushman JC. 2003. Tolerance of mannitol-accumulating transgenic wheat to water stress and salinity. *Plant Physiology* **131**:1748-1755.

Aharon R, Shahak Y, Wininger S, Bendov R, Kapulnik Y, Galili G. 2003. Overexpression of a plasma membrane aquaporin in transgenic tobacco improves plant vigor under favourable growth conditions but not under drought or salt stress. *The Plant Cell* **15**:439-447.

Aharoni A, de Vos CHR, Verhoeven HA, Maliepaard CA, Kruppa G, Bino R, Goodenowe DB. 2004. Nontargeted metabolome analysis by use of Fourier transform ion cyclotron mass spectrometry. *OMICS: A Journal of Integrative Biology* **6**(3):217-234.

Alcazar R, Planas J, Saxena T, Zarza X, Bortolotti C, Cuevas J, Britian M, Tiburcio AF, Altabella T. 2010. Putrescine accumulation confers drought tolerance in transgenic Arabidopsis plants over-expressing the homologous *Arginine decarboxilase 2* gene. *Plant Physiology and Biochemistry* in press.

Alcazar-Roman AR, Tran EJ, Guo S, Wente SR. 2006. Inositol hexakisphosphate and Gle1 activate the DEAD-box protein Dbp5 for nuclear mRNA export. *Nature Cell Biology* **8**(7):711-720.

Amiard V, Morvan-Bertrand A, Billard JP, Huault C, Keller F, Prud'homme MP. 2003. Fructans, but not the sucrosyl-galactosides raffinose and loliose, are affected by drought stress in perennial ryegrass. *Plant Physiology* **132**:2218-2229.

Andrews M, Scholefield D. Abberton MT, McKenzie BA, Hodge S, Raven JA. 2007. Use of white clover as an alternative to nitrogen fertiliser for dairy pastures in nitrate vulnerable zones in the UK: productivity, environmental impact and economic considerations. *Annals of Applied Biology* **151**(1):11-23.

Anonymous: Food and Agriculture Organisation, Internation Fertiliser Industry Association, International Fertilizer Development Center, International Potash Institute and Phosphate and Potash Institute. 2002. Fertilizer use by crop. Fifth Edition. *FAO Rome*.

Anonymous: European Fertilizer Manufacturers Association. 2009. Forecast of food, farming and fertiliser use in the European Union 2009-2019. http://www.efma.org/content.asp?id=6&sid=30 accessed Thursday 11th March.

Apel K, Hirt H. 2004. Reactive oxygen species: Metabolism, oxidative stress and signal transduction. *Annual Review of Plant Biology* **55**:373-399.

Araya T, Noguchi K, Terashima I. 2010. Effect of nitrogen nutrition on the carbohydrate repression of photosynthesis in leaves of *Phaseolus vulgaris* L. *Journal of Plant Research* **123**:371-379.

Bailey NJC, Oven M, Holmes E, Nicholson JK, Zenk MH. 2003. Metabolomic analysis of the consequences of cadmium exposure in *Silene cucubalus* cell cultures via ^{1}H NMR spectroscopy and chemometrics. *Phytochemistry* **62**(6):851-858.

Bailey-Serres J, Mittler R. 2006. The roles of reactive oxygen species in plants cells. *Plant Physiology* **141**(2):311.

Bartels D, Sunkar R. 2005. Drought and salt tolerance in plants. *Critical Reviews in Plant Sciences* **24**(1):23-58.

Beaudoin F, Wu X, Li F, Haslam RP, Markham JE, Zheng H, Napier JA, Kunst L. 2009. Functional characterization of the Arabidopsis β-Ketoacyl-Coenzyme A reductase candidates of the fatty acid elongase. *Plant Physiology* **150**:1174-1191.

Benning C. 2009. Mechanisms of lipid transport involved in organelle biogenesis in plant cells. *Annual Review of Cell and Developmental Biology* **25**:71-91.

Berliner LJ, Reuben J. 1992. Biological Magnetic Resonance – volume 11 - *In vivo* spectroscopy. New York and London: Plenum Press .

Bino RJ, Hall RD, Fiehn O, Kopka J, Saito K, Draper J, Nikolau BJ, Mendes P, Roessner-Tunali U, Beale MH, Tretheway RN, Lange BM, Wurtele ES, Sumner LW. 2004. Potential of metabolomics as a functional genomics tool. *TRENDS in Plant Science* **9:**418-425.

Brazma A, Hingamp P, Quackenbush J, Sherlock G, Spellman P, Stoeckert C, Aach J, Ansorge W, Ball CA, Causton HC, Gaasterland T, Glenisson P, Holstege FCP, Kim IF, Markowitz V, Matese JC, Parkinson H, Robinson A, Sarkans U, Schulze-Kremer S, Stewart J, Taylor R, Vilo J, Vingron M. 2001. Minimum information about microarray experiment (MIAME) – towards standards for microarray data. *Nature Genetics* **29**:365-371.

Boccard J, Grata E, Thiocone A, Grauvrit JY, Lanteri P, Carrupt PA, Wolfender JL, Rudaz S. 2007. Multivariate data analysis of rapid LC-TOF/MS experiments from *Arabidopsis thaliana* stressed by wounding. *Chemometrics and Intelligent Laboratory Systems* **86**(2):189-197.

Bohnert HJ, Sheveleva E. 1998. Plant stress adaptations - making metabolism move. *Current Opinion in Plant Biology* 1(3):267-274.

Bongue-Bartelsman M, Phillips DA. 1995. Nitrogen stress regulates gene expression of enzymes in the flavonoid biosynthetic pathway of tomato. *Plant Physiology and Biochemistry* **33**(5):539-546.

Borner GHH, Sherrier DJ, Weimar T, Michaelson LV, Hawkins ND, MacAskill A, Napier JA, Beale MH, Lilley KS, Dupree P. 2005. Analysis of detergent-resistant membranes in Arabidopsis. Evidence for plasma membrane lipid rafts. *Plant Physiology* **137**:104-116.

Capanoglu E, Beekwilder J, Boyacioglu D, Hall R, de Vos R. 2008. Changes in antioxidant and metabolite profiles during production of tomato paste. *Journal of Agricultural and Food Chemistry* **56**(3):964-973.

Chaves MM, Flexas J, Pinheiro C. 2009. Photosynthesis under drought and Salt stress: regulation mechanisms from whole plant to cell. *Annals of Botany* **103**:551-560.

Chen THH, Murata N. 2002. Enhancement of tolerance of abiotic stress by metabolic engineering of betaines and other compatible solutes. *Current Opinion in Plant Biology* **5**(3):250-257.

Chiwocha SDS, Abrams SR, Ambrose SJ, Cutler AJ, Loewen M, Ross ARS, Kermode AR. 2003. A method for profiling classes of plant hormones and their metabolites using liquid chromatography-electrospray ionization tandem mass spectrometry: an analysis of hormone regulation of thermodormancy of lettuce (*Lactuca sativa* L.) seeds. *The Plant Journal* **35**:405-417.

Choi YH, Tapias EC, Kim HK, Lefeber AWM, Erkelens C, Verhoeven JTJ, Brzin J, Zel J, Verpoorte R. 2004. Metabolic discrimination of *Catharanthus roseus* leaves infected by phytoplasma using 1H-NMR spectroscopy and multivariate data analysis. *Plant Physiology* **135**:2398-2410.

Conklin PL, Williams EH, Last RL. 1996. Environmental stress sensitivity of an ascorbic acid-deficient Arabidopsis mutant. *Proceedings of the National Academy of Sciences* **93**:9970-9974.

Cowling DW, Lockyer DR. 1970. The response of perennial ryegrass to nitrogen in various periods of the growing season. *The Journal of Agricultural Science* **75**:539-546.

Davies A. 1971. Changes in growth rate and morphology of perennial ryegrass swards at high and low nitrogen levels. *The Journal of Agricultural Science* **77**:123-134.

Defernez M, Colquhoun IJ. 2003. Factors affecting the robustness of metabolite fingerprinting using ^{1}H NMR spectra. *Phytochemistry* **62**(2):1009-1017.

Desai S, Hill JE, Trelogan S, Diatchenko L, Siebert PD. 2000. Identification of differentially expressed genes by suppression subtractive hybridization. In: *Functional genomics a practical approach* Oxford University Press, USA.

Diaz C, Salia-Colombani V Loudet O, Belluomo P, Moreau L, Daniel-Velede F, Morot-Gaudry JF, Masclaux-Daubresse C. 2006. Leaf yellowing and anthocyanin

accumulation are two genetically independent strategies in response to nitrogen limitation in *Arabidopsis thaliana. Plant Cell Physiology* **47**(1):74-86.

Dickin E, Wright D. 2008. The effects of winter waterlogging and summer drought on the growth and yield of winter wheat (Triticum aestivum L.). *European Journal of Agronomy* **28**(3):234-244.

Dixon RA. 2001. Natural products and plant disease resistance. *Nature* **411:**843-847

Dobson G, Shepherd T, Verrall SR, Griffiths WD, Ramsay G, McNicol JW, Davies HV, Stewart D. 2010. A metabolomics study of cultivated potato (*Solanum tuberosum*) groups Andigena, Phureja, Stenotomum, and Tuberosum using Gas Chromatography-mass spectrometry. *Journal of Agricultural and Food Chemistry* **58**:1214-1223.

Donahue JL, Alford SR, Torabinejad J, Kerwin RE, Nourbakhsh A, Ray WK, Hernick M, Huang X, Lyons BM, Hein PP, Gillaspy GE. 2010. The Arabidopsis thaliana myo-inositol 1-phosphate synthase 1 gene is required for myo-inositol synthesis and suppression of cell death. *The Plant Cell* **22**:888-903.

Dowdell RJ, Webster CP. 1979. A lysimeter study using nitrogen-15 on the uptake of fertilizer nitrogen by perennial ryegrass swards and losses by leaching. *European Journal of Soil Science* **31**(1):65-75.

Doyle JJ, Doyle JL. 1987. A rapid DNA isolation procedure for small amounts of fresh leaf tissue. *Phytochemical Bulletin* **19**:11-15.

Duan K, Yi K, Dang L, Huang H, Wu W, Wu P. 2008. Characterization of a sub-family of Arabidopsis genes with the SPX domain reveals their diverse functions in plant tolerance to phosphorus starvation. *The Plant Journal* **54**(6):965-975.

Ducreux LJM, Morris WL, Prosser IM, Morris JA, Beale MH, Wright F, Shepherd T, Bryan GJ, Hedley PE, Taylor MA. 2008. Expression profiling of potato germplast differentiated in quality traits leads to the identification of candidate flavour and texture genes. *Journal of Experimental Botany* **59**:4219-4231.

Duff SMG, Moorhead GBG, Lefebvre DD, Plaxton WC. 1989. Phosphate starvation inducible 'bypasses' of adenylate and phosphate dependent glycolytic enzymes in *Brassica nigra* suspension cells. *Plant Physiology* **90**:1275-1278.

Duff SMG, Sarath G, Plaxton WC. 1994. The role of acid phosphatases in plant phosphorus metabolism. *Physiologia Plantarum* **90**(4):791-800.

Dunn WB, Ellis DI. 2005. Metabolomics: Current analytical platforms and methodologies. *Trends in Analytical Chemistry* **24**(4):285-294.

Elbein AD, Pan YT, Pastuszak I, Carroll D. 2003. New insights on trehalose: a multifunctional molecule. *Glycobiology* **13**(4):17-27.

Enstone DE, Peterson CA, Ma F. 2003. Root endodermis and exodermis: structure, function, and responses to the environment. *Journal of Plant Growth Regulation* **21**:335-351.

Fiehn O. 2002. Metabolomics – the link between genotypes and phenotypes. *Plant Molecular Biology* **48:**155-171.

Fiehn O, Kopka J, Dormann P, Altmann T, Trethewey RN, Willmitzer L. 2000. Metabolite profiling for plant functional genomics. *Nature Biotechnology* **18**:1157-1161.

Fiehn O, Robertson D, Griffin J, Werf MVD, Nikolau B, Morrison N, Sumner LW, Goodacre, Hardy NW, Taylor C, Fostel J, Kristal B, Kaddurah-Daouk R, Mendes P, van Ommen B, Lindon JC, Sansone SA. 2007. The metabolomics standards initiative (MSI). *Metabolomics* **3**:175-178.

Fiehn O, Wohlgemuth G, Sholz M, Kind T, Lee DY, Lu Y, Moon S, Nikolau B. 2008. Quality control for plant metabolomics: reporting MSI-compliant studies. The *Plant Journal* **53**:691-704.

Foito A, Byrne SL, Shepherd T, Stewart D, Barth S. 2009. Transcriptional and metabolic profiles of *Lolium perenne* L. genotypes in response to a PEG-induced water stress. *Plant Biotechnology Journal* **7**(8):719-732.

Foito A, Byrne SL, Hedley PE, Morris JA, Stewart D, Barth S. 2010. Early response mechanisms of perennial ryegrass (*Lolium perenne* L.) to phosphorus deficiency. *Submitted.*

Forrest KL, Bhave M. 2008. The PIP and TIP aquaporins in wheat form a large and diverse family with unique gene structures and functionally important features. *Functional and Integrative Genomics* **8**(2):115-133.

Foyer C, Spencer C. 1986. The relationship between phosphate status and photosynthesis in leaves. *Planta* **167**(3):369-375.

Foyer CH, Noctor G. 2005. Oxidant and antioxidant signalling in plants: a re-evaluation of the concept of oxidative stress in a physiological context. *Plant, Cell and Environment* **28**:1056-1071.

Frederich M, Choi YH, Angenot L, Harnischfeger G, Lefeber AWM, Verpoorte R. 2004. Metabolic analysis of *Strychnos nux-vomica*, *Strychnos icaja* and *Strychnos ignatii* extracts by ^{1}H nuclear magnetic resonance spectrometry and multivariate analysis techniques. *Phytochemistry* **65**(13):1993-2001.

Fry SC. 1998. Oxidative scission of plant cell wall polysaccharides by ascorbate-induced hydroxyl radicals. *Biochemical Journal* **332**:507-515.

Garg AK, Kim JK, Owens TG, Ranwala AP, Choi YD, Kochian LV, Wu RJ. 2002. Trehalose accumulation in rice plants confers high tolerance levels to different abiotic stresses. *Proceeding of the National Academy of Sciences* **99**(25):15898-15903.

Gaude N, Brehelin C, Tischendorf G, Kessler F, Dormann P. 2007. Nitrogen deficiency in Arabidopsis affects galactolipid composition and gene expression and results in accumulation of fatty acid phytil esters. *The Plant Journal* **49**:729-739.

Gidman E, Goodacre, Emmett B, Smith AR, Gwynn-Jones D. 2003. Investigating plant-plant interference by metabolic fingerprinting. *Phytochemistry* **63**(6):705-710.

Gigon A, Matos AR, Laffray D, Zuily-Fodil Y, Pham-Thi AT. 2004. Effect of drought stress on lipid metabolism in the leaves of *Arabidopsis thaliana* (ecotype Columbia). *Annals of Botany* **94**(3):345-351.

Glass ADM, Britto DT, Kaiser BN, Kinghorn JR, Kronzucker HJ, Kumar A, Okamoto M, Rawat S, Siddiqi MY, Unkles SE, Vidmar JJ. 2002. The regulation of nitrate and ammonium transport systems in plants. *Journal of Experimental Botany* **53**(370):855-864.

Glazebrook J, Ausubel FM. 1994. Isolation of phytoalexin-deficient mutants of Arabidopsis thaliana and characterization of their interactions with bacterial pathogens. *Proceedings of the National Academy of Sciences* **91**:8955-8959.

Gonzalez B, Boucaud J, Salette J, Longlois J, Duyme M. 1989. Changes in stubble carbohydrate content during regrowth of defoliated perennial ryegrass (*Lolium perenne* L.) on two nitrogen levels. *Grass and Forage Science* **44**(4):411-415.

Goodacre R, Vaidyanathan S, Dunn WB, Harrigan GG, Kell DB. 2004. Metabolomics by numbers: acquiring and understanding metabolite data. *Trends in Biotechnology* **22**(5):245-252.

Green MA, Fry SC. 2005. Vitamin C degradation in plant cells via enzymatic hydrolysis of 4-*O*-oxalyl-L-threonate. *Nature* **433**:83-87.

Greenhouse SW, Geisser S. 1959. On methods in the analysis of profile data. *Psychometrika* **24**(2):95-112.

Gong Q, Li P, Ma S, Rupassara SI, Bohnert HJ. 2005. Salinity stress adaptation competence in the extremophile *Thellungiella halophila* in comparison with its relative *Arabidopsis thaliana*. *The Plant Journal* **44**:826-839.

Good P, Barring L, Giannakopoulos C, Holt T, Palutikof J. 2006. Non-linear regional relationships between climate extremes and annual mean temperatures in model projections for 1961-2099 over Europe. *Climate Research* **31**:19-34.

Guerrand D, Prud'homme MP, Boucaud J. 1996. Fructan metabolism in expanding leaves, mature leaf sheaths and mature leaf blades of *Lolium perenne*. Fructan synthesis, fructosyltransferase and invertase activities. *New Phytologist* **134**:205-214.

Guo FQ, Wang R, Crawford NM. 2002. The Arabidopsis dual-affinity nitrate transporter gene AtNRT1.1 (CHL1) is regulated by auxin in both shoots and roots. *Journal of Experimental Botany* **53**(310):835-844.

Guo W, Zhang L, Zhao J, Liao H, Zhuang C, Yan X. 2008. Identification of temporally and spatially phosphate-starvation responsive genes in *Glycine max. Plant Science* **175**(4):574-584.

Guy C, Kaplan F, Kopka J, Selbig J, Hincha DK. 2007. Metabolomics of temperature stress. *Physiologia Plantarum* **132**(2):220-235.

Guy C, Kopka J, Moritz T. 2008. Plant metabolomics coming of age. *Physiologia Plantarum* **132:**113-116.

Haake V, Cook D, Riechmann JL, Pineda O, Thomashow MF, Zhang JZ. 2002. Transcription factor CBF4 is a regulator of drought adaptation in Arabidopsis. *Plant Physiology* **130**:639-648.

Hagel JM, Weljie AM, Vogel HJ, Facchini PJ. 2008. Quantitative 1H Nuclear magnetic resonance metabolite profiling as a functional genomics platform to investigate alkaloid biosynthesis in opium poppy. *Plant Physiology* **147**:1805-1821.

Halket JM, Waterman D, Przyborowska AM, Patel RKP, Fraser PD, Bramley PM. 2005. Chemical derivatization and mass spectral libraries in metabolite profiling by GC/MS and LC/MS/MS. *Journal of Experimental Botany* **56**(410):219-243.

Halsted M, Lynch J. 1996. Phosphorus responses of C_3 and C_4 species. *Journal of Experimental Botany* **47**(297):497-505.

Hammond JP, Bennett MJ, Bowen HC, Broadley MR, Eastwood DC, May ST, Rahn C, Swarup R, Woolawat KE, White PJ. 2003. Changes in gene expression in Arabidopsis shoots during phosphate starvation and the potential for developing smart plants. *Plant Physiology* **132**:578-596.

Hammond JP, Broadley MR, White PJ. 2004. Genetic responses to phosphorus deficiency. *Annals of Botany* **94**(3):323-332.

Hammond JP, White PJ. 2008. Sucrose transport in the phloem: integrating root responses to phosphorus starvation. *Journal of Experimental Botany* **59**(1):93-109.

Hancock RD, Viola R. 2005. Biosynthesis and catabolism of L-ascorbic acid in plants. *Critical Reviews in Plant Sciences* **24**:167-188.

Hare PD, Cress WA, van Staden J. 1998. Dissecting the roles of osmolyte accumulation during stress. *Plant, Cell and Environment* **21**:535-553.

He Z, Honeycutt CW. 2005. A modified molybdenum blue method for orthophosphate determination suitable for investigating enzymatic hydrolysis of organic phosphates. *Communications in Soil Science and Plant Analysis* **36**(9-10):1373-1383.

Hellemans J, Mortier G, Paepe AD, Speleman F, Vandesompele J. 2007. qBase relative quantification framework and software for management and automated analysis of real-time quantitative PCR data. *Genome Biology* **8**(2):R19.

Hermans C. Hammond JP, White PJ, Verbruggen N. 2006. How do plants respond to nutrient shortage by biomass allocation? *Trends in Plant Sciences* **11**(12):610-617.

Hernandez G, Ramirez M, Valdes-Lopez O, Tesfaye M, Graham MA, Czechowski T, Schlereth A, Wandrey M, Erban A, Cheung F, Wu HC, Lara M, Town CD, Kopka J, Udvardi MK, Vance CP. 2007. Phosphorus stress in common bean: root transcript and metabolic responses. *Plant Physiology* **144**:752-767.

Hernandez G, Valdes-Lopez O, Ramirez M, Goffard N, Weiller G, Aparicio-Fabre R, Fuentes SI, Erban A, Kopka J, Udvardi MK, Vance CP. 2009. Global changes in the transcript and metabolic profiles during symbiotic nitrogen fixation in phosphorus-stressed common bean plants. *Plant Physiology* **151**:1221-1238.

Hirai MY, Yano M, Goodenowe DB, Kanaya S, Kimura T, Awazuhara M, Arita M, Fujiwara T, Saito K. 2004. Integration of transcriptomics and metabolomics for understanding of global responses to nutritional stresses in *Arabidopsis thaliana. Proceedings of the National Academy of Sciences* **101**(27):10205-10210.

Hoch WA, Zeldin EL, McCown BH. 2001. Physiological significance of anthocyanins during autumnal leaf senescence. *Tree Physiology* **21**(1):1-8.

Hodge A, Robinson D, Fitter A. 2000. Are microorganisms more effective than plants at competing for nitrogen? *Trends in Plant Science* **5**(7):304-308.

Hsu SY, Hsu YT, Kao CH. 2003. The effect of polyethylene glycol on proline accumulation in rice leaves. *Biologia Plantarum* **46**(1):73-78.

Huang CY, Roessner U, Eickmeier I, Genc Y, Callahan DL, Shirley N, Langridge P, Bacic A. 2008. Metabolite profiling reveals distinct changes in carbon and nitrogen metabolism in phosphate-deficient barley plants (*Hordeum vulgare* L.) *Plant Cell Physiology* **49**(5):691-703.

Humphreys MO. 2005. Genetic improvement of forage crops – past, present and future. *Journal of Agricultural Science* **143**:441-448.

Humphreys MW, Yadav RS, Cairns AJ, Turner LB, Humphreys J, Skot L. 2005. A changing climate for grassland research. *New Phytologist* **169**(1):9-26.

Ideker T, Thorsson V, Ranish JA, Christmas R, Buhler J, Eng JK, Bumgarner R, Goodlett DR, Aebersold R, Hood L. 2001. Integrated genomic and proteomic analyses of a systematically perturbed metabolic network. *Science* **292**(5518):929-934.

Jang JY, Kim DG Kim YO, Kim JS, Kang H. 2004. An expression analysis of a gene family encoding plasma membrane aquaporins in response to abiotic stresses in *Arabidopsis thaliana. Plant Molecular Biology* **54**(5):713-725.

Jang JY, Lee SH, Rhee JY, Chung GC, Ahn SJ, Kang H. 2007. Transgenic Arabidopsis and tobacco plants overexpressing an aquaporin respond differently to various abiotic stresses. *Plant Molecular Biology* **64**(6):621-632.

Jenkins H, Hardy N, Beckmann M, Draper J, Smith AR, Taylor J, Fiehn O, Goodacre R, Bino RJ, Hall R, Kopka J, Lane GA, Lange M, Liu JR, Mendes P, Nikolau BJ, Oliver SG, Paton NW, Rhee S, Roessner-Tunali U, Saito K, Smedsgaard J, Sumner LW, Wang T, Walsh S, Wurtele ES, Kell DB. A proposed framework for the description of plant metabolomics experiments and their results. *Nature Biotechnology* **22**:1601-1606

Johnson HE, Broadhurst D, Goodacre R, Smith AR. 2003. Metabolic fingerprinting of salt stressed tomatoes. *Phytochemistry* **62**(6):919-928.

Jones MM, Turner NC. 1978. Osmotic adjustment in leaves of sorghum in response to water deficits. *Plant Physiology* **61**:122-126.

Kaderbhai NN, Broadhurst DI, Ellis DI, Goodacre R, Kell DB. 2003. Functional genomics via metabolic footprinting: monitoring metabolite secretion by Escherichia coli tryptophan metabolism mutants using FT-IR and direct injection electrospray mass spectrometry. *Comparative and Functional Genomics* **4**(4):376-391.

Kaida R, Satoh Y, Bulone V, Yamada Y, Kaku T, Hayashi T, Kaneko TS. 2009. Activation of β-glucan synthases by wall-bound purple acid phosphatase in tobacco cells. *Plant Physiology* **150**:1822-1830.

Kalt W, Forney CF, Martin A, Prior RL. 1999. Antioxidant capacity, vitamin C, phenolics , and anthocyanins after fresh storage of small fruits. *Journal of Agricultural and Food Chemistry* **47**:4638-4644.

Kaplan F, Kopka J, Haskell DW, Zhao W, Schiller KC, Gatzke N, Sung DY, Guy CL. 2004. Exploring the temperature-stress metabolome of Arabidopsis. *Plant Physiology* **136**:4159-4168.

Kaplan F, Kopka J, Sung DY, Zhao W, Popp M, Porat R, Guy CL. 2007. Transcript and metabolite profiling during cold acclimation of Arabidopsis reveals an intricate relationship of cold-regulated gene expression with modifications in metabolite content. *The Plant Journal* **50**(6):967-981.

Kasuga M, Liu Q, Miura S, Yamaguchi-Shinozaki K, Shinozaki K. 1999. Improving plant drought, salt and freezing tolerance by gene transfer of a single stress-inducible transcription factor. *Nature Biotechnology* **17**:287-291.

Kaur H, Heinzel N, Schottner M, Baldwin IT, Galis I. 2010. R2R3-NaMYB8 regulates the accumulation of phenylpropanoid-polyamine conjugates, which are essential for local and systemic defense against insect herbivores in *Nicotiana atteuata. Plant Physiology* **152**:1731-1747.

Kell DB, Brown M, Davey HM, Dunn WB, Spasic I, Oliver SG. 2005. Metabolic footprinting and systems biology: the medium is the message. *Nature Reviews Microbiology* **3**:557-565.

Keurentjes JJB, Koornneef M, Vreugdenhil D.2008. Quantitative genetics in the age of omics. *Current Opinion in Plant Biology* **11**(2):123-128.

Kim SW, Min SR, Kim J, Park SK, Kim TI, Liu JR. 2009. Rapid discrimination of commercial strawberry cultivars using Fourier transform infrared spectroscopy data combined by multivariate analysis. *Plant Biotechnology Reports* **3**:87-93.

Kim H, Park SH. 2009. Metabolic profiling and discrimination of two cacti cultivated in Korea using HPLC-ESI-MS and multivariate statistical analysis. *Journal of Korean Society of Applied Biological Chemistry* **52**(4):346-352.

Koch KE. 1996. Carbohydrate-modulated gene expression in plants. *Annual Review of Plant Physiology and Plant Molecular Biology* **47**:509-540.

Kopka J, Fernie AR, Weckwerth W, Gibon, Stitt M. 2004. Metabolite profiling in plant biology: platforms and destinations. *Genome Biology* **5**(6):109.

Kopka J, Schauer N, Krueger S, Birkemeyer C, Usadel B, Bergmuller E, Dormann P, Weckwerth W, Gibon Y, Stitt M, Willmitzer L, Fernie AR, Steinhauser D. 2005. GMD@CSB.DB: The Golm metabolome database. *Bioinformatics* **21**(8):1635-1638.

Koulman A, Lane GA, Christensen MJ, Fraser K, Tapper BA. 2007. Peramine and other fungal alkaloids are exuded in the guttation fluid of endophyte-infected grasses. *Phytochemistry* **68**(3):355-360.

Krishnan P, Kruger NJ, Ratcliffe RG. 2005. Metabolite fingerprinting and profiling in plants using NMR. *Journal of Experimental Botany* **56**:255-265.

Kutchan TM. 2001. Ecological arsenal and developmental dispatcher. The Paradigm of secondary metabolism. *Plant Physiology* **125**:58-60.

Lagerwerff JV, Ogata G, Eagle HE. 1961. Control of osmotic pressure of culture solutions with polyethylene glycol. *Science* **133**(3463):1486-1487.

Lange BM, Ketchum REB, Croteau RB. 2001. Isoprenoid biosynthesis. Mteabolite profiling of peppermint oil gland secretory cells and application to herbicide target analysis. *Plant Physiology* **127**:305-314.

Lasseur B, Lothier J, Djoumad A, Coninck BD, Smeekens S, van Laere A, Moravn-Bertrand A, van den Ende W, Prud'homme MP. 2006. Molecular and functional characterization of a cDNA encoding fructan:fructan 6G-fructosyltransferase (6G-FFT)/fructan:fructan 1-fructosyltransferase (1-FFT) from perennial ryegrass (*Lolium perenne* L.). *Journal of Experimental Botany* **57**(11):2719-2734.

Last RL, Jones AD, Sachar-Hill Y. 2007. Towards the plant metabolome and beyond. *Nature Reviews Molecular Cell Biology* **8**:167-174.

Lauer MJ, Pallardy SG, Blevins DG, Randall DD. 1989. Whole leaf carbon exchange characteristics of phosphate deficient soybeans (*Glycine max* L.). *Plant Physiology* **91**:848-854.

Lay PL, Isaure MP, Sarry JE, Kuhn L, Fayard B, Bail JLL, Bastien O, Garin J, Roby C, Bourguignon J. 2006. Metabolomic, proteomic and biophysical analyses of *Arabidopsis thaliana* cells exposed to a caesium stress. Influence of potassium supply. *Biochimie* **88**:1533-1547.

Lea PJ, Azevedo RA. 2006. Nitrogen use efficiency. 1. Uptake of nitrogen from the soil. *Annals of Applied Biology* **149**:243-247.

Ledgard SF, Sprosen MS, Penno JW, Rajendram GS. 2001. Nitrogen fixation by white clover in pastures grazed by dairy cows: temporal variation and effects of nitrogen fertilization. *Plant and Soil* **229**:177-187.

Lejay L, Tillard P, Lepetit M, Olive FD, Filleur S, Daniel-Vedele F, Gojon A. 1999. Molecular and functional regulation of two NO_3^- uptake systems by N- and C- status of Arabidopsis plants. *The Plant Journal* **18**(5):509-519.

Lemaitre T, Gaufichon L, Boutet-Mercey S, Christ A, Masclaux-Daubresse C. 2008. Enzymatic and metabolic diagnostic of nitrogen deficiency in *Arabidopsis thaliana Wassileskija* Acession. *Plant Cell Physiology* **49**(7):1056-1065.

Lenz EM, Bright J, Knight R, Wilson ID, Major H. 2004. Cyclosporin A-induced changes in endogenous metabolites in rat urine: a metabonomic investigation using high field ^{1}H NMR spectroscopy, HPLC-TOF/MS and chemometrics. *Journal of Pharmaceutical and Biomedical Analysis* **35**(3):599-608.

Li Q, Eigenbrode SD, Stringam GR, Thiagarajah MR. 2000. Feeding and growth of *Plutella xylostella* and *Spodoptera eridania* on *Brassica juncea* with varying glucosinolate concentrations and myronase activities. *Journal of Chemical Ecology* **26**(10):2401-2419.

Li M, Welti R, Wang X. 2006. Quantitative profiling of Arabidopsis polar glycerolipids in response to phosphorus starvation role of phospholipases Dζ1 and Dζ2 in phosphatidylcholine hydrolysis and digalactosyldiacylglycerol accumulation in phosphorus-starved plants. *Plant Physiology* **142**:750-761.

Lian HL, Yu X, Ye Q, Ding XS, Kitagawa Y, Kwak SS, Su WA, Tang ZC. 2004. The role of aquaporin RWC3 in drought avoidance in rice. *Plant Cell Physiology* **45**(4):481-489.

Liang H, Yao N, Song JT, Luo S, Lu H, Greenberg JT. 2003. Ceramides modulate programmed cell death in plants. *Genes and Development* **17**:2636-2641.

Lindon JC, Nicholson J, Holmes E, Keun H, Craig A, Pearce J, Bruce S, Hardy N, Sansone SA, Antti H, Jonsson P, Daykin C, Navarange M, Beger R, Verheji E, Amberg A, Baunsgaard D, Cantor G, Lehmann-McKeeman L, Earll M, Wold S, Johansson E, Haselden J, Kramer K, Thomas C, Lindberg J, Schuppe-Koistinen I, Wilson I, Reily M, Robertson D, Senn H, Krotzky A, Kochhar S, Powell J, Van der Ouderaa F, Plumb R, Schaefer H, Spraul M. 2005. Summary recommendations for standardization and reporting metabolic analyses. *Nature Biotechnology* **23**:833-838.

Little DY, Rao H, Oliva S, Daniel-Vedele F, Krapp A, Malamy JE. 2005. The putative high-affinity nitrate transporter NRT2.1 represses lateral root initiation in response to nutritional cues. *Proceeding of the National Academy of Sciences* **102**(38):13693-13698.

Liu Q, Kasuga M, Sakuma Y, Abe H, Miura S, Yamaguchi-Shinozaki K, Shinozaki K. 1998. Two transcription factors, DREB1 and DREB2, with an EREBP/AP2 DNA binding domain separate two cellular signal transduction pathways in drought- and low-temperature-responsive gene expression, respectively, in Arabidopsis. *The Plant Cell* **10**:1391-1406.

Liu HL, Dai XY, Xu YY, Chong K. 2007. Over-expression of OsUGE-1 altered raffinose level and tolerance to abiotic stress but not morphology in Arabidopsis. *Journal of Plant Physiology* **164**(10):1384-1390.

Lorence A, Chevone BI, Mendes P, Nessler CL. 2004. *myo*-Inositol oxygenase offers a possible entry point into plant ascorbate biosynthesis. *Plant Physiology* **134**:1200-1205.

Lynch JP, Brown KM. 2001. Topsoil foraging – an architectural adaptation of plants to low phosphorus availability. *Plant and Soil* **237**:225-237.

Marschner H. 1995. Mineral nutrition of higher plants. Second edition. Academic Press, London.

Masclaux-Daubresse C, Daniel-Vedele F, Dechorgnat J, Chardon F, Gaufichon L, Suzuki A. 2010. Nitrogen uptake, assimilation and remobilization in plants: challenges for sustainable and productive agriculture. *Annals of Botany* in press.

Matos AR, d'Arcy-Lameta A, Franca M, Petres S, Edelman L, Kader JC, Zuily-Fodil Y, Pham-Thi AT. 2001. A novel patatin-like gene stimulated by drought stress encodes a galactolipid acyl hydrolase. *FEBS letters* **491**(3):188-192.

Matt P, Schurr U, Klein D, Krapp A, Stitt M. 1998. Growth of tobacco in short-day conditions leads to high starch, low sugars, altered diurnal changes in the *Nia* transcript and low nitrate reductase activity, and inhibition of amino acid synthesis. *Planta* **207**:27-71.

McDougall G, Martinussen I, Stewart D. 2008. Towards fruitful metabolomics: high throughput analyses of polyphenol composition in berries using direct infusion mass spectrometry. *Journal of Chromatography B* **871**(2):362-369.

McElwain L, Sweeney J. 2007. Key meteorological indicators of climate change in Ireland. Johnstown Castle: Wexford, Environmental Protection Agency.

Meijer HJG, Munnik T. 2003. Phospholipid-based signalling in plants. *Annual Review of Plant Biology* **54**:265-306.

Meng PH, Raynaud C, Tcherkez G, Blanchet S, Massoud K, Domenichini S, Henry Y, Soubigou-Taconnat L, Lelarge-Trouverie C, Saindrenan P, Renou JP, Bergounioux C. 2009. Crosstalks between myo-inositol metabolism, programmed cell death and basal immunity in Arabidopsis. *PLoS ONE* **4**(10):e7364

Mercke P, Kappers IF, Verstappen FWA, Vorst O, Dicke M, Bouwmeester HJ. 2004. Combined transcript and metabolite analysis reveals genes involved in spider mite induced volatile formation in cucumber plants. *Plant Physiology* **135**:2012-2024.

Messenguy F, Dubois E. 2003. Role of MADS box proteins and their cofactors in combinatorial control of gene expression and cell development. *Gene* **316**:1-21.

Michelet L, Zaffagnini M, Marchand C, Collin V, Decottignies, Tsan P, Lancelin JM, Trost P, Miginiac-Maslow M, Noctor G, Lemaire SD. 2005. Glutathionylation of chloroplast thioredoxin f is a redox signalling mechanism in plants. *Proceedings of the National Academy of Sciences* **102**(45):16478-16483.

Misson J, Raghothama KG, Jain A, Jouhet J, Block MA, Bligny R, Ortet P, Creff A, Somerville S, Rolland N, Doumas P, Nacry P, Herrerra-Estrella L, Nussaume L, Thibaud MC. 2005. A genome-wide transcriptional analysis using *Arabidopsis thaliana* affymetrix gene chips determined plant responses to phosphate deprivation. *Proceedings of the National Academy of Sciences* **102**(33):11934-11939.

Mittler R. 2002. Oxidative stress, antioxidants and stress tolerance. *Trends in Plant Science* **7**(9):405-410.

Moll RH, Kamprath EJ, Jackson WA. 1987. Development of nitrogen efficient prolific hybrids of maize. *Crop Science* **27**:181-186.

Molina I, Li-Beisson Y, Beisson F, Ohlrogge JB, Pollard M. 2009. Identification of an Arabidopsis feruloyl-Coenzyme A transferase required for suberin synthesis. *Plant Physiology* **151**:1317-1328.

Monteiro de Paula F, Pham-Thi AT, Zuily-Fodil Y, Ferrari-Iliou R, Vieira da Silva J, Mzliak P. 1993. Effects of water stress on the biosynthesis and degradation of polyunsaturated lipid molecular species in leaves of *Vigna unguiculata*. *Plant Physiology and Biochemistry* **31**(5):707-715.

Monton MRN, Soga T. 2007. Metabolome analysis by capillary electrophoresis-mass spectrometry. *Journal of Chromatography A* **1168**(1-2):237-246.

Muller R, Morant M, Jarmer H, Nilsson L, Nielsen TH. 2007. Genome-wide analysis of the Arabidopsis leaf transcriptome reveals interaction of phosphate and sugar metabolism. *Plant Physiology* **143**:156-171.

Munne-Bosch S, Penuelas J. 2003. Photo- and oxidative protection, and a role for salicylic acid during drought and recovery in field-grown *Phillyrea angustifolia* plants. *Planta* **217**:758-766.

Mylona P, Pawlowski K, Bisseling T. 1995. Symbiotic nitrogen fixation. *The Plant Cell* **7**:869-885.

Nadas E, Balogh A, Kiss F, Szente K, Nagy Z, Martinez-Carrasco R, Tuba Z. 2008. Role of fructose-1,6-biphosphatase, fructose phosphotransferase, and phosphofructokinase in saccharide metabolism of four C_3 grassland species under elevated CO_2. *Photosynthetica* **46**(2):255-261.

Nakashima K, Ito Y, Yamaguchi-Shinozaki K. 2009. Transcriptional regulatory networks in response to abiotic stresses in Arabidopsis and grasses. *Plant Physiology* **149**:88-95.

Nasholm T, Ekblad A, Nordin A, Giesler R, Hogberg M, Hogberg P. 1998. Boreal forest plants take up organic nitrogen. *Nature* **392**:914-916.

Nielsen J, Oliver SG. 2005. The next wave in metabolome analysis. *Trends in Biotechnology* **23**(11):544-546.

Nishizawa A, Yabute Y, Shigeoka S. 2008. Galactinol and raffinose constitute a novel function to protect plants from oxidative damage. *Plant Physiology* **147**:1251-1263.

Noctor G, Foyer CH. 1998. Ascorbate and glutathione: Keeping active oxygen under control. *Annual Review of Plant Physiology and Plant Molecular Biology* **49**:249-279.

Oikawa A, Nakamura Y, Ogura T, Kimura A, Suzuki H, Sakurai N, Shinbo Y, Shibata D, Kanaya S, Ohta D. 2006. Clarification of pathway-specific inhibition by Fourier transform ion cyclotron resonance/mass spectrometry-based metabolic phenotyping studies. *Plant Physiology* **142**:398-413.

Oliver SG, Winson MK, Kell DB, Baganz F. 1998. Systematic functional analysis of the yeast genome. *Trends in Biotechnology* **16:**373-378.

Opitz S, Kunert G, Gershenzon J. 2008. Increased terpenoid accumulation in cotton (*Gossypium Hirsitum*) foliage is a general wound response. *Journal of Chemical Ecology* **34**(4):508-522.

Parent B, Hachez C, Redondo E, Simonneau T, Chaumont F, Tardieu F. 2009. Drought and abscisic acid effects on aquaporin content translate into changes in hydraulic conductivity and leaf growth rate: a trans-scale approach. *Plant Physiology* **149**:2000-2012.

Pata MO, Hannun YA, Ng CKY. 2009. Plant sphingolipids:decoding the enigma of the sphinx. *New Phytologist* **185**:611-630.

Paul MJ, Driscoll SP. 1997. Sugar repression of photosynthesis: the role of carbohydrates in signalling nitrogen deficiency through source:sink imbalance. *Plant, Cell and Environment* **20**:110-116.

Pavis N, Chatterton NJ, Harrison PA, Baumgartner S, Praznik W, Boucaud J, Prud'homme MP. 2001. Structure of fructans in roots and leaf tissues of *Lolium perenne*. *New Phytologist* **150**(1):83-95.

Peng M, Hudson D, Schofield A, Tsao R, Yang R, Gu H, Bi YM, Rothstein SJ. 2008. Adaptation of Arabidopsis to nitrogen limitation involves induction of anthocyanin synthesis which is controlled by the NLA gene. *Journal of Experimental Botany* **59**(11):2933-2944.

Petersen K, Didion T, Andersen CH, Nielsen KK. 2004. MADS-box genes from perennial ryegrass differentially expressed during transition from vegetative to reproductive growth. *Journal of Plant Physiology* **161**(4):439-447.

Pfaffl MW, Horgan GW, Dempfle L. 2002. Relative expression software tool (REST(c)) for group-wise comparison and statistical analysis of relative expression results in real-time PCR. *Nucleic Acids Research* **30**:e36.

Pilon-Smits EAH, Ebskamp MJM, Paul MJ, Jeuken MJW, Weisbeek PJ, Smeekens SCM. 1995. Improved performance of transgenic fructan-accumulating tobacco under drought stress. *Plant Physiology* **107**:125-130.

Plaxton WC. 2004. Plant response to stress: biochemical adaptations to phosphate deficiency. *Encyclopedia of Plant and Crop Science* pp. 976-980. Marcel Dekker, Inc., New York, USA.

Podmore ID, Griffiths HR, Herbert KE, Mistry N, Mistry P, Lunec J. 1998. Vitamin C exhibits pro-oxidant properties. *Nature* **392**:559.

Pollard M, Beisson F, Li Y, Ohlrogge JB. 2008. Building lipid barriers: biosynthesis of cutin and suberin. *Trends in Plant Science* **13**(5):236-246.

Raamsdonk LM, Teusink B, Broadhurst D, Zhang N, Hayes A, Walsh MC, Berden JA, Brindle KM, Kell DB, Rowland JJ, Westerhoff HV, van Dam K, Oliver SG. 2001. A functional genomics strategy that uses metabolome data to reveal the phenotype of silent mutations. *Nature Biotechnology* **19**:45-50.

Raghothama KG. 1999. Phosphate acquisition. *Annual Review of Plant Physiology and Plant Molecular Biology* **50**:665-693.

Rasmussen S, Parsons AJ, Fraser K, Xue H, Newman JA. 2008. Metabolic profiles of *Lolium perenne* are differentially affected by nitrogen supply, carbohydrate content and fungal endophyte infection. *Plant Physiology* **146**:1440-1453.

Ratcliffe RG. 1997. *In vivo* NMR studies of the metabolic response of plant tissues to anoxia. *Annals of Botany* **79**:39-48.

Reymond P, Weber H, Damond M, Farmer EE. 2000. Differential gene expression in response to mechanical wounding and insect feeding in Arabidopsis. *Plant Cell* **12**:707-720.

Rhizky L, Liang H, Shuman J, Shulaev V, Davletova S, Mittler R. 2004. When defense pathways collide. The response of Arabidopsis to a combination of drought and heat stress. *Plant Physiology* **134**(4):1683-1696.

Richardson AE, Hocking PJ, Simpson RJ, George TS. 2009. Plant mechanisms to optimise access to soil phosphorus. *Crop and Pasture Science* **60**:124-143.

Robert HS, Friml J. 2009. Auxin and other signals on the move in plants. *Nature Chemical Biology* **5**(5):325-332.

Rodriguez D, Keltjens WG, Goudriaan J. 1998. Plant leaf area expansion and assimilate production in wheat (*Triticum aestivum* L.) growing under low phosphorus conditions. *Plant and Soil* **200**:227-240.

Roessner U, Patterson JH, Forbes MG, Fincher GB, Langridge P, Bacic A. 2006. An investigation of boron toxicity in barley using metabolomics. *Plant Physiology* **142**:1087-1101.

Roudier F, Gissot L, Beaudoin F, Haslam R, Michaelson L, Marion J, Molino D, Lima A, Bach L, Morin H, Tellier F, Palauqui JC, Bellec Y, Renne C, Miquel M, DaCosta M, Vignard J, Rochat C, Markham JE, Moreau P, Napier J, Faure JD. 2010. Very-long-chain fatty acids are involved in polar auxin transport and developmental patterning in Arabidopsis. *The Plant Cell* **22**:364-375.

Saito S, Soga T, Nishioka T, Tomita M. 2004. Simultaneous determination of the main metabolites in rice leaves using capillary electrophoresis mass spectrometry and capillary electrophoresis diode array detection. *The Plant Journal* **40:**151-163.

Sakuma Y, Maruyama K, Osakabe Y, Qin F, Seki M, Shinozaki K, Yamaguchi-Shinozaki K. 2006. Functional analysis of an Arabidopsis transcription factor, DREB2A, involved in drought responsive gene expression. *The Plant Cell* **18**:1292-1309.

Sanchez DH, Siahpoosh MR, Roessner U, Udvardi M, Kopka J. 2007. Plant metabolomics reveals conserved and divergent metabolic responses to salinity. *Physiologia Plantarum* **132**(2):209-219,

Sattelmacher B, Gerendas J, Thoms K, Bruck H, Bagdady NH. 1993. Interaction between root growth and mineral nutrition. *Environmental and Experimental Botany* **33**(1):63-73.

Schaller H. 2003. The role of sterols in plant growth and development. *Progress in Lipid Research* **42**:163-175.

Schauer N, Semel Y, Roessner U, Gur A, Balbo I, Carrari F, Pleban T, Perez-Melis A, Bruedigam C, Kopka J, Willmitzer L, Zamir D, Fernie AR. 2006. Comprehensive metabolic profiling and phenotyping of interspecific introgression lines for tomato improvement. *Nature Biotechnology* **24**:447-454.

Scheible WR, Lauerer M, Schulze ED, Caboche M, Stitt M. 1997. Accumulation of nitrate in the shoot acts as a signal to regulate shoot-root allocation in tobacco. *The Plant Journal* **11**(4):671-691.

Scheible WR, Pauly M. 2004. Glycosyltransferases and cell wall biosynthesis: novel players and insights. *Current Opinion in Plant Biology* **7**(3):285-295.

Scheible WR, Morcuende R, Czechowski T, Fritz C, Osuna D, Palacios-Rojas N, Schindelasch D, Thimm O, Udvardi MK, Stitt M. 2004. Genome-wide reprogramming of primary and secondary metabolism, protein synthesis, cellular growth processes, and the regulatory infrastructure of Arabidopsis in response to nitrogen. *Plant Physiology* **136**:2483-2499.

Schreiber L, Franke R, Hartmann K. 2005. Effects of NO_3 deficiency and NaCl stress on suberin deposition in rhizo- and hypodermal (RHCW) and endodermal cell walls (ECW) of castor bean (*Ricinus communis* L.) roots. *Plant and Soil* **269**:333-339.

Schurmann P, Jacquot JP. 2000. Plant thioredoxin systems revisited. *Annual Review of Plant Physiology and Plant Molecular Biology* **51**:371-400.

Seki M, Narusaka M, Ishida J, Najo T, Fujita M, Oono Y, Kamiya A, Nakajima M, Enju A, Sakurai T, Satou M, Akiyama K, Taji T, Yamaguchi-Shinozaki K, Carninci P, Kawai J, Hayashizaki Y, Shinozaki K. 2002. Monitoring the expression profiles of 7000 Arabidopsis genes under drought, cold and high-salinity stresses using a full-length cDNA microarray. *The Plant Journal* **31**(3):279-292.

Seki M, Umezawa T, Urano K, Shinozaki K. 2007. Regulatory metabolic networks in drought stress responses. *Current Opinion in Biology* **10**(3):296-302.

Semel Y, Schauer N, Roessner U, Zamir D, Fernie AR. 2007. Metabolite analysis for the comparison of irrigated and non-irrigated field grown tomato of varying genotype. *Metabolomics* **3**(3):289-295.

Shah J. 2005. Lipids, lipases, and lipid-modifying enzymes in plant disease resistance. *Annual Review of Phytopathology* **43**:229-260.

Shen W, Wei Y, Dauk M, Tan Y, Taylor DC, Selvaraj G, Zou J. 2006. Involvement of a glycerol-3-phosphate dehydrogenase in modulating the NADH/$NADH^+$ ratio provides evidence of a mitochondrial glycerol-3-phosphate shuttle in Arabidopsis. *The Plant Cell* **18**:422-441.

Shi WM, Muramoto Y, Ueda A, Takabe T. 2001. Cloning of peroxisomal ascorbate peroxidase gene from barley and enhanced thermotolerance by overexpressing in *Arabidopsis thaliana. Gene* **273**(1):23-27.

Shih CY, Kao CH. 1996. Growth inhibition in suspension-cultured rice cells under phosphate deprivation is mediated through putrescine accumulation. *Plant Physiology* **111**(3):721-724.

Shin R, Berg RH, Schachtman DP. 2005. Reactive oxygen species and root hairs in Arabidopsis root response to nitrogen, phosphorus and potassium deficiency. *Plant and Cell Physiology* **46**(8):1350-1357.

Shinano T, Nanamori M, Dohi M, Wasaki J, Osaki M. 2005. Evaluation of phosphorus starvation inducible genes relating to efficient phosphorus utilization in rice. *Plant and Soil* **269**(1-2):81-87.

Shinozaki K, Yamaguchi-Shinozaki K, Seki M. 2003. Regulatory network of gene expression in the drought and cold stress responses. *Current Opinion in Plant Biology* **6**(5):410-417.

Shinozaki K, Yamaguchi-Shinozaki K. 2007. Gene networks involved in drought stress response and tolerance. *Journal of Experimental Botany* **58**(2):221-227.

Shore P, Sharrocks AD. 1995. The MADS-box family of transcription factors. *European Journal of Biochemistry* **229**(1):1-13.

Shulaev V. 2006. Metabolomics technology and bioinformatics. *Briefings in Bioinformatics* **7**(2):128-139.

Shulaev V, Cortes D, Miller G, Mittler R. 2008. Metabolomics for plant stress response. *Physiologia Plantarum* **132:**199-208.

Shutzendubel A, Polle A. 2002. Plant responses to abiotic stresses: heavy metal-induced oxidative stress and protection by mycorrhization. *Journal of Experimental Botany* **53**(372):1351-1365.

Slama I, Ghnaya T, Hessini K, Messedi D, Savoure A, Abdelly C. 2007. Comparative study of the effects of mannitol and PEG osmotic stress on growth and solute accumulation in *Sesuvium portulacastrum. Environmental and Experimental Botany* **61**(1):10-17.

Smith AM, Stitt M. 2007. Coordination of carbon supply and plant growth. *Plant, Cell and Environment* **30**:1126-1149.

Sprenger N, Schellenbaum L, van Dun K, Boller T, Wiemken A. 1997. Fructan synthesis in transgenic tobacco and chicory plants expressing barley sucrose:fructan 6-fructosyl transferase. *FEBS letters* **400**(3):355-358.

Stewart D, McDougall GJ, Sungurtas J, Verrall S, Graham J, Martinussen I. 2007. Metabolomic approach to identifying bioactive compounds in berries: advances towards fruit nutritional enhancement. *Molecular Nutrition and Food Research* **51**(6):645-651.

Strehmel N, Praeger U, Konig C, Fehrle I, Erban A, Geyer M, Kopka J, van Dongen JT. 2010. Time course effects on primary metabolism of potato (*Solanum tuberosum*) tuber tissue after mechanical impact. *Postharvest Biology and Technology* **56**:109-116.

Stitt M. 1999. Nitrate regulation of metabolism and growth. *Current Opinion in Plant Biology* **2**(3):178-186.

Stryer L. 1995. Biochemistry – Fourth edition. WH Freeman &Co. New York. pp. 493-495.

Taji T, Ohsumi C, Iuchi S, Seki M, Kasuga M, Kobayashi M, Yamaguchi-Shinozaki K, Shinozaki K. 2002. Important roles of drought- and cold-inducible genes for galactinol synthase in stress tolerance in *Arabidopsis thaliana. The Plant Journal* **29**(4):417-426.

Tan X, Calderon-Villalobos LIA, Sharon M, Zheng C, Robinson CV, Estelle M, Zheng N. 2007. Mechanism of auxin perception by the TIR1 ubiquitin ligase. *Nature* **446**:640-645.

Taylor CF, Paton NW, Garwood KL, Kirby PD, Stead DA, Yin Z, Deutsch EW, Selway L, Walker J, Riba-Garcia I, Mohammed S, Deery MJ, Howard JA, Dunkley T, Aebersold R, Kell DB, Lilley KS, Roepstorff P, Yates JR, Brass A, Brown AJP, Cash P, Gaskell SJ, Hubbard SJ, Oliver SG. 2003. A systematic approach to modelling, capturing, and dissemination proteomics experimental data. *Nature Biotechnology* **21**:247-254.

Theissen G, Becker A, Rosa AD, Kanno A, Kim JT, Munster T, Winter KU, Saedler H. 2000. A short history of MADS-box genes in plants. *Plant Molecular Biology* **42**:115-149.

Theodorou ME, Cornel FA, Duff SMG, Plaxton WC. 1992. Phosphate starvation inducible synthesis of the α-subunit of the pyrophosphate-dependent phosphofructokinase in black mustard suspension cells. *The Journal of Biological Chemistry* **267**(30):21901-21905.

Theodorou ME, Plaxton WC. 1993. Metabolic adaptations of plant respiration to nutritional phosphate deprivation. *Plant Physiology* **101**(2):339-344.

Thomas H. 1991. Accumulation and consumption of solutes in swards of *Lolium perenne* during drought and after rewatering. *New Phytologist* **118**:35-48.

Thornton B, Osborne SM, Paterson E, Cash P. 2007. A proteomic and targeted metabolomic approach to investigate change in *Lolium perenne* roots when challenged with glycine. *Journal of Experimental Botany* **58**(7):1581-1590.

Ticconi CA, Delatorre CA, Lahner B, Salt DE, Abel S. 2004. Arabidopsis *pdr2* reveals a phosphate-sensitive checkpoint in root development. *The Plant Journal* **37**:801-814.

Tierens KFMJ, Thomma BPHJ, Brouwer M, Schmidt J, Kistner K, Porzel A, Mauch-Mani B, Cammue BPA, Broekaert WF. 2001. Study of the role of antimicrobial glucosinolate-derived isothiocyanates in resistance of Arabidopsis to microbial pathogens. *Plant Physiology* **125**:1688-1699.

Timerbaev AR. 2009. Capillary electrophoresis coupled to mass spectrometry for biospeciation analysis: critical evaluation. *Trends in Analytical Chemistry* **28**(4):416-425.

Tomscha JL, Trull MC, Deikman J, Lynch JP, Guiltinan MJ. 2004. Phosphatase under-producer mutants have altered phosphorus relations. *Plant Physiology* **135**:334-345.

Townley HE, McDonald K, Jenkins GI, Knight MR, Leaver CJ. 2005. Ceramides induce programmed cell death in Arabidopsis cells in a calcium-dependent manner. *Biological Chemistry* **386**(2):161-166.

Trenkamp S, Martin W, Tietjen K. 2004. Specific and differential inhibition of very-long-chain fatty acid elongases from *Arabidopsis thaliana* by different herbicides. *Proceedings of the National Academy of Sciences* **101**(32):11903-11908.

Trethewey RN, Krotzky AJ, Willmitzer L. 1999. Metabolic profiling: a rosetta stone for genomics. *Current Opinion in Plant Biology* **2:**83-85.

Troufflard S, Roscher A, Thomasset B, Barbotin JN, Rawsthorne S, Portais JC. 2007. *In vivo* ^{13}C NMR determines metabolic fluxes and steady state in linseed embryos. *Phytochemistry* **68**:2341-2350.

Trull MC, Guiltinan MJ, Lynch JP, Deikamn J. 1997. The responses of wild-type and ABA mutant *Arabidopsis thaliana* plants to phosphorus starvation.*Plant, Cell and Environment* **20**:85-92.

Turner LB, Cairns AJ, Armstead IP, Thomas H, Humphreys MW, Humphreys MO. 2008. Does fructan have a functional role in physiological traits? Investigation by quantitative trait locus mapping. *New Phytologist* **179**(3):765-775.

Uhde-Stone C, Gilbert G, Johnson JMF, Litjens R, Zinn KE, Temple SJ, Vance CP, Allan DL. 2003. Acclimation of white lupin to phosphorus deficiency involves enhanced expression of genes related to organic acid metabolism. *Plant and Soil* **248**(1-2):99-116.

Urbanczyk-Wochniak E, Fernie AR. 2005. Metabolic profiling reveals altered nitrogen nutrient regimes have diverse effects on the metabolism of hydroponically-grown tomato (*Solanum lycopersicum*) plants. *Journal of Experimental Botany* **56**(410):309-321.

Valliyodan B, Nguyen HT. 2006. Understanding regulatory networks and engineering for enhanced drought tolerance in plants. *Current Opinion in Plant Biology* **9**:189-195.

Vance CP, Uhde-Stone C, Allan DL. 2003. Phosphorus acquisition and use: critical adaptations by plants for securing a non-renewable resource. *New Phytologist* **157**:423-447.

Vasquez-Flota F, Carillo-Pech M, Minero-Garcia Y, Miranda-Ham ML. 2004. Alkaloid metabolism in wounded *Catharanthus roseus* seedlings. *Plant Physiology and Biochemistry* **42**(7-8):623-628.

Verslues PE, Bray EA. 2004. LWR1 and LWR2 are required for osmoregulation and osmotic adjustment in Arabidopsis. *Plant Physiology* **136**:2831-2842.

Vinocur B, Altman A. 2005. Recent advances in engineering plant tolerance to abiotic stress: achievements and limitations. *Current Opinion in Biotechnology* **16**(2):123-132.

Walch-Liu P, Ivanov II, Filleur S, Gan Y, Remans T, Forde BG. 2006. Nitrogen regulation of root branching. *Annals of Botany* **97**:875-881.

Wallace RJ. 2004. Antimicrobial properties of plant secondary metabolites. *Proceedings of the Nutrition Society* **63**:621-629.

Wang J, Zhang H, Allen RD. 1999. Overexpression of an Arabidopsis peroxisomal ascorbate peroxidase gene in tobacco increases protection against oxidative stress. *Plant and Cell Physiology* **40**(7):725-732.

Wang SY, Lin HS. 2003. Compost as a soil supplement increases the level of antioxidant compounds and oxygen radical absorbance capacity in strawberries. *Journal of Agricultural and Food Chemistry* **51**:6844-6850.

Wang Y, Ribot C, Rezzonico E, Poirier Y, 2004. Structure and expression profile of the Arabidopsis PHO1 gene family indicates a broad role in inorganic phosphate homeostasis. *Plant Physiology* **135**:400-411.

Wang H, Siopongco J, Wade LJ, Yamauchi A. 2009a. Fractal analysis on root systems of rice plants in response to drought stress. *Environmental and Experimental Botany* **65**:338-344.

Wang X, Wang Y, Tian J, Lim BL, Yan X, Liao H. 2009b. Overexpressing *AtPAP15* enhances phosphorus efficiency in soybean. *Plant Physiology* **151**:233-240.

Ward JL, Harris C, Lewis J, Beale MH. 2003. Assessment of ^{1}H NMR spectroscopy and multivariate analysis as a technique for metabolite fingerprinting of *Arabidopsis thaliana. Phytochemistry* **62**(6):949-957.

Wasaki J, Yonetani R, Kuroda S, Shinano T, Yazaki J, Fuji F, Shimbo K, Yamamoto K, Sakata K, Sasaki T, Kishimoto N, Kikuchi S, Yamagishi M, Osaki M. 2003. Transcriptomic analysis of metabolic changes by phosphorus stress in rice plant roots. *Plant, Cell and Environment* **26**(9):1515-1523.

Wasaki J, Shinano T, Onishi K, Yonetani R, Yazaki J, Fujii F, Shimbo K, Ishikawa M, Shimatani Z, Nagata Y, Hashimoto A, Ohta T, Sato Y, Miyamoto C, Honda S, Kojima K, Sasaki T, Kishimoto N, Kikuchi S, Osaki M. 2006. Transcriptomic analysis indicates putative metabolic changes caused by manipulation of phosphorus availability in rice leaves. *Journal of Experimental Botany* **57**(9):2049-2059.

Wassen MJ, Venterink HO, Lapshina ED, Tanneberger F. 2005. Endangered plants persist under phosphorus limitation. *Nature* **437**:547-550.

Weckwerth W, Loureiro ME, Wenzel K, Fiehn O. 2004a. Differential metabolic networks unravel the effects of silent plant phenotypes. *Proceedings of the National Academy of Sciences* **101**(20):7809-7814.

Wilkins PW, Humphreys MO. 2003. Progress in breeding perennial forage grasses for temperate agriculture. *Journal of Agricultural Science* **140**(2):129-150.

Wishart DS, Tzur D, Knox C, Eisner R, Guo AC, Young N, Cheng D, Jewell K, Arndt D, Sawhney S, Fung C, Nikolai L, Lewis M, Coutouly MA, Forsythe I, Tang P, Shrivastava S, Jeroncic K, Stothard P, Amegbey G, Block D, Hau DD, Wagner J, Miniaci J, Clements M, Gebremedhin M, Guo N, Zhang Y, Duggan GE, MacInnis GD, Weljie AM, Dowlatabadi R, Bamforth F, Clive D, Greiner R, Li L, Marrie T, Sykes BD, Vogel HJ, Querengesser L. 2007. HMDB: the human metabolome database. *Nucleic Acids Research* **35**:521-526.

Wissuwa M, Gamat G, Ismail A. 2005. Is root growth under phosphorus deficiency affected by source or sink limitations. *Journal of Experimental Botany* **56**(417):1943-1950.

Wittstock U, Kliebenstein DJ, Lambrix V, Reichelt M, Gershenzon J. 2003. Glucosinolate hydrolysis and its impact on generalist and specialist insect herbivores. *Recent Advances in Phytochemistry* **37**:101-125.

Wu P, Ma L, Hou X, Wang M, Wu Y, Liu F, Deng XW. 2003. Phosphate starvation triggers distinct alterations of genome expression in Arabidopsis roots and leaves. *Plant Physiology* **132**:1260-1271.

Wu X, Kishitani S, Ito Y, Toriyama K. 2009. Accumulation of raffinose in rice seedlings overexpressing OsWRKY11 in relation to dessication tolerance. *Plant Biotechnology* **26**:431-434.

Yang YH, Dudoit S, Luu P, Lin DM, Peng V, Ngai J, Speed TP. 2002. Normalization for cDNA microarray data: a robust composite method addressing single and multiple slide systematic variation. *Nucleic Acids Research* **30**:e15.

Yang J, Xu G, Hong Q, Liebich HM, Lutz K, Schmulling RM, Wahl HG. 2004. Discrimination of type 2 diabetic patients from healthy controls by using metabonomics method based on their serum fatty acid profiles. *Journal of Chromatography B* **813**(1-2):53-58.

Yu B, Xu C, Benning C. 2002. Arabidopsis disrupted in *SQD2* encoding sulfolipid synthase is impaired in phosphate-limited growth. *Proceedings of the National Academy of Sciences* **99**(8):5732-5737.

Yuan L, Loque D, Kojima S, Rauch S, Ishiyama K, Inoue E, Takahashi H, von Wiren N. 2007. The organization of high-affinity ammonium uptake in Arabidopsis

roots depends on the spatial arrangement and biochemical properties of AMT1-type transporters. *The Plant Cell* **19**:2936-2652.

Zhang FS, Ma J, Cao YP. 1997. Phosphorus deficiency enhances root exudation of low-molecular weight organic acids and utilization of sparingly soluble inorganic phosphates by radish (*Raghanus satiuvs* L.) and rape (*Brassica napus* L.) plants. *Plant and Soil* **196**(2):261-264.

Zhang H, Forde BG. 1998. An Arabidopsis MDS box gene that controls nutrient-induced changes in root architecture. *Science* **279**:407-409.

Zhang H, Jennings A, Barlow PW, Forde BG. 1999. Dual pathways for regulation of root branching by nitrate. *Proceedings of the National Academy of Sciences* **96**:6529-6534.

Zhang H, Forde BG. 2000. Regulation of Arabidopsis root development by nitrate availability. *Journal of Experimental Botany* **51**(342):51-59.

Zhang P, Foerster H, Tissier CP, Mueller L, Paley S, Karp PD, Rhee SY. 2005. Metacyc and Aracyc. Metabolic pathway databases for plant research. *Plant Physiology* **138**:27-37.

Zheng H, Rowland O, Kunst L. 2005. Disruptions of the Arabidopsis Enoyl-CoA reductase gene reveal an essential role for very-long-chain fatty acid synthesis in cell expansion during plant morphogenesis. *The Plant Cell* **17**:1467-1481.

Zheng J, Zhao J, Zhang J, Fu J, Gou M, Dong Z, Hou W, Huang Q, Wang G. 2006. Comparative expression profiles of maize genes from a water stress-specific cDNA macroarray in response to high-salinity, cold or abscisic acid. *Plant Science* **170**(6):1125-1132.

Zhou J, Wang X, Jiao Y, Qin Y, Liu X, He K, Chen C, Ma L, Wang J, Xiong L, Zhang Q, Fan L, Deng XW. 2007. Global genome expression analysis of rice in response to drought and high-salinity stresses in shoot, flag leaf, and panicle. *Plant Molecular Biology* **63**(5):591-608.

Zywicki B, Catchpole G, Draper, Fiehn, O. 2005. Comparison of rapid liquid chromatography-electrospray ionization-tandem mass spectrometry methods for determination of glycoalkaloids in transgenic field-grown potatoes. *Analytical Biochemistry* **336**(2):178-186.

Appendices

Appendix A

Metabolomics Quality control for PEG-induced water-limitation

Solanum tuberosum (variety 'Desiree') tubers and blank samples were extracted and processed simultaneously with *L. perenne* samples as described previously. Multivariate analysis was performed in both polar and non-polar extracts to check for any abnormalities and the principal component analysis (PCA) revealed that *S. tuberosum* tuber samples and the blank segregated from the *L. perenne* dataset (Figures A1 and A2). The reference samples did not reveal significant changes throughout the sequence of injections suggesting that the GC-MS remained stable throughout the analysis process. Further PCA plots were analyzed, and revealed that no pattern related to the technical replicates (Figure A3).

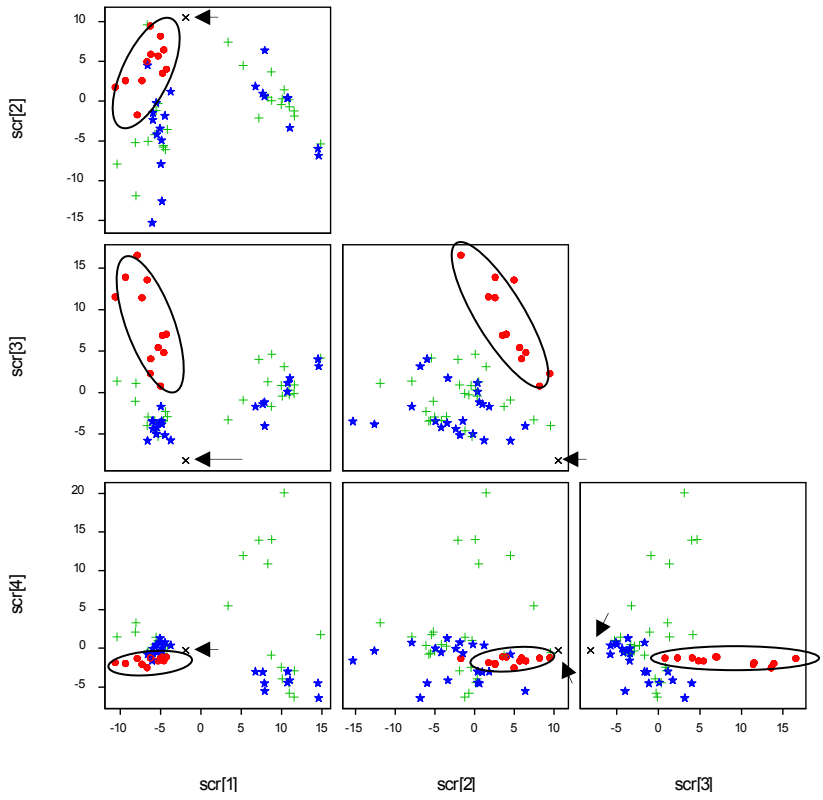

Figure A.1 – Representation of the PCA plots for the first four principal components of the non-polar mass peaks detected in the samples, reference samples and blank injection following GC-MS analysis. ● – Desiree potato reference; × - Blank ; + - Cashel; ★- PI462336.

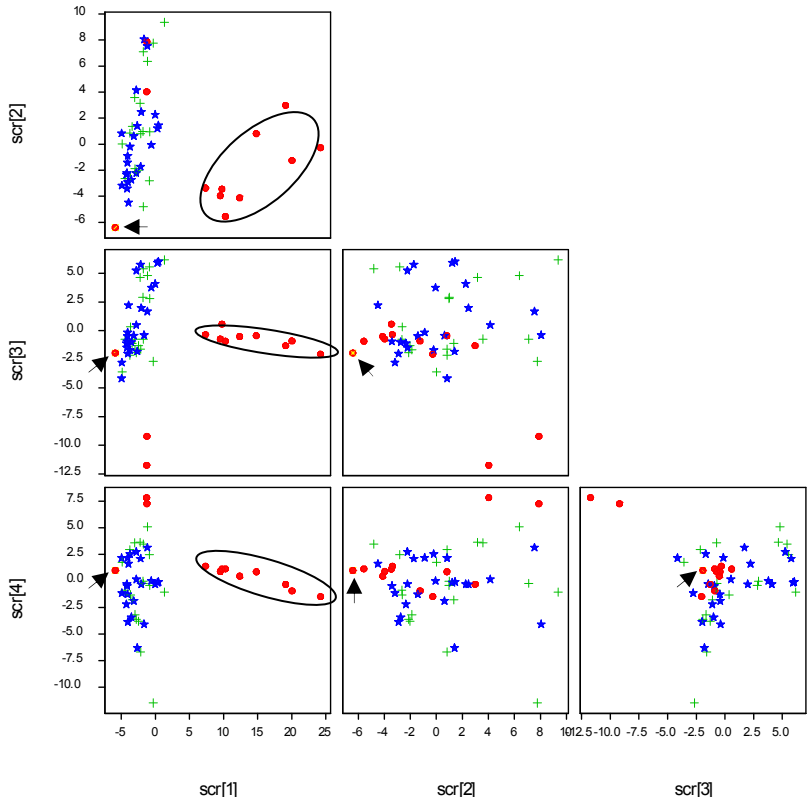

Figure A.2 - A plot representing PCA plots for the first four principal components of the polar mass peaks detected in the samples, reference samples and blank injections following GC-MS analysis. ● – Desiree potato reference; × - Blank ; + - Cashel; ★- PI462336 (note that one of the Desiree sample is overlapping the blank).

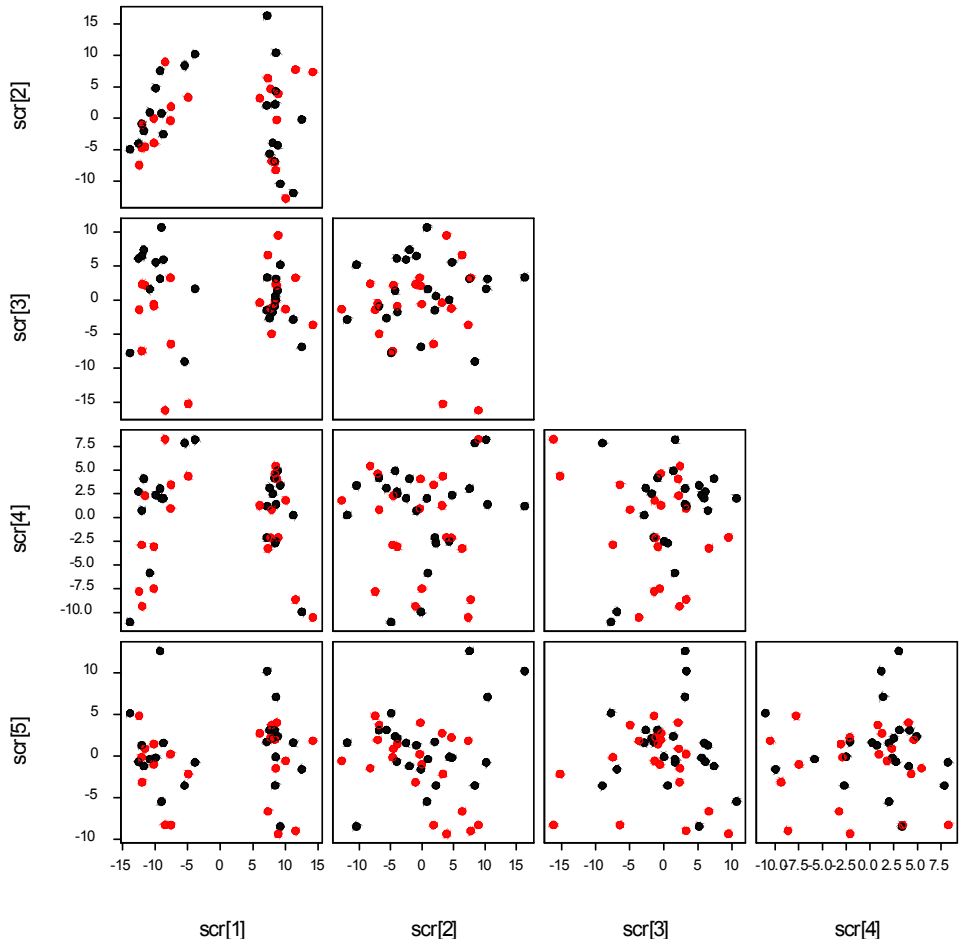

Figure A.3 - A plot representing PCA plots for the first five principal components of the polar mass peaks detected in the samples following GC-MS analysis. ● – first injection; ● – second injection.

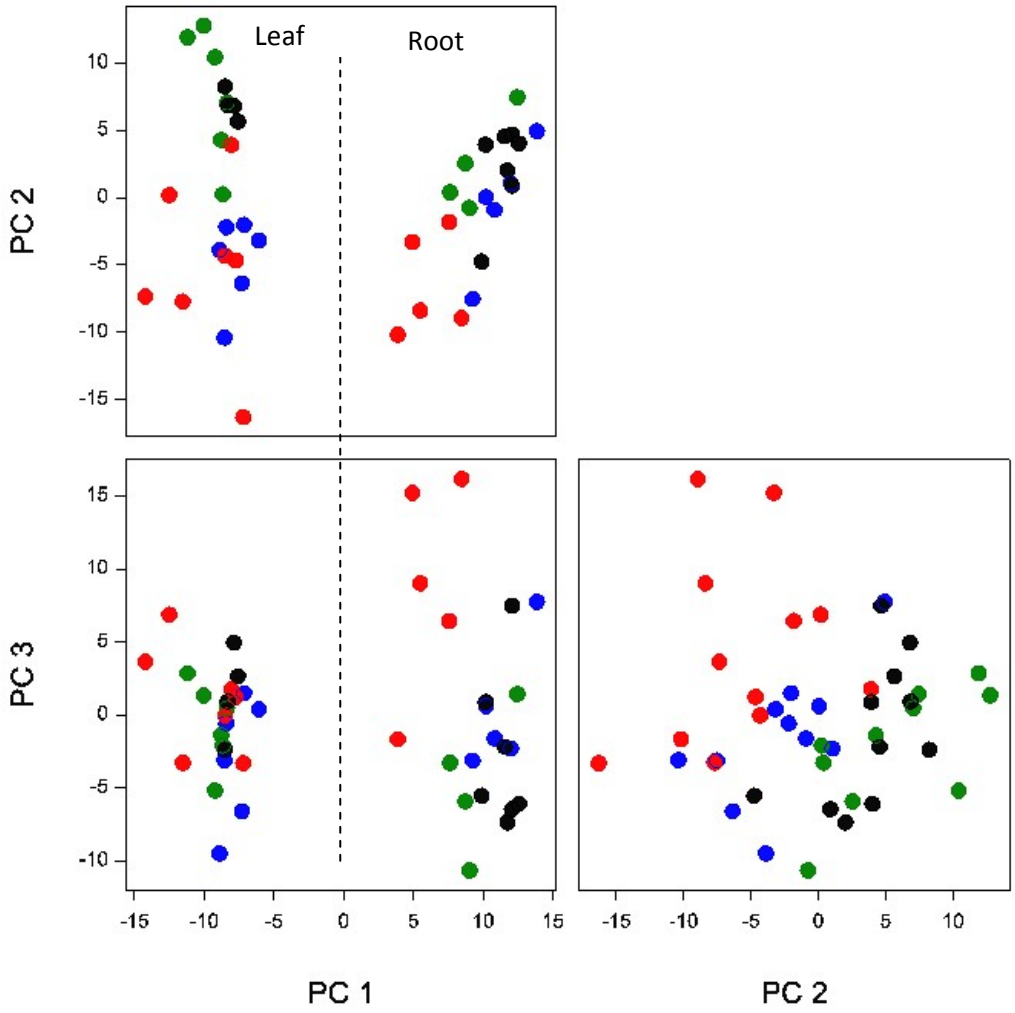

Figure A.4- Principal component analysis (PCA) plot of all metabolite compounds found, following GC-TOF-MS analysis of the root and leaf tissues of Cashel and PI 462336. Components 1, 2 and 3 explained up to 23.9% 10.7 and 8.2% of the variation, respectively. ● – Cashel Stress ●- PI 462336 stress ●- Cashel control ●- PI462336 control.

Appendix B

The approximate DP of the metabolites in leaf tissue was estimated using maltose polymers with different degrees of polymerization (DP) in combination with chicory fructo-oligosaccharide standards (Figure B.1). This allowed to determine the approximate degree of polymerization (DP) of the peaks present in the fructo-oligosaccharide standard solution. For example, Maltotriose is a maltose polymer with a DP of 3, which co-elutes with one of the peaks present in the fructo-oligosaccharide standard solution. The co-eluting peak was then tentatively assigned a DP of 3. This was performed for all of the maltose polymers from DP3 to DP7. The assignment of the DP of the peaks present in the fructo-oligosaccharide standard solution beyond DP7 was extrapolated from the pattern observed in the previous peaks (Figure B.1).

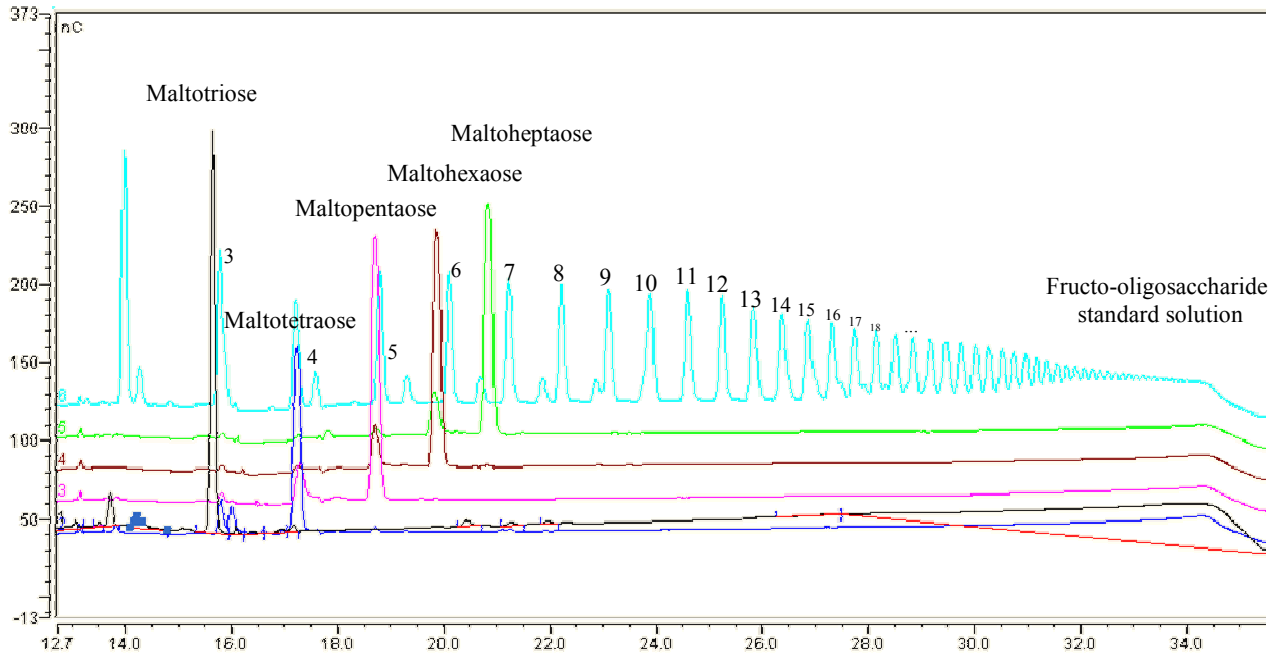

Figure B.1- Stacked chromatograms of the maltose polymer standards and fructo-oligosaccharides used. The numbers present represent the estimated degree of polymeryzation of the peaks present in the fructo-oligosaccharide standard solution. These have not been illustrated for peaks with estimated DP>18, although they have been assigned.

The assignment of the DP to the peaks of the fructo-oligosaccharide standard solution was used to estimate the approximate degree of polymerization in the samples analysed in a similar approach (Figure B.2).

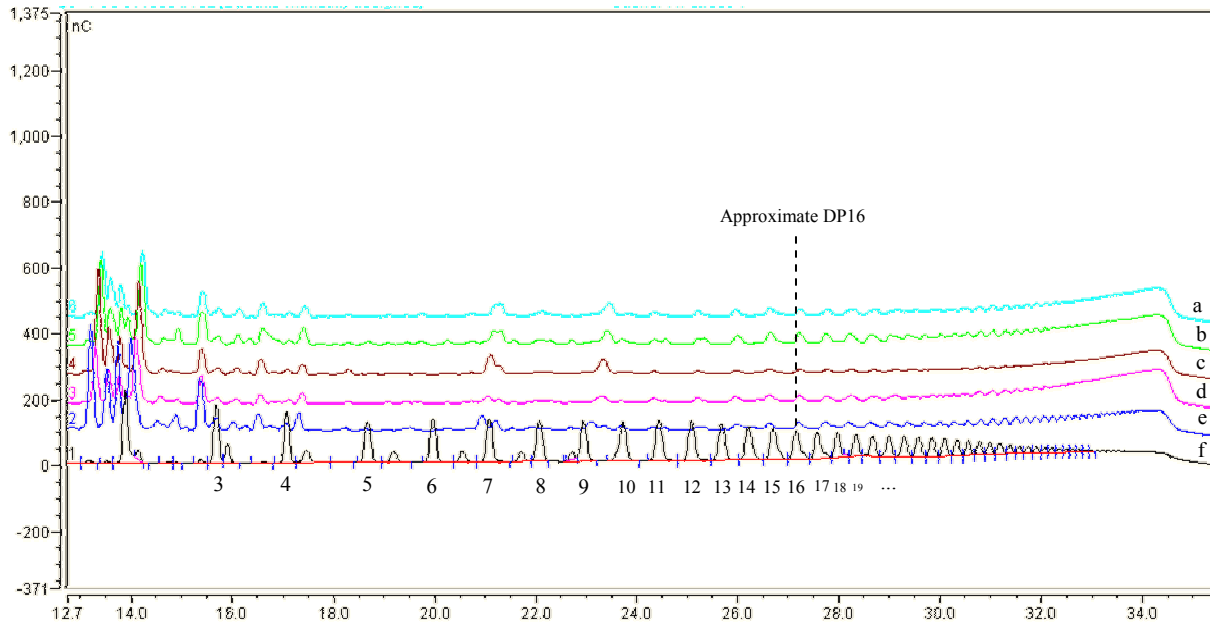

Figure B.2 - Stacked chromatograms of a subset of leaf samples and fructo-oligosaccharides used. The numbers present represent the estimated degree of polymeryzation of the peaks present in the fructo-oligosaccharide standard solution. These have been used to estimate the approximate DP of the peaks present in the samples as demonstrated for peaks assigned with an approximate DP of 16. a- Cashel after one week of exposure to stress; b- Cashel after one week under control conditions; c- Cashel after 24 hours of exposure to stress; d- Cashel after 24 hours under control conditions; e- Cashelsample at time 0; f- Fructo-oligosaccharide standard solution.

Peaks from the latter regions of the chromatogram (retention time >14.1min) corresponding to a DP>2 were integrated generating 53 individual peaks. Principal component analysis was performed and revealed that neither different environmental conditions (Figure B.3) nor different times of sampling (Figure B.4) appeared to have a significant effect over the fructan profile.

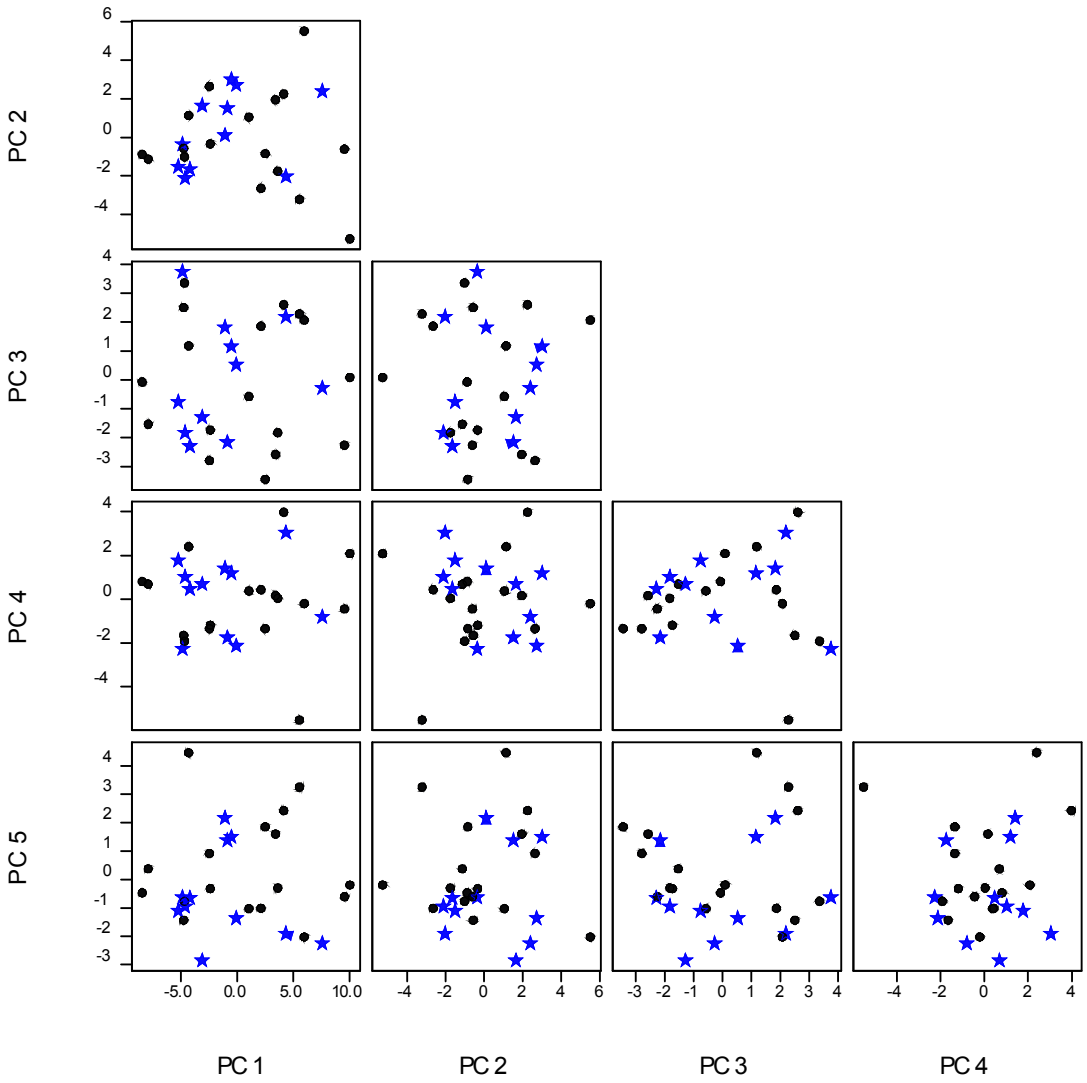

Figure B.3- Principal component analysis (PCA) plots for the first 5 principal components of all metabolites with DP ≥2 found, following HPAEC-PAD analysis of leaf blades of Cashel and PI 462336. No significant pattern was found for treatment effects: ● - Control conditions ; ★ - Stress conditions.

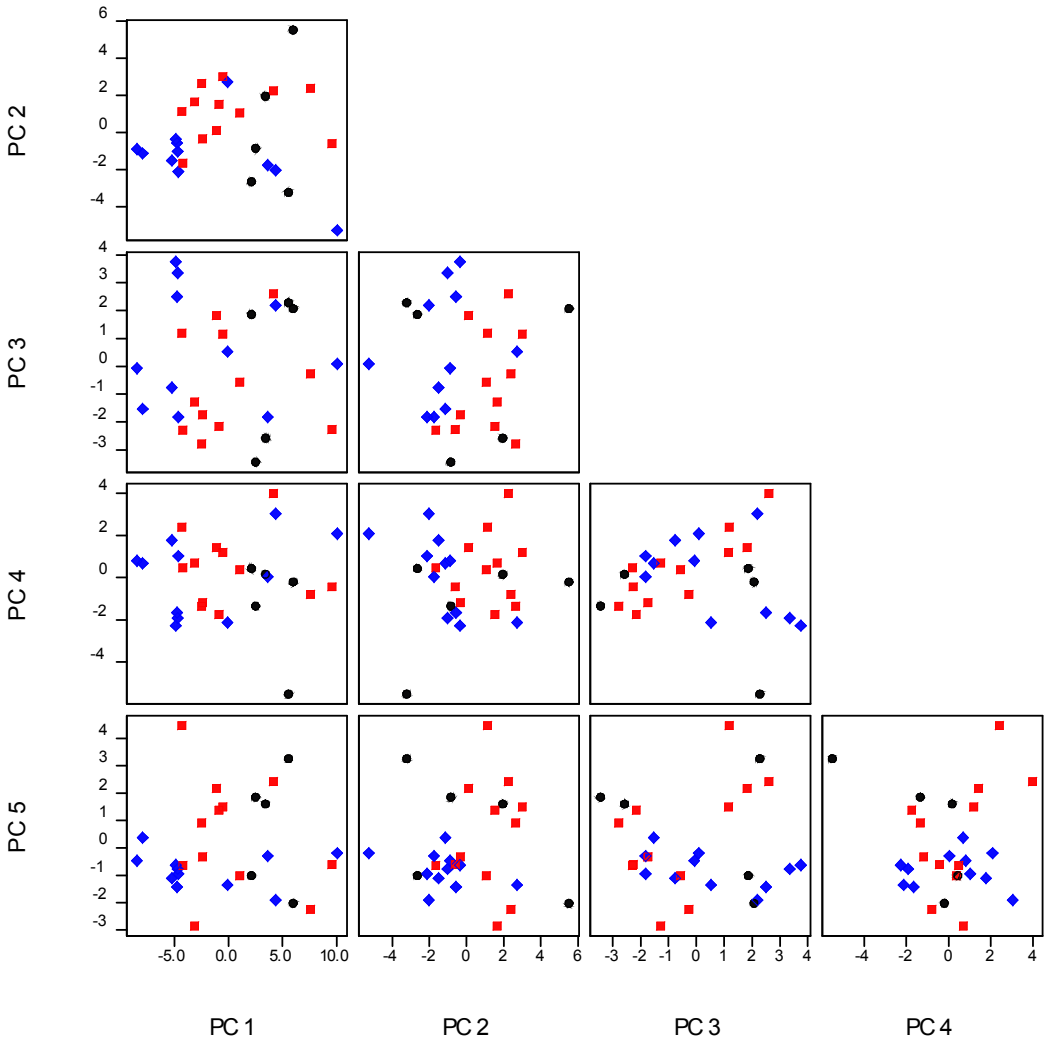

Figure B.4 - Principal component analysis (PCA) plots for the first 5 principal components of all metabolites with DP ≥2 found, following HPAEC-PAD analysis of leaf blades of Cashel and PI 462336. No significant pattern was found for in samples collected at different time points: ● – Time 0 ; ■ – 24 hours; ◆- 1 week.

Appendix C

Table C.1 - Primer sequences used in real-time RT-PCR to verify array results. The primers were designed from barley sequences close to array probe region.

Target	Forward Sequence	Reverse Sequence	Product
U35_44k_v1_12109	GCGGATTTTGGAAGAAAGC	CCCTAGGTGCCAGCTTAACA	208
U35_44k_v1_37470	CGTACCTGCTCCGCTTCAG	AGGAACTCCACCGTGTAGCA	175
U35_44k_v1_8347	AGTACTGGTTTCCGGTGTCG	CGTCGCCATAATTGTTCTCA	174
U35_44k_v1_7335	ATGATGGACCCTTCTGTTGG	CATAAACCGGTCCTTGGATG	154
U35_44k_v1_22715	GAAGTGACCCGAAACGTGAT	GATTCCATTTCTTCGCCTTG	157
U35_44k_v1_49610	TCATCCAAGAGCTGCAAGTG	CTGGCCTTGGTCAATAGCAT	166
U35_44k_v1_43490	AAGAACTGCACCGAGAAGGA	CAGAAGTTGCAGCTCGTTGA	198

Appendix D

Table D.1 - Genes significantly (P<*0.05*) induced ≥ 2 fold after 24 hrs P deficiency in leaf and root tissue of IRL-OP-02538_P genotypes.

Array ID	Best hit rice PP5	Fold-change	P-value
Leaf			
U35_44k_v1_4715	ER33 protein putative expressed	5.353163	0.004579871
U35_44k_v1_24626	phosphatase DCR2 putative expressed	4.3364162	3.77E-04
U35_44k_v1_46976	expressed protein	4.1165686	2.22E-04
U35_44k_v1_43038	phosphatase DCR2 putative expressed	3.5080466	2.47E-04
U35_44k_v1_14109	aquaporin TIP2.2 putative expressed	3.2708807	0.051294126
U35_44k_v1_21032	anthranilate phosphoribosyltransferase-like protein putative expressed	3.1456864	0.009722576
U35_44k_v1_25279	NHL25 putative expressed	2.9791517	0.04822036
U35_44k_v1_20252	calcium-transporting ATPase 2 plasma membrane-type putative expressed	2.6219265	0.04829745
U35_44k_v1_45379	transcription factor RF2a putative expressed	2.536482	0.05069122
U35_44k_v1_46982	No hits found	2.4950936	0.045132954
U35_44k_v1_9740	expressed protein	2.4831276	0.04874199
U35_44k_v1_32125	catalytic/ hydrolase putative expressed	2.4359844	0.0291131
U35_44k_v1_31817	flavonol synthase/flavanone 3-hydroxylase putative expressed	2.4348772	0.059639182
U35_44k_v1_9264	glycerol-3-phosphate dehydrogenase putative expressed	2.387155	0.02705172
U35_44k_v1_41114	expressed protein	2.315359	0.012871884
U35_44k_v1_7148	CESA2 - cellulose synthase expressed	2.2434945	0.005836656
U35_44k_v1_23909	organic anion transporter putative expressed	2.2204297	0.06372753
U35_44k_v1_17337	DNA binding like putative expressed	2.2054417	0.057473686
U35_44k_v1_46617	protein CCC1 putative expressed	2.1908963	0.026788821
U35_44k_v1_1717	protein kinase putative expressed	2.1717	0.007043802
U35_44k_v1_31614	hydrolase acting on ester bonds putative expressed	2.1583903	0.04197502
U35_44k_v1_20943	calmodulin-binding heat-shock protein putative expressed	2.1495454	9.74E-04
U35_44k_v1_35508	expressed protein	2.149482	0.005633004
U35_44k_v1_26832	hypothetical protein	2.1415029	0.01852961
U35_44k_v1_10949	acid phosphatase 1 precursor putative expressed	2.0864272	0.005143785
U35_44k_v1_507	expressed protein	2.0811558	0.04000649
U35_44k_v1_29934	phospholipase A1 putative expressed	2.0523036	0.02149714
U35_44k_v1_23388	PB1 domain containing protein expressed	2.0109181	0.027393483
U35_44k_v1_36515	pyrophosphate--fructose 6-phosphate 1-phosphotransferase alpha subunit putative expressed	2.0027926	0.011530221
U35_44k_v1_47804	oligopeptide transporter 3 putative expressed	0.48743993	0.009662489
U35_44k_v1_28321	oxidoreductase putative expressed	0.43841368	0.014756436
U35_44k_v1_24254	metal transporter Nramp3 putative expressed	0.40853974	1.94E-02
U35_44k_v1_24173	ACR5 putative expressed	0.3655308	5.33E-02
U35_44k_v1_45378	amelogenin precursor like protein putative expressed	0.22104369	2.41E-02
U35_44k_v1_45390	protein kinase domain containing protein expressed	0.11671274	0.027787734
Root			
U35_44k_v1_29895	TPR Domain containing protein expressed	2.3748653	0.041500494
U35_44k_v1_3112	cell differentiation protein rcd1 putative expressed	2.35383	0.04637834
U35_44k_v1_22436	receptor-like protein kinase homolog RK20-1 putative expressed	0.46992186	0.0464881
U35_44k_v1_22289	6b-interacting protein 1 putative expressed	0.456207	0.042473815
U35_44k_v1_44716	expressed protein	0.3988931	0.03349033
U35_44k_v1_31611	germin-like protein subfamily 1 member 7 precursor putative expressed	0.3361492	0.017426532
U35_44k_v1_13014	LOL3 putative expressed	0.31968546	0.00857045
U35_44k_v1_11424	expressed protein	0.31652027	0.036116105

Table D.2 - Genes significantly (P<*0.05*) induced ≥ 2 fold after 24 hrs P deficiency in leaf and root tissue of Cashel_P genotypes.

Array ID	Best hit rice PP5	Fold-change	P-value
Leaf			
U35_44k_v1_46527	endo-14-beta-xylanase putative expressed	7.6987286	0.009854835
U35_44k_v1_7335	CESA4 - cellulose synthase expressed	6.997706	0.03846657
U35_44k_v1_44101	fasciclin-like arabinogalactan protein 7 precursor putative expressed	6.5980825	5.50E-04
U35_44k_v1_15240	MFS18 protein precursor putative expressed	6.2584515	0.004333986
U35_44k_v1_38236	carboxylic ester hydrolase putative expressed	6.2356076	0.016659632
U35_44k_v1_23833	expressed protein	6.2316704	0.006222245
U35_44k_v1_10210	ankyrin protein kinase-like putative expressed	6.1242423	0.016497424
U35_44k_v1_23473	integral membrane protein like putative expressed	5.99986	0.006024993
U35_44k_v1_37470	glycerol-3-phosphate acyltransferase 1 putative	5.828603	0.005029339
U35_44k_v1_37369	ubiquitin-protein ligase putative expressed	5.6448894	0.0153908
U35_44k_v1_16816	anther-specific proline-rich protein APG precursor putative expressed	5.628794	0.025180155
U35_44k_v1_37093	No hits found	5.5770855	0.001592943
U35_44k_v1_10516	ankyrin protein kinase-like putative expressed	5.3768253	3.91E-04
U35_44k_v1_36893	receptor-like protein kinase precursor putative expressed	5.3477926	0.021656243
U35_44k_v1_7774	AFH1 putative expressed	5.2848964	0.003834122
U35_44k_v1_25319	sulfate transporter 3.4 putative expressed	5.1601253	2.97E-04
U35_44k_v1_37262	sucrose synthase 2 putative expressed	5.1558213	0.041007455
U35_44k_v1_29247	phenylalanine ammonia-lyase putative expressed	5.0413713	0.005855679
U35_44k_v1_21741	expressed protein	4.988921	0.015559816
U35_44k_v1_44510	Lsecondary cell wall-related glycosyltransferase family 47 putative expressed	4.634985	0.002605371
U35_44k_v1_5025	beta3-glucuronyltransferase putative expressed	4.513899	0.013111986
U35_44k_v1_44716	expressed protein	4.375929	0.025472803
U35_44k_v1_37452	No hits found	4.3251615	0.013877661
U35_44k_v1_9360	rho GDP-dissociation inhibitor 1 putative expressed	4.3171244	0.025317622
U35_44k_v1_18686	expressed protein	4.219376	0.019662017
U35_44k_v1_24503	CESA9 - cellulose synthase expressed	4.113323	0.003908644
U35_44k_v1_46614	cytochrome P450 93A2 putative expressed	4.108423	0.00780343
U35_44k_v1_7531	BRASSINOSTEROID INSENSITIVE 1-associated receptor kinase 1 precursor putative expressed	4.0944204	0.022634652
U35_44k_v1_471	fasciclin domain putative expressed	4.0936255	0.00441704
U35_44k_v1_31483	xylem serine proteinase 1 precursor putative expressed	4.042759	0.037852287
U35_44k_v1_2770	fasciclin-like arabinogalactan protein 7 precursor putative expressed	3.9659424	0.020347372
U35_44k_v1_38350	pyrophosphate-energized vacuolar membrane proton pump putative expressed	3.9655414	0.007010639
U35_44k_v1_31352	tubulin beta-3 chain putative expressed	3.8711135	0.010508534
U35_44k_v1_38954	peroxidase 1 precursor putative expressed	3.870684	3.93E-04
U35_44k_v1_4878	transposon protein putative unclassified expressed	3.850636	0.002693078
U35_44k_v1_7849	subtilisin-like protease precursor putative expressed	3.8165941	0.021842556
U35_44k_v1_23995	copper transporter 1 putative expressed	3.7964957	0.04388529
U35_44k_v1_38816	bHLH transcription factor GBOF-1 putative expressed	3.7918432	0.007071115
U35_44k_v1_47599	esterase precursor putative expressed	3.787295	0.013639119
U35_44k_v1_38674	hydrolase hydrolyzing O-glycosyl compounds putative expressed	3.7720122	0.028347103
U35_44k_v1_37360	spotted leaf protein 11 putative expressed	3.7103434	0.010224841
U35_44k_v1_14077	tubulin alpha-3 chain putative expressed	3.6658146	0.015694456
U35_44k_v1_3919	expressed protein	3.6505506	0.011005798
U35_44k_v1_31931	expressed protein	3.6362703	0.009043105
U35_44k_v1_12040	patatin-like phospholipase family protein expressed	3.5811014	0.013189553
U35_44k_v1_46386	flavonoid 35-hydroxylase 2 putative expressed	3.5499873	6.79E-04
U35_44k_v1_30293	calmodulin binding protein putative expressed	3.5416565	0.018438462
U35_44k_v1_21619	10-deacetylbaccatin III 10-O-acetyltransferase putative expressed	3.4809747	0.028786067
U35_44k_v1_21802	cytochrome P450 94A2 putative expressed	3.4516048	0.055622853
U35_44k_v1_23933	QRT3 putative expressed	3.4484549	0.031269874
U35_44k_v1_7233	amino acid permease 6 putative expressed	3.4347916	0.001439464
U35_44k_v1_10847	expressed protein	3.398042	0.002971879
U35_44k_v1_1069	alpha-expansin 10 precursor putative expressed	3.3554995	0.00403159
U35_44k_v1_50272	periplasmic beta-glucosidase precursor putative expressed	3.3535528	7.01E-04
U35_44k_v1_38741	myb-related protein Hv33 putative expressed	3.3408115	0.01678029
U35_44k_v1_16083	ACS-like protein putative expressed	3.2929628	0.036667116
U35_44k_v1_5221	expressed protein	3.2654822	0.03369299
U35_44k_v1_22989	expressed protein	3.2394123	0.03149179
U35_44k_v1_50734	mitogen-activated protein kinase kinase kinase 1 putative expressed	3.2207363	0.027514638
U35_44k_v1_31797	dopamine beta-monooxygenase putative expressed	3.2164345	0.030634198

U35_44k_v1_31565	xyloglucan endotransglucosylase/hydrolase protein 23 precursor putative expressed	3.206143	0.005810197
U35_44k_v1_31702	inorganic phosphate transporter 1-5 putative expressed	3.198314	0.04246473
U35_44k_v1_15344	AP2 domain containing protein expressed	3.1795838	0.019653529
U35_44k_v1_31926	esterase precursor putative expressed	3.1706119	0.024928464
U35_44k_v1_24754	expressed protein	3.1561525	0.038593728
U35_44k_v1_921	phi-1-like phosphate-induced protein putative expressed	3.15069	0.028682858
U35_44k_v1_1034	peroxidase 68 precursor putative expressed	3.15031	0.001308297
U35_44k_v1_34528	phytochelatin synthetase-like conserved region family protein expressed	3.1263137	0.009115248
U35_44k_v1_9048	transferase transferring glycosyl groups putative expressed	3.112705	5.70E-04
U35_44k_v1_24549	zinc finger RING-type putative expressed	3.1008186	0.005227685
U35_44k_v1_15794	CESA1 - cellulose synthase expressed	3.047775	0.009843318
U35_44k_v1_39318	sterility protein 2 putative expressed	3.0262222	0.029735455
U35_44k_v1_622	non-cyanogenic beta-glucosidase precursor putative expressed	3.00397	0.022988575
U35_44k_v1_29418	pherophorin like protein putative expressed	2.9944637	0.008614841
U35_44k_v1_31695	HGA6 putative expressed	2.9900587	0.007786733
U35_44k_v1_2422	No hits found	2.9896312	0.037186593
U35_44k_v1_44392	FAD binding domain containing protein putative expressed	2.98386	0.001575453
U35_44k_v1_49679	respiratory burst oxidase 2 putative expressed	2.9814563	0.024788218
U35_44k_v1_29568	CSLD4 - cellulose synthase-like family D expressed	2.973788	0.001243573
U35_44k_v1_23094	expressed protein	2.9731622	0.046042234
U35_44k_v1_10937	transposon protein putative Mutator sub-class expressed	2.9565804	0.008151896
U35_44k_v1_46699	germin-like protein subfamily 2 member 4 precursor putative expressed	2.955034	0.002189577
U35_44k_v1_13283	cyclin-like F-box putative expressed	2.9470835	0.036255512
U35_44k_v1_31708	ATP binding protein putative expressed	2.9213395	0.04224274
U35_44k_v1_14920	quercetin 3-O-methyltransferase 1 putative expressed	2.892111	0.006272628
U35_44k_v1_5239	expressed protein	2.8729205	0.003536929
U35_44k_v1_19768	pollen-specific kinase partner protein putative expressed	2.8680437	0.05563761
U35_44k_v1_7431	systemin receptor SR160 precursor putative expressed	2.8659892	0.01132083
U35_44k_v1_36603	cytochrome P450 86A2 putative expressed	2.8592389	0.005924989
U35_44k_v1_25749	protein binding protein putative expressed	2.8569732	0.011045317
U35_44k_v1_15882	fasciclin-like arabinogalactan protein 8 precursor putative expressed	2.82947	0.029250527
U35_44k_v1_41922	hydrolase acting on ester bonds putative expressed	2.8141446	0.08163687
U35_44k_v1_48830	peroxidase 52 precursor putative expressed	2.814126	0.003069209
U35_44k_v1_31197	S-adenosylmethionine synthetase 1 putative expressed	2.8096354	0.016571559
U35_44k_v1_41629	protein kinase putative expressed	2.808123	0.032023832
U35_44k_v1_46650	CCT motif family protein expressed	2.804794	0.027838321
U35_44k_v1_18189	No hits found	2.7907634	0.03188138
U35_44k_v1_47738	fasciclin-like arabinogalactan protein 8 precursor putative expressed	2.7834933	0.001495949
U35_44k_v1_47366	myb-like DNA-binding domain containing protein expressed	2.7671535	0.006858582
U35_44k_v1_26100	zinc finger RING-type putative expressed	2.75704	0.009709187
U35_44k_v1_422	xyloglucan endotransglucosylase/hydrolase protein 23 precursor putative expressed	2.748535	0.006719182
U35_44k_v1_12317	No hits found	2.743528	3.69E-02
U35_44k_v1_24761	calcium-dependent protein kinase isoform AK1 putative expressed	2.7332249	0.032799073
U35_44k_v1_46642	No hits found	2.7248154	0.021869717
U35_44k_v1_31706	fasciclin-like arabinogalactan protein 8 precursor putative expressed	2.7129107	0.019968668
U35_44k_v1_11067	steroid dehydrogenase KIK-I putative expressed	2.7084906	0.01162494
U35_44k_v1_5349	cytochrome P450 90D2 putative expressed	2.6982863	8.69E-02
U35_44k_v1_31803	periplasmic beta-glucosidase precursor putative expressed	2.696676	0.001116825
U35_44k_v1_43537	glycerol-3-phosphate acyltransferase 1 putative	2.693213	0.0297494
U35_44k_v1_3291	esterase precursor putative expressed	2.6745846	0.001588343
U35_44k_v1_33444	xylanase inhibitor protein 1 precursor putative	2.6682112	0.10393236
U35_44k_v1_47297	glucose-1-phosphate adenylyltransferase large subunit chloroplast precursor putative expressed	2.663975	0.010795747
U35_44k_v1_2833	early nodulin-like protein 1 precursor putative expressed	2.65949	2.22E-02
U35_44k_v1_25570	elicitor inducible gene product EIG-I24 putative expressed	2.6584978	0.001273611
U35_44k_v1_24265	carbonyl reductase 3 putative expressed	2.656853	2.59E-02
U35_44k_v1_46631	10-deacetylbaccatin III 10-O-acetyltransferase putative expressed	2.6514919	0.001969357
U35_44k_v1_32514	tripeptidyl-peptidase 2 putative expressed	2.6498108	5.59E-03
U35_44k_v1_30732	indole-3-acetate beta-glucosyltransferase putative expressed	2.6283958	0.09834122
U35_44k_v1_21777	ATMAP70-2 putative expressed	2.6265001	0.018182814
U35_44k_v1_14126	heat shock protein 82 putative expressed	2.5954683	0.029581029
U35_44k_v1_21808	glycosyltransferase putative expressed	2.514107	6.87E-04
U35_44k_v1_46684	serine carboxypeptidase 1 precursor putative expressed	2.5075119	0.020112116

U35_44k_v1_23199	Lesterase precursor putative expressed	2.5019774	0.04503105
U35_44k_v1_15246	periplasmic beta-glucosidase precursor putative expressed	2.498429	0.002513281
U35_44k_v1_28420	electron transporter putative expressed	2.4983263	0.050779678
U35_44k_v1_38079	AAPT1 putative expressed	2.4982316	0.001347365
U35_44k_v1_29738	patatin-like protein 3 putative expressed	2.483181	0.03618839
U35_44k_v1_27639	harpin-induced protein putative expressed	2.4554622	0.01655597
U35_44k_v1_40706	No hits found	2.4521985	0.041720767
U35_44k_v1_31983	expressed protein	2.4516525	0.060153265
U35_44k_v1_13863	peroxidase 16 precursor putative expressed	2.4405103	0.009900116
U35_44k_v1_14787	beta-expansin 1a precursor putative expressed	2.4381955	0.03822182
U35_44k_v1_8915	expressed protein	2.4357762	8.27E-04
U35_44k_v1_29379	expressed protein	2.433485	0.008015425
U35_44k_v1_29943	alpha-glucosidase precursor putative expressed	2.423989	0.016407773
U35_44k_v1_36859	coiled-coil protein putative expressed	2.4195914	0.031183623
U35_44k_v1_12379	beta3-glucuronyltransferase putative expressed	2.4120233	0.026345225
U35_44k_v1_37347	acyltransferase putative expressed	2.380071	0.004095034
U35_44k_v1_15652	beta-fructofuranosidase 1 precursor putative expressed	2.3620036	0.002151549
U35_44k_v1_24586	OsSAUR38 - Auxin-responsive SAUR gene family member expressed	2.3551404	0.008286722
U35_44k_v1_38510	acyltransferase putative expressed	2.3535845	0.023993237
U35_44k_v1_37436	xyloglucan endotransglucosylase/hydrolase protein 23 precursor putative expressed	2.3493469	0.001145816
U35_44k_v1_29438	3-N-debenzoyl-2-deoxytaxol N-benzoyltransferase putative expressed	2.347938	0.002164841
U35_44k_v1_24570	fatty acid elongase putative expressed	2.3348892	0.004524017
U35_44k_v1_14072	fatty acid elongase putative expressed	2.3336928	0.015302975
U35_44k_v1_46357	peroxidase 39 precursor putative expressed	2.3214066	0.01999973
U35_44k_v1_30856	esterase precursor putative expressed	2.3192694	0.04573317
U35_44k_v1_38673	transposon protein putative unclassified expressed	2.3160493	0.091692284
U35_44k_v1_41615	S-adenosylmethionine synthetase 1 putative expressed	2.30693	0.003922387
U35_44k_v1_38339	glycosyltransferase putative expressed	2.2944586	0.006720561
U35_44k_v1_49709	beta-galactosidase precursor putative expressed	2.2763777	0.031734455
U35_44k_v1_22085	BGAL9 putative expressed	2.2744813	0.033226177
U35_44k_v1_8614	catalytic/ hydrolase putative expressed	2.2741382	0.011335806
U35_44k_v1_46745	S-adenosylmethionine synthetase 1 putative expressed	2.274059	1.41E-02
U35_44k_v1_40281	OsWAK11 - OsWAK receptor-like protein kinase expressed	2.2485623	0.043480173
U35_44k_v1_27403	K-exchanger-like protein putative expressed	2.2418897	0.014316399
U35_44k_v1_29435	circumsporozoite protein precursor putative expressed	2.2316022	0.00949601
U35_44k_v1_38463	No hits found	2.229039	0.009099354
U35_44k_v1_22131	hydrolase/ protein serine/threonine phosphatase putative expressed	2.2280085	0.044406455
U35_44k_v1_5832	dehydration-responsive element-binding protein 1A putative expressed	2.227828	0.018490134
U35_44k_v1_12475	regulator of chromosome condensation RCC1 putative expressed	2.2181396	0.08006384
U35_44k_v1_21435	dihydroflavonol-4-reductase putative expressed	2.2154536	0.015771909
U35_44k_v1_22921	PB1 domain containing protein expressed	2.2091463	0.0372322
U35_44k_v1_19858	ankyrin protein kinase-like putative expressed	2.2030265	0.016331552
U35_44k_v1_13324	RING finger and CHY zinc finger domain-containing protein 1 putative expressed	2.1992414	0.001546581
U35_44k_v1_29679	patatin-like protein 3 putative expressed	2.1979434	0.03199037
U35_44k_v1_47818	polygalacturonase precursor putative expressed	2.1965408	0.02092444
U35_44k_v1_22346	peroxidase 45 precursor putative expressed	2.196504	0.02412561
U35_44k_v1_23431	galactosyltransferase/ transferase transferring hexosyl groups putative expressed	2.193832	6.85E-02
U35_44k_v1_45533	tubulin beta-6 chain putative expressed	2.1894934	0.012594179
U35_44k_v1_10939	protein kinase putative expressed	2.1893947	0.005696818
U35_44k_v1_47693	cyclin-like F-box putative expressed	2.1808844	0.001075693
U35_44k_v1_13217	subtilisin-like protein putative expressed	2.1788564	0.005646007
U35_44k_v1_9428	endoglucanase 1 precursor putative expressed	2.165164	0.003029826
U35_44k_v1_47630	BRASSINOSTEROID INSENSITIVE 1 precursor putative expressed	2.1560192	0.004844051
U35_44k_v1_38565	CESA8 - cellulose synthase expressed	2.1552207	0.008092012
U35_44k_v1_31473	dnaJ protein homolog 1 putative expressed	2.1460986	1.43E-02
U35_44k_v1_21091	mannitol dehydrogenase putative expressed	2.142711	0.03705627
U35_44k_v1_17561	outer membrane protein OMP85 family protein expressed	2.133408	0.069458656
U35_44k_v1_5738	beta-13-galactosyltransferase sqv-2 putative expressed	2.1290567	0.02493711
U35_44k_v1_12492	expressed protein	2.1249514	0.008534043
U35_44k_v1_4543	protein fluG putative expressed	2.1234612	0.001380086
U35_44k_v1_28777	COBRA-like protein 4 precursor putative expressed	2.1224632	0.04006102
U35_44k_v1_2721	ethylene-responsive element binding protein 2 putative expressed	2.1212478	0.004238681
U35_44k_v1_36709	2-oxoglutarate/malate translocator chloroplast precursor putative expressed	2.1077132	0.014254804

U35_44k_v1_45318	5-methyltetrahydropteroyltriglutamate--homocysteine methyltransferase putative expressed	2.1054373	0.013084044
U35_44k_v1_5195	expressed protein	2.104448	0.001757666
U35_44k_v1_13843	aquaporin PIP2.1 putative expressed	2.0883682	0.011158382
U35_44k_v1_39830	BGAL9 putative expressed	2.0863736	3.01E-02
U35_44k_v1_11392	No hits found	2.0808713	0.003270959
U35_44k_v1_607	catalytic/ hydrolase putative expressed	2.0784388	0.005896847
U35_44k_v1_28152	prenyltransferase/ zinc ion binding protein putative expressed	2.074741	0.018788574
U35_44k_v1_26777	caffeoyl-CoA O-methyltransferase 2 putative expressed	2.074394	0.014138627
U35_44k_v1_44030	auxin transporter-like protein 1 putative expressed	2.065403	0.00697697
U35_44k_v1_27989	serine/threonine-protein kinase ICK putative expressed	2.0647557	0.02434274
U35_44k_v1_6789	gibberellin receptor GID1L2 putative expressed	2.0625353	0.04828868
U35_44k_v1_3201	beta3-glucuronyltransferase putative expressed	2.0610719	0.016169172
U35_44k_v1_12880	RING-H2 finger protein ATL5I putative expressed	2.054674	0.022519603
U35_44k_v1_4186	OsIAA12 - Auxin-responsive Aux/IAA gene family member expressed	2.054369	0.021807073
U35_44k_v1_28596	ion channel DMI1 chloroplast precursor putative expressed	2.0542972	0.0911765
U35_44k_v1_23159	SEC14-like protein 1 putative expressed	2.0468514	0.014743507
U35_44k_v1_1454	apospory-associated protein C putative expressed	2.043557	0.03865891
U35_44k_v1_9374	expressed protein	2.0382116	2.59E-02
U35_44k_v1_49704	receptor-like protein kinase 5 precursor putative expressed	2.0359564	0.030475775
U35_44k_v1_9129	expressed protein	2.029731	0.01464792
U35_44k_v1_13488	methyltransferase putative expressed	2.0283234	0.03244721
U35_44k_v1_1050	methylenetetrahydrofolate reductase putative expressed	2.0240793	9.59E-03
U35_44k_v1_41753	metal ion binding protein putative expressed	2.016623	0.007561685
U35_44k_v1_38406	CONSTANS interacting protein 6 putative expressed	2.014175	0.015658814
U35_44k_v1_39002	multiple stress-responsive zinc-finger protein ISAP1 putative expressed	2.0135374	1.22E-02
U35_44k_v1_18212	myb-related protein Hv33 putative expressed	2.0002992	0.043826498
U35_44k_v1_21609	chaperone protein dnaJ 10 putative expressed	0.49555278	0.034209497
U35_44k_v1_26584	No hits found	0.47887254	0.007592123
U35_44k_v1_4163	aspartokinase putative expressed	0.45796496	0.006719958
U35_44k_v1_19632	charged multivesicular body protein 5 putative expressed	0.4533487	0.003614257
U35_44k_v1_31617	aspartic proteinase nepenthesin-1 precursor putative expressed	0.44651634	0.024987886
U35_44k_v1_9376	mtN3-like protein putative expressed	0.4213701	0.019502277
U35_44k_v1_5433	ubiquitin-protein ligase/ zinc ion binding protein putative expressed	0.41520798	0.023678007
U35_44k_v1_28262	CBS domain containing protein expressed	0.39231133	0.002032228
U35_44k_v1_749	CBS domain containing protein expressed	0.38303074	3.17E-03
U35_44k_v1_41584	elongation factor 1-beta putative expressed	0.3739457	0.013123808
U35_44k_v1_102	No hits found	0.3424653	0.001793052
Root			
U35_44k_v1_22715	60S ribosomal protein L5-2 putative expressed	3.6359375	0.03252972
U35_44k_v1_49610	conserved hypothetical protein	3.1135428	0.024956087
U35_44k_v1_41629	protein kinase putative expressed	2.6390605	0.03997762
U35_44k_v1_25497	integral membrane protein expressed	2.5639265	0.0010031
U35_44k_v1_32022	membrane protein putative expressed	2.4371758	0.00912594
U35_44k_v1_26701	expressed protein	2.328416	0.00682608
U35_44k_v1_23558	hydrolase hydrolyzing O-glycosyl compounds putative expressed	2.2152772	0.002031798
U35_44k_v1_8985	methionine aminopeptidase 1B chloroplast precursor putative expressed	2.1079657	0.034236446
U35_44k_v1_25645	No hits found	2.0917227	0.03725131
U35_44k_v1_12109	histidine decarboxylase putative expressed	2.0261323	0.030582085
U35_44k_v1_12441	FIP1 putative expressed	0.48339948	0.011099009
U35_44k_v1_50238	universal stress protein putative expressed	0.46407613	0.045051638
U35_44k_v1_46812	peroxidase putative expressed	0.43063173	0.025026688
U35_44k_v1_26576	methylcrotonoyl-CoA carboxylase subunit alpha mitochondrial precursor putative expressed	0.43043846	0.012192863
U35_44k_v1_29225	fructose-16-bisphosphatase cytosolic putative expressed	0.36784196	0.01619678
U35_44k_v1_37077	No hits found	0.36117163	0.039715894
U35_44k_v1_36348	No hits found	0.35701743	0.037084587
U35_44k_v1_798	asparagine synthetase putative expressed	0.33301896	0.042291213
U35_44k_v1_47121	nodulin-like protein putative expressed	0.3123153	0.013095643
U35_44k_v1_15187	sedoheptulose-17-bisphosphatase chloroplast precursor putative expressed	0.2973487	0.008851505
U35_44k_v1_43490	serine--glyoxylate aminotransferase putative expressed	0.27901918	0.021865902
U35_44k_v1_27334	thaumatin-like protein precursor putative expressed	0.26853362	0.003520957
U35_44k_v1_14852	serine--glyoxylate aminotransferase putative expressed	0.26479635	0.007528276
U35_44k_v1_3950	Ser/Thr-rich protein T10 in DGCR region putative expressed	0.19901338	0.01776676
U35_44k_v1_31263	60S ribosomal protein L32 putative expressed	0.19251043	0.007134674
U35_44k_v1_31218	50S ribosomal protein L6 putative expressed	0.19074225	0.004654094

Appendix E

Metabolomics Quality control for P-limitation

Solanum tuberosum (variety 'Desiree') tubers and blank samples were extracted and processed simultaneously with *L. perenne* samples as described previously. Multivariate analysis was performed in the combined dataset for polar and non-polar metabolites. The principal component analysis (PCA) revealed that *S. tuberosum* tuber samples and the blank segregated from the *L. perenne* dataset in the second and third principal components respectively, while the first principal component separated leaf samples from root samples (Figure E1). The reference samples did not reveal significant changes throughout the sequence of injections suggesting that the GC-MS remained stable throughout the analysis process. Further PCA plots were analyzed, and revealed no pattern related to the technical replicates (Figure E2).

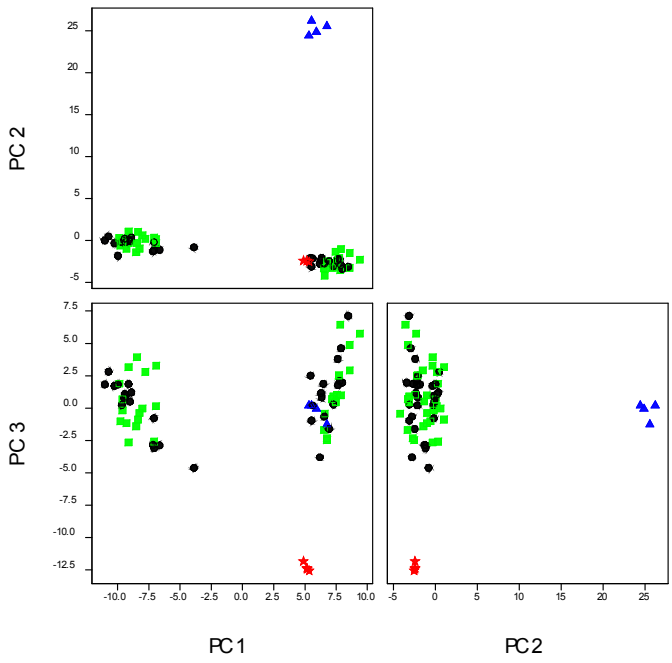

Figure E.1 - Representation of the PCA plots for the first three principal components of the polar and non-polar mass peaks detected in the samples, reference samples and blank injection following GC-MS analysis. The first, second and third principal components explained 36.1, 23.3 and 8.4% of the variation, respectively. ▲ – Desiree potato reference; ★ - Blank ; ■ - Cashel; ● - PI462336.

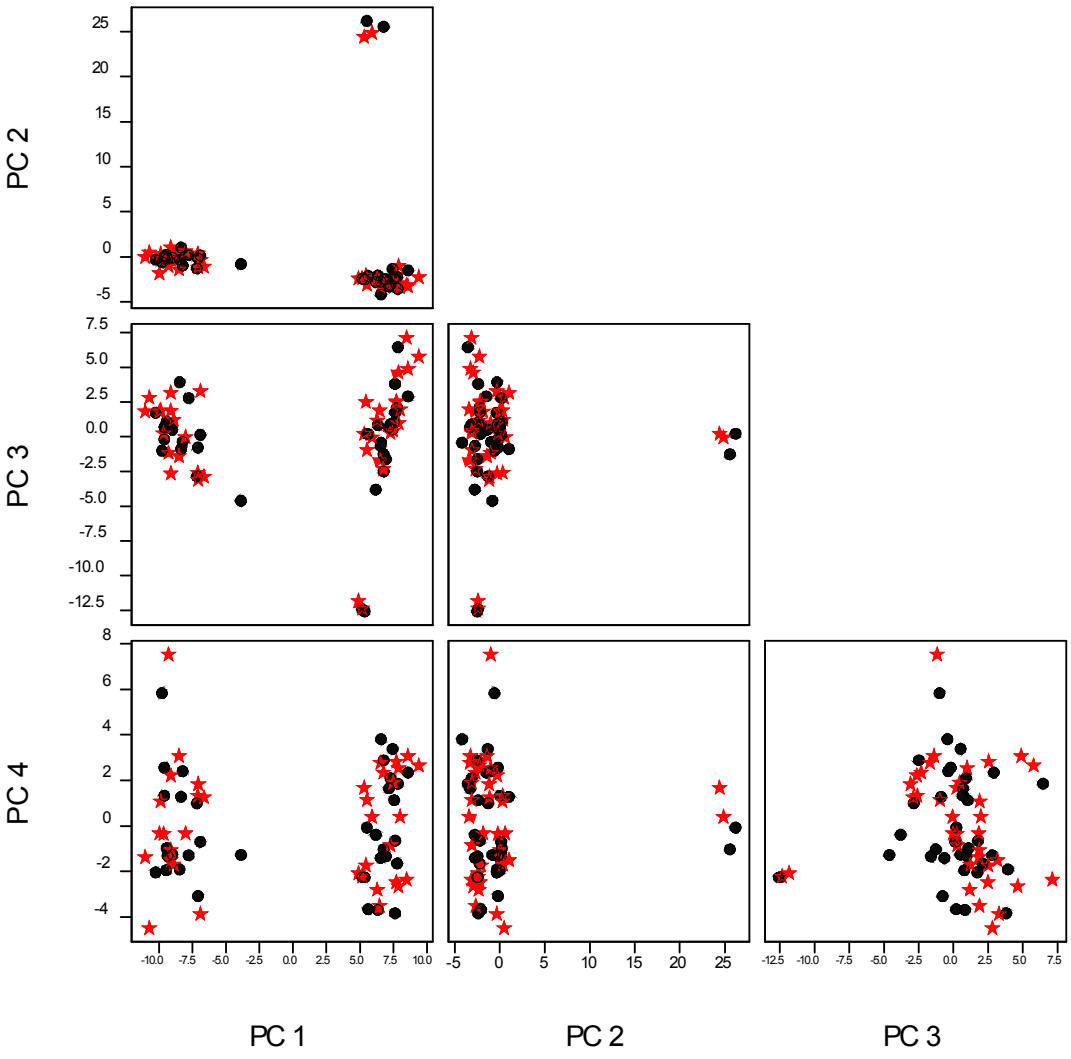

Figure E.2 - Representation of the PCA plots for the first four principal components of the polar and non-polar mass peaks detected in the samples, reference samples and blank injection following GC-MS analysis. The first, second, third and fourth principal components explained 36.1, 23.3, 8.4 and 3.4% of the variation, respectively. ★ - injection 1; ●- injection 2.

Appendix F

FT-IR Quality control for P-limitation experiment

Wheat flour was used as external biological reference sample to for FT-IR analysis. Multivariate analysis was performed to check for any unusual patterns and the principal component analysis (PCA) revealed that wheat samples segregated from the *L. perenne* dataset (Figure F1) on the first principal component. The reference samples did not reveal significant changes throughout the sequence suggesting that the FT-IR remained stable throughout the analysis process. This seems to suggest a high amount of biological variation in the samples collected.

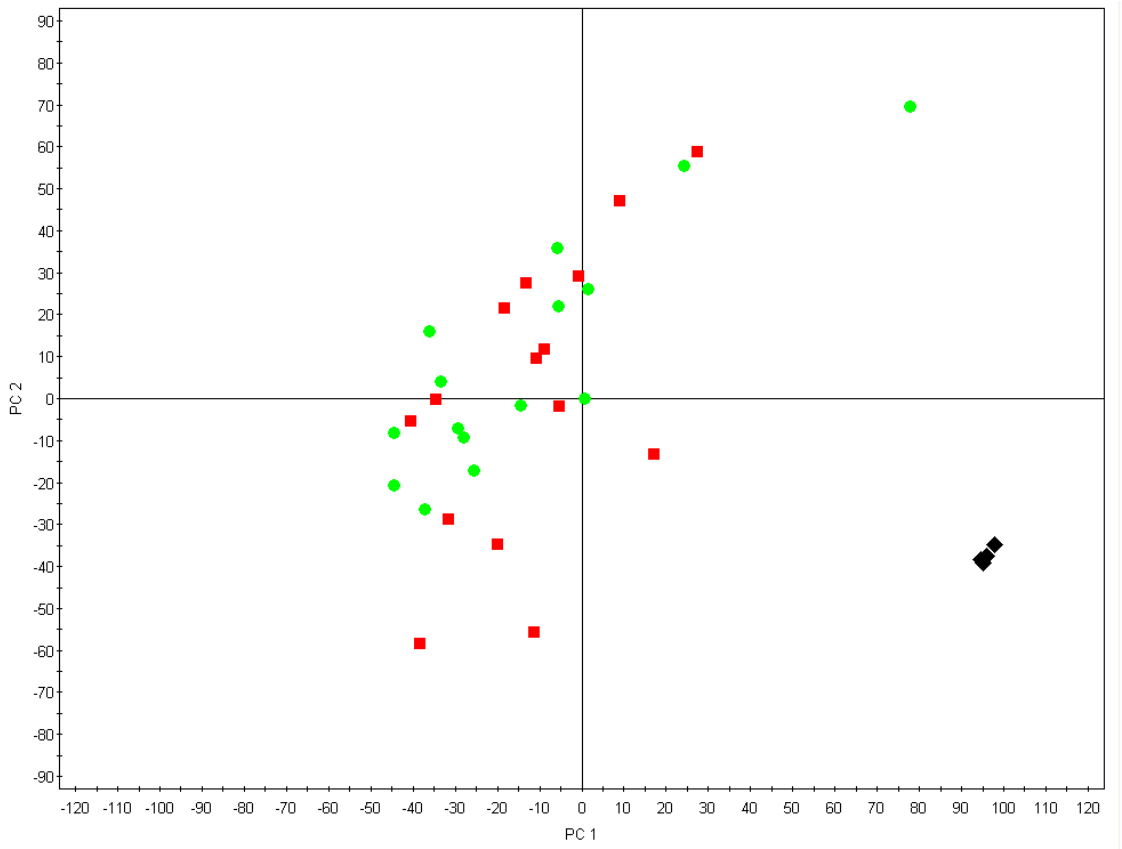

Figure F.1- PCA plot of leaf and root samples from perennial ryegrass and wheat flour analysed by FT-IR. The first and second component explained 52.1 and 29.4% of the variation respectively. Symbols represent samples from: ■ - IRL-OP-02538 genotype; ● - Cashel_P genotype; ♦ - Wheat flour reference sample.

PCA of FT-IR spectra *Lolium perenne* samples

Analysis was subsequently focused solely on the perennial ryegrass samples.PCA revealed that both tissue types can be differentiated based on their FT-IR spectra (Figure F2). Therefore, it was decided to analyse each tissue individually.

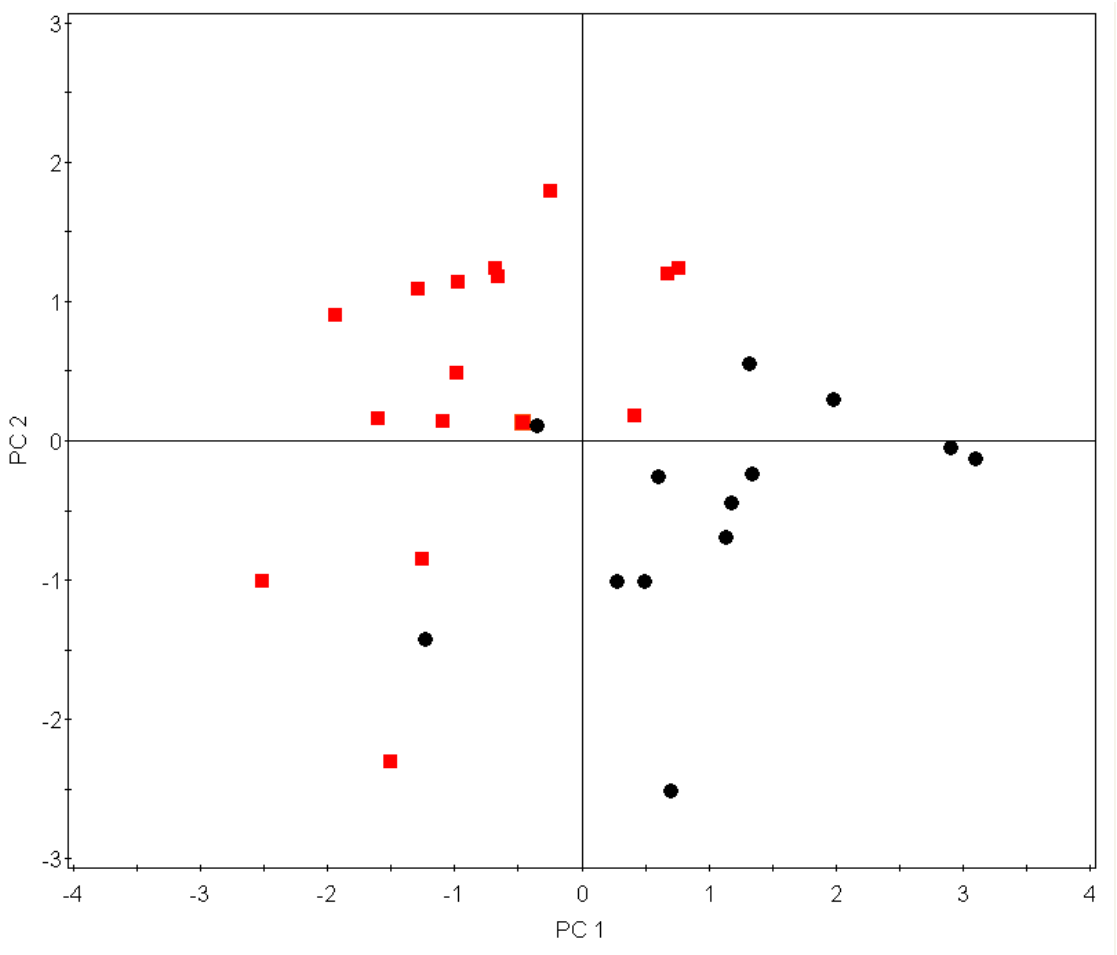

Figure F.2- PCA plot of leaf and root samples from perennial ryegrass analysed by FT-IR. The first and second component explained 47.9 and 27.5% of the variation respectively. Symbols represent samples from: ■ -Leaf; ● – Root.

FT-IR loading plots for principal components 1 and 4 of root tissue

Principal components 1 and 4 appeared to separate control samples from IRL-OP-02538_P and Cashel_P respectively. In order to visualise the regions of the spectra that are driving the response of the principal components, loading plots were created and the respective region in the FT-IR spectra were annotated (Figure F.3)

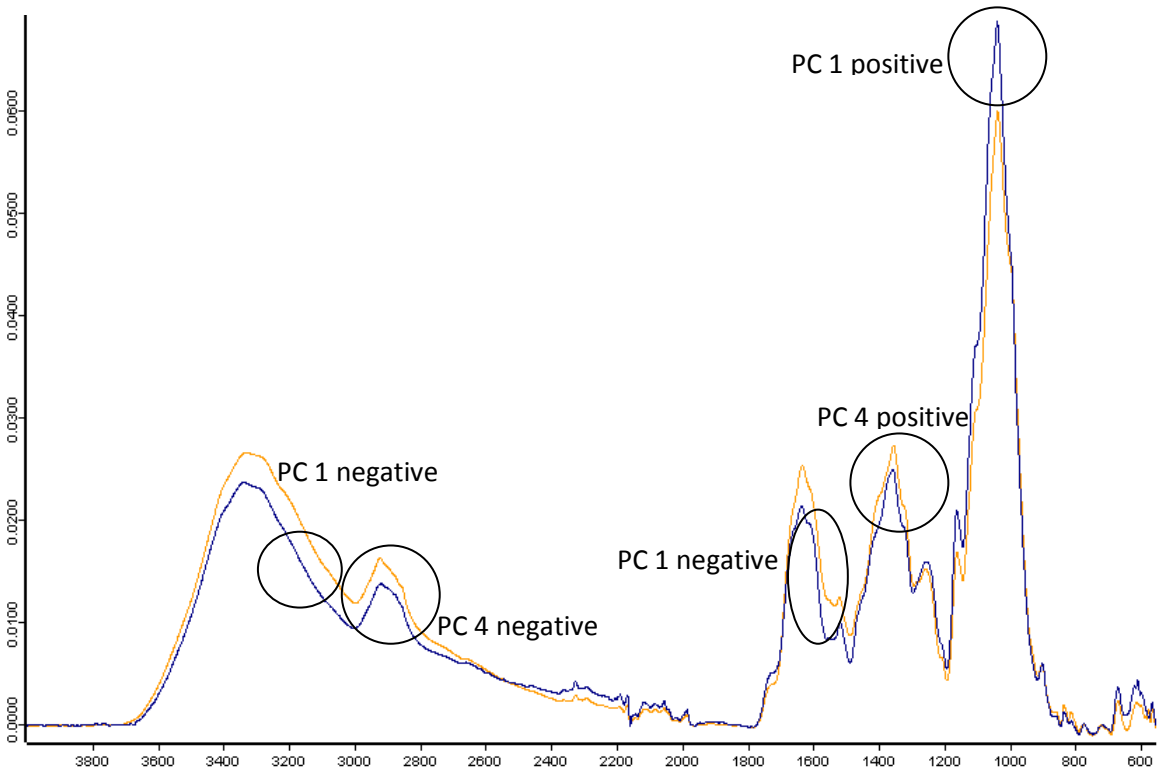

Figure F.3 – FT-IR spectra of root samples. The circled regions represent regions of the spectra which have a significant contribution for the respective principal component (1 or 4). The blue line corresponds to the spectra of a sample from IRL-OP-2538_P grown under P-sufficient conditions. The orange line corresponds to the spectra of a sample from IRL-OP-2538_P grown under P-depleted conditions.

Appendix G

Metabolomics Quality control for PEG-induced water-limitation

Solanum tuberosum (variety 'Desiree' and 'Phureja') tubers, perennial ryegrass samples used as references and blank samples were extracted and processed simultaneously experimental with *L. perenne* samples as described previously. Multivariate analysis was performed in both polar and non-polar extracts to check for any abnormalities and the principal component analysis (PCA) revealed that *S. tuberosum* tuber samples and the blank segregated from the *L. perenne* dataset (Figure G1 and G2). In the polar fraction (Figure G1), it was found that tuber samples segregated from perennial ryegrass samples in the first principal component. The perennial ryegrass reference samples also segregate from the experimental samples, however , it seems that both a combination of principal component 1 and 2 are affecting this group of samples.

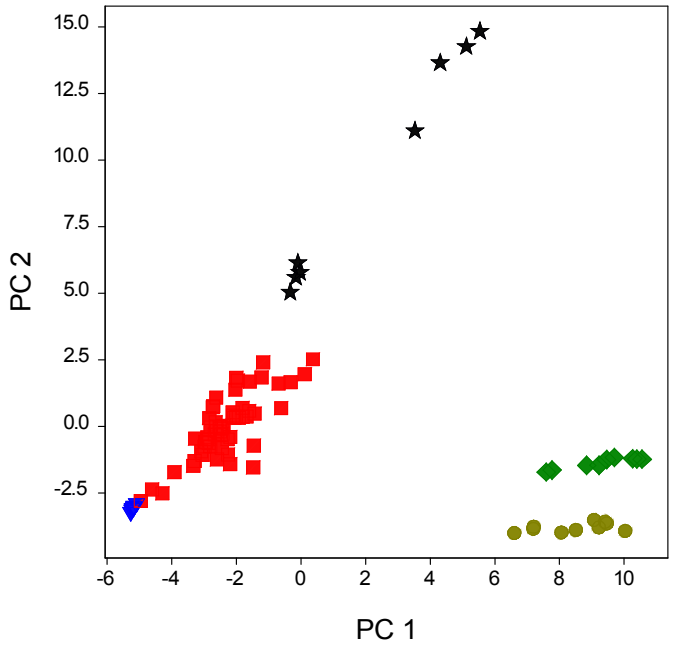

Figure G.1- Principal component analysis plot representing principal components 1 and 2 of the polar fraction. Principal component 1 and 2 represent 46.3% and 24.6% of the variability, respectively. ▼- blank ; ● - Desiree ; ◆ - Phureja; ★ - reference perennial ryegrass samples; ■ - experimental perennial ryegrass samples.

The non-polar fraction also displays segregation between perennial ryegrass samples and tuber samples, although it is not as clear as observed for the polar fraction. The first principal component appears to allow the segregation between perennial ryegrass samples and Blank and tubers. However, as observed in the polar fraction there is segregation between reference and experimental perennial ryegrass samples. However, in this case the segregation appears to be explained mainly through principal component 2.

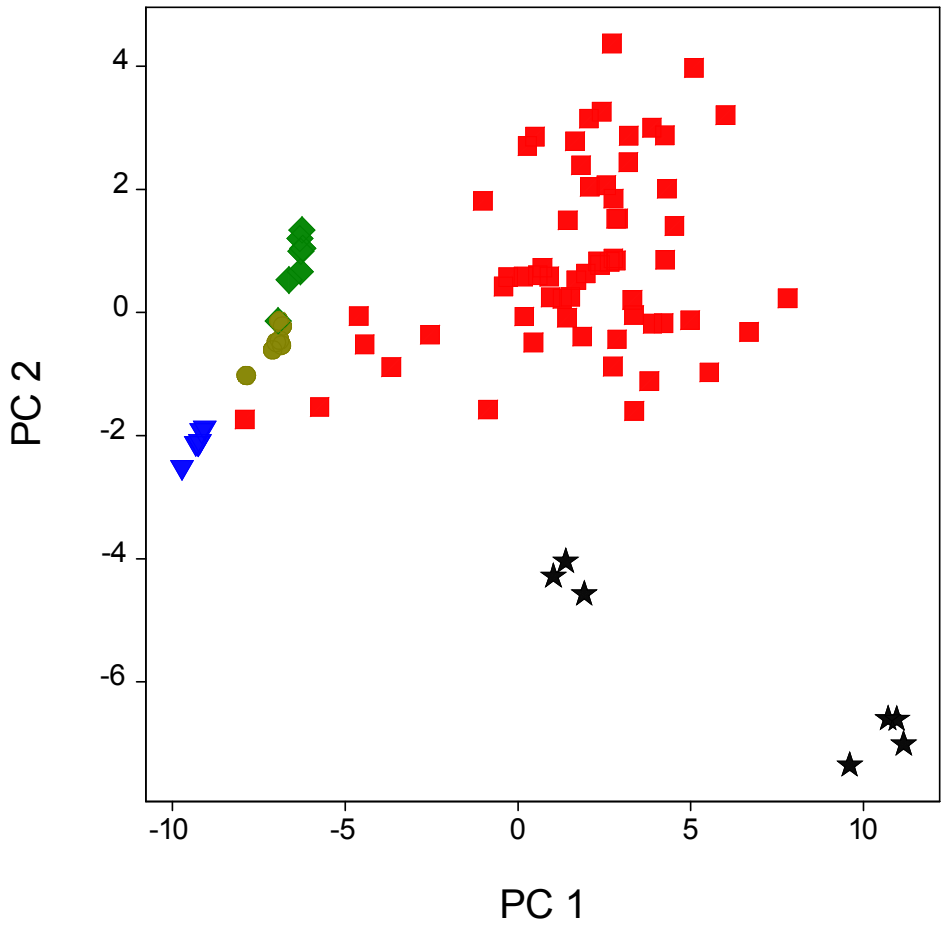

Figure G.2- Principal component analysis plot representing principal components 1 and 2 of the non-polar fraction. Principal component 1 and 2 represent 57.4% and 11.1% of the variability, respectively. ▼- blank ; ● - Desiree ; ◆ - Phureja; ★ - reference perennial ryegrass samples; ■ - experimental perennial ryegrass samples.

Appendix H

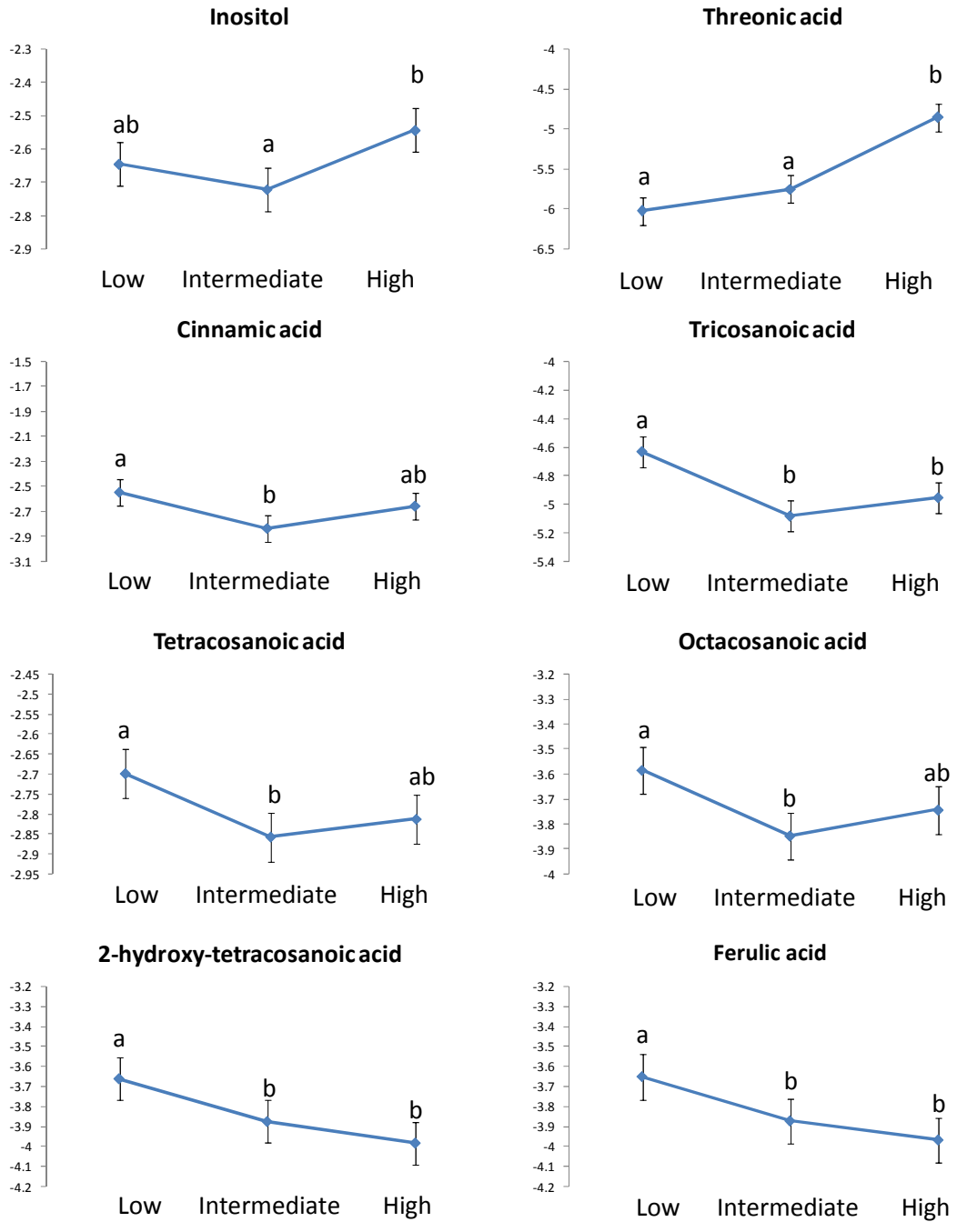

Figure H.1 - Graphical representation of the logarithm of the mean value of each metabolite (no amino acids) found to be significantly regulated by N levels. ANOVAs between means with different letters (a, b or c) were found to be significantly different ($p<0.05$) while ANOVAs between means containing the same letters were found to be non-significant ($p>0.05$).

Appendix I

Table I.1 – List of mass peaks used in the processing method of polar extracts analysed on the GC-MS used for the water-stress experiments (TOF).

retention time (min)	Name	m/z	identity process	comments	retention index
1.20	1.20_228.05	228.05	na		1086.3
1.25	1.25_174.00	174.00	na		1092.0
1.27	L-alanine (TMS)2	116.00	Compared with SCRI standard database		1094.3
1.29	1.29_204.00	204.00	na		1096.6
1.33	1.33_116	116.00	na		1101.1
1.38	Hydroxylamine (TMS)3	133.00	Compared with SCRI standard database		1106.9
1.39	1.39_228	228.00	na		1108.0
1.47	1.47_218	218.00	na		1117.1
1.55	1.55_220	220.00	na		1126.3
1.58	1.58_262	262.14	na		1129.7
1.68	1.68_174	174.10	na		1141.1
1.86	1.86_144	144.10	na		1161.7
1.89	1.89_154	154.00	na		1165.1
1.90	urea	261.20	Compared with SCRI standard database		1166.3
1.91	1.91_171	171.10	na		1167.4
1.94	1.94_174.1	174.10	na		1170.9
2.16	2.16_198	198.10	na		1196.0
2.29	L-Valine (TMS)2	144.10	Compared with SCRI standard database		1210.9
2.31	2.31_130	130.10	na		1213.1
2.44	ethanolamine (TMS)3	174.00	Compared with SCRI standard database		1228.0
2.54	Possible Carbamic acid (TMS)3	278.00	NIST query		1239.4
2.60	Benzoic acid TMS ester	179.10	NIST query		1246.3
2.75	N-ethydiethanoamine (TMS)2	174.00	Compared with SCRI standard database		1263.4
2.80	Phosphate (TMS)3	299.20	Compared with SCRI standard database		1269.1
2.81	Leucine (TMS)2	158.00	Compared with SCRI standard database		1270.3
2.84	Glycerol (TMS)3	205.00	Compared with SCRI standard database		1273.7
2.88	N-acetylglycine/2-ketobutryric acid	218.10	NIST query		1278.3
2.98	L-isoleucine (TMS)2	158.00	Compared with SCRI standard database		1289.7
3.00	L-proline (TMS)2	142.00	Compared with SCRI standard database		1292.0
3.13	3.13_240	240.10	na		1309.8
3.16	succinic acid (TMS)2	247.00	Compared with SCRI standard database		1314.7
3.24	Unknown(similar to phosphate)	299.07	na		1327.7
3.25	3.25_285	285.07	na		1329.3
3.27	2,3-dihydroxypropanoic acid (TMS)2	189.00	Compared with SCRI standard database		1332.6
3.43	Fumaric acid (TMS)2	245.00	Compared with SCRI standard database		1358.7
3.49	L-serine (TMS)3	204.00	Compared with SCRI standard database		1368.5
3.51	2-phenoxyethanol (TMS)	151.00	NIST query		1371.7
3.56	dihydroxyhydrofuranone (TMS)2	247.00	Compared with SCRI standard database		1379.9
3.64	3.64_240	240.12	na		1392.9

3.66	L-threonine (TMS)3	218.20	Compared with SCRI standard database		1396.2
3.81	3.81_156	156.00	na		1420.7
3.83	3.83_170	170.00	na		1423.9
3.92	b-alanine	174.00	Compared with SCRI standard database		1438.6
4.03	4.03_170	170.10	na		1456.5
4.07	Homoserine (TMS)3	218.00	Compared with SCRI standard database		1463.0
4.24	4.24_234	234.10	na		1490.8
4.30	Malic acid (TMS)3	233.00	Compared with SCRI standard database		1500.5
4.31	4.31_155	155.00	na		1502.2
4.34	4.34_156	156.07	na		1507.1
4.42	4.42_256	256.11	na		1520.1
4.44	4.44_116	116.00	na		1523.4
4.46	5-oxoproline (TMS)2	156.11	NIST query		1526.6
4.48	L-Aspartic acid (TMS)3	232.10	Compared with SCRI standard database		1529.9
4.52	gamma-aminobutyric acid	174.10	Compared with SCRI standard database		1536.4
4.56	4.56_156	156.10	na	similar to 5-oxoproline	1542.9
4.57	4.57_305	305.20	na		1544.6
4.60	4.60_174	174.00	na		1549.5
4.66	dipyridine	156.10	NIST query	removed from statistical analysis	1559.2
4.69	2,3,4-trioxybutyric acid (TMS)4	292.12	Compared with SCRI standard database		1564.1
4.72	4.72_218.10	218.10	na	similar to methylcisteine (TMS)2	1569.0
4.74	4.74_185	185.10	na		1572.3
4.75	4.75_243	243.20	na		1573.9
4.80	4.80_186	186.11	na		1582.1
4.83	4.83_218	218.10	na		1587.0
4.89	4.89_116	116.00	na		1596.7
5.00	Glutamic acid (TMS)3	246.20	Compared with SCRI standard database		1620.2
5.03	Asparagine (TMS)4	188.00	Compared with SCRI standard database	combine with asparagine (TMS)3 *	1627.0
5.09	Diamino(1,3)propane (TMS)4	174.00	NIST query		1640.4
5.17	Gluconic acid o methyloxime (TMS)5	217.10	Compared with SCRI standard database		1658.4
5.22	5.22_275	275.00	na		1669.7
5.23	5.23_245	245.00	na		1671.9
5.24	Asparagine (TMS)3	116.00	Compared with SCRI standard database	combine with asparagine (TMS)4 *	1674.2
5.29	Ribose-o-methyloxime (TMS)5	307.20	Compared with SCRI standard database		1685.4
5.38	5.38_275	275.20	na		1705.6
5.41	5.41_204	204.20	na		1712.4
5.44	5.44_204	204.20	na		1719.1
5.54	Putrescine (TMS)4	174.10	Compared with SCRI standard database		1741.6
5.66	5.66_392	392.20	na		1768.5
5.69	5.69_129	129.10	na		1775.3
5.72	L-glutamine (TMS)3	245.15	Compared with SCRI standard database		1782.0
5.74	5.74_334	334.14	na		1786.5
5.76	5.76_429	429.10	na		1791.0

5.84	5.84_489	489.20	na		1809.0
5.89	Shikimic acid (TMS)4	204.11	NIST query		1820.2
5.91	Ornithine (TMS)4	142.12	Compared with SCRI standard database		1824.7
5.92	Citric acid (TMS)4	273.16	Compared with SCRI standard database		1827.0
6.08	Quinic acid (TMS)4	255.15	NIST query		1862.9
6.14	Fructose-o-methyloxime (TMS)5	217.10	Compared with SCRI standard database	combine with Fructose-O-methyloxime (TMS)5 2nd peak	1876.4
6.18	Fructose-o-methyloxime (TMS)5 2nd peak	217.10	Compared with SCRI standard database	combine with Fructose-O-methyloxime (TMS)5	1885.4
6.19	Allantoin (TMS)4	431.20	NIST query		1887.6
6.24	Glucose-O-methyloxime (TMS)5	319.11	Compared with SCRI standard database	combine with Glucose-O-methyloxime (TMS)5 2nd peak	1898.9
6.27	6.27_174	174.10	na		1905.6
6.27	Allantoic acid	188.10	NIST query		1905.6
6.32	Glucose-O-methyloxime (TMS)5 2nd peak	319.11	Compared with SCRI standard database	combine with Glucose-O-methyloxime (TMS)5	1916.9
6.35	L-lysine (TMS)4	156.14	Compared with SCRI standard database		1923.6
6.37	6.37_304	304.12	na		1928.1
6.37	Sorbitol (TMS)6	319.20	Compared with SCRI standard database		1928.1
6.42	L-tyrosine (TMS)4	218.20	Compared with SCRI standard database		1939.3
6.77	6.77_319	319.16	na		2022.1
6.94	6.94_259	259.11	na		2069.0
7.00	Inositol (TMS)6	217.10	Compared with SCRI standard database		2085.5
7.07	7.07_319	319.20	na	carbohydrate	2104.8
7.16	7.16_319	319.00	na	carbohydrate	2129.7
7.18	7.18_319	319.20	na	carbohydrate	2135.2
7.20	Caffeic acid (TMS)3	396.17	Compared with SCRI standard database		2140.7
7.33	7.33_475	475.14	na		2176.6
7.37	7.37_204	204.11	na	polysaccharide	2187.6
7.79	Fructose 6P methyloxime (TMS)6	315.00	Compared with SCRI standard database		2303.4
7.82	7.82_204	204.10	na		2311.7
7.89	Glucose 6P methyloxime (TMS)6	387.00	Compared with SCRI standard database		2331.0
8.19	8.19_623	623.20	na		2416.5
8.30	8.30_623	623.20	na		2452.7
8.45	8.45_204	204.11	na		2502.2
8.57	8.57_219	219.10	na	sugar acid phosphate	2541.8
8.60	8.60_186	186.10	na	sugar phosphate	2551.6
8.72	8.72_186	186.00	na	polysaccharide	2591.2
8.87	Sucrose (TMS)8	361.19	Compared with SCRI standard database		2640.7
9.03	9.03_274	274.13	na		2693.4
9.16	Maltose(TMS)8	204.00	Compared with SCRI standard database		2736.3
9.18	Trehalose (TMS)8	361.18	Compared with SCRI standard database		2742.9
9.94	9.94_204	204.00	na		2993.4
10.24	Chlorogenic acid (TMS)6	345.17	Compared with SCRI standard database		3105.7
10.28	10.28_597	597.40	na		3120.8

10.97	Raffinose (TMS)11	361.18	NIST query	3381.1
11.06	11.06_361	361.18	na	3410.5

Table I.2 – List of mass peaks used in the processing method of non-polar extracts analysed on the GC-MS used for the water-stress experiments (TOF).

retention time (min)	Name	m/z	identity process	comments	retention index
1.19	1.19_228	228.30	na		1085.1
1.25	1.25_154	154.20	na		1092.0
1.27	1.27_147	147.10	na		1094.3
1.28	1.28_204	204.20	na		1095.4
1.32	n-Butylamine (TMS)2	174.20	Compared with SCRI standard database		1100.0
1.37	1.37_154	154.20	na		1105.7
1.42	1.42_220	220.20	na		1111.4
1.46	146_218	218.00	na		1116.0
1.49	1.49_130	130.20	na		1119.4
1.50	1.5_147	147.00	na		1120.6
1.55	1.55_258	258.20	na		1126.3
1.59	1.59_255	255.30	na		1130.9
1.65	1.65_228	228.20	na		1137.7
1.77	1.77_201	201.00	na		1151.4
1.85	1.85_188	188.20	na		1160.6
1.87	1.87_211	211.00	na		1162.9
1.93	1.93_185	185.00	na		1169.7
2.29	2.29_140	140.10	na		1210.9
2.30	2.30_130	130.20	na		1212.0
2.43	2.43_174	174.20	na		1226.9
2.54	2.54_147	147.20	na		1239.4
2.57	2.57_174	174.30	na		1242.9
2.68	2.68_228	228.00	na		1255.4
2.74	2.74_259	259.00	na		1262.3
2.83	2.83_205	205.00	na		1272.6
2.87	2.87_218	218.20	na		1277.1
2.90	2.90_273	273.40	na		1280.6
2.96	2.96_244	244.46	na		1287.4
3.10	3.10_191	191.20	na		1304.9
3.14	3.14_232	232.28	na		1311.4
3.22	3.22_196	196.20	na		1324.5
3.24	3.24_184	184.10	na		1327.7
3.27	3.27_267	267.30	na		1332.6
3.30	3.30_228	228.24	na		1337.5
3.43	3.43_159	159.20	na		1358.7
3.49	3.49_159	159.20	na		1368.5
3.50	3.50_151	151.20	na		1370.1
3.54	3.54_211	211.20	na		1376.6

3.65	3.65_270	270.30	na		1394.6
3.66	3.66_143	143.20	na		1396.2
3.69	3.69_130	130.20	na		1401.1
3.80	3.80_156	156.20	na		1419.0
3.88	3.88_143	143.10	na		1432.1
3.95	3.95_270	270.30	na		1443.5
3.96	3.96_184	184.20	na		1445.1
4.02	4.02_170	170.20	na		1454.9
4.12	4.12_165	165.20	na		1471.2
4.14	4.14_220	220.30	na		1474.5
4.19	4.19_189	187.20	na		1482.6
4.23	4.23_255	255.40	na		1489.1
4.26	BHT derivative	165.20	NIST query		1494.0
4.31	4.31_209	209.20	na		1502.2
4.32	4.32_141	141.10	na		1503.8
4.36	4.36_293	293.40	na		1510.3
4.39	Butylated hidroxytoluene (BHT)	205.30	Compared with SCRI standard database		1515.2
4.42	4.42_99	99.00	na		1520.1
4.43	4.43_116	116.10	na		1521.7
4.50	4.50_205	205.30	na		1533.2
4.53	4.53_199	199.20	na		1538.0
4.54	4.54_111	111.00	na		1539.7
4.56	4.56_263	263.40	na		1542.9
4.61	4.61_218	218.20	na		1551.1
4.64	4.64_177	177.20	na		1556.0
4.66	4.66_156	156.20	na		1559.2
4.74	4.74_243	243.40	na		1572.3
4.76	4.76_197	197.40	na		1575.5
4.77	4.77_184	184.20	na		1577.2
4.80	4.80_257	257.30	na		1582.1
4.88	4.88_201	201.30	na		1595.1
4.94	4.94_173	173.20	na		1606.7
4.97	4.97_197	197.20	na		1613.5
4.99	4.99_257	257.40	na		1618.0
5.00	5.00_240	240.30	na		1620.2
5.03	5.03_309	309.30	na		1627.0
5.04	5.04_121	121.10	na		1629.2
5.04	5.04_355	355.20	na		1629.2
5.09	5.09_257	257.30	na		1640.4
5.13	PEG-related peak	324.40	NIST query	related with PEG	1649.4
5.15	5.15_314	314.00	na		1653.9
5.20	5.20_156	156.20	na		1665.2
5.22	5.22_163	163.20	na		1669.7
5.24	5.24_247	247.40	na		1674.2
5.26	5.26_281 (siloxane)	281.00	NIST query	Plastisizer contaminants	1678.7
5.28	5.28_270	270.30	na		1683.1

5.29	5.29_129	129.20	na		1685.4
5.31	5.31_312	312.30	na		1689.9
5.33	BHT_related	277.30	NIST query		1694.4
5.34	5.34_250.3	250.30	NIST query		1696.6
5.38	5.38_314	314.40	na		1705.6
5.41	5.41_PEG	105.00	NIST query	related with PEG	1712.4
5.44	5.44_242	242.40	na		1719.1
5.51	Tetradecanoic acid methyl ester	242.40	Compared with SCRI standard database		1734.8
5.56	5.56_266	266.40	na		1746.1
5.60	5.60_155	155.19	na		1755.1
5.66	5.66_253	253.30	na		1768.5
5.69	5.69_271	271.40	na		1775.3
5.71	5.71_289	289.20	na		1779.8
5.73	5.73_155	155.20	na		1784.3
5.78	5.78_250.3	250.30	na		1795.5
5.79	5.79_241	241.30	na		1797.8
5.79	Iso-pentadecanoic acid methyl ester	143.19	Compared with SCRI standard database		1797.8
5.83	5.83_229	229.00	na		1806.7
5.83	Anteiso-pentadecanoic acid methyl ester	199.30	Compared with SCRI standard database		1806.7
5.87	5.87_236	236.30	na		1815.7
5.88	5.88_187	187.30	na		1818.0
5.91	5.91_311.30	311.30	na		1824.7
5.93	4- or 3- hydroxy cinnamic acid*	250.20	Compared with SCRI standard database	4- or 3- hydroxy 3- or 4- methoxy cinnamic acid (Ferulic acid)	1829.2
5.96	pentadecanoic acid methyl ester	256.40	Compared with SCRI standard database		1836.0
5.99	5.99_239	239.30	na		1842.7
6.01	Phytol A	123.00	NIST query	Phytol derivative	1847.2
6.05	6.05_255	255.30	na		1856.2
6.06	6.06_285	285.30	na		1858.4
6.07	6.07_365	365.50	na		1860.7
6.09	6.09_242	242.20	na		1865.2
6.10	6.10_149	149.10	na		1867.4
6.12	Phytol B	123.00	NIST query	Phytol derivative	1871.9
6.16	6.16_103	103.00	na		1880.9
6.19	Phytol C	123.10	NIST query	Phytol derivative	1887.6
6.22	6.22_204	204.20	na		1894.4
6.22	6.22_259	259.30	na		1894.4
6.23	iso-Hexadecanoic acid methyl ester	270.40	Compared with SCRI standard database		1896.6
6.24	6.24_266	266.40	na		1898.9
6.29	anteiso-hexadecanoic acid methyl ester	236.40	Compared with SCRI standard database		1910.1
6.36	Hexadecenoic acid methyl ester	236.30	na		1925.8
6.38	Hexadecanoic acid methyl ester	270.40	Compared with SCRI standard database		1930.3
6.41	6.41_563	563.50	na		1937.1
6.43	Phytol derivative	293.30	NIST query	Phytol derivative	1941.6
6.45	6.45_219	219.00	na		1946.1

6.46	3- or 4- hydroxy cinnamic acid*	250.20	Compared with SCRI standard database	4- or 3- hydroxy 3- or 4- methoxy cinnamic acid (Ferulic acid)	1948.3
6.52	6.52_209	209.20	na		1961.8
6.54	6.54_250	250.40	na		1966.3
6.54	6.54_85	85.00	na		1966.3
6.56	6.56_99	99.00	na		1970.8
6.57	6.57_204	204.10	na		1973.0
6.60	Hexadecenoic acid ethyl ester	236.00	NIST query		1979.8
6.63	Iso-15-methyl hexadcanoic acid methyl ester	74.00	NIST query		1986.5
6.66	6.66_333	333.37	na		1993.3
6.66	Hexadecanoic acid ethyl ester	284.50	NIST query		1993.3
6.67	anteiso-(n-7)methyl hexadecanoic acid methyl ester	74.00	Compared with SCRI standard database		1995.5
6.71	6.71_215	215.30	na		2005.5
6.72	6.72_250	250.40	na		2008.3
6.73	6.73_219	219.30	na		2011.0
6.73	6.73_233	233.30	na		2011.0
6.75	6.75_237	237.40	na		2016.6
6.77	6.77_163	163.10	na		2022.1
6.78	6.78_284	284.40	na		2024.8
6.81	Phytil methyl ether	123.10	NIST query	Phytol derivative	2033.1
6.86	Hexadecanoic acid (TMS)	313.50	NIST query		2046.9
6.92	Phytil methyl ether 2	123.10	NIST query	Phytol derivative	2063.4
6.97	6.97_291	291.40	na		2077.2
6.99	6.99_172	172.20	na		2082.8
7.00	7.00_136	136.00	na		2085.5
7.01	7.01_415	415.00	na		2088.3
7.05	Octadecadienoic acid methyl ester	294.50	Compared with SCRI standard database		2099.3
7.06	Octadecatrienoic acid methyl ester	292.50	Compared with SCRI standard database		2102.1
7.09	(n-9)Octadecenoic acid methyl ester	264.40	Compared with SCRI standard database		2110.3
7.14	(n-7)Octadecenoic acid methyl ester	343.40	NIST query		2124.1
7.17	Octadecanoic acid methyl ester	298.40	Compared with SCRI standard database		2132.4
7.23	7.23_436	436.30	na		2149.0
7.26	7.26_251	251.20	na		2157.2
7.27	Octadecanol (TMS)	327.40	NIST query		2160.0
7.31	7.31_306	306.40	na		2171.0
7.33	7.33_475	475.40	na		2176.6
7.34	7.34_117	117.10	na		2179.3
7.38	7.38_291	291.40	na		2190.3
7.48	7.48_175	175.20	na		2217.9
7.49	7.49_335	335.40	na		2220.7
7.51	7.51_259	259.30	na		2226.2
7.62	Nonadecanol (TMS)	341.60	NIST query		2256.6
7.70	7.70_175	175.20	na		2278.6
7.72	7.72_271	271.30	na		2284.1
7.74	7.74_227	227.30	na		2289.7

7.77	7.77_326	326.50	na	2297.9
7.80	7.80_292	292.00	na	2306.2
7.81	7.81_183	183.20	na	2309.0
7.82	Phytol (TMS)	143.16	NIST query	2311.7
7.83	7.83_223	223.30	na	2314.5
7.85	7.82_327	327.50	na	2320.0
7.89	Eicosanoic acid methyl ester	326.50	Compared with SCRI standard database	2331.0
7.90	7.90_133	133.20	na	2333.8
7.93	Nonadecanoic acid (TMS)	183.20	NIST query	2342.1
7.97	Eicosanol (TMS)	355.50	NIST query	2353.1
7.99	7.99_311	311.40	na	2358.6
8.07	8.07_259	259.33	na	2380.7
8.08	8.08_171	171.20	na	2383.4
8.18	8.18_201	201.00	na	2413.2
8.21	8.21_290	290.30	na	2423.1
8.22	Heneicosanoic acid methyl ester	340.50	Compared with SCRI standard database	2426.4
8.25	8.25_141	141.10	na	2436.3
8.26	8.26_215	215.23	na	2439.6
8.26	Eicosanoic acid (TMS)	369.00	NIST query	2439.6
8.27	8.27_311	311.40	na	2442.9
8.30	Heneicosanol (TMS)	369.60	NIST query	2452.7
8.31	8.31_270	270.30	na	2456.0
8.34	8.34_259	259.30	na	2465.9
8.35	8.35_378	378.50	na	2469.2
8.37	8.37_292	292.40	na	2475.8
8.40	8.40_290	290.40	na	2485.7
8.43	8.43_175	175.20	na	2495.6
8.45	8.45_290	290.40	na	2502.2
8.47	(n-9)Eicosenoic acid methyl ester	294.50	NIST query	2508.8
8.50	Hydroxy- Eicosanoic acid methyl ester (TMS)	355.50	NIST query	2518.7
8.52	8.52_131	131.20	na	2525.3
8.54	8.52_378	378.50	na	2531.9
8.62	Docosanol (TMS)	383.50	NIST query	2558.2
8.65	8.65_290	290.30	na	2568.1
8.77	8.77_225	225.30	na	2607.7
8.87	Tricosanoic acid methyl ester	368.60	Compared with SCRI standard database	2640.7
8.92	Tricosanol (TMS)	397.70	NIST query	2657.1
8.94	8.94_133	133.20	na	2663.7
9.09	(n-9)Tetracosenoic acid methyl ester	348.60	NIST query	2713.2
9.09	9.09_380	380.50	na	2713.2
9.10	2-Hydroxy-Docosanoic acid methyl ester	383.50	NIST query	2716.5
9.18	9.18_363	362.60	na	2742.9
9.21	9.21_117	117.00	na	2752.7
9.22	Tetracosanol (TMS)	411.60	Compared with SCRI standard database	2756.0

9.38	9.38_395	394.60	na	2808.8
9.39	9.39_398	397.70	na	2812.1
9.47	Pentacosanoic acid methyl ester	396.60	Compared with SCRI standard database	2838.5
9.49	9.49_135	135.10	na	2845.1
9.51	9.51_426	425.70	na	2851.6
9.59	9.59_396	395.60	na	2878.0
9.61	9.61_409	409.50	na	2884.6
9.64	9.64_131	131.00	na	2894.5
9.67	9.67_409	408.70	na	2904.4
9.68	2-Hydroxy-Tetracosanoic acid methyl ester	411.50	Compared with SCRI standard database	2907.7
9.76	Hexacosanoic acid methyl ester	410.70	Compared with SCRI standard database	2934.1
9.79	9.79_129	129.20	na	2944.0
9.79	Hexacosanol (TMS)	439.70	Compared with SCRI standard database	2944.0
9.86	9.86_395	395.00	na	2967.0

Table I.3 – List of retention times, retention indexes and masses used for the detection of retention and internal standards analysed on the GC-MS used for the water-stress experiments (TOF).

Standards	retention time	mass	retention index
Undecane	1.32	57.00; 71.00; 85.00	1100
Tridecane	3.07	57.00; 71.00; 85.00	1300
Hexadecane	4.91	57.00; 71.00; 85.00	1600
Eicosane	6.69	57.00; 71.00; 85.00	2000
Tetracosane	8.14	57.00; 71.00; 85.00	2400
Triacontane	9.96	57.00; 71.00; 85.00	3000
Tetratriacontane	11.02	57.00; 71.00; 85.00	3400
Octatriacontane	12.55	57.00; 71.00; 85.00	3800
Ribitol	5.49	307.2	1730.3
nonadecanoate (TMS)	7.54	269.51	2234.5

Table I.4 – List of mass peaks used in the processing method of polar extracts analysed on the GC-MS used for the phosphorus experiments (DSQI).

retention time (min)	Name	m/z	identity process	comments	retention index
1.28	1.28_147	147.00	na		
1.37	1.37_174	174.00	na		
1.54	1.54_202	202.00	na		
1.58	1.58_174	174.10	na		

1.90	L-Valine (TMS)2	144.10	Compared with SCRI standard database		
2.25	Benzoic acid (TMS)	179.10	NIST query		
2.42	N-ethydiethanoamine (TMS)2	174.00	Compared with SCRI standard database		
2.46	Leucine (TMS)2	158.00	Compared with SCRI standard database		
2.50	Glycerol (TMS)3	205.00	Compared with SCRI standard database		
2.66	L-Isoleucine (TMS)2	158.00	Compared with SCRI standard database		
2.68	L-Proline (TMS)2	142.00	Compared with SCRI standard database		
2.85	Succinic acid (TMS)2	247.00	Compared with SCRI standard database		1313.0
2.95	2,3-dihydroxypropanoic acid (TMS)2	189.00	Compared with SCRI standard database		1329.2
3.12	Fumaric acid (TMS)2	245.00	Compared with SCRI standard database		1356.8
3.17	L-Serine (TMS)3	204.00	Compared with SCRI standard database		1364.9
3.34	L-Threonine (TMS)3	218.20	Compared with SCRI standard database		1392.4
3.51	3.51_141	141.00	na		1420.0
3.92	3.92_234	234.10	na		1486.5
3.98	Malic acid (TMS)3	233.00	Compared with SCRI standard database		1496.2
4.12	5-oxoproline (TMS)2	156.00	NIST query		1518.9
4.16	L-Aspartic acid (TMS)3	232.10	Compared with SCRI standard database		1525.4
4.19	gamma-aminobutyric acid (TMS)3	174.10	Compared with SCRI standard database		1530.3
4.28	4.28_156	156.10	na	similar to 5-oxoproline	1544.9
4.33	4.33_185	185.10	na		1553.0
4.42	2,3,4-trioxybutyric acid (TMS)4	292.12	Compared with SCRI standard database		1567.6
4.50	4.50_218	218.10	na		1580.5
4.67	Glutamic acid (TMS)3	246.20	Compared with SCRI standard database		1611.5
4.69	Asparagine (TMS)4	188.00	compared with SCRI standard database	combine with asparagine (TMS)3 *	1616.1
4.75	Diamino(1,3)propane (TMS)4	174.00	NIST query		1629.9
4.83	Gluconic acid-o-methyloxime	217.10	Compared with SCRI standard database		1648.3
4.94	4.94_245	245.00	na		1673.6
4.94	Asparagine (TMS)3	116.00	Compared with SCRI standard database	combine with asparagine (TMS)4 *	1673.6
5.08	5.08_204	204.20	na		1705.7
5.16	Putrescine (TMS)4	174.10	Compared with SCRI standard database		1724.1
5.19	5.19_174	174.00	na		1731.0
5.30	5.30_129	129.10	na		1756.3
5.37	L-Glutamine (TMS)3	245.15	Compared with SCRI standard database		1772.4
5.55	Shikimic acid (TMS)4	204.11	NIST query		1813.8
5.56	Ornithine (TMS)4	142.12	Compared with SCRI standard database		1816.1
5.57	Citric acid (TMS)4	273.00	Compared with SCRI standard database		1818.4
5.72	Quinic acid (TMS)4	255.15	NIST query		1852.9
5.78	Fructose-o-methyloxime (TMS)5	217.10	Compared with SCRI standard database	combine with Fructose-O-methyloxime (TMS)5 2nd peak	1866.7
5.83	Fructose-o-methyloxime (TMS)5 2nd peak	217.10	Compared with SCRI standard database	combine with Fructose-O-methyloxime (TMS)5	1878.2
5.88	Glucose-O-methyloxime (TMS)5	319.11	Compared with SCRI standard database	combine with Glucose-O-methyloxime (TMS)5 2nd peak	1889.7
5.96	Glucose-O-methyloxime (TMS)5 2nd peak	319.11	Compared with SCRI standard database	combine with Glucose-O-methyloxime (TMS)5	1908.0
5.99	L-Lysine (TMS)4	156.14	Compared with SCRI standard database		1914.9
6.01	Sorbitol (TMS)6	319.20	Compared with SCRI standard database		1919.5

6.06	L-Tyrosine (TMS)3	218.20	Compared with SCRI standard database		1931.0
6.23	6.23_204	204.20	na		1970.1
6.41	6.41_319	319.20	na		2014.0
6.63	Inositol (TMS)6	217.10	Compared with SCRI standard database		2075.5
6.70	7.07_319	319.00	na	carbohydrate, previously found	2095.1
6.80	7.16_319	319.00	na	carbohydrate, previously found	2123.1
6.81	Caffeic acid (TMS)3	396.17	Compared with SCRI standard database		2125.9
7.07	7.07_202	202.00	na		2198.6
7.44	7.44_204	204.10	na		2302.1
8.07	8.07_204	204.00	na		2493.3
8.20	8.20_204	204.00	na		2536.7
8.47	Sucrose (TMS)8	361.19	Compared with SCRI standard database		2626.7
8.76	Maltose (TMS)8	204.00	Compared with SCRI standard database		2723.3
8.78	Trehalose (TMS)8	361.18	Compared with SCRI standard database		2730.0
9.45	9.45_204	204.00	na		2953.3
9.83	Chlorogenic acid (TMS)6	345.17	Compared with SCRI standard database		3089.7
9.88	9.88_204	204.00	na		3108.4
10.57	Raffinose (TMS)11	361.18	NIST query		3366.4

Table I.5 – List of mass peaks used in the processing method of non-polar extracts analysed on the GC-MS used for the phosphorus experiments (DSQI).

retention time (min)	**Name**	**m/z**	**identity process**	**comments**	**retention index**
1.35	1.35_228	228.20	na		
1.51	1.51_188	188.20	na		
1.80	1.80_228	228.00	na		
1.93	1.93_130	130.20	na		
2.08	2.08_174	174.20	na		
2.25	2.25_179	179.00	na		
2.42	2.42_259	259.00	na		
2.47	2.47_228	228.00	na		
2.51	2.51_147	147.20	na		
2.55	2.55_147	147.20	na		
2.63	2.63_244	244.26	na		
2.78	2.78_191	191.20	na		1301.6
2.88	2.88_196	196.20	na		1317.8
2.92	2.92_285	285.00	na		1324.3
2.95	2.95_267	267.30	na		1329.2
3.18	3.18_151	151.20	na		1366.5
3.33	3.33_270	270.30	na		1390.8
3.49	3.49_156	156.20	na		1416.8
3.54	3.54_211	211.20	na		1424.9
3.93	3.93_184	184.20	na		1488.1

3.95	3.95_165	165.20	na		1491.4
4.00	4.00_141	141.10	na		1499.5
4.02	4.02_187	187.20	na		1502.7
4.03	4.03_209	209.20	na		1504.3
4.03	4.03_293	293.40	na		1504.3
4.17	Butylated hydroxy toluene (BHT) (TMS)	205.30	Compared with SCRI standard database		1527.0
4.20	4.20_199	199.20	na		1531.9
4.23	4.23_263	263.40	na		1536.8
4.27	4.27_218	218.20	na		1543.2
4.36	4.36_156	156.20	na		1557.8
4.41	4.41_243	243.40	na		1565.9
4.42	4.42_197	197.40	na		1567.6
4.55	4.55_201	201.30	na		1588.6
4.72	4.72_355	355.20	na		1623.0
4.81	4.81_314	314.00	na		1643.7
4.95	4.95_129	129.20	na		1675.9
4.98	4.98_277	277.30	na	BHT-related	1682.8
5.16	5.16_129	129.20	na		1724.1
5.18	Tetradecanoic acid methyl ester	242.40	Compared with SCRI standard database		1728.7
5.34	5.34_289	289.20	na		1765.5
5.40	5.40_253	253.30	na		1779.3
5.44	5.44_250.3	250.30	na		1788.5
5.48	5.48_229	229.00	na		1797.7
5.53	5.53_187	187.30	na		1809.2
5.59	3- or 4- hydroxy cinnamic acid*	250.20	Compared with SCRI standard database	4- or 3- hydroxy 3- or 4- methoxy cinnamic acid (Ferulic acid)	1823.0
5.64	5.64_239	239.30	na		1834.5
5.65	Phytol A	123.00	NIST query	Phytol derivative	1836.8
5.72	5.72_242	242.20	na		1852.9
5.75	5.75_149	149.10	na		1859.8
5.76	Phytol B	123.00	NIST query	Phytol derivative	1862.1
5.81	5.81_103	103.00	na		1873.6
5.83	Phytol C	123.10	NIST query	Phytol derivative	1878.2
5.87	5.87_259	259.30	na		1887.4
6.00	Hexadecenoic acid methyl ester	236.30	Compared with SCRI standard database		1917.2
6.02	Hexadecanoic acid methyl ester	270.40	Compared with SCRI standard database		1921.8
6.09	6.09_219	219.00	na		1937.9
6.10	4- or 3- hydroxy cinnamic acid*	250.20	Compared with SCRI standard database	4- or 3- hydroxy 3- or 4- methoxy cinnamic acid (Ferulic acid)	1940.2
6.15	6.15_209	209.20	na		1951.7
6.17	6.17_85	85.00	na		1956.3
6.19	6.19_99	99.00	na		1960.9
6.29	Hexadecanoic acid ethyl ester	284.50	NIST query		1983.9
6.34	6.34_215	215.30	na		1995.4
6.40	6.40_163	163.10	na		2011.2
6.42	6.42_74	74.00	na		2016.8

6.42	6.42_284	284.40	na		2016.8
6.44	Phytil methyl ether	123.10	NIST query	Phytol derivative	2022.4
6.49	Hexadecanoic acid (TMS)	313.50	NIST query		2036.4
6.55	Phytil methyl ether 2	123.10	NIST query	Phytol derivative	2053.1
6.67	Octadecadienoic acid methyl ester	294.50	Compared with SCRI standard database		2086.7
6.70	Octadecatrienoic acid methyl ester	292.50	Compared with SCRI standard database		2095.1
6.73	(n-9)Octadecenoic acid methyl ester	264.40	Compared with SCRI standard database		2103.5
6.76	(n-7)Octadecenoic acid methyl ester	343.40	NIST query		2111.9
6.79	Octadecanoic acid methyl ester	298.40	Compared with SCRI standard database		2120.3
6.90	Octadecanol (TMS)	327.30	NIST query		2151.0
6.97	6.97_117	117.10	na		2170.6
7.09	7.09_175	175.20	na		2204.2
7.12	7.12_259	259.30	na		2212.6
7.21	Octadecanoic acid (TMS)	341.00	NIST query		2237.8
7.32	7.32_175	175.20	na		2268.5
7.34	7.34_271	271.30	na		2274.1
7.43	7.43_183	183.20	na		2299.3
7.50	Eicosanoic acid methyl ester	326.50	Compared with SCRI standard database		2318.9
7.53	Nonadecanoic acid (TMS)	183.20	NIST query		2327.3
7.57	Eicosanol (TMS)	355.50	NIST query		2338.5
7.67	7.67_259	259.33	na		2366.4
7.68	7.68_171	171.20	na		2369.2
7.81	7.81_201	201.00	na		2406.7
7.83	Heneicosanoic acid methyl ester	340.50	Compared with SCRI standard database		2413.3
7.85	7.85_141	141.10	na		2420.0
7.90	Eicosanoic acid (TMS)	369.00	NIST query		2436.7
7.90	Heneicosanol (TMS)	369.60	NIST query		2436.7
7.96	7.96_259	259.30	na		2456.7
8.03	8.03_175	175.20	na		2480.0
8.10	Hydroxy- Eicosanoic acid methyl ester (TMS)	355.50	NIST query		2503.3
8.12	8.52_131	131.20	na		2510.0
8.15	8.15_311	311.40	na		2520.0
8.22	Docosanol (TMS)	383.50	NIST query		2543.3
8.47	Tricosanoic acid methyl ester	368.60	Compared with SCRI standard database		2626.7
8.52	Tricosanol (TMS)	397.70	NIST query		2643.3
8.70	2-Hydroxy-Docosanoic acid methyl ester	383.50	NIST query		2703.3
8.77	Tetracosanoic acid methyl ester	382.60	Compared with SCRI standard database		2726.7
8.81	Tetracosanol (TMS)	411.60	Compared with SCRI standard database		2740.0
8.99	8.99_398	397.70	na		2800.0
9.06	9.06_259	259.00	na		2823.3
9.07	Pentacosanoic acid methyl ester	396.60	Compared with SCRI standard database		2826.7
9.11	9.11_426	425.70	na		2840.0
9.18	9.18_396	395.60	na		2863.3
9.20	9.20_410	409.50	na		2870.0
9.27	9.27_409	408.70	na		2893.3

9.28	2-Hydroxy-Tetracosanoic acid methyl ester	411.50	Compared with SCRI standard database	2896.7
9.34	Hexacosanoic acid methyl ester	410.70	Compared with SCRI standard database	2916.7
9.37	Hexacosanol (TMS)	439.70	Compared with SCRI standard database	2926.7
9.46	9.46_85	85.00	na	2956.7
9.81	9.81_99	99.00	na	3082.2
10.00	10.00_75	75.00	na	3153.3
10.14	10.14_129	129.20	na	3205.6
10.15	10.15_75	75.00	na	3209.3
10.20	10.20_129	129.00	na	3228.0
10.33	10.33_71	71.00	na	3276.6
10.36	10.36_75	75.00	na	3287.9
10.37	10.37_129	129.00	na	3291.6
10.42	10.42_218	218.00	na	3310.3
10.44	10.44_204	204.20	na	3317.8
10.52	10.52_75	75.00	na	3347.7
11.07	11.07_75	75.00	na	3553.3

Table I.6 – List of retention times, retention indexes and masses used for the detection of retention and internal standards analysed on the GC-MS used for the phosphorus experiments (DSQI).

Standards	**retention time**	**mass**	**retention index**
Undecane	na	na	na
Tridecane	2.77	57.00; 71.00; 85.00	1300
Hexadecane	4.62	57.00; 71.00; 85.00	1600
Eicosane	6.36	57.00; 71.00; 85.00	2000
Tetracosane	7.79	57.00; 71.00; 85.00	2400
Triacontane	9.59	57.00; 71.00; 85.00	3000
Tetratriacontane	10.66	57.00; 71.00; 85.00	3400
Octatriacontane	12.08	57.00; 71.00; 85.00	3800
Ribitol	5.15	307.2	1721.8
Nonadecanoate (TMS)	7.19	269.51	2232.2

Table I.7 – List of mass peaks used in the processing method of polar extracts analysed on the GC-MS used for the nitrogen experiments (DSQII).

retention time (min)	Name	m/z	identity process	comments	retention index
1.44	L-Alanine (TMS)2	116.00	Compared with SCRI standard database		
2.49	L-Valine (TMS)2	144.00	Compared with SCRI standard database		1191.3
2.61	Ethanolamine (TMS)3	174.00	Compared with SCRI standard database		1207.4
3.04	Leucine (TMS)2	158.00	Compared with SCRI standard database		1265.1
3.05	Phosphate (TMS)3	299.00	Compared with SCRI standard database		1266.4
3.05	Glycerol (TMS)3	205.00	Compared with SCRI standard database		1266.4
3.22	L-Isoleucine (TMS)2	158.00	Compared with SCRI standard database		1289.3
3.24	L-Proline (TMS)2	142.00	Compared with SCRI standard database		1291.9
3.31	Glycine (TMS)3	174.00	Compared with SCRI standard database		1301.7
3.38	Succinic acid (TMS)2	247.00	Compared with SCRI standard database		1313.3
3.49	2,3-dihydroxypropanoic acid (TMS)2	189.00; 292.00	Compared with SCRI standard database		1331.7
3.67	Fumaric acid (TMS)2	245.00	Compared with SCRI standard database		1361.7
3.72	L-Serine (TMS)3	204.00	Compared with SCRI standard database		1370.0
3.88	L-Threonine (TMS)3	218.50	Compared with SCRI standard database		1396.7
4.26	Homoserine (TMS)3	218.00	Compared with SCRI standard database		1460.0
4.48	Malic acid (TMS)3	233.00	Compared with SCRI standard database		1496.7
4.50	4.50_155	155.00	na		1500.0
4.54	4.54_234	234.00	na	looks like arabinohexose	1506.7
4.60	L-methionine	176.00	Compared with SCRI standard database		1516.7
4.65	5-oxoproline (TMS)2	156.00	Compared with SCRI standard database		1525.0
4.66	L-aspartic acid	232.00	Compared with SCRI standard database		1526.7
4.70	gamma-aminobutyric acid (TMS)3	174.00	Compared with SCRI standard database		1533.3
4.73	4.73_156	156.00	na		1538.3
4.87	Threonic acid (TMS)4	292.00	Compared with SCRI standard database		1561.7
5.00	5.00_227	227.00; 301.00; 304.00	na		1583.3
5.08	5.08_188	188.00; 216.00	na		1596.7
5.18	Glutamic acid (TMS)3	246.00	Compared with SCRI standard database		1618.1
5.20	L-phenylalanine (TMS)3	192.00; 218.00	Compared with SCRI standard database		1622.6
5.22	Asparagine (TMS)4	188.00	Compared with SCRI standard database	combine with asparagine (TMS)3 *	1627.1
5.41	Asparagine (TMS)3	116.00	Compared with SCRI standard database	combine with asparagine (TMS)4 *	1670.1
5.72	L-glutamine (TMS)4	227.00	Compared with SCRI standard database	combine with glutamine (TMS)3 *	1740.1
5.74	Putrescine (TMS)4	174.00	Compared with SCRI standard database		1744.6
5.90	L-glutamine (TMS)3	156.00	Compared with SCRI standard database	combine with glutamine (TMS)4 *	1780.8
6.06	6.06_217	217.00	na		1816.9
6.08	Shikimic acid (TMS)4	255.00; 357.00; 372.00; 462.00	NIST query		1821.5
6.09	Citric acid (TMS)4	273.00; 363.00; 465.00	Compared with SCRI standard database		1823.7
6.25	Quinic acid (TMS)4	345.00	Compared with SCRI standard database		1859.9

6.30	6.30_188	188.00	na		1871.2
6.31	Fructose-o-methyloxime (TMS)5	217.10	Compared with SCRI standard database	combine with Fructose-O-methyloxime (TMS)5 2nd peak	1873.4
6.34	Fructose-o-methyloxime (TMS)5 2nd peak	217.10	Compared with SCRI standard database	combine with Fructose-O-methyloxime (TMS)5	1880.2
6.36	Allantoin (TMS)4	331.00	Compared with SCRI standard database		1884.7
6.37	Galactose	319.00	Compared with SCRI standard database	minor peak	1887.0
6.41	Glucose-O-methyloxime (TMS)5	319.11	Compared with SCRI standard database	combine with Glucose-O-methyloxime (TMS)5 2nd peak	1896.0
6.43	Allantoic acid	188.00; 428.00; 518.00	NIST query		1900.6
6.48	Glucose-O-methyloxime (TMS)5 2nd peak	319.11	Compared with SCRI standard database	combine with Glucose-O-methyloxime (TMS)5	1911.9
6.52	L-lysine (TMS)4	174.00	Compared with SCRI standard database		1920.9
6.52	Sorbitol (TMS)6	319.00	Compared with SCRI standard database		1920.9
6.59	L-tyrosine (TMS)4	218.00	Compared with SCRI standard database		1936.7
7.17	Inositol (TMS)6	217.00; 305	Compared with SCRI standard database		2083.3
7.37	Caffeic acid (TMS)3	219.00; 396.00	Compared with SCRI standard database		2138.9
7.65	Tryptophan (TMS)3	202.00; 291.00	Compared with SCRI standard database		2216.7
7.98	Galactose/glycerol conjugate	204.00; 337.00	Compared with SCRI standard database		2308.3
7.99	7.99_387	387.00	na		2311.1
9.03	Sucrose (TMS)8	217.00; 361.00	Compared with SCRI standard database		2636.1
10.05	10.05_204	204.00	na	polysaccharide	2970.5
10.13	10.13_204	204.00	na	polysaccharide	2996.7
10.43	Chlorogenic acid (TMS)6	255.00; 345.00	Compared with SCRI standard database		3102.7

Table I.8 – List of mass peaks used in the processing method of non-polar extracts analysed on the GC-MS used for the nitrogen experiments (DSQII).

retention time (min)	Name	m/z	identity process	comments	retention index
2.62	2.62_174	174.20	na		1208.7
3.44	3.44_196	196.20	na		1323.3
3.48	3.48_285	285.00	na		1330.0
4.08	4.08_156	156.00	na		1430.0
4.52	4.52_141	141.10	na		1503.3
4.75	4.75_263	263.40	na		1541.7
5.08	5.08_201	201.10	na		1596.7
5.22	5.22_355	355.20	na		1627.1
5.70	Tetradecanoic acid methyl ester	74.00; 242.40	Compared with SCRI standard database		1735.6
6.02	6.02_74	74.00	na		1807.9
6.03	6.03_229	229.00	na		1810.2
6.17	6.17_239	239.20			1841.8
6.18	Phytol A	123.00	NIST query		1844.1
6.28	Phytol B	123.00	NIST query		1866.7
6.39	Phytol C	123.10	NIST query		1891.5

6.54	(n-9)Hexadecenoic acid methyl ester	236.30	Compared with SCRI standard database		1925.4
6.56	Hexadecanoic acid methyl ester	270.20	Compared with SCRI standard database		1929.9
6.64	Ferulic acid	250.20	Compared with SCRI standard database	4- or 3- hydroxy 3- or 4-methoxy cinnamic acid (Ferulic acid)	1948.0
6.95	Heptadecanoic acid methyl ester	284.30	Compared with SCRI standard database		2022.2
6.99	Phytil methyl ether	123.10	NIST query		2033.3
7.05	Hexadecanoic acid (TMS)	313.50	NIST query		2050.0
7.10	Phytil methyl ether 2	123.10	NIST query		2063.9
7.23	Octadecadienoic acid methyl ester	294.20	Compared with SCRI standard database		2100.0
7.23	Octadecatrienoic acid methyl ester	292.30	Compared with SCRI standard database		2100.0
7.26	Octadecenoic acid methyl ester	264.40	Compared with SCRI standard database		2108.3
7.33	Octadecanoic acid methyl ester	298.40	Compared with SCRI standard database		2127.8
7.45	Octadecanol (TMS)	327.30	NIST query		2161.1
7.75	Octadecanoic acid (TMS)	341.00	NIST query		2244.4
7.88	7.88_175	175.20	na		2280.6
8.05	Eicosanoic acid methyl ester	326.50	Compared with SCRI standard database		2327.8
8.15	Eicosanol (TMS)	355.50	NIST query		2355.6
8.39	Heneicosanoic acid methyl ester	340.30	Compared with SCRI standard database		2426.2
8.43	Heneicosanol (TMS)	369.50	NIST query		2439.3
8.43	7.85_141	141.10	na		2439.3
8.60	8.03_175	175.20	na		2495.1
8.67	Hydroxy- Eicosanoic acid methyl ester (TMS)	355.50	NIST query		2518.0
8.72	Docosanoic acid methyl ester	354.50	Compared with SCRI standard database		2534.4
8.78	Docosanol (TMS)	383.50	NIST query		2554.1
9.04	Tricosanoic acid methyl ester	368.60	Compared with SCRI standard database		2639.3
9.28	2-Hydroxy-docosanoic acid methyl ester	383.50	NIST query		2718.0
9.35	Tetracosanoic acid methyl ester	382.50	Compared with SCRI standard database		2741.0
9.39	Tetracosanol (TMS)	411.50	Compared with SCRI standard database		2754.1
9.86	2-Hydroxy-tetracosanoic acid methyl ester	411.60	Compared with SCRI standard database		2908.2
9.94	Hexacosanoic acid methyl ester	410.50	Compared with SCRI standard database		2934.4
9.97	Hexacosanol (TMS)	439.50	Compared with SCRI standard database		2944.3
10.24	Heptacosanol (TMS)	453.60	Compared with SCRI standard database		3035.4
10.50	Octacosanoic acid methyl ester	438.50	Compared with SCRI standard database		3127.4
10.50	Octacosanol (TMS)	467.70	Compared with SCRI standard database		3127.4
10.61	10.61_75	75.00	na		3166.4
11.02	beta-sitosterol (TMS)	357.50	Compared with SCRI standard database		3311.5

Table I.9 – List of retention times, retention indexes and masses used for the detection of retention and internal standards used on the GC-MS used for the nitrogen experiments (DSQII).

Standards	retention time	mass	retention index
Undecane	1.81	57.00; 71.00; 85.00	1100
Tridecane	3.30	57.00; 71.00; 85.00	1300
Hexadecane	5.10	57.00; 71.00; 85.00	1600
Eicosane	6.87	57.00; 71.00; 85.00	2000
Tetracosane	8.31	57.00; 71.00; 85.00	2400
Triacontane	10.14	57.00; 71.00; 85.00	3000
Tetratriacontane	11.27	57.00; 71.00; 85.00	3400
Octatriacontane	13.27	57.00; 71.00; 85.00	3800
Ribitol	5.66	307.2	1726.6
nonadecanoate (TMS)	7.70	269.51	2230.6

Appendix: List of posters and publications

International Peer-Refereed publications

Foito, A, Byrne, S., Hedley, P., Morris, J., Stewart, D., Barth, S. (2010) "Analysis of transcriptomic and metabolic response of *Lolium perenne* to phosphorous limited growth conditions" (awaiting decision)

Foito, A., Byrne, S, Shepherd, T., Stewart D, Barth, S. (2009) "Transcriptional and metabolic profiles of *Lolium perenne* L. genotypes in response to a PEG-induced water stress." Plant Biotechnology Journal 7, 1-14.

Posters and presentations

Foito, A., Byrne, S, Shepherd, T., Stewart D, Barth, S. (2009) "Transcriptional and metabolic profiles of *Lolium perenne* L. genotypes in response to a PEG-induced water stress." EUCARPIA XXVIIIth meeting of the Fodder crops and amenity grasses section - La Rochelle, 11-14th May, 2009

Foito, A., Stephen Byrne, S., Barth, S, Shepherd, T.. & Stewart D (2009) "Drought in perennial ryegrass- A metabolomics perspective." Monogram Network workshop – Bristol 29th April-1st May 2009

Foito, A., Stephen Byrne, S., Barth, S, Shepherd, T.. & Stewart D (2009) "Transcriptional and metabolic profiles of *Lolium perenne* L. genotypes in response to a PEG-induced water stress." Plant abiotic stress tolerance international conference – Vienna 8-11th February 2009

Foito, A., Stephen Byrne, S., Barth, S. & Stewart D (2008) A combined transcriptomic and metabolomic approach to understand the mechanisms underlying drought response in

perennial ryegrass. XVII Eucarpia General Congress, September 9th-12th 2008, Valencia, Spain (poster)

Foito, A., Stephen Byrne, S., Barth, S. & Stewart D (2008) A combined transcriptomic and metabolomic approach to understand the mechanisms underlying drought response in perennial ryegrass. (ABIC) August 24th-27th 2008, Cork, Ireland

Foito, A., Stephen Byrne, S., Barth, S. & Stewart D (2008) Investigating the metabolomic response of *Lolium perenne* to a PEG induced drought stress. Metabomeeting 2008 28th-29th April 2008, Lyon, France